The University Of Sheffield.

Efficient Polymer Electrolyte Fuel Cells for Portable Applications

Fatma Calili Cankir

A thesis submitted in partial fulfilment of the requirements for the degree of Doctor of Philosophy

The University of Sheffield
Faculty of Engineering
Department of Mechanical Engineering

30 June 2023

Acknowledgement

Firstly, I would like to express my deepest appreciation to my supervisor, Dr Mohammed S. Ismail, for his enormous support, guidance and patience during my PhD education. I extend sincere gratitude to my other supervisors Prof Derek B. Ingham and Prof Mohamed Pourkashanian who were always there when I needed their support. Special thanks to Professor Lin Ma and Dr Kevin J. Hughes for their suggestions and discussions that we had during weekly group meetings. I would also like to thank all the members of the Energy 2050 research group. Rahima, in particular, has been a great friend to me in both good and bad times. My appreciation extends to my friends in the fuel cell research group: Jinbei, Mustafa, Fernando, Fahad, Isaac, Florence, and Qizhi. I will never forget the coffee breaks of the fuel cell group just after Tuesday's meetings.

Many thanks to myself, as I take pride in the great achievements I have accomplished despite all the difficult times I experienced during my PhD.

My deepest gratitude goes to my beloved parents who always respect and support my decisions and my husband, Umut, for his love, encouragement and patience. I want to express my appreciation to my sister, Havva, who has been always a role model for me, and her beloved husband, Serhat, who has been always a nice brother to me.

Finally, I acknowledge the Ministry of National Education in the Republic of Turkey for funding my PhD studentship at the University of Sheffield.

This thesis is dedicated to my mother who has made me a strong and independent woman and has always given me her unconditional and never-ending love.

Abstract

Fuel cells offer a promising future for the production of clean energy by efficiently converting chemical energy into electricity without combustion, thereby minimising the environmental impact. Air-breathing polymer electrolyte fuel cells (PEFCs) distinguish themselves from other types of fuel cell due to their simplified design, which utilises ambient air, supplied by natural convection, as an oxidant. This novel approach reduces the system complexity and has the potential to improve the scalability of the fuel cell technology for portable applications. The main motivation of this thesis is to numerically investigate how to improve the output power and the operation stability of air-breathing PEFCs used for portable applications. It consists of a collection of a review paper and three published research papers.

There has been a knowledge gap in the literature on how the air-breathing PEFC responds to sudden and large load alterations under different ambient conditions, design parameters and operating conditions. In this context, a dynamic model for an air-breathing PEFC has been developed and then the sensitivity of the transient response and the steady state performance of the fuel cell to the ambient temperature and relative humidity, the thickness and the thermal conductivity of the cathode GDL, and the fuel utilisation have been studied.

Further, there has been a lack of knowledge on how natural convection limits the steady-state performance and the transient response of the air-breathing PEFC. To this end, two steady-state, non-isothermal mathematical models have been developed for both air-breathing and conventional polymer electrolyte fuel cells. Namely, with these models, a comparative parametric study has been performed to understand how each type of fuel cell responds to changes in some key parameters (i.e. the porosity and the thickness of the GDL,

the membrane thickness and the overall electrical resistance) and subsequently obtain some insights on how to design an efficient air-breathing PEFC.

Finally, two dynamic models have been developed for air-breathing and conventional PEFCs to conduct a parametric study on the impact of natural convection and some key parameters (i.e. the GDL porosity, the membrane thickness and the electrical resistance) on the transient response to load alterations and the steady-state performance of the air-breathing PEFC. This has been achieved by comparing the outcomes of the dynamic model with those of the dynamic model of the higher-in-performance and more responsive conventional PEFC.

Overall, the results show that not only the performance of the air-breathing PEFC but also its dynamic response to rapid and large load alterations are significantly sensitive to the ambient conditions due to reliance on natural convection. The results also show that it is possible to enhance the transient response and the steady-state performance of the air-breathing PEFCs by optimising some key design parameters.

Publications

Journal Papers

1. Calili-Cankir F, Ismail MS, Ingham DB, Hughes KJ, Ma L, Pourkashanian M. Air-breathing polymer electrolyte fuel cells: A review. Renewable Energy. 2023 Jun 1. (Impact Factor = 8.634) – Chapter 2.

   https://doi.org/10.1016/j.renene.2023.05.134

2. Calili F, Ismail MS, Ingham DB, Hughes KJ, Ma L, Pourkashanian M. A dynamic model of air-breathing polymer electrolyte fuel cell (PEFC): A parametric study. International Journal of Hydrogen Energy. 2021 May 13;46(33):17343-57 (Impact Factor = 7.139) – Chapter 3 .

   https://doi.org/10.1016/j.ijhydene.2021.02.133

3. Calili-Cankir F, Ismail MS, Ingham DB, Hughes KJ, Ma L, Pourkashanian M. Air-breathing versus conventional polymer electrolyte fuel cells: A parametric numerical study. Energy. 2022 Jul 1;250:123827 (Impact Factor = 8.857) – Chapter 4.

   https://doi.org/10.1016/j.energy.2022.123827

4. Calili-Cankir F, Ismail MS, Berber MR, Alrowaili ZA, Ingham DB, Hughes KJ, Ma L, Pourkashanian M. Dynamic models for air-breathing and conventional polymer electrolyte fuel cells: A comparative study. Renewable Energy. 2022 Aug 1;195:1001-14 (Impact Factor = 8.634) – Chapter 5

   https://doi.org/10.1016/j.renene.2022.06.092

Declaration

I, the author Fatma Calili Cankir, confirm that the Thesis is my own work. I am aware of the University's Guidance on the Use of Unfair Means (www.sheffield.ac.uk/ssid/unfair-means). This work has not been previously presented for an award at this, or any other, university.

Table of Contents

List of Tables

List of Figures

Chapter 1: Introduction

In the 21st century, global warming resulting from urbanization and industrialization has been a serious threat to the ecosystem. With the increasing human population, the energy demand has been increasing year by year and the combustion of fossil fuels is the main source of carbon emissions into the atmosphere, leading to global warming and environmental pollution. The percentage of carbon dioxide, the most abundant greenhouse gas, in the air has increased by approximately 30% since the industrial revolution [1]. Although renewable energy has become popular around the world, fossil fuels are still utilised to meet most of the global energy demand. Unless the use of renewable energy sources dominates, the pace of the current usage of fossil fuels, such as natural gas and coal, will result in serious and irreversible damage to the environment and the welfare of human beings. Furthermore, it is clear that fossil fuels, which are finite, will not meet the world energy demand in the future.

Fuel cells, electrochemical energy converters, have a great potential to contribute to the reduction of carbon emissions [2]. Unlike heat engines that produce electricity in several steps, fuel cells generate electricity in a single process using renewable energy resources as reactants [3]. This simple single process produces only pure water and heat as by-products when pure hydrogen, the most abundant element in the universe, is used as fuel.

There are many benefits of fuel cells over conventional heat engines, for example, fuel cells have high energy efficiency since they directly convert chemical energy to electrical energy.

Also, they do not normally have moving parts, which means that their maintenance cost is lower than that of heat engines. Despite their several advantages, there are a number of technical and economical obstacles that this technology must overcome, mainly, the low durability and high manufacturing cost of the fuel cell power systems [2], in order to be widely deployed in the marketplace. The Department of Energy (DOE) [4] has outlined specific technical targets for integrated transportation fuel cell power systems with a net capacity of 80 kilowatts electric (kW_e) operating on direct hydrogen in the context of fuel cell technologies. The specified performance criteria include a durability goal of 8,000 operational hours and a cost goal of 30 dollars per net watt (30 \$/W_{net}). In addition, distinct cost targets for fuel cell systems designed for portable power and auxiliary power applications have been established [5]. Specifically, the ultimate cost target for fuel cells with capacities between 5 and 50 Watts is set at \$7 per watt (\$7/W) whilst the ultimate cost target for fuel cells with a capacity between 100 and 200 kilowatts is reduced to \$5 per watt (\$5/W). In addition, the ultimate durability target for fuel cells in these categories is 5,000 operational hours.

1.1 Overview of Fuel Cell Technology

A fuel cell is a device that directly converts chemical energy into electricity by electrochemical reactions. Figure 1.1 shows the main components of a typical fuel cell. Similar to batteries, it mainly consists of two electrodes (anode and cathode) and an electrolyte. Batteries have a finite capacity to store energy and, once the latter has been depleted, the battery must be either discarded (if non-rechargeable) or recharged and the recharging time is relatively long. However, energy generation is a continuous process in the fuel cells as long as the fuel, e.g. hydrogen, and oxidant, e.g. oxygen, are supplied.

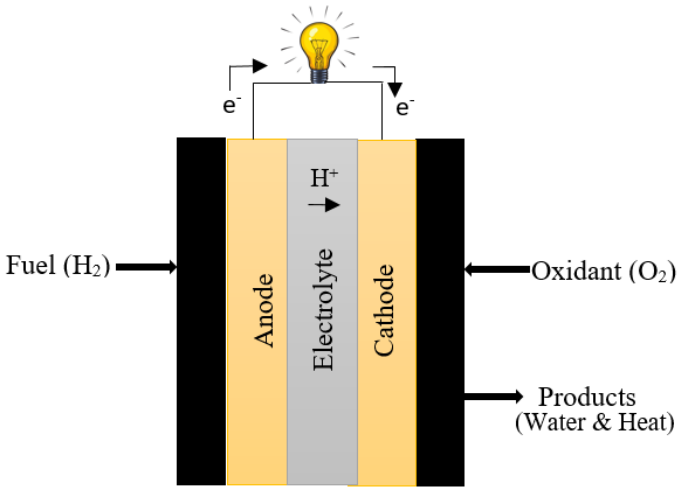

Figure 1.1 Schematic representation of a fuel cell.

Fuel and oxidant are typically supplied to the anode side and the cathode side of the fuel cell, respectively as shown in Figure 1.1. These two sides of the cell are separated by an ion-conducting electrolyte to prevent a direct chemical combustion reaction. After the hydrogen atoms are oxidized, they split into protons and electrons. Protons produced by the half-reaction (i.e., hydrogen oxidation reaction) at the anode travel across the electrolyte while the electrons are forced to travel to the cathode through an external circuit, thus powering a load. At the cathode, oxygen molecules react with protons and electrons to produce water; this reaction is known as the oxygen reduction reaction. Direct electrical current is the net result of these simultaneous half reactions due to electron migration through the external circuit.

1.2 Types of Fuel Cells

Fuel cells may be categorised based on the material of the electrolyte or the fuel type as: alkaline fuel cell, molten-carbonate fuel cell, solid oxide fuel cell, phosphoric acid fuel cell, direct methanol fuel cell and polymer electrolyte fuel cell.

According to their operating conditions and design, alkaline fuel cells may operate over a wide range of temperatures: 60-250 °C. This type of fuel cell has a lifespan of between 5,000 and 20,000 operating hours [6]. The liquid electrolyte used in alkaline fuel cells is a potassium hydroxide-water solution, whose concentration is approximately 85 wt.% at high operating temperatures (i.e. 250 °C) and 35-50 wt.% at low operating temperatures (below 120 °C) [3]. The use of an alkaline electrolyte provides high performance and lowers the material cost. In the 1950s, alkaline fuel cells were developed for space applications through collaboration between the United States and the Soviet Union [7]. Since the 1960s, they have served many space programs, such as the Space Shuttle Orbiter and Apollo programs. However, apart from space applications, other commercial applications for alkaline fuel cells are relatively limited since the electrolyte is highly sensitive to carbon dioxide that reacts with the liquid electrolyte to form the poisonous potassium carbonate. This not only adversely affect the performance of alkaline fuel cells but also limits their lifetime. This limitation can be prevented by using a carbon dioxide filter but it is quite expensive, especially for practical applications.

Alkali (Lithium, Sodium and Potassium) carbonates are used in combination as the electrolyte material for molten carbonate fuel cells. The carbonate combination is retained in a ceramic matrix [3]. The operating temperature of molten carbonate fuel cells is around 650 °C which is the temperature at which the mixture of alkali metal carbonates in the electrolyte melt to provide ionic conduction [8]. In the 1950s and 1960s, the molten carbonate fuel cells were originally developed by the US Army to operate power sources requiring high temperatures for internal fuel reformation. Nowadays, molten carbonate fuel cells are commercially available in up to 3.7 MW fuel cell units [9].

As inferred from their name, solid oxide fuel cells, the high-temperature fuel cells utilize a solid, nonporous ceramic type oxide as the electrolyte. YZS – Y_2O_3 stabilized ZrO_2 – is usually used in solid oxide fuel cells. Their operating temperature varies between 600 °C and 1000 °C since ionic conduction of oxygen ions occurs at high temperatures in the ceramic electrolyte [3]. The high operating temperature allows for the use of non-noble cost-effective metal catalysts such as nickel. Due to the non-corrosive components of solid oxide fuel cells, they have a long lifetime (40,000-80,000 operating hours) and high efficiency [10].

The electrolyte of phosphoric acid fuel cells uses concentrated (almost 100%) phosphoric acid and a silicon carbide matrix is commonly used to hold the acid. Platinum is the electro-catalyst used in both electrodes. Typically, these fuel cells operate at 150 °C to 220 °C, which provides flexible design parameters for the balance of the plant [2]. The liquid electrolyte, consisting of highly concentrated acid, supplies sufficient proton conductivity without the need to supply water, making water management simple. 1-2% carbon monoxide can be allowed in the fuel stream due to the high operating temperatures. Phosphoric acid fuel cells, with these advantages, demonstrate a long lifetime ranging from 40,000 to 80,000 hours of operation [11]. This fuel cell type was developed to be used for commercial purposes in the 1960s. However, the commercialisation of this technology has not been fully realised and this is due to the high cost of the fuel cell system. Phosphoric acid fuel cells have made some commercial success when used in stationary power plants [7].

Due to their low operating temperatures (20-90 °C), low power and long lifetime [12], direct methanol fuel cells (DMFCs) are one of the most applicable alternatives to lithium-ion batteries used in portable electronic devices. In this type of fuel cell, a platinum catalyst is used at the cathode side (for oxygen reduction reaction), a platinum-ruthenium catalyst is

used at the anode side (for methanol oxidation) and a Teflon-based solid polymer is used as an electrolyte for the conduction of protons. Methanol is directly consumed as a fuel in liquid form, hence the name is 'direct methanol' [12]. Compared to hydrogen, the use of liquid fuel brings several advantages: reduced cost and simpler storage of fuel. On the other hand, several technical restrictions adversely affect the performance of the fuel cell, such as methanol crossover (referring to the unwanted passage of methanol from the anode side to the cathode side through the membrane), managing two-phase flow in the electrodes and high catalyst loading requirements due to insufficient catalyst activity [7]. As a result of these technical issues, the power output of the fuel cell is relatively low, and this has led to limited commercial development and success.

Polymer electrolyte fuel cell (PEFC) technology has, amongst other fuel cell types, attracted a great deal of attention due to its appealing features: high efficiency, high power density, simplicity and low operating temperatures (20-90 °C). This technology has been widely used in automotive, stationary and portable applications. PEFCs employ a thin (normally less than 50 μm) proton conductive polymeric membrane (e.g. Nafion) as an electrolyte. Also, they have been called proton exchange membrane (PEM) fuel cells. Platinum nanoparticles supported on carbon black are mostly used as catalysts at both electrodes and the use of solid electrolyte allows for the PEFCs to be operated in any orientation. Also, the fuel cell start-up is fast and this is due to the low-temperature operation [7]. The PEFC is fed with oxygen, reduced at the cathode and hydrogen, oxidized at the anode. A polymer electrolyte and two catalyst layers are assembled in the PEFC and this assembly is called the membrane electrode assembly (MEA). Two more porous layers, which are known as gas diffusion layers (GDLs), are added to both sides of the MEA, which is then sandwiched between two flow

field plates. The polymer membrane offers proton conductivity during the oxidation of hydrogen and the electrons migrate through an external circuit to power the load. Polymer electrolytes were first applied in fuel cells, using an auxiliary power source for space flights in the 1960s [13]. There was no significant enhancement in the development of this technology between the 1960s and 1980s. Afterwards, significant technical advances, novel configurations and new fabrication methods have made the PEFCs much more technically and commercially feasible.

1.3 Polymer Electrolyte Fuel Cells for Portable Applications

Portable electronic devices, such as laptops and smartphones, have captured a great deal of attention and have a huge market demand due to the fact that they have substantially improved the life quality of human beings. Hence, it is expected that portable devices will keep progressing with new designs, varieties, sophistication and built-in functionalities. In addition to these improvements, advances in the power systems of these devices will be equally required in order to run the devices adequately. High-tech military-related portable electronics (e.g. night vision devices, personal cooling systems, radios and computers) are normally used for various purposes in the enemy environment, where recharging of the devices is sometimes limited. Therefore, a longer operating power source with lower weight is essential for portable applications [14].

Power sources of small electronics are normally batteries; however, the time between recharges is relatively short. In this context, PEFCs are strong candidates to be used as portable power sources due to their attractive features: long lifetime, high efficiency, low operating temperatures, independence from electricity, zero emissions, a refilled fuel cartridge, reliability and convenience [15].

It is clear that portable fuel cells must be miniaturized and simplified to compete with the state-of-the-art battery technology. The use of an open cathode to the ambient is a convenient way to minimize the stack size and simplify the fuel cell. Unlike the conventional PEFC where oxygen or air is actively supplied by forced convection using, for example, a compressor, the oxygen required for the completion of the electrochemical reaction and water vapour needed for the initial humidification of the solid membrane are extracted from the ambient air via natural convection in the open-cathode portable PEFCs. In other words, open cathode fuel cell units do not require an oxygen storage device and humidifier. This type of PEFC is described as 'open-cathode', 'passive', 'free-breathing', 'self-breathing' or 'air-breathing'. In this study, they are called air-breathing PEFCs.

As mentioned earlier, DMFCs are also an alternative to batteries. Among fuel cell types, the market for small electronic devices is equally dominated by air-breathing PEFC and DMFC technologies [16]. Both fuel cell types offer similar advantages such as high power density, silent operation, and low weight to portable small batteries [17]. However, methanol crossover from the anode to the cathode poses a significant issue in DMFCs, severely reducing cell voltage, current density and fuel utilisation [18]. One major concern in the commercialisation of DMFCs is the stability of the fuel cell during long-term operation. Degradation rates of DMFCs are presumably high due to poisoning by intermediates produced from methanol oxidation reaction, mainly CO_2, to MEA [19]. Given these concerns, air-breathing PEFCs are more favourable alternatives than DMFCs for portable applications.

On the other hand, the general design of a battery is usually simpler compared to fuel cells, primarily due to the absence of fuel and oxidant delivery and water management systems [17]. Further, the miniaturisation of the portable fuel cell-based power systems is

significantly affected by these complexities. Addressing these challenges is crucial for successful commercialization of such systems. When comparing these three technologies in terms of economic feasibility, Metzger and Li [20] recently conducted a study comparing the life cycle cost of batteries, PEFCs and DMFCs as the primary power source of electrical forklifts. While the battery exhibited the lowest cost over 10 years ($14,935), the life cycle cost of DMFCs ($41,819) was 12% higher than that of PEFCs ($36,682). In summary, there are several technical and economic issues that the air-breathing PEFC system needs to overcome for substantial market penetration.

1.4 Motivation and Objectives

The main motivation of this study was to numerically investigate how to improve the dynamic and static performance of air-breathing PEFCs. When the air-breathing PEFCs are compared with conventional PEFCs, they are significantly simpler devices due to the reliance on natural convection. However, the output power and the operation stability of air-breathing PEFCs are relatively low compared to the conventional PEFCs and this is due to the low heat and mass transfer coefficients associated with natural convection.

It is evident that the ambient conditions have a significant impact on the efficiency and operation of the air-breathing fuel cell. Furthermore, the power that is needed to power a portable device may significantly change with time when using multiple power-demanding functions. Therefore, one of the main aims for this technology is to improve the transient response of the air-breathing PEFC in the case of sudden and/or large changes in the load of the small electronic device. It has been observed in the literature that there have been no investigations on the effect of ambient conditions and design parameters of the GDL on the transient response of the air-breathing fuel cell. Based on the above, the first main objective

of this thesis is to investigate the effects of the ambient conditions, GDL parameters and hydrogen utilisation on the dynamic response of the air-breathing PEFC to rapid and large load changes. Therefore, a dynamic model for an air-breathing PEFC has been developed within the platform of MATLAB/Simulink to study the sensitivity of the transient response of the fuel cell to the ambient conditions, the cathode GDL parameters and the hydrogen utilisation.

In the air-breathing PEFC, the heat and mass transfer coefficients are, compared to the conventional PEFCs, significantly small due to the passive oxygen supply from the open cathode, thus substantially limiting the cell performance. Mathematical modelling is one of the most efficient and cost-effective ways to investigate the ambient and design parameters on the fuel cell performance. The number of air-breathing PEFC numerical models is limited and there have been no modelling studies in the literature that have simultaneously compared the outcomes of the air-breathing and the conventional PEFCs and analysed the main reasons behind the significant difference in the cell performance. Thus, the second objective of this thesis is to comparatively investigate the impact of some key parameters on the performance of each type of fuel cell and obtain better insights on how to improve the air-breathing fuel cell performance. To this end, two steady-state, non-isothermal and efficient mathematical models have been developed for both conventional and air-breathing PEFCs. Subsequently, a parametric study has been carried out to comparatively assess the effect of the GDL porosity and thickness, the membrane thickness and the electrical resistance on the performance of both types of fuel cell.

The third main objective of this thesis is to reveal the effect of natural convection on the dynamic response of the air-breathing PEFC by comparing its performance with that of the

conventional PEFC. To achieve this objective, two dynamic models for air-breathing and conventional PEFCs have been built and their outcomes have been compared to study the effect of natural convection on the transient response of the air-breathing PEFC. Further, the impacts of some key parameters (i.e. the GDL porosity, the membrane thickness and the electrical resistance) on the transient response of both types of fuel cells have been comparatively investigated to obtain better insights on how these design parameters should be optimised to improve the transient response of the air-breathing PEFC.

1.5 Thesis Outline

The thesis comprises a collection of four journal papers, three of which are published and one of which has been submitted for publication in Applied Energy and it is under review. Each paper forms a chapter that is written and formatted as when it was submitted for publication.

Chapter 2 is a review paper that has been published in Renewable Energy [21]. This paper first provides a general description of the main components and the working principles of the air-breathing PEFC in Section 2.3. Section 2.4 lists and describes the fundamental equations used to create the mathematical models for air-breathing PEFCs. Then, Section 2.5 reviews various ways that have been adopted in the literature to optimise the designs and the materials to enhance the performance of the air-breathing PEFC. In Section 2.6, the impact of the ambient conditions in terms of temperature and humidity is reviewed. Hydrogen delivery, air-breathing PEFC stacks and systems are reviewed in Sections 2.7, 2.8 and 2.9, respectively. Finally, some key concluding remarks and recommendations are given in the last sections of Chapter 2.

Chapter 3 is a research paper published in the International Journal of Hydrogen Energy [22]. This paper proposes a dynamic model for an air-breathing PEFC, developed within the

platform of MATLAB/Simulink. It investigates, for the first time, the sensitivity of the load-following capability of the air-breathing PEFCs to various ambient conditions, the cathode GDL parameters and the hydrogen utilisation during rapid and large load changes. The paper concludes by highlighting the key findings associated with the optimisation of the ambient conditions and GDL parameters to maximise the dynamic performance of the air-breathing PEFC.

Chapter 4 is a research paper published in the Energy Journal [23]. This paper presents two steady-state, non-isothermal and efficient mathematical models for conventional and air-breathing PEFCs. These models are employed in a comparative study, aiming to explore, for the first time, the extent to which natural convection limits the steady-state performance of the air-breathing PEFC. The study also comparatively evaluates the impact of key parameters (i.e., the GDL porosity and thickness, the membrane thickness and the electrical resistance) on the steady-state performance of both fuel cell types. Finally, this paper sheds light on the significant difference in the steady-state performances between the two fuel cell types and provides recommendations for enhancing the performance of the air-breathing PEFC through optimising the key parameters.

Chapter 5 is a research paper published in the Renewable Energy Journal [24]. It introduces two dynamic models for the conventional and air-breathing PEFCs. It elucidates how natural convection influences the load-following capability of the air-breathing PEFC under rapid and substantial load alterations. This is achieved by comparing its dynamic performance with that of the conventional PEFC, where air is supplied though forced convection. Additionally, it demonstrates the sensitivity of the dynamic response of both fuel cell types to the GDL porosity, the membrane thickness and the electrical resistance when the load current

suddenly changes. Furthermore, this paper outlines the key findings on certain parameters to mitigate the adverse impact of natural convection on the dynamic response of the air-breathing PEFC, thereby enhancing its transient response to the load changes.

Chapter 6 is a summary of the main findings of the thesis. This chapter also suggests possible future investigations that could build up on the findings outlined in this thesis.

Chapter 2: Theoretical Background and Literature Review

Air-breathing polymer electrolyte fuel cells: A review

This chapter is published as:

Calili-Cankir F, Ismail MS, Ingham DB, Hughes KJ, Ma L, Pourkashanian M. Air-breathing polymer electrolyte fuel cells: A review. Renewable Energy. 2023 Jun 1. https://doi.org/10.1016/j.renene.2023.05.134

Authorship statement

The principle author of the paper is Calili-Cankir F. The contribution of Calili-Cankir F is conceptualization, methodology, formal analysis, investigation, writing original draft, review and editing.

2.1 Abstract

Air-breathing polymer electrolyte fuel cells have become a promising power source to provide uninterrupted power for small electronic devices. This review focuses primarily on describing how the air-breathing PEFC performance is improved through optimising some key parameters: the design and the material of the current collector; the design and the material of the cathode gas diffusion layer; the catalyst layer and cell orientation. In addition, it reviews the impact of the ambient conditions on the fuel cell performance and describes

the methods adopted to mitigate the effects of extreme conditions of ambient temperature and humidity. Hydrogen storage and delivery technologies used in air-breathing fuel cells are then summarised and their design aspects are discussed critically. Finally, the few reported air-breathing fuel cell stacks and systems are reviewed, highlighting the challenges to the widespread commercialisation of air-breathing fuel cell technology.

Keywords: Air-breathing PEFCs; Portable applications; Open Cathode; Fuel cell performance; Ambient conditions

2.2 Introduction

Hydrogen fuel cells have been a central element in what is known as the "hydrogen economy", where hydrogen is produced from zero/low carbon technologies (e.g., water electrolysers powered by wind turbines), and where the overarching aim is to mitigate the detrimental consequences of global warming [25-27]. Due to their low operating temperature, high efficiency, and fast starting speed, polymer electrolyte fuel cells (PEFCs) are the fuel cell of choice for a magnitude of automotive, stationary, and portable applications [28-30]. Fuel cells designed to power portable applications are classified as battery replacement where the output power is typically under 100 W and portable power generators where the output power is normally up to 1 kW [17, 31]. The scope of this review paper is mainly centred on the first classification, i.e., the battery-replacement PEFCs. As it is evident from this classification, the aim here is not to reduce CO_2 emissions but to replace batteries, which normally contain toxic heavy metals whose disposal poses an environmental challenge [32].

The portable fuel cell has the main advantage that the time taken between charges is significantly longer than batteries, potentially several days versus hours for batteries [15].

However, typical consumer devices require to be reasonably handled by consumers and thus the size and weight of the fuel cell powering these devices need to be significantly reduced to seriously compete with ever-improving batteries [33]. The cost of these fuel cells also needs to be significantly reduced to increase their competitiveness in the consumer device markets [34].

Conventional PEFCs require devices to store oxidant and fuel and pumping devices to supply the oxidant and fuel to the reaction sites in the fuel cell. Further, these reactant gasses normally need to pass through humidifiers to initially humidify the membrane electrolyte and make it functional. Evidently, these conventional PEFCs with all the above ancillary components are not an attractive option for small portable applications where size, weight, and cost play a vital role when selecting the powering devices. Therefore, most of these ancillary components should be removed in order for PEFCs to become competitive with the batteries used in small consumer devices. As the output power required to power the consumer devices is relatively small, it turns out that, in fact, most of the above-mentioned ancillary components could be removed without compromising the main functions of the fuel cell. Namely, the cathode compartment is made open so that oxygen is directly extracted from the ambient air through the process of natural convection, removing the requirement for an oxidant storage device, a pumping device to apply it to the fuel cell, as well as the valves and the flow controllers. Likewise, the water vapour that is required to initially humidify the membrane electrolyte at the start-up of the fuel cells is directly extracted from the ambient air, avoiding the need for a humidifier at the anode side of the fuel cell. All the above arrangements greatly simplify the PEFC system powering small consumer devices and make them much more technically and economically competitive with

batteries. This simplified type of fuel cell is normally termed an air-breathing PEFC and this is due to the passive way to supply oxygen to the cathode of the fuel cell.

While there is no direct comparison between air-breathing PEFC-based and battery-based portable power systems, Belmonte et al. [35] conducted a cost analysis and life cycle assessment for both stationary and mobile applications. They compared the total cost of battery and fuel cell systems to identify the more competitive solutions. Their findings revealed that the cost of fuel cells is approximately twice that of a battery system of the same size and for the same applications. Also, they reported that battery-based systems exhibit a simpler design compared to their fuel cell-based counterparts, necessitating fewer auxiliary components. Further, systems employing battery storage can benefit from a wide commercial diffusion of Li-ion batteries, making their prices more attractive.

Currently, there are only two examples where air-breathing PEFCs experience market penetration. High-tech military-related portable electronics, such as night vision devices, personal cooling systems, radios, and computers, are normally used for various purposes in hostile environments, where recharging the devices is a challenge. Hence, a fast-growing deployment of air-breathing PEFCs into portable military electronic devices has been observed, and this is primarily due to long times between recharges and the light weight of the air-breathing fuel cell [36]. Furthermore, air-breathing PEFCs have been used as implantable power sources (e.g., biosensors and pacemakers) or in the operation of robots used in biomedical applications [37, 38]. Their potential use however is wider than these specialised applications, and Table 2.1 lists more small electronic devices and their corresponding power requirements where air-breathing PEFCs could be potentially used. It

is worth mentioning that air-breathing PEFCs are also used as portable power generators, such as replacement of gasoline or diesel engines [3].

It is crucial to reduce the volume of air-breathing PEFCs in order to facilitate their commercialization. This is consistent with the overarching goal of improving the portability and integration of these energy sources. The power density target outlined by the DOE is 55 W/L for portable fuel cell systems [5]. For example, considering a smartphone with a potential power requirement of 2 W, adhering to the power density criteria reported by the DOE requires the volume of the fuel cell to be no more than 37 mL.

Table 2.1 Power requirements for portable small electronic devices [15, 17, 39].

Electronic Devices	**Power Requirements**
Cellular phone	1 W
Smartphone	2 W
IPhone	2 W
Video camera	1-10 W
Laptop	20-40 W
Tablet personal computer	10 W
Robot	10-15 W
Toy car	5-15 W
Toy airplane	110 W/kg
PlayStation portable	2 W
Flashlights	1-10 W
Insulin pump	10 mW

Notably, numerous review papers on the conventional PEFCs have been published, for example, [40-45]; however, to the best of the authors' knowledge, there have been no comprehensive review papers on air-breathing PEFC. Kurnia et al. [46] recently reviewed the open cathode PEFCs, including forced-convection and air-breathing PEFCs. However, they did not cover some important aspects of air-breathing PEFCs including some components (e.g., gas diffusion layers, catalyst layers, and hydrogen cartridge) and system designs, which

have been thoroughly covered and discussed in this review paper. Namely, this review provides up-to-date research trends and reports on various aspects of air-breathing PEFCs that involve their mathematical models, components, stacks, systems, and applications; thus ultimately providing much better insights on how to improve their efficieny and cost-effectiveness. Also, the review discusses the challenges that face the air-breathing PEFC technology and the potential future work that could be unertaken to boost the penetration of this clean technology into the marketplace. The layout of this review paper is as follows: it first provides a general description of the main components and the working principles of the air-breathing PEFC in Section 2.3. It then lists and describes the equations that are normally used to create air-breathing PEFC mathematical models in Section 2.4. Section 2.5 looks into various ways that have been adopted in the literature to optimise the designs and the materials to maximise the performance of the air-breathing PEFC. The impact of ambient conditions in terms of temperature and humidity is reviewed in Section 2.6. Hydrogen delivery, air-breathing PEFC stacks, and systems are reviewed in Sections 2.7, 2.8, and 2.9, respectively. Section 2.10 discusses the present state of air-breathing PEFC and provides recommendations for future work. Finally, the main points of the review are summarised in the last section.

2.3 Overview of Air-breathing PEFC

An air-breathing PEFC is a portable electrochemical device in which oxygen is taken directly from the ambient air by natural convection and reduced at the cathode and hydrogen is supplied as fuel from a storage device to the anode where it is oxidised. The key components for this type of fuel cell are shown in Figure 2.1; an open cathode current collector, an anode current collector, two gas diffusion layers (GDLs), two catalyst layers, and a polymeric

electrolyte. The hydrogen supplied to the air-breathing PEFC is not normally humidified [47-51]; water, which is directly extracted from the ambient air at the open cathode, should be ideally sufficient for the initial humidification of the membrane. The main functions and the commonly used materials of the fuel cell components are given in Table 2.2.

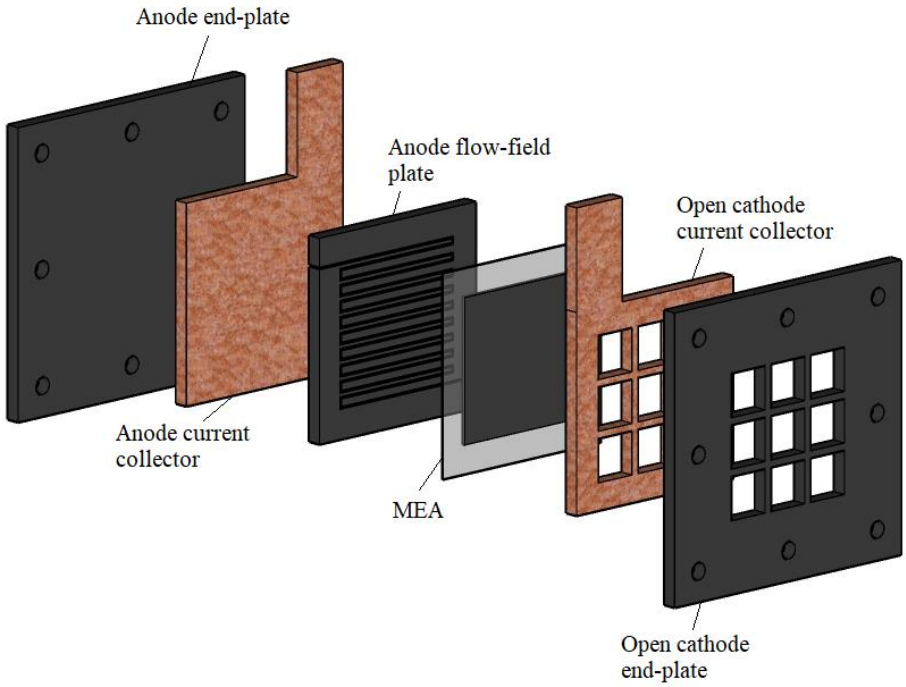

Figure 2.1 Exploded view of an air-breathing PEFC showing its key components.

The polymeric electrolyte membrane, the catalyst layers, and the GDLs are assembled to form what is known as the membrane electrode assembly (MEA). The polymeric electrolyte membrane is ionically conductive, allowing protons (produced at the anode) to be transported to the cathode through the membrane. The catalyst layers are where the half-electrochemical reactions take place, and as such, they need to have voids, an electrically conductive solid phase, and a membrane electrolyte phase to allow for reacting gases, electrons, and protons to transport and/or meet. The GDL is a porous structure whose main function is to distribute the reacting gases as uniformly as possible to the catalyst layers. Also, the position of the GDLs within the fuel cell requires them to be good electrical

conductors, liquid water removers and heat dissipators. The GDLs are typically coated with microporous layers to enhance electrical contact with the catalyst layer and improve water management [52, 53].

Table 2.2 Air-breathing PEFC components: functions and materials [3, 45].

Component	Main Functions	Materials
Open cathode current collector/ flow field plate	• Supply of oxygen and water vapour from/to the ambient to/from the fuel cell by natural convection • Conduction of electrical charge	A variety of metallic (e.g., stainless steel) and non-metallic materials (e.g., silicon wafers and printed circuit boards (PCBs) coated with metals)
Anode current collector/flow field plate	• Supply of hydrogen to the fuel cell • Conduction of electrical charge	Graphite, carbon composite or metallic sheets
GDLs	• Uniform supply of reactant gases to the catalyst layers • Removal of excess liquid water • Conduction of electrical charge • Mechanical support to the catalyst layer • Dissipation of heat	Carbon fibre-based paper or cloth coated with a microporous layer (a mixture of PTFE and carbon black)
Catalyst layers	• Facilitating electrochemical reactions	Platinum nanoparticles supported on carbon black particles
Polymer electrolyte	• Conduction of protonic (or ionic) charge	Perfluorosulfonic acid

The cathode in the air-breathing PEFCs is open to the ambient air to allow for the oxidant (oxygen) to be directly extracted from the ambient air through natural convection and be transported to the active areas in the cathode catalyst layer. On the other hand, hydrogen molecules are oxidised at the anode catalyst layer and split into protons and electrons. Oxygen molecules at the cathode react with protons, migrating from the anode catalyst layer through the membrane electrolyte, and electrons (forced, due to the electrically insulating nature of the membrane electrolyte, to migrate to the cathode) and form water

molecules. The following are the electrochemical half-reactions and the overall reaction for the PEFCs:

Hydrogen Oxidation Reaction (Anode): $\mathrm{H_2 \rightarrow 2H^+ + 2e^-}$ (2.1)

Oxygen Reduction Reaction (Cathode): $\mathrm{\frac{1}{2}O_2 + 2H^+ + 2e^- \rightarrow H_2O}$ (2.2)

Overall reaction: $\mathrm{H_2 + \frac{1}{2}O_2 \rightarrow H_2O}$ (2.3)

Water and most of the heat produced at the cathode catalyst layer should be adequately managed to obtain and sustain high performance. Excess water (normally in the form of liquid) results in water flooding at the cathode, thus hindering the transport of oxygen to the reactive sites in the catalyst layer. On the other hand, insufficient water leads to membrane dehydration, thus decreasing the membrane ionic conductivity and increasing the ohmic losses of the fuel cell. Likewise, thermal management is as important as water management. Excess heat may result in membrane dehydration, and a lack of heat may lead to water flooding. To this end, the amount of water and heat within the MEA of the fuel cell, particularly for air-breathing PEFCs where water and heat are passively transported, should be carefully balanced [54].

Further, in air-breathing PEFCs, the flow of air within the proximity of the open cathode of the air-breathing PEFC is driven by buoyancy effects (i.e., natural convection). Namely, the air adjacent to the surface of the heat-generating open cathode becomes relatively warm, light and in turn rises, replacing the upper and colder portion of air that flows downward adjacent to the warm open cathode. Again, this portion of air becomes relatively warm, light

and in turn rises and so on [55]. Such dynamics and the fact that oxygen is consumed and water is produced at the cathode catalyst layer create gradients in temperature, oxygen and water vapour concentration which govern the heat and mass transport between the open cathode of the air-breathing fuel cell and the ambient air. As mentioned previously, the balance of water and heat within the air-breathing PEFC is crucial to avoid undesirable phenomena that degrade the fuel cell performance, such as water flooding or membrane dehydration. One of the efficient and cost-effective ways to better understand transport phenomena within air-breathing PEFCs is mathematical modelling discussed in the following section, leading to more effective designs that improve the fuel cell performance and potentially mitigate undesirable phenomena.

2.4 Mathematical Modelling

Several modelling tools have been used in the field of fuel cells to: study the effects of some geometrical and operational parameters; understand the transport phenomena within the several components of the fuel cell; and explore the transient response of the fuel cells. In the literature, the number of models for the air-breathing PEFCs is substantially less than for the conventional PEFCs. This is evidently attributable to the significant use of the latter type of fuel cells in a wide range of applications. Typically, the use of air-breathing PEFCs is restricted to portable appliances where the small output power is required.

The models existing in the literature for air-breathing PEFCs are either: numerical, analytical or dynamic; dimensionless, one-dimensional, two-dimensional or three-dimensional; and resembling channel-based or window-based fuel cells.

Table 2.3 lists various mathematical models that have been developed for air-breathing PEFCs, mentioning (among other items) their dimensionality and key findings. More details

on these models are in Section 2.5 and Section 2.6 where the experimental and modelling work on the optimisation of the air-breathing PEFCs and the impact of the ambient conditions on their performance are described.

For completeness, the following are brief descriptions of the mathematical equations (mainly adapted from [56, 57]) that are often used to capture transport phenomena within the PEFCs, namely the equations for conservation of mass, momentum, species, charge, and energy.

The conservation of mass equation is expressed as follows:

$$\nabla.\left(\rho\vec{V}\right) = S_c \tag{2.4}$$

where ρ is the density of the fluid, $\vec{V}$ is the superficial velocity vector, and S_c is the mass source term. Note that the mathematical expressions for the all the source terms for various regions within the fuel cell are listed in Table 2.4. The conservation of momentum equation is given by:

$$\nabla.\left(\rho\vec{V}\vec{V}\right) = -\nabla P + \nabla.\vec{\tau} + \rho\vec{g} + S_V \tag{2.5}$$

Table 2.3 Literature survey on modelling of air-breathing PEFCs.

Authors	Analytical/ Numerical	Model Characteristics	Cathode Type	Software	Focus of Research	Model Validation	Main Findings
Hamel and Frechette [58]	Analytical	1D, isothermal, single phase	Window	N/A	Water transport in the membrane	Validated by experimental data	Anode suffers from dehydration
O'Hayre et al. [59]	Analytical	1D, non-isothermal, single phase	Window	N/A	Heat and mass transfer at the cathode side	Validated by experimental data reported in [60]	Air-breathing PEFC requires maximum heat rejection and minimum water flooding.
Schmitz et al. [61]	Numerical	2D, isothermal, single phase	Window	COMSOL Multiphysics®	Impact of opening ratio	Validated by experimental data	The larger the opening ratio, the better the cell performance.
Hwang [62]	Numerical	3D, isothermal, single phase	Window	COMSOL Multiphysics®	Impact of size and arrangement of opening ratio	Validated by experimental data	There exists an optimum size for the opening ratio, about 30%.
Tabe et al. [63]	Numerical	3D, non-isothermal, single phase	Channel	ANSYS Fluent®	Oxygen profile in flow channels	Validated by experimental data	The depletion rate of oxygen increased with decreasing channel depth
Matamoros and Bruggemann [64]	Numerical	3D, non-isothermal, multi-phase	Channel	In-house code	Concentration losses in the flow channels	N/A	Shorter stacks are needed to maximize the utilisation of the active area; low platinum is sufficient for this type of fuel cell.

Litster et al. [65]	Numerical	2D, non-isothermal, single phase	Window	ANSYS CFX	The feasibility of the use of nano-porous GDL	N/A	The nano-porous GDL could be used in air-breathing PEFCs.
Zhang and Pitchumani [57]	Numerical	2D, non-isothermal, single phase	Window	ANSYS Fluent®	Impact of cell orientation and stack height	Validated by experimental data	The cell performs better with a vertical orientation and worse with a horizontal facing upward orientation; the cell becomes less sensitive to orientation as it becomes smaller.
Zhang et al. [56]	Numerical	3D, non-isothermal, single phase	Window	ANSYS Fluent®	Impact of geometrical parameter of a stack	Validated by experimental data	There must be a minimum spacing between the adjacent cartridges and a minimum gap between the cell and the substrate.
Rajani and Kolar [66]	Numerical	2D, non-isothermal, single phase	Window	ANSYS Fluent®	Natural convection boundary layers	Validated by experimental data reported in [67]	A shorter stack gives better performance; the longer stack has thicker boundary layers and therefore experiences larger mass and thermal resistance.
Ying et al. [68]	Numerical	3D, non-isothermal, single phase	Channel	STAR-CD®	Local distribution	Validated by experimental data	The local distributions showed.
Ying et al. [69]	Numerical	3D, non-isothermal, single phase	Channel	STAR-CD®	Impact of channel width	Validated by experimental data	The channel width must be optimised.
Ying et al. [70]	Numerical	2D, non-isothermal, multi-phase	Channel	Not Mentioned	Impact of channel and rib widths	N/A	Optimum values for these two parameters exist.
Wang and Ouyang [71]	Numerical	3D, non-isothermal, single phase	Channel	STAR-CD®	Local distribution	Validated by experimental data	The membrane resistance decreases with increasing back diffusion.

Ismail et al. [55]	Numerical	2D, non-isothermal, single phase	Window	ANSYS Fluent®	Thermal situation above the open cathode surface	Validated by experimental data reported in [60]	Joule heating has a significant effect on thermal parameters.
Ismail et al. [72]	Numerical	0D, non-isothermal, single phase	Window	MATLAB	Impact of Joule heating and entropic heat sources	Validated by experimental data reported in [60]	The neglect of Joule and entropic heats results in over-prediction of the fuel cell performance.
Chen et al. [73]	Numerical	0D, non-isothermal, single phase	Window	MATLAB	Impact of hydrogen relative humidity	Validated by experimental data reported in [60]	Increased hydrogen humidity enhances the fuel cell performance.
Yalcinoz and Alam [74]	Numerical	0D, dynamic, non-isothermal, single phase	Window	MATLAB/ Simulink	Proposing a dynamic model for an air-breathing PEFC	Validated by experimental data reported in [60]	The proposed air-breathing PEFC-based system provides sufficient power supply for a laptop.
Calili et al. [22]	Numerical	0D, dynamic, non-isothermal, single phase	Window	MATLAB/ Simulink	Impact of ambient conditions and GDL parameters	Validated by experimental data reported in [60]	Both transient response and steady-state performance of the fuel cell are sensitive to ambient conditions and GDL parameters.
Calili-Cankir et al. [23]	Numerical	0D, non-isothermal, single phase	Window	MATLAB	Impact of convection type on the fuel cell performance	Validated by experimental data reported in [60]	The performance of conventional PEFC surpasses that of air-breathing fuel cell due to its superior heat and mass transfer coefficients.
Calili-Cankir et al. [24]	Numerical	0D, dynamic, non-isothermal, single phase	Window	MATLAB/ Simulink	Impact of convection type on the dynamic response	Validated by experimental data reported in [60]	The air-breathing PEFC has a substantially slower dynamic response than conventional fuel cells.
Al-Anazi et al. [75]	Numerical	3D, non-isothermal, multi-phase	Channel	ANSYS Fluent®	Impact of ambient conditions in Saudi Arabia	Validated by experimental data	The fuel cell performance is lower in the winter than in summer by around 12%.

where P is the pressure, $\vec{g}$ is the gravity vector, $\vec{\tau}$ is the stress tensor and S_V is the momentum source term. The conservation of the chemical species equation could be expressed as follows:

$$\nabla.\left(\rho\vec{V}Y_i\right) = \nabla.\left(\rho D_i^{eff}\nabla Y_i\right) + S_i \tag{2.6}$$

where Y_i is the mass fraction of species i and S_i is the source term for species i. The effective diffusion coefficient of the species i, D_i^{eff}, is often calculated using Bruggmann's correlation [76]:

$$D_i^{eff} = \varepsilon^{1.5}.D_i \tag{2.7}$$

where ε is the porosity of the porous medium and D_i is the bulk diffusivity of the species i, given by:

$$D_i = D_i^{ref}\left(\frac{T}{T_{ref}}\right)^{1.5}\left(\frac{P_{ref}}{P}\right) \tag{2.8}$$

where D_i^{ref} is the bulk diffusivity of the species i at the reference temperature (T_{ref}) and pressure (P_{ref}). The conservation of charge equation for the solid (s) or the membrane (m) phases is expressed as follows:

$$\nabla.\left(\sigma_j^{eff}\nabla\varphi_j\right) + S_j = 0; \qquad j = s, m \tag{2.9}$$

where σ_j^{eff}, φ_j, and S_j are respectively the effective electrical conductivity, the potential and the charge source term of either the solid or the membrane phase. σ_s^{eff} is given as follows:

$$\sigma_s^{eff} = (1 - \varepsilon_{eff})\sigma_s \tag{2.10}$$

where σ_s is the electrical conductivity of the solid phase. On the other hand, σ_m^{eff} is given as follows:

$$\sigma_m^{eff} = \varepsilon_m^{1.5}\sigma_m \tag{2.11}$$

where ε_m is the volume fraction of the membrane phase which is equal to unity in the membrane electrolyte. The ionic conductivity of the membrane, σ_m, can be estimated using the well-known Springer's model [77]:

$$\sigma_m = [0.514\lambda - 0.326] \exp\left[1268\left(\frac{1}{303} - \frac{1}{T}\right)\right] \tag{2.12}$$

where λ is the water content of the membrane and is calculated using the following expression:

$$\lambda = \begin{cases} 0.043 + 17.81a - 39.85a^2 + 36a^3, & 0 < a \leq 1 \\ 14 + 1.4(a-1), & 1 < a \leq 3 \end{cases} \tag{2.13}$$

where a is the water activity and is given by:

$$a = \frac{P_{H_2O}}{P_{sat}} \tag{2.14}$$

where P_{H_2O} is the partial pressure of water vapour and P_{sat} is the saturation pressure of water vapour which can be obtained (in atm units) by the following empirical formula [77]:

$$\begin{aligned} log_{10}P_{sat} = {} & -2.1794 + 0.02953(T - 273.15) - 9.1837 \\ & \times 10^{-5}(T - 273.15)^2 + 1.4454 \\ & \times 10^{-7}(T - 273.15)^3 \end{aligned} \tag{2.15}$$

However, Ismail et al. [72] and Litster and Djilali [78] reported that at low humidity operating conditions, the Springer model results in unrealistic predictions for the case of air-breathing PEFCs. Thus, an alternative empirical correlation formula is recommended to be used to estimate the ionic conductivity of the membrane under low-humidity conditions [59, 72, 74, 79]:

$$\sigma_m = (3.46a^3 + 0.0161a^2 + 1.45a - 0.175) \exp\left[1268\left(\frac{1}{303} - \frac{1}{T}\right)\right] \tag{2.16}$$

Table 2.4 Source terms in the conservation equations for different regions of the air-breathing PEFC (all the symbols are defined in the nomenclature). Adapted from [31, 56, 57].

Source Term	GDLs	Anode Catalyst Layer	Cathode Catalyst Layer	Membrane
S_C	0	$-\frac{I_a}{2F}M_{H_2}$	$-\frac{I_c}{4F}M_{O_2}+\left(\frac{I_c}{2F}+nd\frac{I_c}{F}\right)M_{H_2O}$	0
S_V	$-\frac{\mu}{k}\varepsilon_{eff}\vec{V}$	$-\frac{\mu}{k_p}\varepsilon_{eff}\vec{V}+\frac{k_\varphi}{k_p}z_f c_f F\nabla\varphi_m$	$-\frac{\mu}{k_p}\varepsilon_{eff}\vec{V}+\frac{k_\varphi}{k_p}z_f c_f F\nabla\varphi_m$	$-\frac{\mu}{k_p}\varepsilon_{eff}\vec{V}+\frac{k_\varphi}{k_p}z_f c_f F\nabla\varphi_m$
S_T	$\frac{i_s^2}{\sigma_s^{eff}}$	$\frac{i_s^2}{\sigma_s^{eff}}+\frac{i_m^2}{\sigma_m^{eff}}+I_a\eta_a$	$\frac{i_s^2}{\sigma_s^{eff}}+\frac{i_m^2}{\sigma_m^{eff}}+I_c\left(-\eta_c-\frac{T\Delta S}{2F}\right)$	$\frac{i_m^2}{\sigma_m^{eff}}$
S_i	0	$-\frac{I_a}{2F}M_{H_2}$ (H_2) 0 (O_2)	0 (H_2) $-\frac{I_c}{4F}M_{O_2}$ (O_2) $\left(\frac{I_c}{2F}+nd\frac{I_c}{F}\right)M_{H_2O}$ (H_2O)	0
S_s	0	$-I_a$	I_c	0
S_m	0	I_a	$-I_c$	0

The conservation of energy equation can be expressed as follows:

$$\nabla.\left(\rho C_p \vec{V} T\right) = \nabla.\left(k_{eff} \nabla T\right) + S_T \qquad (2.17)$$

where C_p is the specific heat of the fluid at constant pressure, k_{eff} is the effective thermal conductivity of the medium and S_T is the energy source term.

The boundary conditions typically used to solve the above conservation equations are listed in Table 2.5 and Figure 2.2 shows the interfaces at which these boundary conditions are prescribed.

Table 2.5 Boundary conditions for the layers shown in Figure 2.2. Adapted from [31, 56, 57].

Interface	**Boundary condition**
Ambient | Cathode GDL	$\varphi_s = V_{cell}$ $-k_{eff}\frac{\partial T}{\partial x} = h(T_\infty - T_s)$ $-D_{O_2}^{eff}\frac{\partial Y_{O_2}}{\partial x} = h_{m,O_2}(Y_{\infty,O_2} - Y_{s,O_2})$ $-D_{H_2O}^{eff}\frac{\partial Y_{H_2O}}{\partial x} = h_{m,H_2O}(Y_{\infty,H_2O} - Y_{s,H_2O})$
Cathode GDL | Cathode Catalyst Layer	$\frac{\partial \varphi_m}{\partial x} = 0$
Cathode Catalyst Layer | Membrane	$\frac{\partial Y_{O_2}}{\partial x} = 0; \frac{\partial Y_{H_2O}}{\partial x} = 0;\ \frac{\partial \varphi_s}{\partial x} = 0$
Membrane | Aanode Catalyst Layer	$\frac{\partial Y_{H_2}}{\partial x} = 0;\ \frac{\partial \varphi_s}{\partial x} = 0$
Anode Catalyst Layer | Anode GDL	$\frac{\partial \varphi_m}{\partial x} = 0$
Anode GDL | H_2 Chamber	$T_a = const.;\ Y_{H_2} = const.; Y_{H_2O} = const.;\ \varphi_s = 0$

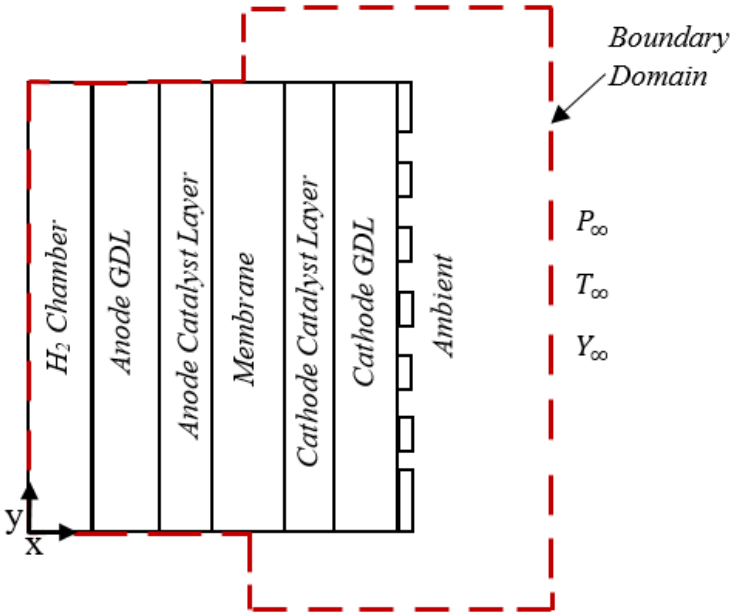

Figure 2.2 A cross-section schematic of an air-breathing PEFC showing the boundary domain.

2.5 Optimisation of Air-breathing PEFC

As mentioned in Section 2.3, water and heat within the air-breathing PEFC should be carefully balanced to avoid undesirable phenomena of either water flooding or membrane dehydration that badly affect the fuel cell performance. Therefore, the designs and/or materials of the various components of the fuel cell should be optimised to ensure this water and thermal balance and ultimately sustain the fuel cell performance. Further, the design and the materials are often optimised to reduce the size, weight, complexity or cost of the air-breathing fuel cell used for portable applications. Surveying the literature, the following elements are normally optimised to maximise the performance of the air-breathing PEFC or minimise cost, size, and weight: the design and the material of the cathode current collector; the thickness and the material of the GDL; the catalyst loading and thickness; and the fuel cell orientation. The following subsections review the attempts that have been made under each of the above-mentioned elements.

2.5.1 Design of Cathode Current Collector

The design of the open cathode current collector (also known as the cathode flow distributor) directly influences the performance of air-breathing PEFCs, and this is due to its substantial impact on the mass and heat exchange between the ambient air and the fuel cell. The open cathode current collectors are mainly classified as follows: window-based (ribbed or open-slit) and channel-based (ducted) current collectors; see Figure 2.3. The main difference between them is the airflow direction. As shown in Figure 2.3a, the flow direction of the ambient air is primarily from the bottom to the top of the channel in the ducted flow fields; therefore, oxygen reacts more in the bottom part of the channel and its concentration becomes more diluted as it flows towards the upper outlet of the channel. In the horizontal orientation, ambient air is drawn in from both sides of the channels. This positioning allows oxygen to react more at the inlets of the channels, and its concentration becomes more diluted in the central region of the fuel cell. Therefore, the channel-based open cathode leads to a high degree of non-uniformity in the current density distribution. On the other hand, the whole cathode surface of the window-based type cell is exposed to the air (Figure 2.3b). In other words, the concentration of oxygen is, compared to that of the ducted channel, more uniform over the cell active area. Likewise, the produced water primarily evaporates through the openings by diffusion. To this end, there has been a trend towards the use of window-based current collectors for air-breathing PEFC. The design criteria for each type of current collector are different; they are mainly the size and shape of the openings in the window-based current collectors and the dimensions of the channels in the channel-based current collectors. These design criteria need to be optimised since efficient mass transport to and from the cathode electrode and good contact between the collector and the MEA are typically in conflict with each other. To illustrate, in window-based current collectors, oxygen

transport to the cathode and water removal rate are enhanced if the size of the openings is increased; however, the contact between the current collector and the MEA becomes poorer with increasing size of the openings. It should be noted that the term 'opening ratio' is normally used to indicate how large the openings of the collector are relative to the active area of the fuel cell. The optimisation of the design of the cathode current collectors in air-breathing PEFCs has been a major theme for a number of investigations in the literature, as will be shown in the following paragraphs.

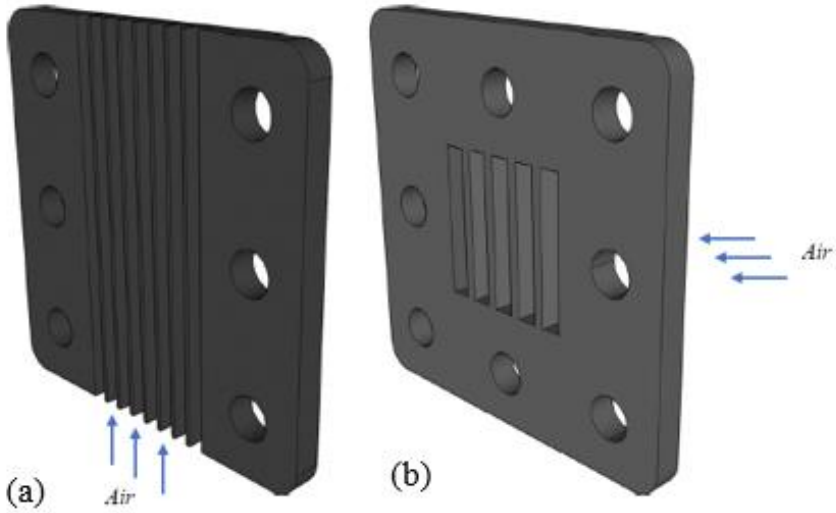

Figure 2.3 Channel-based and (b) window-based cathode current collectors. Reproduced from [55] with permission from Elsevier.

Ying et al. [69] developed a three-dimensional mathematical model for an air-breathing PEFC and showed that the distributions of the temperature, partial pressure of gas species, the flow rate of water and gas species, local current density, and over-potential are significantly influenced by the size of the cathode opening. They concluded that a larger opening size provides an improvement in the performance of the fuel cell; however, the level of this improvement decreases as the opening ratio increases beyond an optimum value.

Schmitz et al. [80] investigated the effect of cathode current collectors with rectangular openings on the performance of air-breathing PEFCs. They found that the cell performance

is more or less the same in the low current density regions; however, it significantly improves with increasing opening ratio in the high current density regions due to better mass transport of oxygen and liquid water. They experimentally showed that the amount of liquid water collected from the anode side becomes less with increasing opening ratio; this signifies that the water removal from the cathode is better for the current collectors with larger openings. Later, the same research group [61] developed a two-dimensional computational model that confirmed the above experimental results. In a relevant work [81], they demonstrated that increasing the opening ratio improves cell performance regardless of the hydrophobicity of the GDL.

The effects of cathode current collectors with an array of rectangular openings were experimentally investigated by Jeong et al. [82]. They showed that, in the low current density regions, the fuel cell performance degrades with increasing opening ratio; they suggested that this is because of the increased in-plane resistance. However, in the high current density regions, there exists an optimum opening ratio at which the peak power is a maximum, namely 77% (Figure 2.4). The charge transfer resistance shown by the electrochemical impedance spectroscopy measurements is a minimum for this geometry; this is most likely due to the improved activity of the catalyst layer.

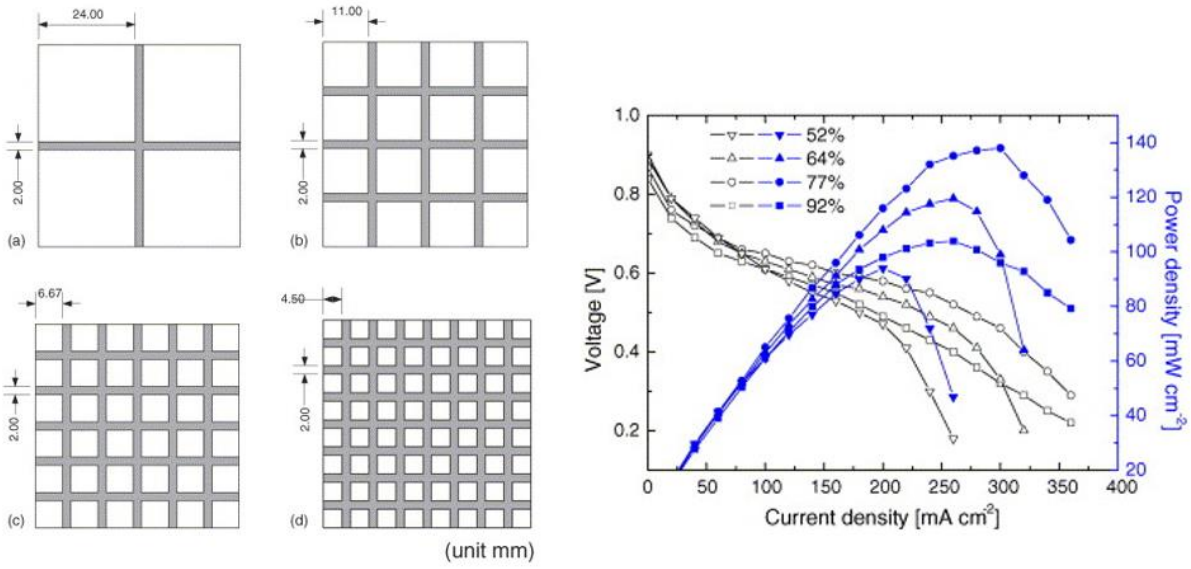

Figure 2.4 Open cathode designs with opening ratio of: (a) 92%; (b) 77%; (c) 64% and (d) 52%. The left graph shows the corresponding polarisation curves at 35 °C and relative humidity of 80%. Reproduced from Ref. [82] with permission from Elsevier.

Bussayajarn and co-workers [83] investigated the effects of the shape of the opening on the performance of the fuel cell. The openings investigated were parallel slits, oblique slits and circular. They found that, for a given opening ratio of 47%, the fuel cell performed better with the circular openings. The authors thought that the reason behind this was the shortest rib width and the smallest hydraulic diameter presented by the investigated circular openings. However, Kim et al. [84] found that each opening shape has its own optimum opening ratio. They experimentally showed that the optimum opening ratios for arrays of rectangular, triangular, and circular openings are about 70%, 50%, and 38%, respectively. A six-cell stack was subsequently made from cathode collectors with rectangular openings since their optimum opening ratio is sufficiently large to allow for more efficient water removal.

Hottinen et al. [67] showed that the negative effects of increased opening ratios can be significantly mitigated, especially in the low current density regions, if one employs a thick and stiff GDL. Current collectors with large openings show a slightly better performance in the high current density regions. However, the authors showed that there exists an optimum

opening ratio for the openings and that the performance is significantly better than that with thick GDLs if one employs conventional thin GDLs. They also [85] designed an air-breathing PEFC consisting of a Z-shape flow field anode current collector, a window-based cathode current collector, and rigid GDLs. This study aimed to minimise the size of the cell for portable applications. There were no separate end plates in the fuel cell since the current collectors act as end plates in both the anode and cathode sides, thus reducing the size of the fuel cell and its manufacturing costs.

Babcock et al. [86] deployed a stiff and porous mesh between the GDL and cathode current collector. They showed that the use of the mesh significantly decreases the ohmic losses of the fuel cell in such a way that one can use a current collector with an extremely high opening ratio, which will significantly improve the fuel cell performance due to improved oxygen and water transport.

Kumar and Kolar [87] built a three-dimensional, single-phase, and non-isothermal model under steady-state conditions to predict the performance change of an air-breathing fuel cell with channel widths of 2, 4, and 6 mm, depths of 2, 6, and 10 mm and heights of 15, 30, and 45 mm. They found that open channels with 4 mm width, 6 mm depth and 45 mm height maximise the fuel cell power density (240 $\mathrm{mW/cm^2}$). Kumar and Parthasarathy [88] carried out a similar but experimental study and found out that the best performance was obtained with the open channel of the largest cross-section (i.e. 6 mm× 6 mm) which is somewhat in line with the outcomes of their model [87].

Kumar and Kolar [89] investigated how the cathode collector type (channel- and window-based) influences the fuel cell performance using a three-dimensional, steady-state, non-isothermal, and single-phase model. They demonstrated that the transport rate of

generated heat and water is higher in the fuel cell with a window-based cathode current collector than in a fuel cell with a channel-based current collector, allowing for better fuel cell performance. On the other hand, Tabe et al. [63] found that the air-breathing PEFC with a channel-based cathode current collector performs better than that with a window-based cathode current collector. This is, according to the authors, due to the increased contact resistance presented by the latter current collector. However, it appears that the authors did not optimise the opening ratio of the window-based current collector; the opening ratio of the cathode current collector used was estimated to be no more than 65%. As shown earlier in [80, 82, 84], the fuel cell performance is very sensitive to the opening ratio of the current collector. For the fuel cell running with channel-based current collectors, the authors reported that the mass transport and, consequently, the cell performance are improved with increasing channel dimensions [63].

The efficient removal of heat is critical for ensuring the optimal performance and durability of air-breathing PEFCs. In addition to prevent material deterioration, heat management improves the overall performance and safety. However, a few studies have investigated the use of fin structures in the open cathode to enhance heat dissipation. Chun et al. [90] manufactured two prototype top layers for a window-based air-breathing PEFC: thin-fin and duct top layer arrangements as shown in Figure 2.5. They reported that a cathode collector with thin-fin structures offers better heat dissipation, thus preventing overheating of the air-breathing PEFC. In a later work [91], they tested the air-breathing fuel cell using two different fin structures, illustrated in Figure 2.6, at four different temperatures controlled by an external heater (room temperature, 30, 40 and 50 °C). They showed that the proposed fin designs do not substantially enhance the performance of the fuel cell at room temperature,

30 and 40 ℃; however, at 50 ℃, the convective heat transfer rate increases with the presence of fins, thus improving heat dissipation and subsequently the fuel cell performance. The fuel cell performance was found to be better at 50 ℃ with the left design than with the right design shown in Figure 2.6.

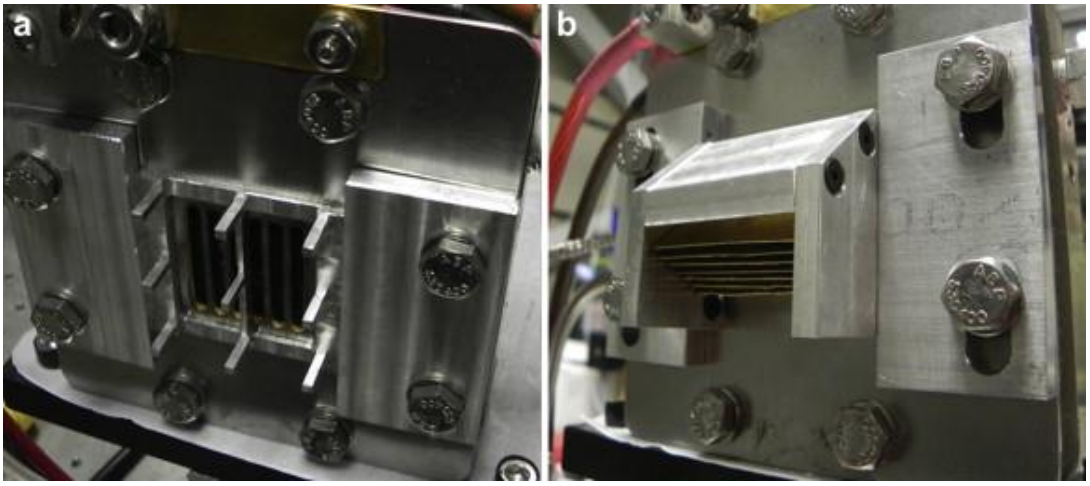

Figure 2.5 Fin structures: (a) thin-fin top-layer and (b) duct top-layer. Reprinted with permission from Elsevier [90].

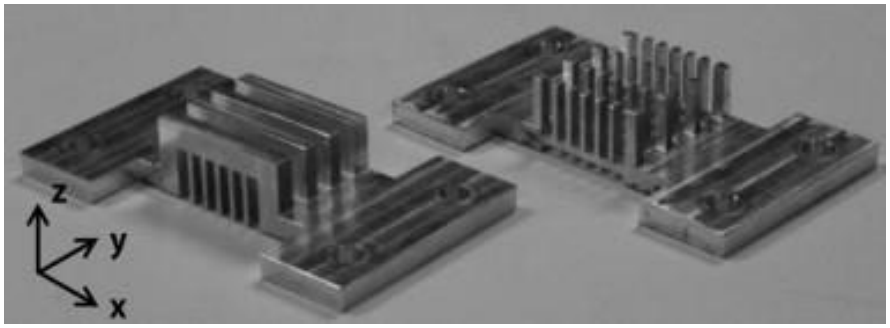

Figure 2.6 The two fin structures investigated in [91]. Reprinted with permission from Elsevier.

Karst et al. [92] developed a cover with openings for the open cathode, as shown in Figure 2.7, to investigate the effect of the opening ratio on water management. They found that the amount of water rejected from anode side increases by more than 30% at 150 $\mathrm{mA/cm^2}$ when the fuel cell is equipped with a cover with 5% opening ratio.

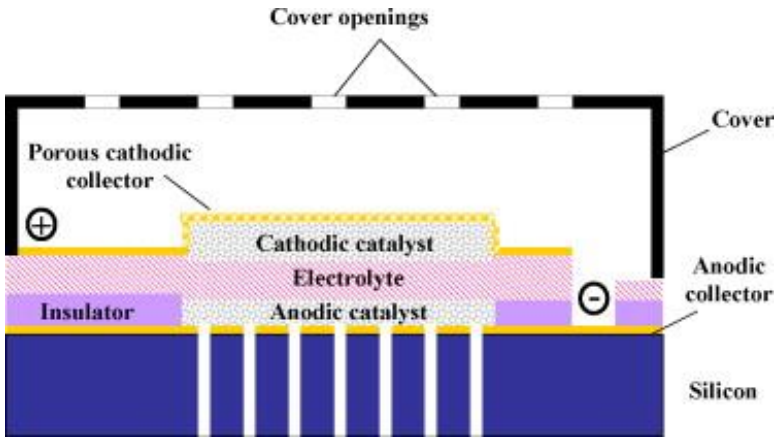

Figure 2.7 A schematic of the cross-section of the air-breathing PEFC equipped with the perforated cover. Reprinted with permission from Elsevier [92].

Suseendiran et al. [93] proposed a cathode current collector consisting of two hollow semi-cylindrical parts for an air-breathing PEFC. Figure 2.8 shows exploded and assembled views of the proposed cylindrical air-breathing PEFC. They reported that the fuel cell has better performance with a rib width of 2.5 mm and a slot size of 1 mm, and the peak output power is 2 W at 800 $\mathrm{mA/cm^2}$.

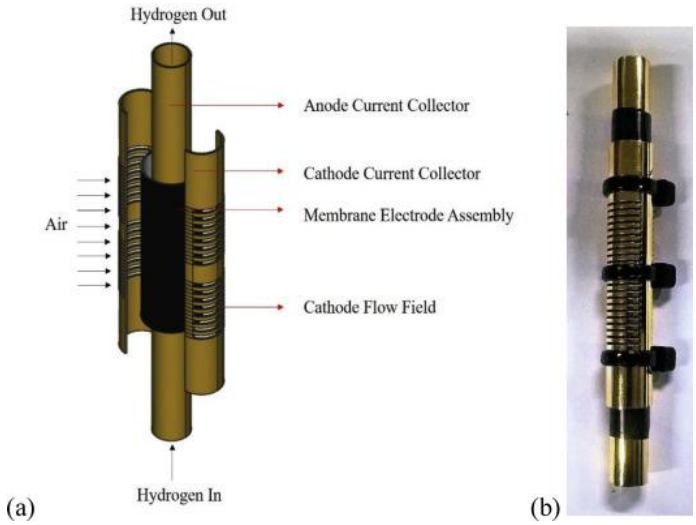

Figure 2.8 A cylindrical PEFC: (a) an exploded view of the fuel cell and (b) a picture of assembled fuel cell. Reprinted with permission from Elsevier [93].

To conclude, the opening ratio for each window-based design must be optimised to achieve the required balance between good mass transport for oxygen and liquid water, and good contact between the current collector and the MEA. Thick GDLs or a stiff contact layer may

be employed to enhance the electrical contact in the cathode compartment; however, care must be taken not to sacrifice the mass transport through creating undesirable long diffusion paths.

2.5.2 Materials for Cathode Current Collectors

The type of material employed in current collectors directly affects the performance of the fuel cell since the properties of each material, such as the electrical conductivity and the corrosion resistance, differ [85]. A variety of metallic (e.g., stainless steel) and non-metallic materials (e.g., silicon wafers and printed circuit boards (PCBs) coated with metals) can be used as current collectors for air-breathing PEFCs [94].

Graphite is attractive to be used for air-breathing PEFC current collectors, and this is due to its high corrosion resistance; however, it is rather brittle, and as, such the current collectors made from graphite are relatively thick (of the order of 5 mm), resulting in "bulky" fuel cells [95]. On the other hand, current collectors made of metals are mechanically stronger than graphite, and they could be made substantially thinner than graphite collectors. However, the most commonly used metals are mostly vulnerable to corrosion, and they, therefore, need to be covered with some corrosion-resistant coating. For example, Jeong et al. [82] coated a copper cathode current collector with gold. Similarly, gold-coated aluminium-metallic current collectors were used by Bussayajarn et al. [83].

Silicon wafers have also been used as a base material for the current collectors for air-breathing PEFCs [96-98]. Namely, a silicon wafer is transformed into a porous layer by electrochemical etching and is then partially filled with platinum to form electrically conductive paths [99].

Some researchers used thin PCBs as current collectors to minimise the size of the stack volume of the air-breathing PEFCs; PCBs feature some compelling characteristics such as cost efficiency, lightweight composite materials, and fast prototype cycle times. The multilayer PCB technology enables different circuit layers to overlap so that it improves some of its features, such as functionality and mechanical strength [100]. O'Hayre et al. [101] were the first to report that PCB technologies can be applied to improve power density, design flexibility, and ease of integration. Schmitz et al. [80] designed a planar air-breathing PEFC using a standard PCB consisting of a thin copper layer (for electrical conduction) and a rigid fibreglass epoxy (to act as a mechanical support). They showed that this fuel cell achieved a power density of 100 $\mathrm{mW/cm^2}$ at 0.5 V and long-term operation (more than 1500 h) without degradation. In another study by the same authors [79], an air-breathing PEFC was constructed using both anodic and cathodic plates made from PCB materials. Jaouen et al. [99] combined a PCB cathode current collector with a stainless steel net while a copper foil with an adhesive and conductive layer was used as an anode current collector. In doing so, good electrical conduction was obtained for both collectors. Kim et al. [84] coated a flexible PCB—a non-conductive polyimide film—with gold, which collects the current on both the anode and cathode sides. In doing so, they achieved a highly thin monopolar six-cell stack of 6 mm.

2.5.3 Gas Diffusion Layer

The GDL is a multifunctional layer that allows for the exchange of reactant gasses and water between the ambient and the catalyst layer, and it therefore has an influential role in terms of water and heat management in air-breathing PEFCs. A typical GDL is coated with a microporous layer (MPL) which is meant to adequately manage water within the MEA and

enhance the electrical contact between the GDL and the catalyst layer. Several studies have been conducted to investigate the effects of the cathode GDL (specifically its thickness and wetting properties) on the performance of air-breathing PEFCs.

Hottinen et al. [85] employed two thick rigid GDLs in their air-breathing PEFCs. One of the GDLs was characterised by high porosity (i.e., 78% vs 58%), whereas the other was of low electrical resistance. They showed that the cell performs better with the latter GDL achieving a peak power density of 115 $\mathrm{mW/cm^2}$ at 250 $\mathrm{mA/cm^2}$ in the intermediate current density region, and this is due to reduced cell resistance; however, because of the reduced mass transport losses, the fuel cell performs better with the high-porosity GDL in the high current density region. In a later work [67], they used three different types of GDLs: thick carbon sheet; carbon paper; and titanium sinter to investigate the impact of the cathode structure on the cell performance. They showed that carbon paper, which is thinner and more compressible than other tested GDLs, achieved a significant performance gain with relatively high opening ratios. Ferreira-Aparicio and Chaparro [102] compared the performance of woven and non-woven carbon paper GDLs in an air-breathing PEFC. They demonstrated that the fuel cell performed better with the woven carbon paper GDLs than with the highly tortuous non-woven carbon paper GDLs as the mass transport is highly limited with the latter GDLs, particularly at high current densities (Figure 2.9).

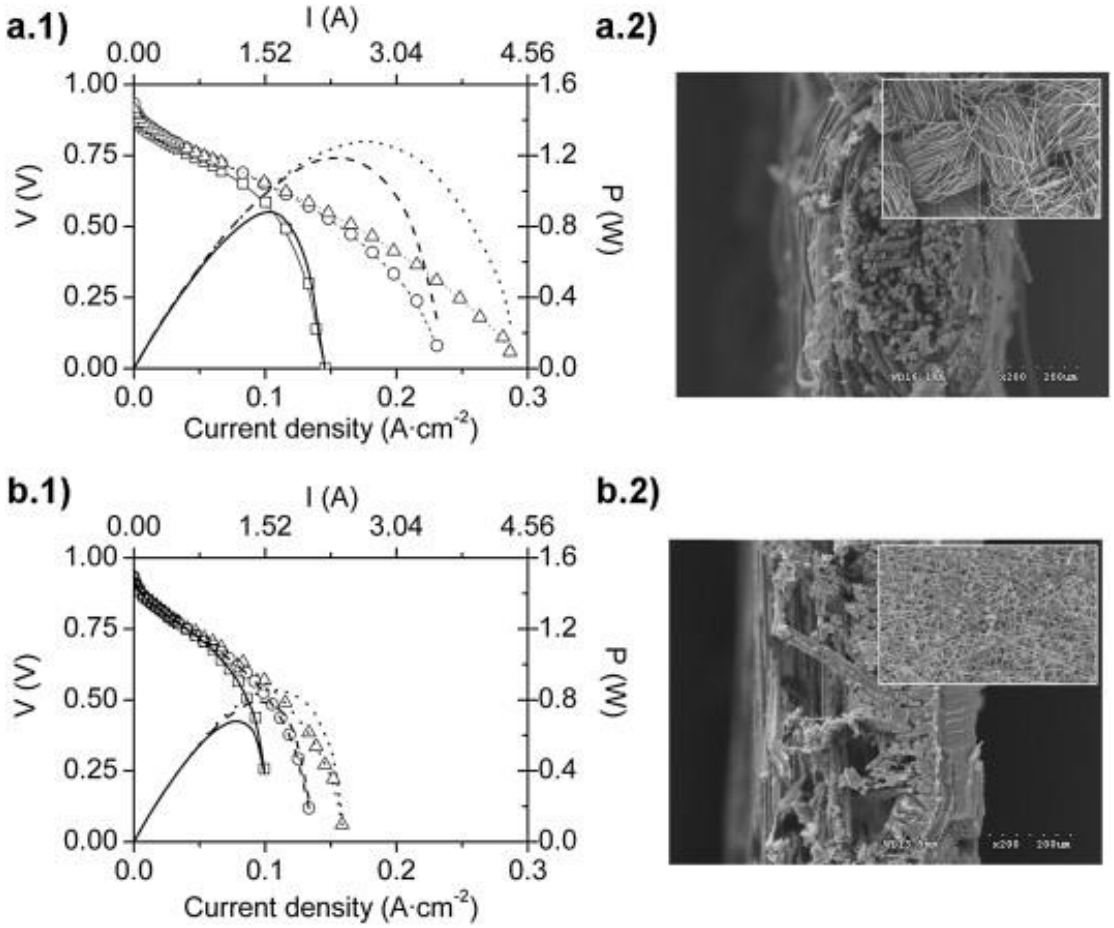

Figure 2.9 Polarisation curves of the air-breathing PEFC with: a) woven GDL; b) non-woven GDL and with fan-driven air with maximum power (··Δ··), 18% of fan's maximum power (--o--), and natural convection (–□–). Reprinted with permission from Elsevier [102].

The thickness of the GDL in an air-breathing PEFC (particularly in the cathode side) should be optimised as either too thin or too thick GDLs could lead to membrane dry-out, oxygen starvation or water flooding [55]. If the GDL is too thin, the rejection rate of water from the catalyst layer becomes extremely high, leading to membrane dry-out. On the other hand, if the GDL is too thick, depending on whether the fuel cell is low or high performing, the fuel cell may experience water flooding and/or oxygen starvation due to increased mass transport resistance for product water and oxygen, or membrane dry-out due to increased thermal resistance of the GDL.

Jeong et al. [103] demonstrated that the air-breathing PEFC performance was improved by increasing the thickness of the GDL from 100 to 280 μm; however, the performance of the

fuel cell degraded when using a 370 µm thick GDL. They explained these results stating that the relatively thin GDLs lead to membrane dry-out, which is due to the high evaporation rate of water while the relatively thick GDLs hinder oxygen transport from the ambient air.

Schmitz et al. [80] experimentally showed that the thickness of the cathode GDL must be optimised to improve the performance of the air-breathing PEFC. A very low limiting current was shown by the fuel cell operating with the relatively thick GDL, and this is most likely due to increased diffusion paths for oxygen extracted from the ambient air. Similarly, Tabe et al. [63] showed that, for both window and channel-based current collectors, the limiting current decreases with increasing GDL thickness. Further, they stated that, for window-based current collectors, the contact pressure becomes more uniform with increasing GDL thickness, which translates into reduced cell resistance. However, the effect of GDL thickness on the cell resistance was reported to be negligible in the case of channel-based current collectors, owing to their geometry, which allows for uniform contact pressure. Notably, in these two studies (i.e. [80] and [63]), the activation losses are minimal with thick GDLs. The reason is most likely that the good contact between the current collector and the GDL in these cases induces better electronic conduction, a higher reaction rate, more water produced to humidify the catalyst layer, and, therefore, more catalytic activity.

Using a dynamic model, Calili et al. [22] studied the impacts of GDL thickness and thermal conductivity on the dynamic response and steady-state performance of an air-breathing PEFC. They demonstrated that there is an optimal GDL thickness at which the load-following ability of the fuel cell is enhanced. In addition, they reported that both the dynamic responsiveness and the steady-state performance of the fuel cell could be improved with increasing GDL thermal conductivity. In later studies, they studied the influence of GDL porosity on the steady-state performance [23] and the dynamic response [24] of the air-

breathing PEFC. They found that both the dynamic and steady-state performances of the air-breathing PEFC increased with decreasing GDL porosity. This is because the rate of water vapour removal from the catalyst layer decreases with decreasing GDL porosity, enhancing the humidification of the membrane, and therefore decreasing ohmic losses, and improving the cell performance and dynamic response of the fuel cell. Litster et al. [65] developed a two-dimensional model for an air-breathing cathode electrode consisting of a nano-porous GDL. They showed that this new design for the GDL is able to passively supply reactants and regulate the fuel cell temperature by natural convection and Knudsen diffusion.

The wettability of the GDL is another important factor that affects the fuel cell performance [103]. Carbon paper GDLs are typically treated with polytetrafluoroethylene (PTFE) to assist in driving water away from the MEA and prevent water flooding at the cathode [33].

Xiang et al. [104] showed that the air permeability of the GDL (and evidently the hydrophobicity) increases when increasing the PTFE content beyond 10 wt. % (i.e., 15–25 wt. %), which, according to the authors, results in higher cell performance. They also investigated the impacts of the MPL thickness on the mass and charge transfer by testing the GDLs with MPLs ranging from 0 to 0.16 mm in thickness. Their results show that the optimal MPL thickness that maximises the fuel cell performance is 0.14 mm; this was explained as follows: (i) no MPL or too thin MPL potentially causes water flooding in the catalyst layer and/or the GDL, which in turn hinders the supply of the reactant gas to the reactive sites in the catalyst layer and (ii) too thick MPL evidently increases both the mass and charge transfer resistances due to the increased diffusion path and the tendency to retain condensed water within the MPL.

Open pore cellular foam has been recently increasingly used as a GDL material in PEFCs as they offer low-pressure drop, excellent gas flow and low electrical resistance [105-108].

Baroutaji et al. [105] designed a GDL using a PTFE-coated open cellular nickel foam that they used in an air-breathing PEFC. They demonstrated that the PTFE coating of the cellular foam improved its corrosion resistance and hydrophobicity, and subsequently resulted in better fuel cell performance. Schmitz et al. [81] investigated the impacts of the wetting properties of the GDL employed in air-breathing PEFCs. They found that the fuel cell operates more efficient with non-treated GDL, which is considered slightly hydrophobic; neither the hydrophobic nor the hydrophilic GDL improves the cell performance. The hydrophobic and hydrophilic GDLs were found to have higher contact resistance than the non-treated GDL due to reduced porosity and increased electrical resistance of the GDL after applying non-conducting coatings. Notably, the fuel cell was found to perform better with the hydrophobic GDL than with the hydrophilic GDL, although the contact resistance of the hydrophilic GDL is less than that of the hydrophobic GDL. The authors suggested that the hydrophilic GDL absorbs and uniformly distributes the produced water into its pores. This causes the evaporation rate to increase and the membrane to dry out, particularly at higher temperatures. On the other hand, the hydrophobic GDL rejects the water produced at the catalyst layer, which allows for the membrane to be reasonably humidified at high temperatures. The authors' rationales were supported by the amount of water collected at the anode side, which was found to be a minimum for the hydrophilic GDL case, signalling efficient water evaporation for this case at the cathode side.

Dang et al. [109] proposed GDLs that were made from natural wood and characterised by three-dimensional, interconnected perpendicular channels for air-breathing PEFCs. Figure 2.10 shows how the natural wood-based GDL is processed and the configuration of the employed air-breathing PEFC. The wood carbon sheets were treated with PTFE dispersion and heated at 400 °C for 30 min to uniformly disperse the PTFE. The fuel cell was occupied

with the proposed GDL at the cathode, and the peak power density was found to be 102 mW/cm^2 at 318 mA/cm^2 with the optimal 20 wt.% PTFE.

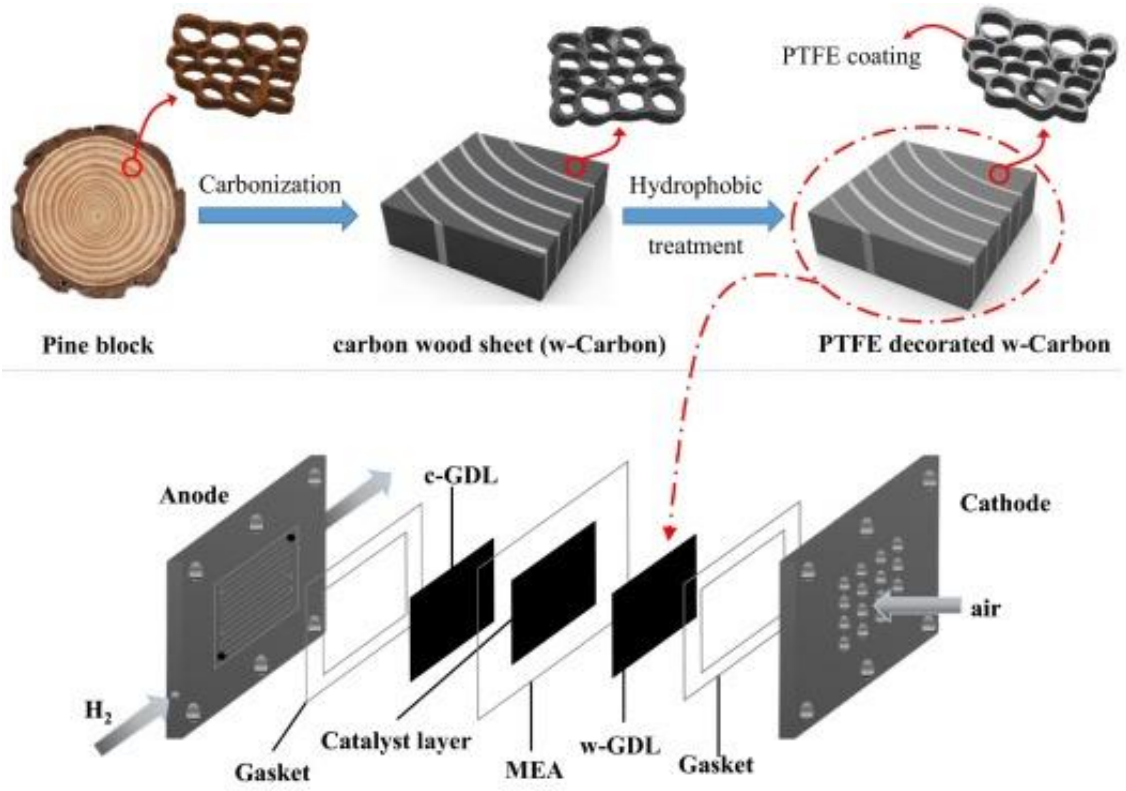

Figure 2.10 A schematic diagram showing the natural wood-based GDL is processed and configuration of the employed air-breathing PEFC. Reprinted with permission from Elsevier [109].

In summary, there exists an optimum thickness for the GDL; very thick GDLs induce increased mass transport losses and increased thermal resistance, whereas very thin GDLs increase the likelihood of membrane dry-out and, consequently, ohmic losses. Likewise, moderately hydrophobic GDLs are recommended to be employed. Very hydrophobic GDLs might result in water flooding, whereas very hydrophilic GDLs result in membrane dry-out.

2.5.4 Catalyst Layer

Catalyst layers (or electrodes) are where half-reactions take place and are in direct contact with both the GDLs and the polymer electrolyte membrane at each side of the fuel cell. Platinum is typically used as a catalyst in PEFCs due to its high chemical activity and stability.

The catalyst layers in PEFCs consist of platinum nanoparticles supported on carbon (20–40 wt.% Pt/C), Nafion (20–60 wt.% Nafion content), and voids [78, 80, 101]. Since platinum-based catalysts are precious, lowering the catalyst loading or using alternative cheaper catalysts is of great interest to the fuel cell community. Furthermore, as will be shortly shown, optimisation of the catalyst in terms of loading and composition has proven to be vital for improving the performance of the air-breathing PEFCs.

Ferreira-Aparicio and Chaparro [102] investigated the effect of the thickness of the catalyst layer on the performance of the air-breathing PEFCs. Three catalyst layers with thicknesses of 8 (20 wt.% Pt), 4.0 (40 wt.% Pt), and 2.5 μm (60 wt.% Pt) were prepared for the cathode side based on platinum loading of 0.17 mg /cm^2 and applied to the membrane electrolyte. They show that maximum power is obtained with the thinnest catalyst layer (i.e., 2.5 μm), particularly at the cathode side. Jeong et al. [103] investigated the effect of platinum loading (from 0.3 to 1.6 mg/cm^2) on the performance of the air-breathing fuel cell at 30 and 60% relative humidities. They showed that the platinum loading needs to be optimised: the fuel cell performance was found to decrease with substantially high platinum loadings, and this is due to increased mass transport resistance for product water. Similar findings were reported in the numerical study undertaken by Matamoros and Brüggemann [64].

Xiang et al. [104] improved the water management in an air-breathing PEFC using a dual cathode catalyst layer including a thin hydrophilic layer in contact with the membrane electrode (where Nafion was used as a catalyst binder) and a hydrophobic layer in contact with the GDL (where a mixture of Nafion and PTFE was used as a catalyst binder). They showed that, compared to the fuel cell with a single catalyst layer, the fuel cell performs better when a dual catalyst layer is used. The hydrophilic catalyst layer enhances the ionic

conductivity of the membrane phase while the hydrophobic catalyst layer traps water that is most needed for membrane humidification under low-humidity conditions and equally expels excess water produced at high current densities. Jung et al. [110] added 40 wt.% hydrophilic silica nanoparticles to the anode catalyst layer so that these nanoparticles could absorb the excess liquid water migrating from the cathode. They showed that, with this arrangement, the fuel cell performance improves by around 27%, and this is due to increased water rejection from the cathode to the anode and substantially decreased mass transport resistance for oxygen.

2.5.5 Cell Orientation

One of the main factors that affects the performance of air-breathing PEFCs is the orientation of the fuel cell as the natural convection heat and mass transfer coefficients are sensitive to this orientation [111]. As shown in Figure 2.11, there are typically three different fuel cell orientations (see vertical where the fuel cell is parallel to the gravitational force (Figure 2.11a); horizontal upward where the open cathode of the fuel cell is normal to the gravitational force and facing upwards (Figure 2.11b); and horizontal downward where the open cathode of the fuel cell is normal to the gravitational force and facing downwards (Figure 2.11c) [57].

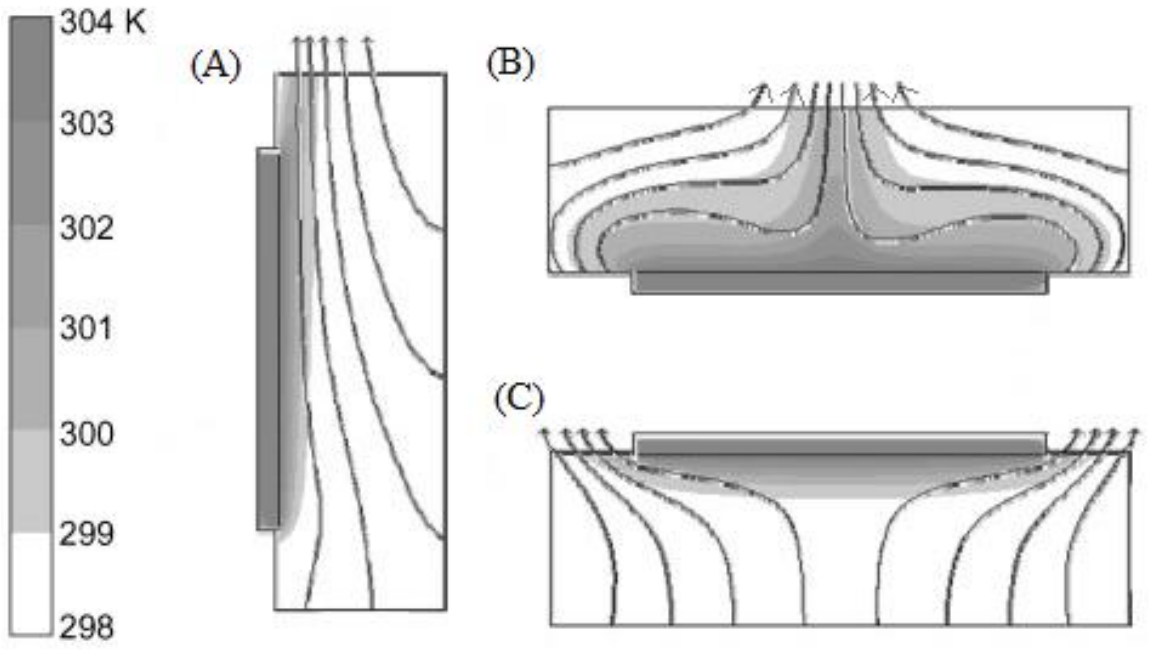

Figure 2.11 Schematic of the temperature distributions and air flow patterns for window-based air-breathing PEFCs under three different fuel cell orientations: (a) vertical, (b) horizontally facing upward and (c) horizontally facing downward. Reproduced from [57] with the permission from Elsevier.

Li et al. [111] developed a numerical model for an air-breathing PEFC and found that a much higher concentration of oxygen at the cathode surface could be obtained with vertical or horizontally facing upward orientations. Also, they experimentally showed that the horizontally upward-oriented fuel cell, compared to other orientations, demonstrates better performance while the downward-oriented fuel cell shows the worst performance. This phenomenon was attributed to the potential enhancement of the mass transport characteristics associated with the natural convection, which could be facilitated by the appropriate orientation of the open-cathode surface. They reported that, compared to the horizontally facing downward, the horizontally facing upward orientation resulted in a potential increase in the maximum output power of the fuel cell by around 10%. Obeisun et al. [112] evaluated the effect of cell orientation on the performance of a channel-based air-breathing PEFC by visualising water accumulation using thermal imaging, optical visualisation, electrochemical impedance spectroscopy, and gravimetric analysis. They

found that the horizontally facing upward orientation is favoured for the fuel cell due to less build-up of liquid water in the channels. However, most of the relevant studies show that the best performance of the air-breathing PEFC is obtained when the fuel cell is vertically oriented [60, 67]. Zhang and Pitchumani [57] developed a numerical two-dimensional model for an air-breathing PEFC and showed that the best performance is obtained with vertical orientation. They showed that, with this orientation, the air is initially drawn from the bottom of the fuel cell. Air adjacent to the open cathode of the fuel cell becomes heated, rises, and is replaced by cold air. This cold air in turn becomes hot, rises, and so on. Such dynamics create buoyancy effects and allow, compared to the horizontal orientations, for a relatively more effective supply of oxygen to the fuel cell and the removal of excess water and heat from the fuel cell. Vijay Babu et al. [113] experimentally investigated the effect of cell orientation on the performance of window-based and channel-based air-breathing PEFCs. Vertical orientation was found to be the best orientation for both types of fuel cells; this is due to higher natural convection heat transfer coefficients compared to other cell orientations. They also showed that the gravitational force assists in the removal of liquid water from the catalyst layer when the fuel cell is oriented vertically.

Hottinen et al. [85] experimentally showed that the performance of a single-cell air-breathing PEFC demonstrated similar performance when orienting it vertically or horizontally facing upwards. However, they [67] reported that, compared with horizontal orientation, an air-breathing PEFC with vertical orientation showed a longer stable operation. Similar findings were obtained by Kim et al. [84] but with a six-cell mono-polar stack attributing this to better expulsion of water when orienting the fuel cell vertically or horizontally facing upwards compared.

Ismail et al. [55] created a two-dimensional thermal model and investigated how the fuel cell orientation affects the thermal dissipation from the air-breathing PEFCs; the heat was found to be dissipated more efficiently when the fuel cell is oriented vertically or horizontally facing upward compared to horizontally facing downward orientation. Kumar and Kolar [89] conducted a numerical study and investigated the effect of the fuel cell orientation on the performance of both fuel cells with window- and channel-based cathodes. They reported that as the thickness of the boundary layer increases along the height of the cell, the cell orientation substantially affects the natural convection heat and mass transport. Hence, they concluded that the best performance of the air-breathing PEFC is obtained when it is oriented vertically in both types of open-cathode designs.

Fabian et al. [60] visualised the thermal plumes around the cathode surface of an air-breathing PEFC in vertical and horizontal cell orientations using a thermal imaging system: shadowgraphy. The average air speed above the cathode surface was found to be higher with the vertical orientation than with the horizontally facing upward orientation (11 $\mathrm{cm/s}$ vs 9 $\mathrm{cm/s}$); this is due to the higher density gradient of the plume in the former orientation.

To summarise, the relevant literature has shown that the cell orientation of the air-breathing PEFC could have a significant impact on the natural convection heat and mass transfer coefficients and subsequently the fuel cell performance. Namely, it has been shown that, depending on the design parameters, particularly those associated with the open cathode, the performance of the fuel cell improves when orienting it vertically and/or horizontally facing upward. However, the variation in the performance between the fuel cells that are oriented vertically and those oriented horizontally facing upward is mostly small or even negligible [85].

2.6 The Effect of Ambient Conditions

Since the cathode side is open to ambient air, the performance of air-breathing fuel cells is highly dependent on the ambient conditions of temperature and humidity, which are practically out of control. Instead, one may change or refine the design and the material of the components that make up the fuel cell to mitigate the detrimental consequences of some ambient conditions. As will be shown in the following paragraphs, the impact of ambient conditions on the air-breathing PEFCs has been studied by several research groups through mathematical models or experiments.

Matamoros and Brüggemann [64] created a three-dimensional model for a channel-based air-breathing PEFC. They demonstrated that as the ambient temperature rises, the performance of the fuel cell improves. This mainly results from the improved natural convection that is induced by the temperature gradient between the fuel cell and the ambient air. They discovered, on the other hand, that the impact of ambient humidity is negligible for fully humidified inlet gasses. They also demonstrated that the current density reaches the highest value near the ends of the channel and decreases towards its centre since the natural convection is inefficient to drive air towards the central regions. Further, only a small amount of platinum was found to be required for a fuel cell with a realistic channel length; the primary rate-limiting issue is the concentration losses resulting from the insufficient oxygen supply due to natural convection. Any increase in the platinum loading would have a negligible impact on the local current densities at the channel ends. Rajani and Kolar [66] developed a two-dimensional model for a window-based air-breathing PEFC. They showed that the thicknesses of the boundary layers associated with natural convection significantly affect the cell performance. The shorter the height of the fuel cell and the lower

the overall thicknesses of the velocity, thermal, and concentration boundary layers, the higher the temperature and concentration gradients at the cathode surface, leading to the higher heat and mass transfer coefficients. As a result, shorter fuel cells perform better owing to: lower concentration losses, a result of increased oxygen supply; higher activation losses, which are inversely proportional to temperature; and lower ohmic losses, a result of improved heat dissipation.

Ismail et al. [72] built a steady-state zero-dimensional model and found that favourable ambient conditions depend on the cell potential of air-breathing PEFC. Moderate ambient temperatures (e.g., 20 °C) and low humidities (e.g., 20%) are preferred at intermediate fuel cell potentials (e.g., 0.6 V) while low ambient temperatures (e.g., 10 °C) and high humidities (e.g., 80%) are preferred at low cell potentials (e.g., 0.4 V). Chen et al. [73] developed a numerical model and investigated how hydrogen relative humidity influences the performance of air-breathing PEFCs at ambient temperatures of 10, 20 and 30 °C; it was shown to have a great impact on the fuel cell performance. For instance, at an ambient temperature of 30 °C, when the relative humidity of hydrogen rises from 0% to 100%, the limiting current density could increase by more than 40%. Calili et al. [22] developed a dynamic model for an air-breathing PEFC to study the dynamic response of the fuel cell to sudden current changes at various ambient conditions: 10, 20 and 30 °C; and 20, 40, 60, and 80% RH. They found that there exists an optimum ambient temperature (i.e., 20 °C) at which overshoots are minimised during load changes and the steady-state fuel cell performance is maximised. Furthermore, they showed that both the transient response and the steady-state performance of the fuel cell are improved with increasing ambient relative humidity. Al-Anazi et al. [75] developed a three-dimensional, non-isothermal, steady-state model for an air-breathing PEFC stack to explore the influence of Riyadh City's (Saudi Arabia) ambient

conditions on the performance of the fuel cell. It was discovered that the performance of the fuel cell stack is enhanced by warm and humid ambient circumstances (summer) in which the membrane is sufficiently humidified. In the winter, the output power of the fuel cell stack is approximately 12% lower than in the summer.

Fabian et al. [60] conducted a comprehensive experimental study regarding the impacts of ambient humidity and temperature on the performance of planar air-breathing fuel cells. They found that the effect of ambient humidity on cell performance is dependent on the ambient temperature. To illustrate, if the ambient temperature is 40 °C, the cell performance improves with increasing ambient humidity. When the ambient temperature decreases to 20 °C, there is an optimal relative humidity at which the cell performance is a maximum, namely 40% as higher or lower relative humidity results in flooding or membrane dry-out, respectively. Unlike the 40 °C case, the cell performance degrades with increasing ambient humidity at 10 °C. Likewise, they showed that the effect of ambient temperature on the performance of the fuel cell is dependent on the ambient humidity; however, this dependency is rather weak. For example, the optimum temperature at a relative humidity of 20% is 20°C. The optimum temperature slightly increases with increasing relative humidity; it is 30 °C at a relative humidity of 80%.

Hottinen et al. [114] conducted a similar but earlier experimental study. Notably, they found that, at relatively high ambient temperatures, the fuel cell performance degrades with increasing relative humidity; this appears to be in contradiction with that of Fabian and his co-workers [60]. This is not the case. The relevant polarisation curves show that, for a given low cell potential, the amount of electric current generated by the fuel cell used by Fabian et al. [60] is significantly higher than that generated by the fuel cell used by Hottinen et al. [114]. The high electric current in Fabian et al.'s case dictates a higher heat of reaction, and, as a

consequence, higher heat generation. This amount of heat appears to be sufficiently high to raise the cell temperature to a level where the rate of water evaporation is higher than the rate of water generation. As a result, the membrane starts to dry out. Therefore, any increase in the ambient humidity will assist in humidifying the membrane, mitigating the ionic resistance, and improving the performance of the fuel cell. In contrast, since the amount of heat generated is relatively low in Hottinen's et al fuel cell, the rate of water generation is higher than the rate of water evaporation. Therefore, any increase in the ambient humidity will exacerbate water flooding and oxygen mass transport resistance. This was evident from the current distribution measurements which show that the non-uniformity of the current distribution increases with increasing relative humidity [114]. The same rationales can be used to interpret the results reported by Chu and Jiang [115, 116] which are similar to those of Fabian et al. and those reported by Jeong et al. [82], which are similar to those of Hottinen et al. [114]. Notably, Jeong et al. [82] showed that if the fuel cell is to be operated at low current densities, then its performance increases with increasing ambient humidity; the increased humidity assists in humidifying the membrane and the catalyst layer and, as a result, reducing the ohmic and charge transfer resistances. On the other hand, Chu and Jiang [115, 116] found that when the fuel cell operates at high current densities, the performance of the fuel cell stack increases with increasing relative humidity. This improvement is attributed to the self-humidification of the fuel cell.

As stated earlier in this section, the design of the air-breathing fuel cell and the materials from which the components of the fuel cell are made can be refined or changed to alleviate the detrimental effects of some environmental conditions on the performance of the fuel cell. It has been found that the fuel cell performance is improved with an increasing

temperature difference between the fuel cell and the ambient [59, 64, 114]. The buoyancy force, which is the driving force for natural convection, increases with increasing temperature difference between the surface of the cell and the ambient. This leads to increased air velocity near the cathode, better oxygen transport to the cathode, and better water removal from the cathode [114]. On the other hand, as the temperature difference between the cell and the ambient becomes smaller, the heat rejection rate from the cell becomes less. As a consequence, the cell temperature increases; the rate of water evaporation increases; the membrane starts to dry-out; the ionic resistance increases; and the fuel cell performance degrades [60]. This is normally the case when the ambient temperature is high, e.g., 40 °C. In accordance with this, the fuel cell was found to perform better at moderate ambient temperatures, e.g., 20 °C [60]. At such temperatures, the effect of humidity is minimal since the rate of water evaporation is low and the water produced is largely sufficient to humidify the membrane. However, it must be stressed that water flooding typically occurs at low ambient temperatures and high relative humidities [60] owing to the decrease in the rate of water removal [59]. One way to increase the temperature gradient is to use a GDL with low thermal conductivity [59, 114]. However, as discussed in Section 2.5.3, this may lead to excessive self-heating and, as a consequence, membrane dry-out.

Numerous investigations aim to address the adverse effects of ambient conditions on the air-breathing PEFC performance through the development of various passive and active methods to effectively manage the liquid water. Ous and Arcoumanis [117] investigated the effect of ambient conditions on the formation and accumulation of water droplets in the flow channels of an air-breathing PEFC by using two CDD cameras. The images of the water

droplets captured during the cell operation showed that their contact angles were approximately equal when they were advancing and receding. The water droplets were found to evaporate significantly when the ambient temperature increased beyond 23 ℃This study showed that the ambient temperature significantly influences water removal from the cathode of the air-breathing PEFC. As shown above, some ambient conditions may create undesirable phenomena for the air-breathing PEFCs, such as water flooding or membrane dry-out. Below are summaries of some investigations, aimed at mitigating undesirable phenomena induced by ambient conditions. Ma and Huang [118] innovated an air-breathing PEFC design incorporating a micro-diaphragm pump with a piezoelectric actuator to enhance both oxygen supply and liquid water removal. The piezoelectric actuator was able to pump most of the water out of the open cathode and, at the same time, transport more air towards the MEA of the fuel cell. Fabian et al. [119] introduced a water-collecting wick, which is electrically conductive and hydrophilic, to provide a water balance for an air-breathing PEFC. It was located between the cathode current collector and the catalyst layer. To test the water-rejection capability, they used an environmental chamber and set the ambient relative humidity and temperature to 80% and 10 ℃, respectively, to induce severe flooding conditions at the open cathode; they showed that the wick adequately mitigated water flooding. In subsequent work, for active water management, they integrated an electroosmotic pump into the air-breathing fuel cell system [120]. Their experimental results demonstrated that, with only 2% of the cell power, the use of the electroosmotic pump in conjunction with the wick can completely prevent water flooding at the open cathode. Coz et al. [121] positioned an insulating water management layer, i.e., a 190 μm thick microporous PTFE membrane, between a cathode current collector made of PCB and a metal grid in an air-breathing PEFC to retain liquid water. The metal grid, having no electrical

contribution, was used to maintain a constant compression and dissipate the heat. They aimed to investigate the nucleation of liquid water and its relationship with natural convection. They found that the proposed method improves water condensation, thus increasing the water activity at the cathode region, and reported that the performance of the fuel cell is stable between 0.6 and 0.65 V with a power density of 150 $\mathrm{mW/cm^2}$.

In summary, the impact of the ambient humidity on the air-breathing PEFC in general depends on the ambient temperature. Low ambient humidity is preferred in conjunction with low ambient temperature (e.g., 10 °C); relatively high relative humidity causes flooding. High relative humidity, on the other hand, is associated with a high ambient temperature (40 °C); low relative humidity results in membrane dry-out. There have been attempts to mitigate the negative impact of some ambient conditions on the performance of the air-breathing PEFC by innovating some passive and active means (e.g., electroosmotic pump) to appropriately manage liquid water. However, these means mostly add to the size of the fuel cell system and subsequently lower its commercial potential. It is clear that there is a need to innovate designs for the open cathode that substantially mitigate the detrimental impacts of the extreme ambient conditions on the performance of the air-breathing PEFC and minimally increase its size and weight, rendering it more practical and commercially attractive.

2.7 Air-breathing PEFC Stacks

Single cells are typically connected to each other in order to meet the load of the end application, forming what is known as a fuel cell stack. Stacking air-breathing fuel cells, in particular when operating with window-based cathode current collectors, is rather challenging as the design of the stack must ensure the supply of adequate amount of oxygen

to all the cells. Equally, the size and weight of the air-breathing PEFC stack should be minimised so that it could fit within the housing of the portable device to be powered. The following paragraphs list the key findings of the investigations in which air-breathing PEFC stacks were developed. Further, Table 2.6 shows the key features of these stacks and the cells used to form them.

Santa Rosa et al. [122] fabricated an eight-cell air-breathing PEFC stack and investigated the impact of the type of convection (forced versus natural) at the open cathode on the performance of the fuel cell stack. They showed that the performance of the PEFC stack operating with forced convection is almost five times higher than that operating with natural convection (9.7 W versus 2 W). Yang and Shi [123] fabricated a six-cell air-breathing stack where the cells are connected in series in a stair configuration as shown in Figure 2.12. Such a configuration allowed for a compact design and, at the same time, allowed all the open cathodes of all the cells to be in direct contact with the ambient air. Moreover, hydrogen was circulated within the stack by fans to improve the uniformity of the fuel supply. They reported that this design produced a peak power density of 350 $\mathrm{mW/cm^2}$. Kim et al. [84] designed a miniaturised air-breathing six-cell planar stack (18 $\mathrm{cm^3}$) in which cells are connected in series and the anode and cathode current collectors are gold-plated PCB-based. The maximum output power from the stack was 3.5 W.

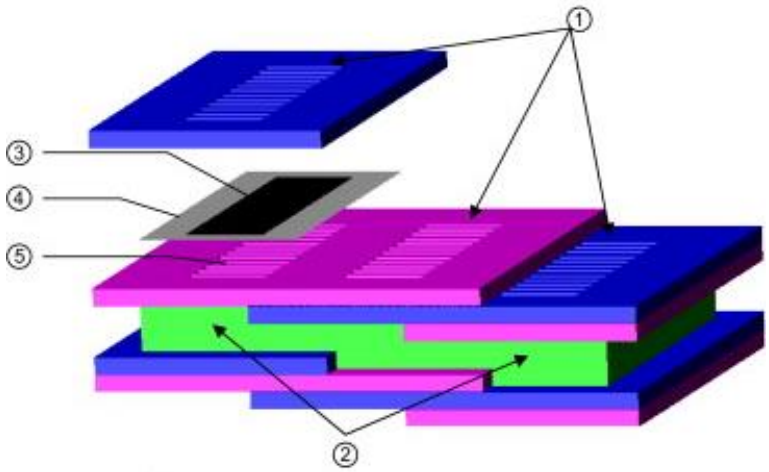

Figure 2.12 A stair configuration air-breathing six-cell PEFC stack: (1) window-based cathode current collectors, (2) hydrogen fans, (3) a GDL and catalyst layer, (4) a polymer electrolyte membrane and (5) an anode flow field. Reproduced from [123] with permission from Elsevier.

Bussayajarn et al. [83] manufactured a two-cell planar air-breathing PEFC without using endplates. They tested the fuel cell for 2 hours and showed that the best performance is obtained with circular openings, where the power density (347 $\mathrm{mW/cm^3}$) is stable. Isanaka et al. [124] proposed a lighter, smaller, and more cost-effective air-breathing PEFC stack design where the weight and cost were reduced by 90% and 80%, respectively. Namely, their stack did not include end plates, bolts or nuts. The stack consists of polycarbonate flow-field plates, stainless steel current collectors, and silicone gaskets at the anode side. Notably, the peak power of the proposed stack was found to be tenfold higher than the conventional design.

Baroutaji et al. [105] proposed a design for an air-breathing PEFC using open-pore cellular foam as flow distributors. Figure 2.13 shows that the design was to reduce the size and cost of the fuel cell stack by having a single hydrogen chamber for every two cells. They found that the maximum power densities of the fuel cell stack with uncoated and PTFE-coated open-pore cellular foams were 0.09 $\mathrm{W/cm^2}$ and 0.15 $\mathrm{W/cm^2}$, respectively. They noted that

the individual cells did not perform equally, and this was probably due to the different levels of water accumulation demonstrated by each cell.

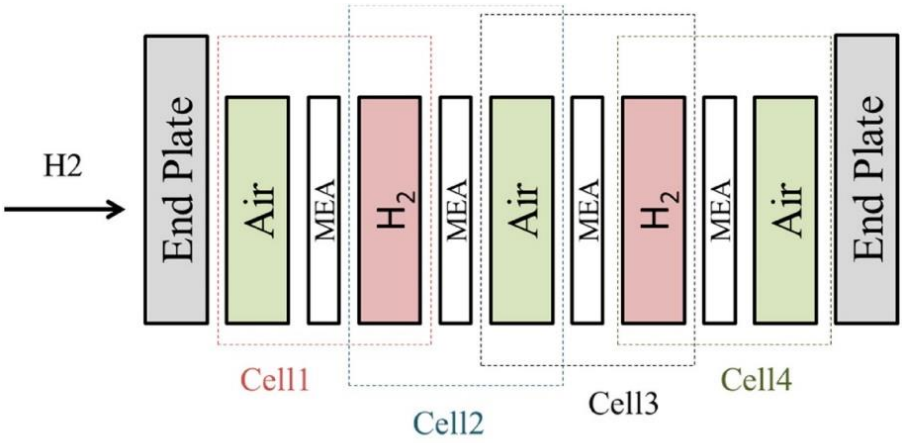

Figure 2.13 Schematic representation of the 4-cell air-breathing PEFC developed by Baroutaji et al. [105]. Reprinted with the permission from Elsevier.

Yan et al. [125] designed a 15-cell channel-based air-breathing PEFC stack and proposed a thermal management method that improves the performance of the fuel cell stack by applying different cathode flow channel opening ratios. They compared the stack performance of the fuel cell with a 58.3% opening ratio under natural and forced convection (through using a fan) and found that the stack performance under forced convection is about twenty-fold higher than that under natural convection. They also showed that the use of a combination of 50% and 58.3% opening ratios decreased the overall stack temperature and therefore improved stack performance.

Table 2.6 Air-breathing PEFC stack designs.

Authors	Stack Design Features	Dimensions of Fuel Cell and MEA Properties	Fuel Cell Performance
Santa Rosa et al. [122]	An 8-cell stack; channel-based gold-plated cathode current collectors, graphite bipolar plates; a fan used for air supply and cooling	Open cathode stack: 10SR4-A (commercially available from SRE—*Soluções Racionais de Energia*); Membrane: Nafion® 111; MEA area: 3.8 cm^2	Maximum output power: 9.7 W (fan working at 5 V) and 2 W (without a fan)
Yang and Shi [123]	A 6-cell stack; window-based cathode current collectors with slit openings; stair configuration; hydrogen fans to supply and circulate hydrogen	MEA area: 5 cm^2; slits dimensions: 10 $mm \times 1$ mm at 1 mm; Pt loading: 0.3 mg/cm^2	Maximum output power: 10.5 W at 650 mA/cm^2
Kim et al. [84]	A planar monopolar 6-cell stack using a flexible PCB-based current collector with rectangular openings; parallel-serpentine flow field anodic plates	Membrane: Nafion® 212; MEA area: 10.08 cm^2; six coplanar electrode pairs: 14 $mm \times 1$ mm; anodic flow channel sizes: 0.5 $mm \times 0.5$ mm with 0.5 mm spacing; cathodic opening ratio: 65%; stack size: 18 cm^3; cathode Pt loading: 1.5 mg/cm^2; anode Pt loading: 4 mg/cm^2	Maximum power density: 350 mW/cm^2 at 750 mA/cm^2
Bussayajarn et al. [83]	A planar 2-cell stack; gold plated aluminium monopolar plates; three window-based cathode collectors with parallel slits, circular openings or oblique slit	Membrane: Nafion® NRE-212; MEA area: 11 cm^2; Pt loading in cathode: 0.4 mg/cm^2; Pt loading in anode: 0.6 mg/cm^2	Maximum power density: 347 mW/cm^3 using circular openings
Isanaka et al. [124]	A stack design free from end plates, bolts, nuts, insulating washers and sleeves; polycarbonate flow field plates	Membrane: Teflon/sulfonic acid; MEA area: 50 cm^2; Pt loading: 0.5 mg/cm^2	Maximum output power: 0.25 W; reduction in weight: 90%; reduction in cost:80%
Baroutaji et al. [105]	A 4-cell stack with only two hydrogen chambers; open pore cellular foams (OPCFs) as flow distributors	Membrane: Nafion® 212; MEA area: 25 cm^2; Pt loading: 0.4 mg/cm^2; GDL: ®SIGRACET SGL 24BC	Maximum power density (with PTFE-coated OPCF): 0.15 W/cm^2 at 0.34 A/cm^2; maximum power density (with uncoated OPCF):0.09 W/cm^2 at 0.23 A/cm^2
Yan et al. [125]	A 15-cell stack with channel-based openings; gold-coated copper current collectors; graphite bipolar plates	Membrane: Nafion® ; MEA area: 130 cm^2; Pt loading: 0.8 mg/cm^2	Maximum power density: 11.98 mW/cm^2 at 20.36 mA/cm^2 under natural convection and 244.75 mW/cm^2 at 414.36 mA/cm^2 under air-forced condition

2.8 Hydrogen Storage and Anode Outlet for Air-breathing PEFCs

Hydrogen storage and supply in air-breathing PEFCs need to be simple, compact, efficient, cost-effective, and safe. This section first reviews how hydrogen is normally stored, with a particular emphasis on metal hydrides, which are typically used for air-breathing PEFCs. It then reviews the modes of hydrogen outlets, with a particular focus on the dead-end mode that is typically adopted for air-breathing PEFCs.

2.8.1 Storage of Hydrogen

Hydrogen can be stored in four different forms: a compressed gas form; a liquid form; a cryo-compressed gas form; and a solid form in hydrides [126]. Among these storage options, solid-state hydrogen storage is favourable for air-breathing PEFC-based portable applications since it is more convenient and safer than other storage methods [127].

Metal hydrides have been promising candidate materials to store hydrogen in solid form as they feature high energy density [128]. In contrast to conventional approaches, such as compressed hydrogen and liquid hydrogen, metal hydrides offer a higher volumetric and gravimetric density, thus allowing for more efficient storage. As they operate at moderate temperature and pressures, metal hydrides render portable applications safer and more feasible. This approach offers a viable solution for compact and safe hydrogen storage in air-breathing PEFCs, where efficiency and safety are of the utmost importance.

There are several metals and alloys that have the capability of reversibly absorbing/desorbing large amounts of hydrogen. Their hydrogen storage performance is based on their thermal stability, durability, volumetric capacity, and the kinetics of hydrogenation/dehydrogenation [129]. In short, the metal hydrides should be thermally

stable and durable within the ranges of the operating temperature and pressure of the target applications.

There have been several reviews on metal hydrides, in particular their materials and applications, in the literature. For example, Rusman and Dahari [128], Bhattacharyya and Mohan [130] and Tarasov et al. [131] comprehensively reviewed studies on materials used for metal and alloy hydrides and the progress made in terms of their absorption/desorption of hydrogen. Hoffman et al. [132] discussed the chemistry of metal hydrides and, for the first time, proposed magnesium-based alloys for hydrogen storage for mobile applications, and this is due to their low material cost and favourable hydrogenation rate.

The reversible sorption process of metal hydrides is exothermic during the absorption of hydrogen, thus requiring heat removal. On the other hand, desorption of hydrogen (when, for example, supplying hydrogen to the fuel cell) is an endothermic process; therefore, heat must be supplied to release hydrogen from the metal hydride. Hence, heat transfer between the hydride and the exterior is a limiting factor that controls hydrogen absorption/desorption in/from the metal hydrides [133]. Hydrogen absorption/desorption rates are also affected by operating conditions, the geometry of the storing cartridge, and the packing density of metal hydrides [134]. Recent studies on metal hydrides have focused on how to enhance hydrogen absorption/desorption rates through optimising design parameters and heat distribution. Lototskyy et al. [135] pointed out that the components of the fuel cell system could be integrated in such a way that the heat released as a result of the exothermic electrochemical reaction taking place within the fuel cell is efficiently utilised to release hydrogen from the metal hydride storage canister.

The plateau pressure of a metal hydride, which is a significant parameter for material selection, is the pressure at which large quantities of hydrogen are absorbed or released in/from the metal hydride [134]. When the plateau pressures of the metal hydrides are close to the ambient pressure, these metal hydrides are considered suitable for lightweight cartridges used in portable air-breathing PEFC systems [134]. Further, the storage material must be thermally stable and durable at operating temperature and pressure ranges for portable applications.

The selection criteria of metal hydrides employed in air-breathing PEFC systems vary and are highly dependent on the requirements of the portable application. The physical and design parameters (e.g., hydrogen absorption/desorption rate, thermal stability, volumetric capacity, and plateau pressure) must be considered when selecting metal hydrides for portable applications. Further, the cost and manufacturability of metal hydride are the other important selection factors. Figure 2.14 shows some examples of commercially available metal hydride hydrogen storage devices for air-breathing PEFCs used in portable applications.

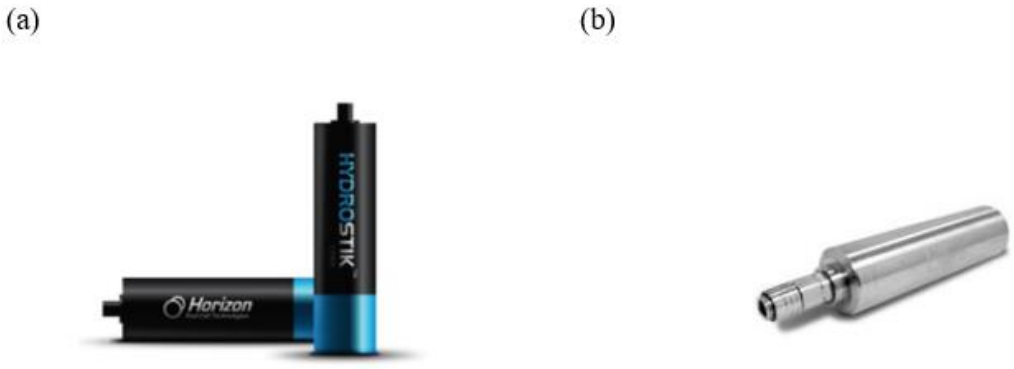

Figure 2.14 Commercially available metal hydrides hydrogen storage devices: (a) HYDROSTIKTM [136] and (b) HB-SC-0010-Q [137].

There have been few studies on employing metal hydride cartridges in air-breathing PEFCs. Coz et al. [121] used a sodium borohydride ($NaBH_4$) cartridge with a hydrogen storage capacity of 24 litres to conduct an experimental study on an air-breathing PEFC. They reported that the hydrogen is supplied from the cartridge through $NaBH_4$ hydrolysis to meet the fuel demand of the fuel cell. This process controls the total amount of hydrogen supplied to the anode chamber and mitigates safety concerns associated with the accumulation of hydrogen. Kim et. al. [51] selected an AB_5 metal hydride hydrogen storage tank for an air-breathing PEFC to power a mobile phone; this is mainly because this type of metal hydride alloy can be packaged in a small hydrogen storage tank and has a sufficient hydrogen absorption/desorption rate at room temperature. Fernández-Moreno et al. [39] used a metal hydride cartridge produced by Horizon Fuel Cell Technologies [138] to supply hydrogen to an air-breathing PEFC system. They reported that the cartridge with one gram of hydrogen capacity provided 20 hours of operation above 1 W.

2.8.2 Anode Outlet

The outlet of the hydrogen side in PEFCs could take one of the following forms shown in Figure 2.15: (a) open ended without recirculation, (b) open ended with recirculation or (c) dead ended [139, 140]. In dead-end mode, the outlet of the anode compartment is sealed off so that the hydrogen fed to the fuel cell can be completely consumed at the anode. The selection of the mode for hydrogen outlets largely depends on the type of application. Rodatz et al. [141] experimentally studied the effects of the hydrogen supply modes on PEFC efficiency. They reported that the dead-end mode is the simplest arrangement in which the amount of hydrogen supplied to the fuel cell is equal to the amount of hydrogen needed to sustain the electrochemical reaction; however, the performance of the fuel cell in dead-end

mode was found to be poor compared to other hydrogen supply arrangements. Hwang [139] performed a similar investigation and found out that the efficiencies of the fuel cell were similar for both dead-end and recirculation modes of hydrogen supply when the power of the fuel cell stack was less than 1.2 kW. At higher stack powers, the recirculation mode was found to be more efficient than the dead-end mode.

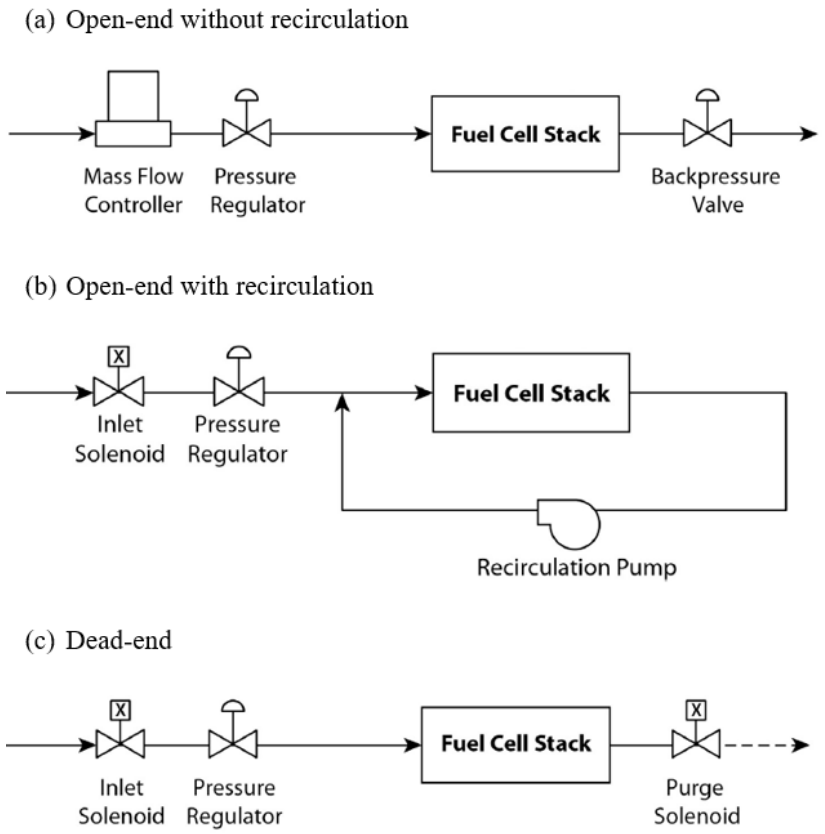

Figure 2.15 Schematics of hydrogen supply modes: (a) open-end without recirculation, (b) open-end with recirculation and (c) dead-end. Reproduced from [139] with the permission from Elsevier.

Evidently, the dead-end mode is the simplest mode as it does not require a downstream treatment arrangement to deal with unreacted excess hydrogen (e.g., recycling or burning of hydrogen). For this reason, it is often the mode of choice for air-breathing PEFCs where size and mass reduction are a priority. In the dead-end mode, hydrogen pressure at the anode compartment is made constant using a pressure regulating valve as shown in Figure

2.15c or simply by displacement arising as a result of reduction of volume of hydrogen in the storage device [33].

However, the use of a dead-end mode for the anode compartment of the PEFC may have some drawbacks, such as the accumulation of inert gases, contaminants, and water [140]. Namely, high purity hydrogen (i.e., >99.99%) should be used to avoid the accumulation of any contaminants and/or inert gases in the porous anode compartment [139]; otherwise, the fuel cell efficiency may be significantly reduced [142-144]. Furthermore, liquid water may form and accumulate at the anode compartment because of the absence of forced convection [145, 146]. To remedy this problem, an anode purging mechanism should be adopted to allow for regular purging and subsequently maintain good operation of air-breathing PEFCs. However, such a purging mechanism requires extra power to automatically open and shut the purging valve. Fernández-Moreno et al. [39] showed that anode purging provides performance stability for long-term operations of an air-breathing PEFC. Chiche et al. [147] proposed an experimental approach to predict the time between two anode purges for an air-breathing PEFC stack operating in dead-end mode. The relative humidity and the current load were found to be influential parameters affecting the time between two purges. They found that the time between two purges increases with decreasing relative humidity and current load; however, the performance of the fuel cell is unstable at low relative humidity and low current.

2.9 Air-breathing PEFC Systems

Air-breathing PEFCs are a cleaner replacement to rechargeable batteries used to power small electronic devices, such as cell phones and laptops, as they do not contain poisonous heavy metals [17, 148, 149]. The literature has shown some experimental (and very few

modelling) studies on developing air-breathing PEFC systems to power small electronic devices; the key findings of these investigations are summarised below.

Kim et al. [51] integrated an air-breathing PEFC system, consisting of an 8-cell air-breathing PEFC stack (8 cm^3), a mini dc-dc voltage converter, a miniature pressure regulator (4 cm^3), and a metal hydride hydrogen canister (8 cm^3 with a hydrogen storage capacity of 4 litres at 25 ℃) at the back of a mobile phone shown in Figure 2.16. The volumetric energy density of this miniaturised fuel cell system (< 25 cm^3) was around 205 $\mathrm{Wh/L}$ and was able to power the mobile phone for roughly 6 hours of uninterrupted voice calling.

Fernández-Moreno et al. [39] presented a portable system including a single air-breathing PEFC cell to power a display screen and four LED lights. A dc-dc converter was used to increase the voltage of the system from 0.5–0.8 V to 3.3 V. The fuel cell was operated with or without a fan installed at the open cathode, an electronic valve for anode purging, and two supercapacitors for auxiliary power requirements. They showed that this system could supply more than 1 W dc electricity with only 1 gram of hydrogen for 20 hours of continuous operation. The fan and the purging valve were proven to be beneficial in terms of water flooding migration. Bussayajarn et al. [83] developed and used an air-breathing PEFC system to power a cell phone charger. The fuel cell system was demonstrated to operate steadily during a 2-hour cell phone charging. The specific power of the fuel cell system was found to be 150 W/kg. Han et al. [50] developed and used around 200 W air-forced PEFC system to power a freezer for outdoor and medical applications. The fuel cell system consists of an air-forced PEFC stack, a dc-dc converter, a control electronic subsystem, two metal hydride hydrogen canisters connected in parallel (to ensure continuous supply of hydrogen to the system while replacing the empty canister), and a lead acid battery (to enhance the transient

response to load change). The authors demonstrated that the fuel cell system provided reliable and continuous power for the portable freezer operating at around -22 ℃ and an ambient temperature of around 27 ℃. Note that, except for the integrated fan, this system is very similar to the air-breathing PEFC system.

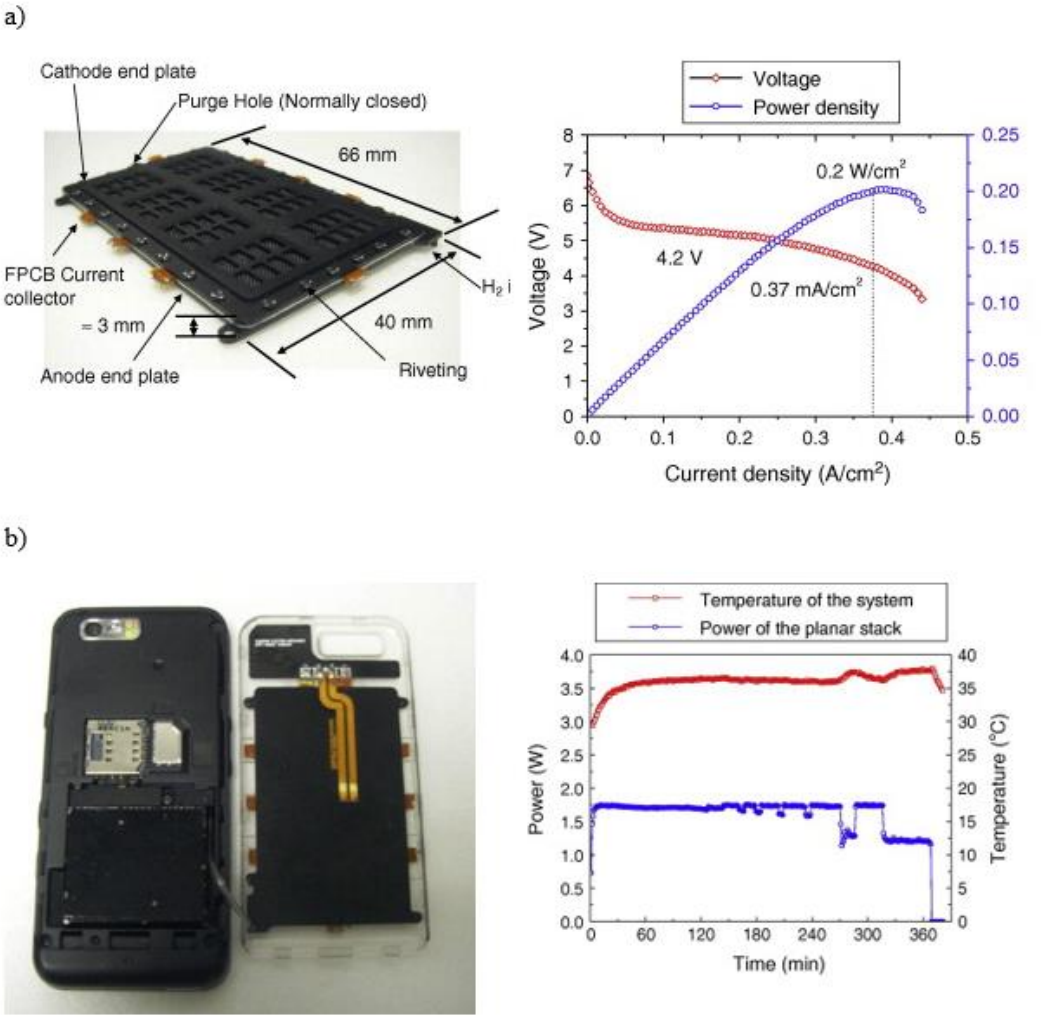

Figure 2.16 Views and performances of (a) an 8-cell air-breathing PEFC stack and (b) a mobile phone powered by an air-breathing PEFC. Reprinted with permission from Elsevier [51].

Yalcinoz and Alam [74] developed a dynamic model for an air-breathing PEFC system to power a laptop. The system consists of a fuel cell stack, a dc-dc converter, a load control, and a feedback controller. The results showed that the power consumption of the laptop depends

on the operating conditions (e.g., load alteration) and that it is possible to keep the voltage of the system at a desirable level for the laptop by the feedback controller.

Ferreira-Aparicio [150] reviewed some of the attempts to widely commercialise air-breathing PEFCs and stated that most (if not all) of these attempts have been unsuccessful. The author discussed and analysed the key research and development bottlenecks that hinder the widespread deployment of air-breathing PEFCs; namely, the reliability of the fuel cell operation under extreme ambient conditions (e.g., extremely high and low ambient temperatures), weight reduction, the safety of hydrogen storage devices, and the high cost of materials.

2.10 Discussion and Recommendations for Future Work

The air-breathing PEFC is a promising technology for a multitude of portable applications and this is due to being more environmentally friendly and less reliable on the national grid when compared to other conventional energy sources. Numerous experimental and modelling studies have been conducted to examine the effects of different design parameters and ambient conditions on the performance of air-breathing PEFC. The main motive behind these investigations is to look for ways to improve the fuel cell performance to make it more reliable and commercially attractive. However, very few studies have been conducted on hydrogen storage and delivery, air-breathing PEFC stacks, and air-breathing PEFC systems. Miniaturising the fuel cell system in order to make it more commercially viable for small portable applications is one of the primary goals of these investigations. In this work, we have exhaustively reviewed the articles on air-breathing PEFCs. Below are key findings and some recommendations for future work:

- The opening ratio of the window-based cathode current collector should be optimised to ensure a sufficient supply of oxygen and water to the cathode of the fuel cell and good electrical contact between the current collector and the MEA of the fuel cell.
- Likewise, the thickness of the cathode GDL in air-breathing PEFCs should be optimised; very thin GDLs increase the likelihood of membrane dry-out while very thick GDLs increase the mass transport and thermal resistances. Similarly, the GDL should be moderately hydrophobic as super-hydrophobic GDLs result in water flooding while hydrophilic GDLs lead to membrane dry-out.
- The impact of the ambient humidity on the air-breathing PEFC performance depends on the ambient temperature. Low ambient humidity is favoured with low ambient temperature (10 ℃) to avoid water flooding while high ambient humidity is favoured with high ambient temperature to avoid membrane dry-out. The ambient conditions are beyond the control of the user and therefore, there have been some passive and active means (e.g., an electroosmotic pump) to manage better the liquid water. However, these mitigation means add to the size of the fuel cell system and may lower its commercial competitiveness.
- The air-breathing PEFC in general performs better when it is oriented vertically or horizontally facing upwards rather than horizontally facing downwards, and this is due to better heat dissipation and supply of oxygen and water to the fuel cell in the former two cases.
- Although the structures and the materials of the components (e.g., GDL, MPL, and catalyst layer) of air-breathing PEFCs are largely similar to those of conventional PEFCs, the characteristics of these components may show different effects on the

performance of the fuel cell. For example, Calili-Cankir et al. [23] reported that the performances of air-breathing and conventional PEFCs are affected by the porosity of the GDL differently: the performance of air-breathing PEFC improves with decreasing porosity while the performance of conventional PEFC improves with increasing porosity. Therefore, the optimal parameters for conventional PEFCs should not be extrapolated to air-breathing PEFCs and the parameters of the latter fuel cells should be optimised separately.

- Reducing the weight and size of the fuel cell components while maintaining good thermal and water management is one of the key challenges for air-breathing PEFCs. Light-weight gold-plated PCB [84] and polycarbonate [124] are promising materials for flow-field plates. It is, therefore, recommended that a variety of cost-effective non-conductive materials coated with highly conductive metals are used for the current collectors and the end plates to reduce the size, weight, and cost of air-breathing PEFCs.
- Many studies have been centred on reducing the catalyst loading or exploring alternative, more cost-effective catalysts for the cathode catalyst layer and this is due to the high-cost of the platinum-based catalysts [102, 103]. Likewise, the above objectives are applicable to the anode catalyst layer and could be considered when seeking an overall cost reduction.
- The incorporation of the MPL between the catalyst layer and macroporous substrate is a crucial aspect in managing liquid water within the MEA. A very well-designed MPL could significantly mitigate undesirable phenomena of water flooding, particularly at the cathode side. On the other hand, poorly designed MPLs may trap water produced at the cathode catalyst layer and consequently result in water flooding, and/or

significantly increase the mass and charge transfer resistances [151]. Reviewing the relevant literature, MPL optimisation in air-breathing PEFCs was limited to the thickness of the MPL [104]. Further research is required to optimise other aspects of the MPLs (e.g., porosity and contact angle) with the aim of enhancing the water management and fuel cell performance.

- Enhancing the wettability of the porous medium (i.e., GDL and MPL) in air-breathing PEFCs is necessary to alleviate the negative effects of ohmic and concentration losses. Recently, Lee et al. [152] provided an overview of novel approaches used for the GDLs and the MPLs of PEFCs. For example, the wettability-patterned GDLs/MPLs are novel designs aiming at creating a hydrophobicity gradient within the surface of the porous media that accelerates the removal of excess water and subsequently the supply of reactant gases to the cathode catalyst layer [153]. Similarly, the perforation of GDLs/MPLs by a laser beam was found to significantly enhance the performance of conventional PEFCs [154]. It will be of great interest to investigate the impact of wettability-patterned or perforated GDLs/MPLs on the performance of air-breathing PEFCs.
- Research on the load-following capability of air-breathing PEFCs has been restricted to a limited number of studies [22, 24, 74]. Additional modelling analyses need to be conducted to assess the impact of the cell numbers on the dynamic response of an air-breathing PEFC. Also, the dynamic response of a small portable electronic device powered by an air-breathing PEFC should be investigated at extreme ambient and operating conditions.
- The efficiency of air-breathing PEFCs is influenced by the orientation of the fuel cell and ambient conditions. The task of rendering air-breathing PEFCs intensive to the

influence of these variables poses an immense challenge. Therefore, novel methodologies need to be explored to eradicate or alleviate these adverse effects of the orientation and ambient conditions in portable air-breathing PEFC powered systems. The integration of a hybrid miniature air-breathing PEFC and battery system into a portable device has the potential to mitigate these adverse effects and provide at the same time a fast dynamic response to sudden and/or substantial load changes.

2.11 Concluding Remarks and Recommendations

Air-breathing PEFCs are attractive alternative power conversion technologies, particularly for small electronic devices, as the time taken between recharges is, compared to batteries, significantly longer. Further, air-breathing PEFCs, again compared to batteries, do not involve toxic heavy metals whose disposal forms an environmental challenge. Furthermore, air-breathing PEFCs, compared to conventional PEFCs, are substantially simpler, and this is due to their reliance on natural convection to transport oxygen and water vapour between ambient air and the open cathode of the fuel cell. However, due to the low heat and mass transfer coefficients associated with natural convection, the output power and the operational stability of air-breathing PEFCs are relatively small compared to conventional PEFCs. Therefore, as reviewed in this paper, there have been considerable experimental and modelling investigations in the literature looking into the impact of various design parameters and ambient conditions on the air-breathing PEFC performance.

For completeness, the mathematical modelling of air-breathing PEFCs has been reviewed listing the conservation equations and how they are adapted to account for natural convection at the open cathode.

The literature has shown that very few investigations have been conducted concerning: hydrogen storage and delivery; air-breathing PEFC stacks; and air-breathing PEFC systems. One of the main aims behind these few investigations is to miniaturise the fuel cell system to make it more commercially attractive for small portable applications. Overall, there are still some technical and economic issues that the air-breathing PEFC system needs to overcome to make a sizeable market penetration. These issues include, but are not limited to: reliability of operation under extreme ambient conditions (very low or very high temperatures); size and weight reduction; the safety of hydrogen storage; and cost reduction. Evidently, relevant research needs to be substantially intensified to appropriately address all the above issues.

Acknowledgements

Fatma Calili thanks the Ministry of National Education at the Republic of Turkey for funding her PhD studentship at the University of Sheffield. The authors would like to thank Havva Kiral for her help with the exploded view of the air-breathing PEFC components.

Nomenclature

Roman symbols

a	Water activity
c_f	Fixed charge site concentration in membrane, $\mathrm{mol/m^3}$
C_p	Specific heat of fluid at constant pressure, $\mathrm{J/(kg.K)}$
D	Diffusion coefficient, $\mathrm{m^2/s}$
F	Faraday's constant, $\mathrm{C/mol}$
g	Gravitational acceleration, $\mathrm{m/s^2}$
h	Heat transfer coefficient, $\mathrm{W/(m^2.K)}$
h_m	Mass transfer coefficient, $\mathrm{m/s}$
i	Electric current, A
I	Current density, $\mathrm{A/m^2}$

k	Permeability of porous media m^2
k_{eff}	Effective thermal conductivity, $\mathrm{W/(m.K)}$
k_p	Hydraulic permeability of membrane, m^2
k_φ	Electro-kinetic permeability of membrane, m^2
M	Molecular weight, $\mathrm{kg/m}^3$
n_d	Electro-osmotic drag coefficient
P	Pressure, atm
S	Source terms of governing equations in Table 2.4
T	Temperature, K
$\vec{V}$	Superficial velocity vector, $\mathrm{m/s}$
V_{cell}	Overall cell potential, V
Y	Mass fraction
z_f	Charge of sulfonate site in membrane

Greek symbols

ε	Porosity
η	Surface over potential, V
λ	Water content
μ	Dynamic viscosity, $\mathrm{kg/(m.s)}$
ρ	Density, $\mathrm{kg/m}^3$
σ	Electrical/ionic conductivity, $\mathrm{S/m}$
$\vec{\tau}$	Stress tensor, $\mathrm{kg/(m.s)}^2$

Subscripts and superscripts

a	Anode
c	Cathode
eff	Effective value
f	Fluid
i	Species i
m	Membrane
ref	Reference
s	Solid
sat	Saturation
∞	Ambient

Abbreviations

GDL	Gas Diffusion Layer
MEA	Membrane Electrode Assembly
MPL	Microporous Layer
PEFC	Polymer Electrolyte Fuel Cell

Chapter 3: A Dynamic Model of Air-breathing Polymer Electrolyte Fuel Cell: A Parametric Study

---

This chapter is published as:

Calili F, Ismail MS, Ingham DB, Hughes KJ, Ma L, Pourkashanian M. A dynamic model of air-breathing polymer electrolyte fuel cell (PEFC): A parametric study. International Journal of Hydrogen Energy. 2021 May 13;46(33):17343-57.

https://doi.org/10.1016/j.ijhydene.2021.02.133

Authorship statement

The principle author of the paper is Calili F. The contribution of Calili F is conceptualization, methodology, software, formal analysis, investigation, validation, writing original draft, review and editing.

3.1 Abstract

A dynamic model for an air-breathing PEFC has been built to investigate the transient response of the fuel cell to load changes. The sensitivities of the dynamic response, as well as the steady state performance, to: the ambient temperature and relative humidity; the thickness and the thermal conductivity of the cathode GDL; and the fuel utilisation, have

been studied. A previously-developed steady-state model of the fuel cell was linked to the dynamic model to feed the latter with the data of the cell temperature as it changes with the current density. It was found that, when there are sudden changes to high loads, there exist optimum values for the ambient temperature and GDL thickness at which the overshoots are mitigated and the steady state performance is improved. Further, the transient and steady state performance were found to improve with increasing the ambient relative humidity and GDL thermal conductivity. Finally, the fuel utilisation was found to have no impact on the dynamic response of the fuel cell. All the above findings have been presented and discussed in the paper.

Keywords: Air-breathing PEFCs; Dynamic model; Transient response; Load changes

3.2 Introduction

Portable electronic devices, such as smartphones and laptops, have become an increasingly essential part of our daily life. In this huge market, power demand is growing fast. Portable polymer electrolyte fuel cells (PEFCs) are strong candidates to act as an alternative power source for small electronic devices due to their appealing features: long charge cycle (i.e. of the order of a few days), high efficiency and grid-independence [17, 33, 56, 65, 94]. The cathode of portable PEFCs is typically open to the ambient in order to directly extract (by natural convection): (i) oxygen required for the completion of the electrochemical reaction and (ii) water vapour required for the initial humidification of the polymeric membrane. Thus, PEFCs, with an open cathode, do not require an air/oxygen storage device and humidifier, thus simplifying the fuel cell system. This type of PEFCs is normally described as air-breathing PEFCs.

Since oxygen is passively supplied from the ambient air by natural convection, the performance of air-breathing PEFCs is sensitive to the ambient conditions. Particularly, liquid water formation at the open porous cathode is strongly affected by the ambient conditions. Some models and experimental studies that investigated the impact of ambient conditions on the performance of air-breathing PEFCs are presented in the following paragraphs.

Rajani and Kolar [66] investigated the effect of various sets of ambient conditions (20-80% ambient relative humidity and 10-40 ℃ ambient temperature) on the performance of the air-breathing PEFC using a two-dimensional, single phase, non-isothermal and steady-state numerical model. They concluded that the ambient temperature dominantly affects the fuel cell performance compared to relative humidity of the ambient. Matamoros and Brüggemann [64] developed a three-dimensional and non-isothermal model to observe how different ambient conditions influence the concentration and ohmic losses in air-breathing PEFCs. They demonstrated that concentration losses were more dominant than ohmic losses on the performance of the air-breathing PEFC at different ambient conditions. Chen et al. [73] built a zero-dimensional mathematical model to investigate the impact of hydrogen relative humidity on the performance of air-breathing PEFCs at ambient temperatures of 10, 20 and 30℃. It was found that the limiting current density increases with increasing hydrogen relative humidity. Ismail et al. [72] developed a zero-dimensional mathematical model for an air-breathing PEFC. They found that a high ambient relative humidity with a low ambient temperature is advantageous at low cell potential while a low ambient relative humidity with a moderate ambient temperature is favourable at intermediate fuel cell potentials.

Hottinen et al. [114] and Fabian et al. [60] experimentally investigated the effects of ambient temperatures and relative humidities on the performance of air-breathing fuel cells using environmental chambers. Hottinen et al. [114] found that the air-breathing PEFC displayed the best performance at low ambient temperatures where the temperature gradient between the open cathode of the fuel cell and the ambient region is a maximum. Fabian et al. [60] showed that the maximum power density was achieved at an ambient temperature of 20°C and a relative humidity of 40%. Jeong et al. [82] also used an environmental chamber and showed that the cell performance at low current densities could be enhanced with increasing the ambient relative humidity from 20 to 100%. Chun et al. [90] improved heat dissipation of the air-breathing PEFC using thin-fin structures in the open cathode design. In a later work [91], the same research group investigated the effects of fin structures at different ambient temperatures (30 °C, 40 °C and 50 °C).

The characteristics of cathode gas diffusion layer (GDL) also play a significant role in managing the water balance within the air-breathing PEFC. O'Hayre et al. [59] developed a non-isothermal, one-dimensional numerical model and investigated the impact of GDL characteristics (i.e. GDL thickness and thermal conductivity) on an air-breathing PEFC. They showed that GDL thickness should be optimised to provide an adequate balance between heat and mass transfers, thus maximising the performance of the air-breathing fuel cell. Jeong et al. [103] reported that the performance of air-breathing PEFC was enhanced with increasing the GDL thickness from 100 to 280 μm; increasing the GDL thickness beyond 280 μm was found to adversely affect the fuel cell performance. Furthermore, the effects of the wettability of the GDL [81, 155-157] and the material and the structure of the GDL [67, 104, 105, 158] on the performance of air-breathing PEFCs have been also investigated.

The dynamic response of air-breathing PEFC is significant for small electronic devices as it directly impacts their performance and reliability. The power demand of portable devices can significantly change over time. For instance, the power demand of a smartphone may suddenly and/or significantly change as a result of the use of multiple power-demanding applications such as social media, location-aware apps, gaming, video streaming and connectivity with other devices, resulting in a power consumption from 25 mW up to 2,000 mW [159]. Hence, one of the main challenges is to make the air-breathing PEFCs as highly responsive as possible to the rapid and/or large load changes in the small electronic device. If the dynamic response of the air-breathing PEFC is sluggish, the device may experience power fluctuations or struggle to meet sudden spikes in power requirements.

MATLAB/Simulink software is often used to create dynamic models for fuel cell-based systems. Several researches have been performed to understand the dynamic characteristics of different types of fuel cells used in various applications with an ultimate aim of improving their load following abilities. Padulles et al. [160] proposed a dynamic model for power systems incorporating solid oxide fuel cells and described some modelling methodologies of the fuel cell stack and the power conditioner. They demonstrated that the dynamic model is an effective tool to determine the safe and durable operating conditions in a solid oxide fuel cell power plant. El-Sharkh et al. [161] proposed a dynamic model for a direct methanol fuel cell power plant used for residential applications and studied its transient under various load changes; they tested the model using an actual residential load profile for a period of 4 h and concluded that the dynamic model of the fuel cell power plant exhibits a good conformity. Uzunoglu and Alam [162] designed a grid-independent system for residential applications that comprises of a PEFC plant and an ultracapacitor-based storage unit that supplies extra

power during peak periods. They created a dynamic model for the system and their results showed that the combination of the above units improves the overall performance of the system and decreases the size and the cost of the PEFC unit. In a later work [163], they investigated the dynamic behaviour of the PEFC power plant operating in parallel with a battery bank to power different loads: a washing machine, a microwave, computers, transformers and a resistive load bank. The experimental data were used to validate the output of the dynamic model. They concluded that the PEFC power plant requires an extra energy storage device, such as a battery bank, to assist the PEFC during large load transients. Yalcinoz [164] proposed a dynamic model of PEFCs used to power electric bicycles. Many researchers have designed different types of controllers to improve the dynamic response of the conventional fuel cells by particularly controlling input gases flowrates such as micro-chip [36] and fuzzy logic controllers [165-168]. Morner and Klein [169] experimentally studied the dynamic behaviour of a PEFC stack to investigate the effects of humidity, temperature and air-flowrate on the transient response of the fuel cell. Unlike conventional PEFCs, there was only one study on the dynamic response of air-breathing PEFCs in the literature [74]; Yalcinoz and Alam [74] developed, using MATLAB/Simulink, a dynamic model for an air-breathing PEFC and validated it against the modelling data at an ambient temperature of 10 °C and relative humidity of 40% reported by O'Hayre et al. [59]. The above model was then integrated into a larger-in-scale dynamic model for a system powering a laptop. Notably, Yalcinoz and Alam [74] run their model for a single set of conditions and parameters.

In this study, a dynamic model for an air-breathing PEFC is developed to investigate, for the first time, the effects of the ambient conditions (temperature and relative humidity), GDL parameters (thickness and thermal conductivity) and fuel (i.e. hydrogen) utilisation on the

transient response of the fuel cell to rapid and large load alterations. Further, a previously-developed steady-state model of the fuel cell was linked to the dynamic model to provide the latter with the data representing the changes of temperature with the current density. This is an attempt to better understand the factors that may affect the response of the air-breathing fuel cells to load changes and how to improve this response.

3.3 Air-breathing PEFC Model

3.3.1 Model Characteristics and Assumptions

The dynamic model of a single air-breathing PEFC used in this study is developed within the platform of MATLAB/Simulink. The modelled fuel cell was originally fabricated and reported by Fabian et al. [60]; the geometry and the physical parameters of the fuel cell are listed in Table 3.1. The dynamics of the fuel cell model are expressed in the Laplace domain. The dynamic model consists of three main subsystems: Nernst voltage, activation losses and ohmic losses (Figure 3.1) The mass concentration losses are not considered in this model as the sharp decline in the cell voltage at high current densities of the modelled fuel cell was found to be due to the increased membrane resistance induced by the exponential increase in cell temperature at these high current densities [72]. The subsystem "Cell Temperature" shown in Figure 3.1 links the dynamic model with a steady-state model for the fuel cell that was developed in an earlier work [59, 60, 72]; namely, the steady-state model was used to feed the dynamic model with the surface temperature of the cathode GDL of the fuel cell (or simply cell temperature as the temperature difference across the components of the PEFC is relatively small, i.e. ≤ 2°C) as it changes with current density (more details are available in the introduction of Section 3.4). It should be noted that the details of the steady-state model were not included in the present in order not to distract the flow of the present work whose

main theme is the transient response of the air-breathing PEFCs; the interested reader is referred to [72] for further details about the steady-state model. The outputs of the dynamic model are the fuel cell voltage and power and below are the assumptions and considerations that have been employed for the model [60].

- Water exists only in vapour form.
- Gases are assumed to be ideal.
- The anode of the fuel cell is in dead-end mode and the fuel used is dry.
- The water activity is uniform through the membrane and is in equilibrium with water vapour activity in the cathode catalyst layer.
- The cathode catalyst layer is infinitely thin so that it could be treated as an interface between the membrane and the cathode GDL.
- The lengths of the fuel cell channels are small (i.e. 3 cm) and therefore the variation of pressure along the channel could be ignored [160].

It should be noted that Fabian et al. [60] found that some water accumulates at the cathode of the fuel cell, particularly at the intermediate current densities for certain operating conditions (low temperatures and high relative humidity). However, as the running air-breathing fuel cell was of high-performance, liquid water accumulation starts to diminish as the current density increases and this is due to the exponential increase of the cell temperature at such high current densities. Under the latter conditions, the sharp decline in the cell potential at high current densities is primarily due to membrane dehydration, not water flooding.

It is appreciated that accounting for water flooding in the steady-state model (originally developed by Ismail et al. [72]) linked to the dynamic model will make the outcomes of the

latter model more accurate. However, as water flooding may only occur in the intermediate current densities of the modelled fuel cell and has therefore no significant impact on the overall trends of the outcomes of the model, we assume that, for simplification, water only exists as a vapour; O'Hayre et al. [59] and Ismail et al. [72] considered the same assumption.

Table 3.1 Parameters in the air-breathing PEFC dynamic model [59, 60, 74].

Parameters	**Value**
Universal gas constant, R	$8.3145\ \mathrm{J/(mol.K)}$
Faraday's constant, F	$96500\ \mathrm{C/mol}$
Standard reversible fuel cell voltage, E_0	$1.23\ \mathrm{V}$
Ambient pressure, P	$1\ \mathrm{atm}$
Binary diffusivity of O_2 in air, $D_{O_2,air}$	$2.1\times10^{-5}\ \mathrm{m^2/s}$
Binary diffusivity of H_2O in air, $D_{H_2O,air}$	$2.6\times10^{-5}\ \mathrm{m^2/s}$
Length of active cell side (square), L_a	$0.03\ \mathrm{m}$
Cell active area, A_{act}	$0.0009\ \mathrm{m^2}$
Membrane thickness, L_{mem}	$5.2\times10^{-5}\ \mathrm{m}$
GDL thickness, L_{GDL}	$3.0\times10^{-4}\ \mathrm{m}$
GDL porosity, ε	0.4
GDL tortuosity, τ	3.0
GDL thermal conductivity, k_{GDL}	$10\ \mathrm{W/(m.K)}$
Activation energy, E_a	$50\ \mathrm{kJ/mol}$
Reference exchange current density, $j^0_{303\ K}$	$5\times10^{-5}\mathrm{A/cm^2}$
Lumped cell electrical resistance, R_{elec}	$12\ \mathrm{m\Omega}$
Charge transfer coefficient, α	0.28
Utilization factor, U	0.7
Hydrogen time constant, τ_{H_2}	0.3096 s
Hydrogen valve constant, K_{H_2}	$3.627\times10^{-5}\ \mathrm{mol/(s.atm)}$

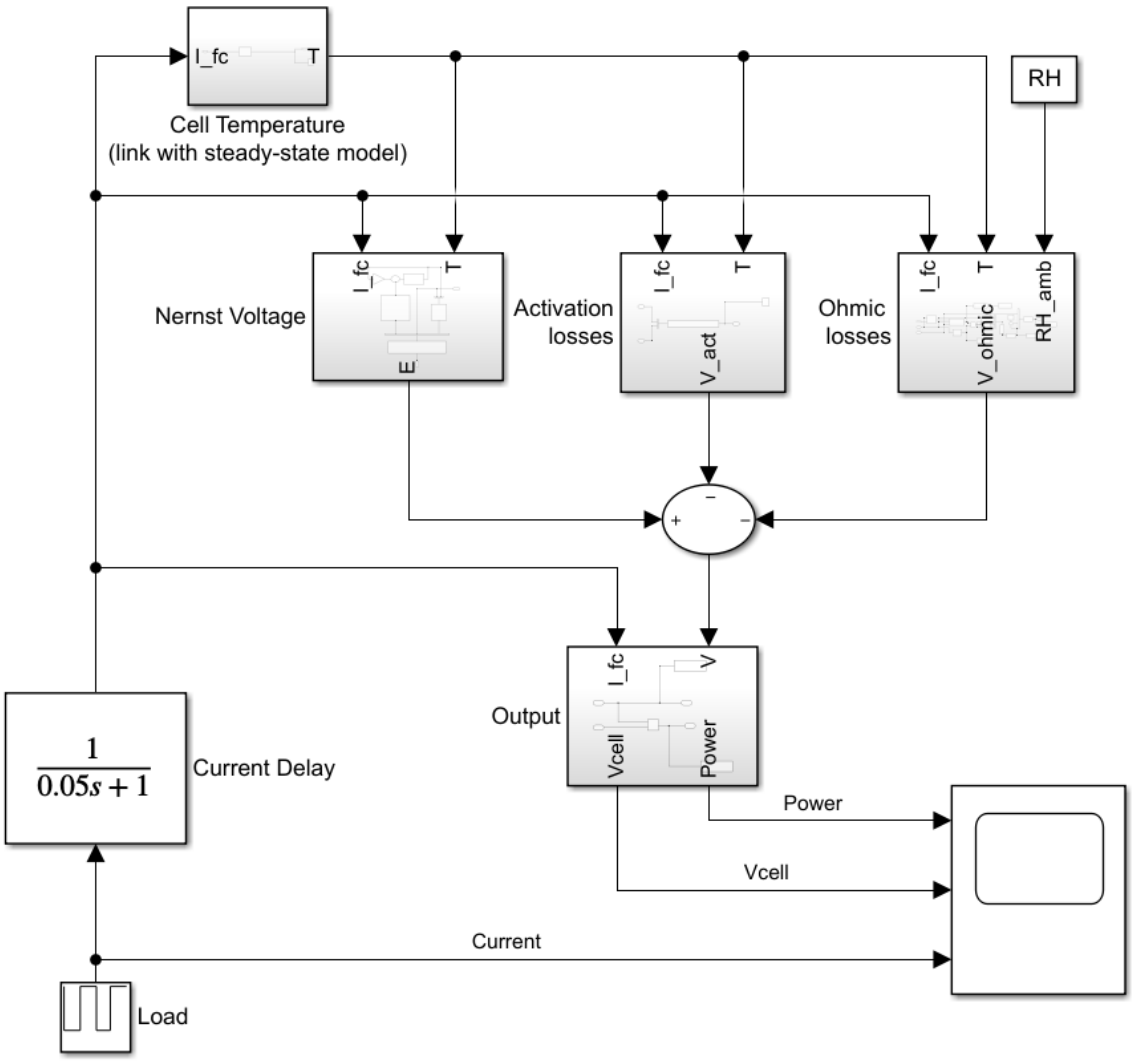

Figure 3.1 The block diagram of the air-breathing PEFC dynamic model. All the details of the subsystems are available in Appendix A.

3.3.2 Calculation of Cell Voltage

The proportional relationship between the hydrogen molar flow through a valve and its partial pressure inside the flow channel can be stated as follows [161, 165]:

$$\frac{q_{H_2}}{P_{H_2}} = K_{H_2} \qquad (3.1)$$

where q_{H_2} is the molar flow rate of hydrogen, P_{H_2} is the partial pressure of hydrogen and K_{H_2} is the molar valve constant for hydrogen.

The partial pressure of hydrogen is obtained using the ideal gas law:

$$P_{H_2} V_{an} = n_{H_2} RT \tag{3.2}$$

where V_{an} is the volume of the anode compartment [160], n_{H_2} is the number of hydrogen moles in the anode channel, R is the universal gas constant and T is the absolute temperature.

The derivation of Eq. (3.2) with respect to time gives:

$$\frac{d}{dt} P_{H_2} = \frac{RT}{V_{an}} q_{H_2} \tag{3.3}$$

The molar flow rate of hydrogen can be calculated using the following expression:

$$q_{H_2} = q_{H_2}^{in} - q_{H_2}^{out} - q_{H_2}^{r} \tag{3.4}$$

where $q_{H_2}^{in}$ is the inlet flow rate of hydrogen, $q_{H_2}^{out}$ is the outlet flow rate of hydrogen and $q_{H_2}^{r}$ is the flow rate of reacting hydrogen.

According to Faraday's second law of electrolysis, the molar flow rate of reacting hydrogen can be expressed as a function of the fuel cell current I:

$$q_{H_2}^{r} = \frac{I}{2F} \tag{3.5}$$

where F is the Faraday's constant. Substituting Eq. (3.4) and Eq. (3.5) into Eq. (3.3) gives:

$$\frac{d}{dt} P_{H_2} = \frac{RT}{V_{an}} \left(q_{H_2}^{in} - q_{H_2}^{out} - \frac{I}{2F}\right) \tag{3.6}$$

After replacing the output hydrogen flow given by Eq. (3.1) into Eq. (3.6), the partial pressure of the hydrogen can be determined in the Laplace domain as [160-163, 165, 170] :

$$P_{H_2} = \frac{1/K_{H_2}}{1 + \tau_{H_2} s}\left(q_{H_2}^{in} - \frac{I}{2F}\right) \tag{3.7}$$

where τ_{H_2} is hydrogen time constant and given by:

$$\tau_{H_2} = \frac{V_{an}}{K_{H_2} RT} \tag{3.8}$$

and the derivation of Eq. (3.7) is given in Appendix B. The partial pressure of the oxygen, P_{O_2}, in the open cathode compartment is given by [74]:

$$P_{O_2} = x_{O_2} P = x_{O_2}^0 - L_{GDL} \frac{jRT}{4F D_{O_2}^{eff}} \tag{3.9}$$

where $x_{O_2}^0$ is the mole fraction of the oxygen in the ambient (i.e. 0.21), L_{GDL} is the GDL thickness, j is the current density, P is the ambient pressure (i.e. 1 atm) and $D_{O_2}^{eff}$ is the effective diffusivity of oxygen into air given by:

$$D_{O_2}^{eff} = \frac{\varepsilon}{\tau} D_{O_2,air} \tag{3.10}$$

where $D_{O_2,air}$ is the binary diffusivity of oxygen into air and ε is the porosity, the ratio of void spaces to the total volume of the GDL (dimensionless). τ is the tortuosity which is dimensionless and is a measure of how tortuous the pathway is for the transport of gases within the GDL.

The reversible (or Nernst) voltage of the fuel cell (E) is obtained using Nernst equation [8]:

$$E = E_0 + \frac{RT}{2F} \ln\left(P_{H_2} . P_{O_2}^{1/2}\right) \tag{3.11}$$

where E_0 represents the standard reversible fuel cell voltage (i.e. 1.23 V). The block diagram of the Nernst voltage is shown in Figure 3.2.

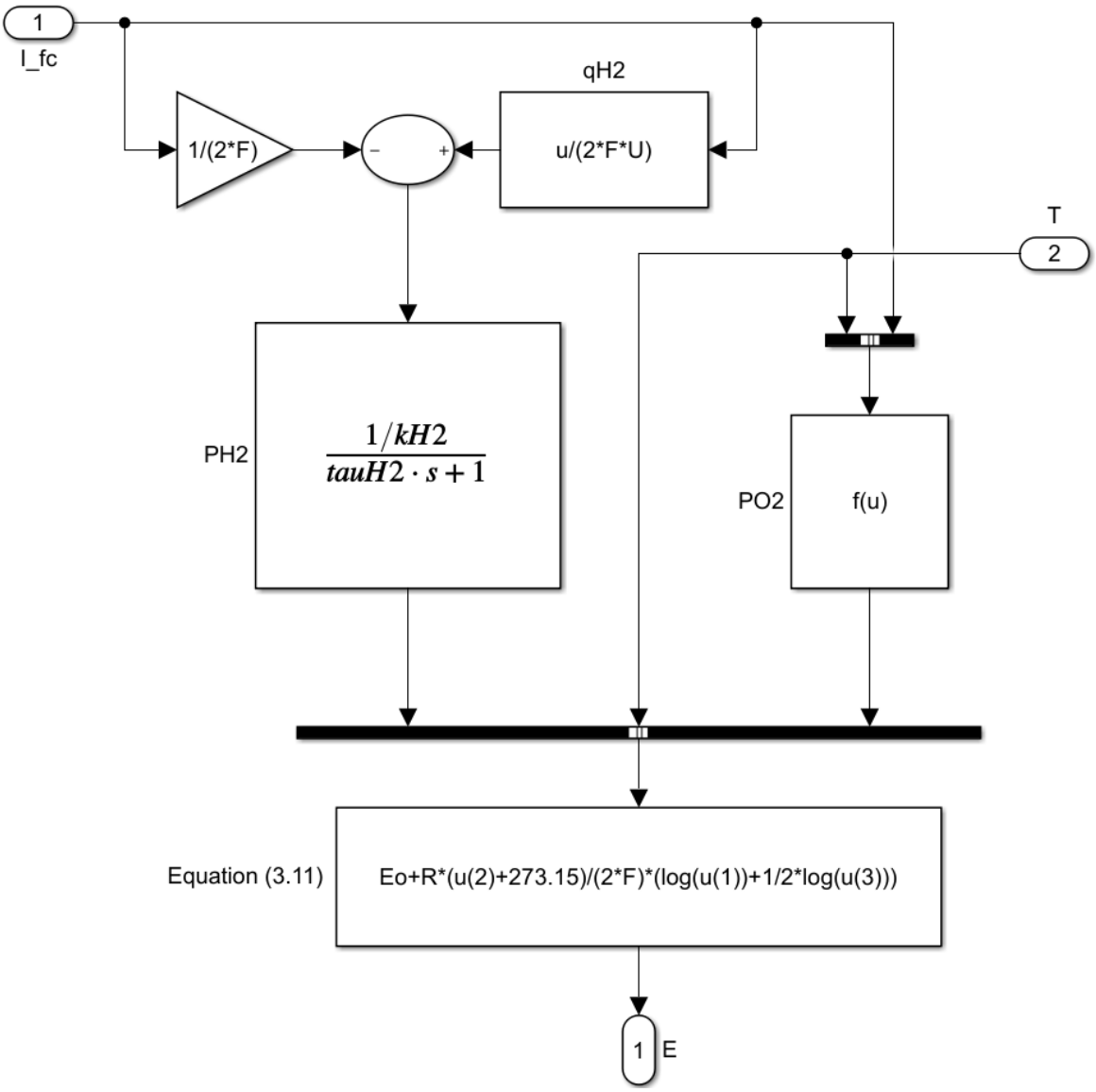

Figure 3.2 The block diagram of the Nernst voltage.

The activation losses associated with the energy required to drive the electrochemical reaction at the catalyst layer, η_{act}, are obtained using the equation [74]:

$$\eta_{act} = \frac{RT}{2\alpha F}\ln\left(\frac{j}{j_0}\right) \qquad (3.12)$$

where α is the charge transfer coefficient and j_0 is the reference exchange current density, which can be corrected for temperature by the following expression:

$$j_0 = j^0_{303\,K} \exp\left[\frac{E_a}{R}\left(\frac{1}{303} - \frac{1}{T}\right)\right] \tag{3.13}$$

where E_a is the activation energy for the oxygen reduction reaction. The ohmic losses occur due to the resistance of the ionic and electronic conductive materials to the flow of protons and electrons, respectively; η_{ohmic}, can be calculated as follows [72]:

$$\eta_{ohmic} = jA_{act}(R_{elec} + R_{mem}) \tag{3.14}$$

where A_{act} is the active area of the fuel cell, R_{elec} represents the lumped electrical resistance of the cell and R_{mem} is the membrane resistance and is defined as follows:

$$R_{mem} = \frac{L_{mem}}{A_{act}\sigma_{mem}} \tag{3.15}$$

where L_{mem} is the thickness of the Nafion® membrane and σ_{mem} represents the ionic conductivity of the membrane which is given by [79]:

$$\sigma_{mem} = (3.46a^3 + 0.0161a^2 + 1.45a - 0.175) \exp\left[1268\left(\frac{1}{303} - \frac{1}{T}\right)\right] \tag{3.16}$$

The water activity a in Eq. (3.16) is defined as follows [8]:

$$a = \frac{P_{H_2O}}{P_{sat}} \tag{3.17}$$

where P_{H_2O} and P_{sat} are respectively the partial pressure and saturation pressure of water vapour at the fuel cell temperature. P_{sat} is obtained by [77]:

$$log_{10}P_{sat} = -2.1794 + 0.02953(T - 273.15) - 9.1837 \times 10^{-5}(T - 273.15)^2 + 1.4454 \times 10^{-7}(T - 273.15)^3 \tag{3.18}$$

A similar equation to Eq. (3.9) can be used to calculate the partial pressure of water vapour:

$$P_{H_2O} = x_{H_2O}P = x^0_{H_2O} + L_{GDL}\frac{jRT}{2FD^{eff}_{H_2O}} \quad (3.19)$$

$$x^0_{H_2O} = \frac{RH \times P_{sat}}{100} \quad (3.20)$$

where $x^0_{H_2O}$ is the mole fraction of the water vapour in the ambient, RH is the ambient relative humidity and $D^{eff}_{H_2O}$ is the effective diffusivity of water into air and is given by:

$$D^{eff}_{H_2O} = \frac{\varepsilon}{\tau} D_{H_2O,air} \quad (3.21)$$

Having calculated the Nernst voltage (Eq. (3.11)), the activation losses (Eq. (3.12)) and ohmic losses (Eq. (3.14)), the cell potential of the air-breathing PEFC, V_{cell}, could be then calculated:

$$V_{cell} = E - \eta_{act} - \eta_{ohmic} \quad (3.22)$$

The concentration losses have not been taken into account in the model as the factors that cause them were always found to be rather insignificant in our simulation: the water activity was always less then unity, thus signalling that there was no liquid water saturation and there was always abundance of reactant gasses available for the reaction even at high current densities.

3.4 Model Validation

The air-breathing PEFC dynamic model is validated against the experimental data reported by Fabian et al. [60]. Figure 3.3a shows the polarisation curves generated by the model (when reaching steady state conditions) at an ambient relative humidity of 40% and ambient temperatures of 10, 20 and 30 °C. The results are in a good agreement with the corresponding experimental polarisation curves, and moreover, the decline in the fuel cell performance with increasing ambient temperature is well captured by the fuel cell model. It is noteworthy that

the only fitting parameter in the model is the reference exchange current density. The data showing the variation of the surface temperature of the open cathode with the current density of the fuel cell for the set of variables investigated in this study (i.e. the ambient conditions of temperature and relative humidity, the thickness and the thermal conductivity of the cathode GDL and hydrogen utilisation) was generated from a steady-state model developed and reported in a previous work [72]. The above data were fitted using high order polynomials and directly linked to the dynamic model; Appendix B presents some example polynomials. Figure 3.3b shows that the model (after reaching steady state conditions) predicts well the change of the surface temperature with ambient temperature and current density. In particular, the sharp increases in the GDL surface temperature at high current densities are captured well by the model. Such good agreements between the outputs of the model and the experimental data over a wide range of ambient temperatures impart a high degree of confidence in the prediction abilities of the developed model.

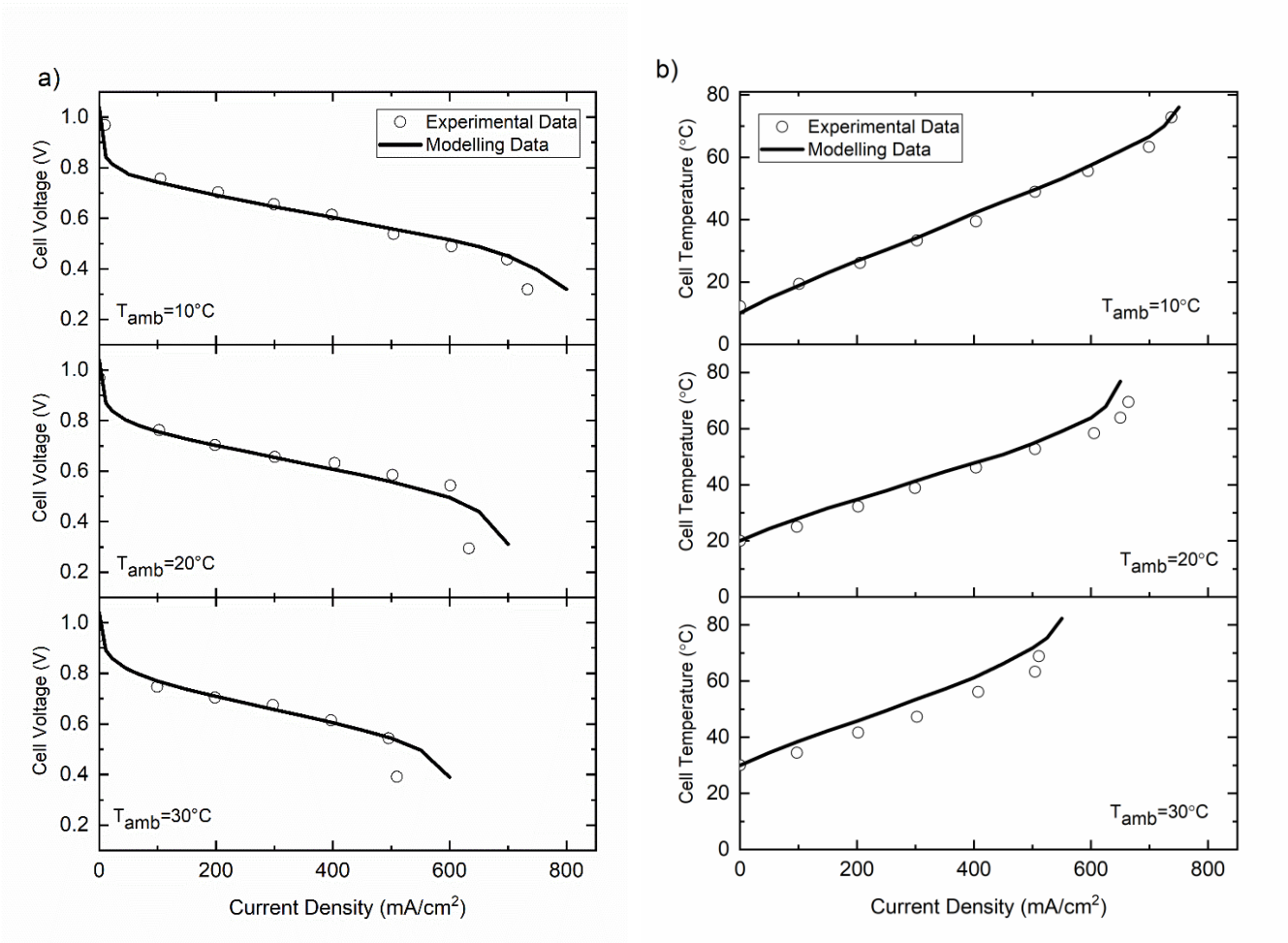

Figure 3.3 Modelling and experimental data for an air-breathing PEFC operating under an ambient RH of 40% and ambient temperatures of 10,20 and 30 ℃: (a) the polarisation curves and (b) the cell temperature of the cathode GDL as a function of current density.

3.5 Results and Discussion

3.5.1 Transient Operation

The current was, using the "Repeating Sequence Stairs" built-in function in Simulink, programmed to rapidly change between low (i.e. 1 A) and high (i.e. 5 A) values after each 300 s for 2400 s; 300 s was experimentally found to be sufficient for the potential of the air-breathing fuel cell to stabilise [60]. The evolution of the fuel cell temperature with time was modelled by Kim et al. [171]:

$$T(t) = T_2 + (T_1 - T_2) \times \exp(-0.0295t) \qquad (3.23)$$

where T_1 is the steady cell temperature before applying the current step change and T_2 is the steady cell temperature after applying the step change. Note that both T_1 and T_2 are provided by the steady-state model linked to the dynamic model as described in Section 3.4.

Figure 3.4 demonstrates that the fuel cell current alternates between 1 and 5 A under ambient conditions of 40% relative humidity and 20 °C. It can be seen that the step change of the current causes the fuel cell temperature to sharply increase/decrease before starting to stabilise after around 100 s of the step change.

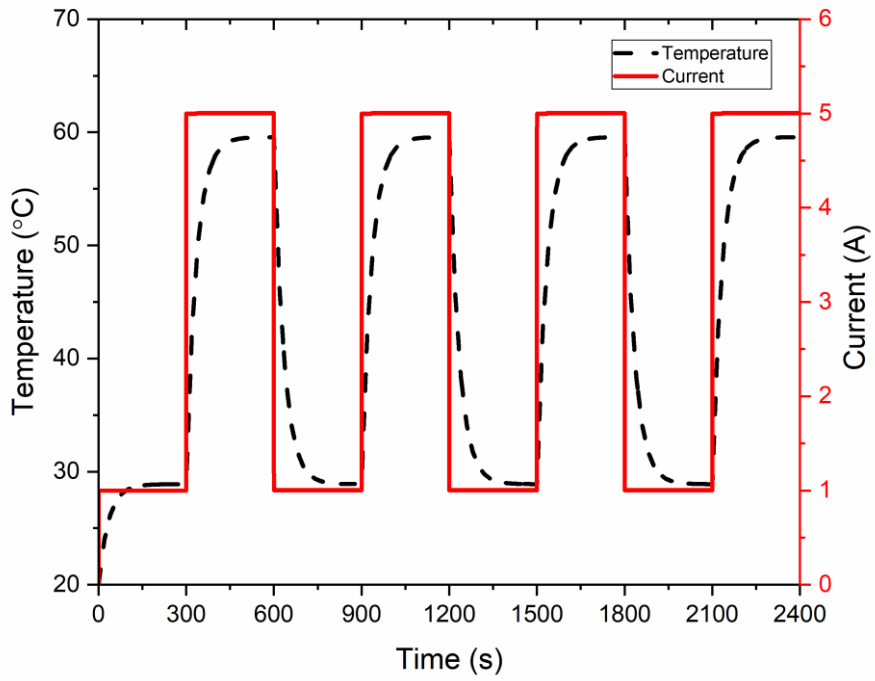

Figure 3.4 The fuel cell temperature as it changes with alternating 4-A step changes in the fuel cell current under ambient conditions of 40% RH and 20 °C.

3.5.2 Effect of Ambient Temperature

Figure 3.5 shows the effects of the ambient temperature on the dynamic behaviour and the performance of the fuel cell for a given ambient relative humidity of 40%. The figure shows

there exists an optimum ambient temperature at which the fuel cell performance is maximised, i.e. 20 ℃. The activation and ohmic losses at this ambient temperature are of reasonable values. On the other hand, a relatively high ambient temperature (i.e. 30 ℃) causes an increase in fuel cell temperature (Figure 3.5a) and an exponential increases in the saturation pressure of the water vapour, thus decreasing the water content and ionic conductivity of the membrane phase and ultimately increasing the ohmic losses (Figure 3.5d). This also causes the output power of the fuel cell to have an increased overshoot when changing to a high current step (Figure 3.5c). It is noteworthy that the overshoots in the output power of the fuel cell that occur as a result of the current step changes are similar to those obtained by Uzunoglu and Alam [162]. On the other hand, a relatively low ambient temperature (i.e. 10 ℃) results in less ohmic losses but higher activation losses compared to those of 20℃ ambient temperature.

Figure 3.5d shows that, when changing to a high current step, the ohmic losses start to decrease and then increase with different rates for different ambient temperatures before stabilisation. This is attributed to the two-field effect of the temperature as evident from Equations (3.16-3.18). Namely, as the current is increased to 5 A, the cell temperature increases causing an initial increase in the ionic conductivity of the membrane phase (Eq. (3.16)). However, as time passes, this positive effect of the cell temperature on the ionic conductivity is outweighed by the exponential increase in the saturation pressure of the water vapour with increasing temperature (Eq. (3.18)) which eventually leads to a decrease in the water content and the ionic conductivity of the membrane phase before reaching the steady state values.

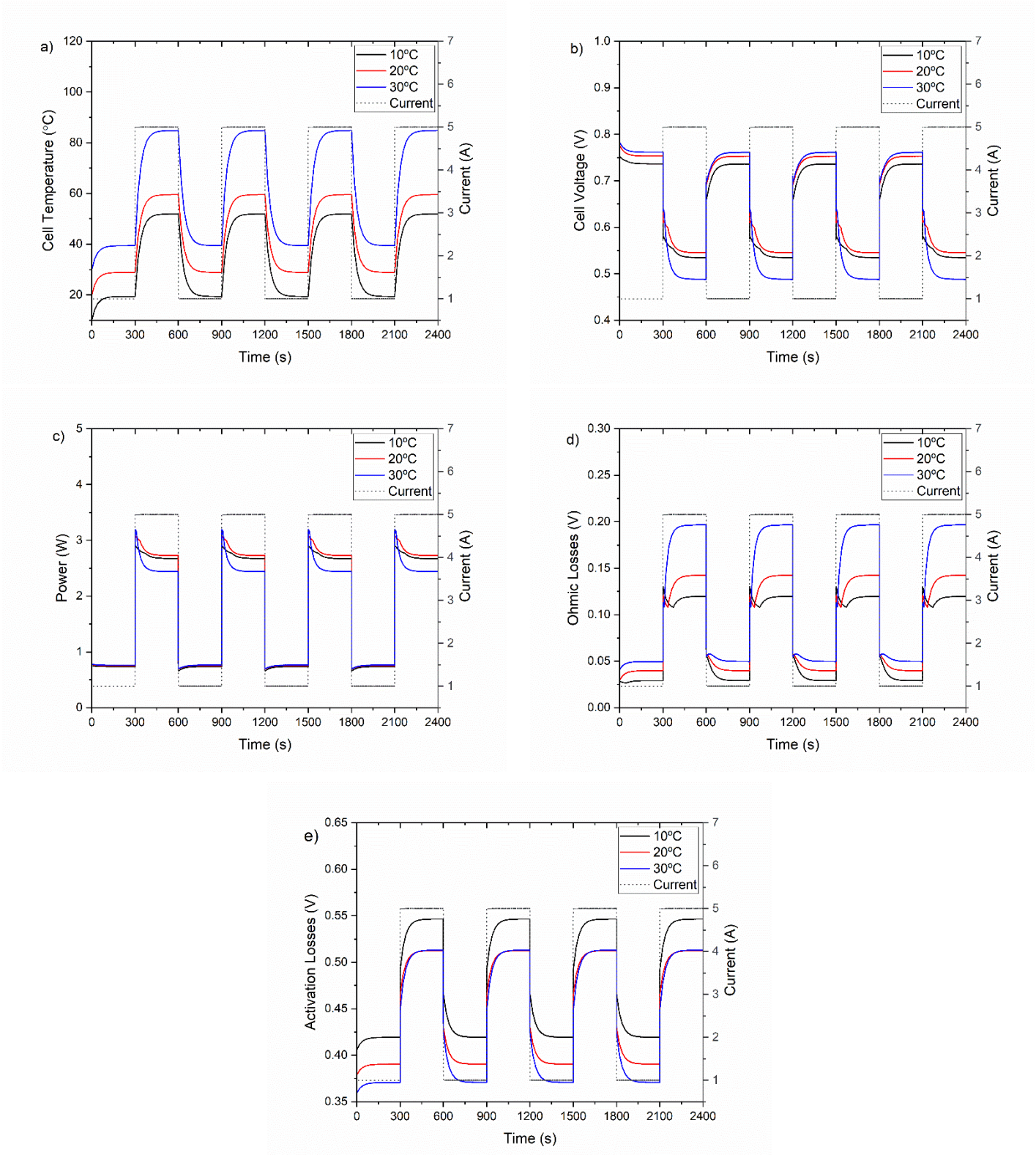

Figure 3.5 Transient profiles for: (a) cell temperature, (b) voltage, (c) output power, (d) ohmic losses and (e) activation losses of air-breathing PEFC under different values for the ambient temperature and a constant ambient relative humidity of 40%.

3.5.3 Effect of Ambient Relative Humidity

Figure 3.6 shows the effect of the ambient relative humidity on the dynamic behaviour and the performance of the fuel cell for a given ambient temperature of 20 °C. The fuel cell temperature is lowest with an ambient relative humidity of 40% (Figure 3.6a); this could be attributed to the heat sources: the product of the current density and each one of the ohmic losses and the activation losses. Namely, the ohmic losses with 40% relative humidity are less than those with 20% relative humidity (Figure 3.6d) and this is due to better membrane hydration with 40% relative humidity. Equally, the activation losses with 40% relative humidity are less than those with 60 and 80% relative humidity (Figure 3.6e) and this is due to less current densities demonstrated by the former case (i.e. 40% relative humidity). Such combined effects of activation and ohmic losses result in 40% relative humidity case having the lowest cell temperature.

Apart from 40% relative humidity, the temperature profile of the fuel cell at 1 A is almost the same for the ambient relative humidity of 20, 60 and 80%, while at 5A the temperature slightly decreases with increasing relative humidity from 20 to 80%. Figure 3.6b and Figure 3.6c show that, when changing to a high current step, the overshoot is a maximum with the lowest relative humidity (i.e. 20%), especially at high current intervals, and this is due to the increased ionic resistance, caused by membrane dry-out, at this low RH; this is evident from the ohmic losses profiles shown in Figure 3.6d. On the other hand, the overshoots become less profound with increasing ambient relative humidity and this is more apparent at high current intervals where the fuel cell is more ohmic losses limited; this signals that the well-hydrated membrane enhances the dynamic behaviour of the air-breathing PEFC.

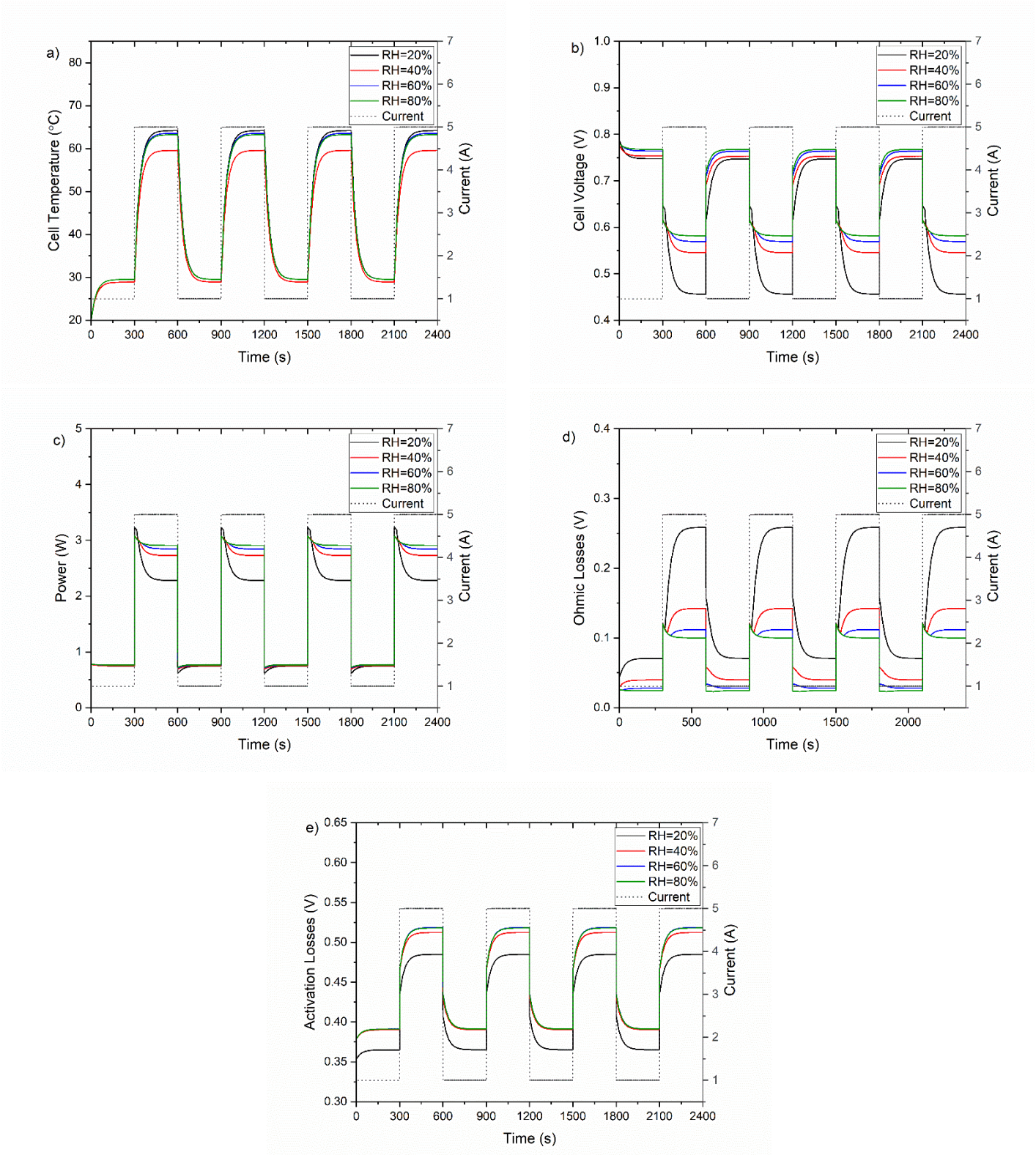

Figure 3.6 Transient profiles for: (a) cell temperature, (b) voltage, (c) output power, (d) ohmic losses and (e) activation losses of air-breathing PEFC under different values for the ambient relative humidity and a constant ambient temperature of 20 °C.

3.5.4 Effect of GDL Thickness

Figure 3.7 shows the effects of the cathode GDL thickness on the dynamic behaviour and the performance of the fuel cell for given ambient conditions of 20°C and 40% RH. Overall, the figure shows that there exists an optimum GDL thickness at which the dynamic response and the performance of the fuel cell are maximised: 500 μm. This thickness provides a good balance between the ohmic and activation losses; see Figure 3.7(d-e). Too thin GDL (i.e. 100 μm) ensures a fast supply of oxygen to the catalyst layer (Figure 3.7f) and subsequently the decrease in the activation losses (Figure 3.7e). However, this too thin GDL (compared to other thicknesses) allows for more transfer of the produced water (required to humidify the membrane phase) from the cathode catalyst layer to the ambient; this leads to a lower ionic conductivity, increased ohmic losses (Figure 3.7d)) and a high overshoot (Figure 3.7c). On the other hand, too thick GDL (i.e. 700 μm) increases the mass transport resistance, leading to: (i) more produced water being available for membrane humidification, higher ionic conductivity and less ohmic losses (Figure 3.7d) and (ii) less oxygen being available for the reaction at the cathode catalyst layer (Figure 3.7f), and higher activation losses (Figure 3.7e). The transient temperature profile (Figure 3.7a) shows a slightly different trend: the lowest surface temperature is demonstrated by not the 500 μm thick GDL but by the 300 μm thick GDL and this is attributed to the shorter thermal pathway of the latter GDL. The highest surface temperature is featured by the 100 μm thick GDL and this is due to the substantial ohmic losses demonstrated by this GDL. It should be noted that, due to the higher consumption of oxygen and production of water rates, all the above effects are significantly more profound at high current steps (i.e. 5 A).

The above results reveal that the GDL thickness should be optimized to ensure obtaining reasonable values for the activation (through increasing the supply rate of oxygen to the catalyst layer) and ohmic (through decreasing the rejection rate of produced water required for humidification of membrane phase) losses.

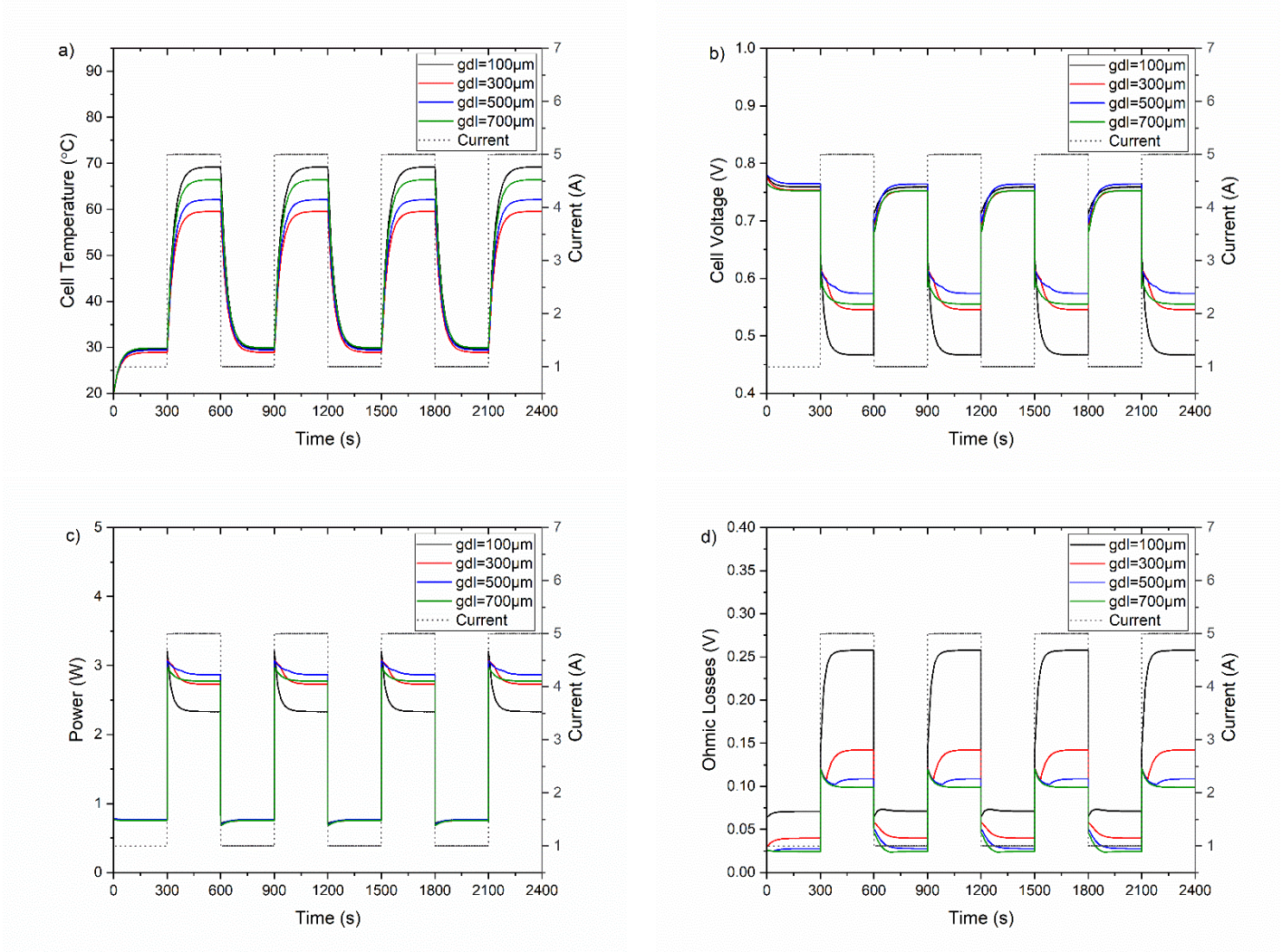

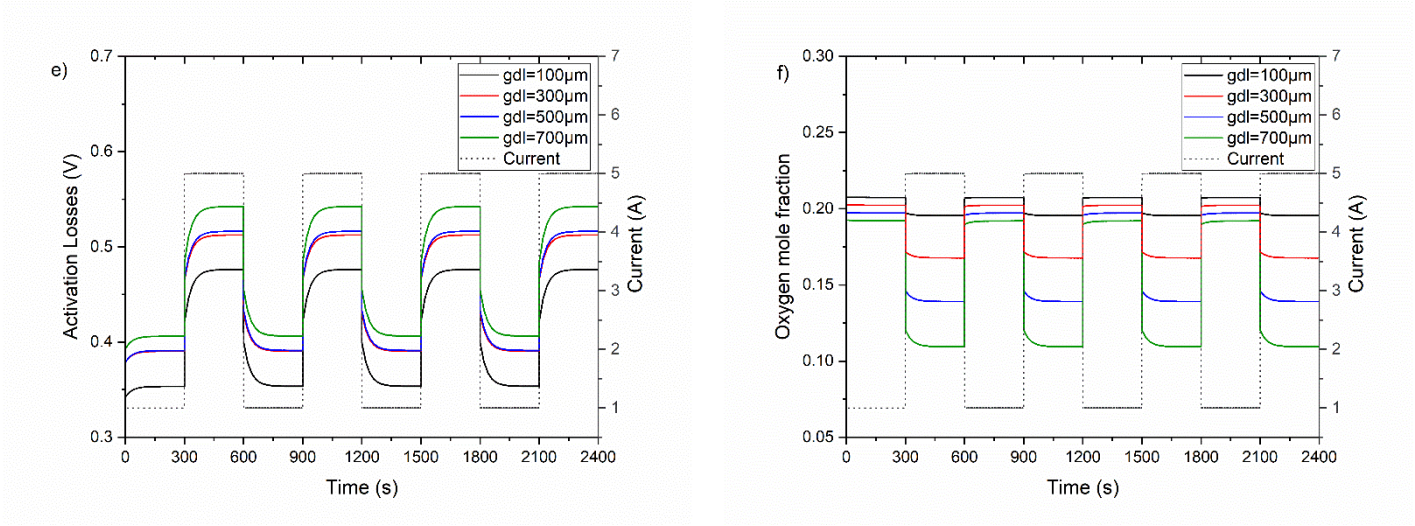

Figure 3.7 Transient profiles for: (a) cell temperature, (b) voltage, (c) output power, (d) ohmic losses, (e) activation losses and (f) oxygen mole fraction of the air breathing PEFC under a variety of GDL thicknesses for the ambient conditions of 20 °C and 40% relative humidity.

3.5.5 Effect of GDL Thermal Conductivity

Figure 3.8 shows the effects of cathode GDL thermal conductivity on the dynamic behaviour and the performance of the fuel cell for given ambient conditions of 20 °C and 40% RH. As with [59], the base value of the GDL thermal conductivity is 10 $\mathrm{W/(m.K)}$. The 1-100 $\mathrm{W/(m.K)}$ range was selected to cover a variety of materials that could be possibly used for the GDLs: the metal-based GDLs whose thermal conductivity is of the order 100 $\mathrm{W/(m.K)}$ and conventional GDLs whose carbon fibres are mainly oriented in the transverse directions (1 $\mathrm{W/(m.K)}$) [172, 173]. The figure shows that the fuel cell performance becomes better as the GDL thermal conductivity increases. The transient behaviour also shows significantly less overshoot with higher thermal conductivities (Figure 3.8c). Nonetheless, the fuel cell demonstrates an asymptotic behaviour with increasing GDL thermal conductivity; no performance gain is obtained with a thermal conductivity higher than 30 $\mathrm{W/(m.K)}$. On the other hand, extremely low thermal conductivity (i.e. 1 $\mathrm{W/(m.K)}$) significantly lowers the fuel cell performance and incurs a substantial overshoot when abruptly changing to a high current step. Such a low thermal conductivity significantly decreases the dissipation rate of

heat and subsequently increases the fuel cell temperature (Figure 3.8a), exponentially increases the saturation pressure of water, decreases the water content and ionic conductivity of the membrane phase and ultimately significantly increases the ohmic losses (Figure 3.8d). It should be noted that the effects of the thermal conductivity are indirectly taken into account through the cell temperature- current density data generated by the steady-state model linked to the dynamic model.

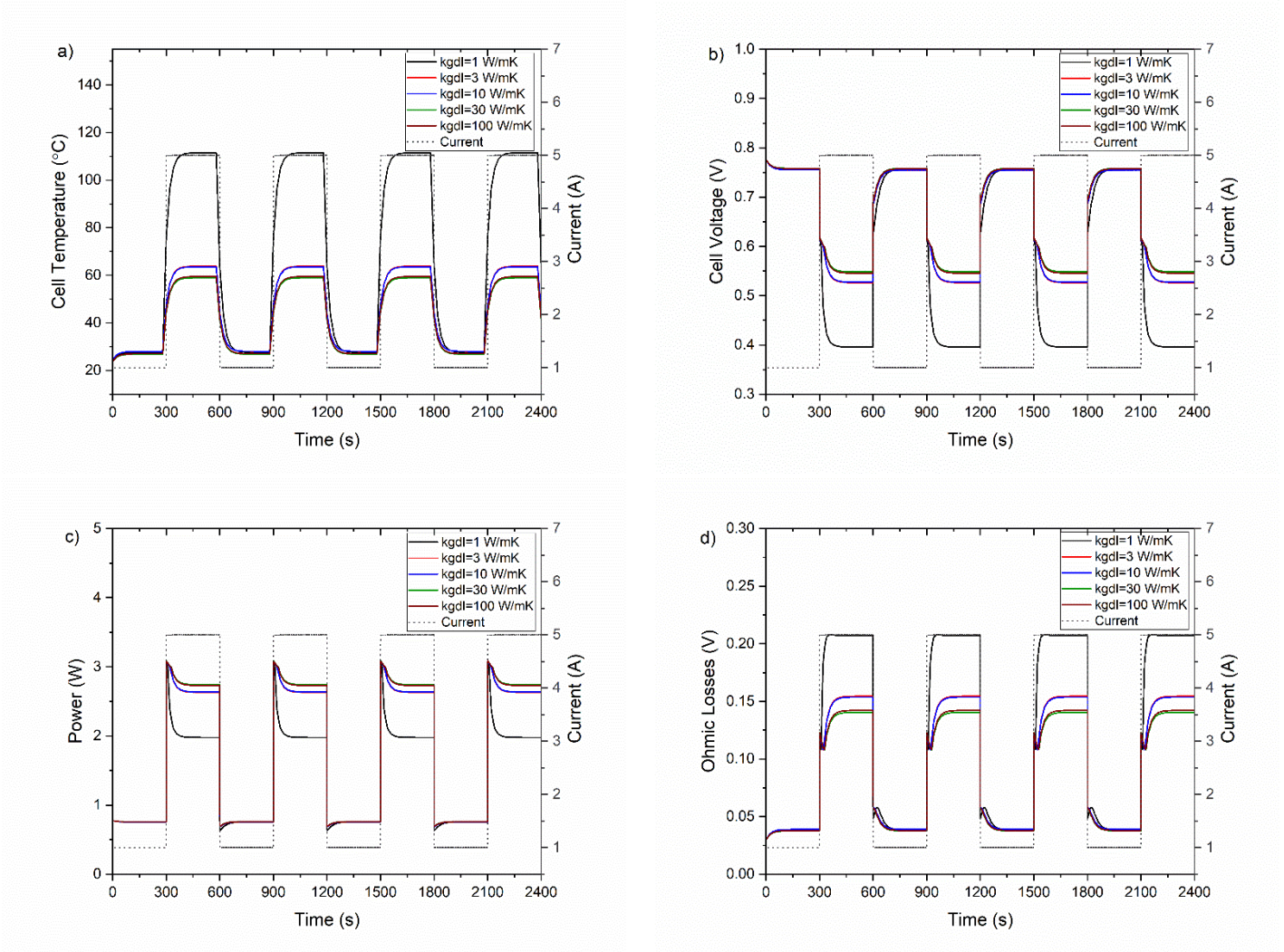

Figure 3.8 Transient profiles for: (a) cell temperature, (b) voltage, (c) output power and (d) ohmic losses of the air breathing PEFC under a variety of GDL thermal conductivity for the ambient conditions of 20 °C and 40% relative humidity.

3.5.6 Effect of Hydrogen Utilisation

Figure 3.9 shows the effects of the hydrogen utilisation (i.e. the portion of the supplied fuel that is consumed in the reaction) on the dynamic behaviour and the performance of the fuel cell for given ambient conditions of 20 °C and 40% RH. It was found that the hydrogen utilisation has no effect on the activation and ohmic losses (not shown) and consequently no impact on the dynamic behaviour of the fuel cell. However, the figure shows that the fuel cell performance improves with decreasing hydrogen utilisation. As the hydrogen utilisation decreases, a higher hydrogen flow rate is provided, thus increasing the partial pressure of hydrogen and subsequently the Nernst voltage of the fuel cell (Eq. (3.11)).

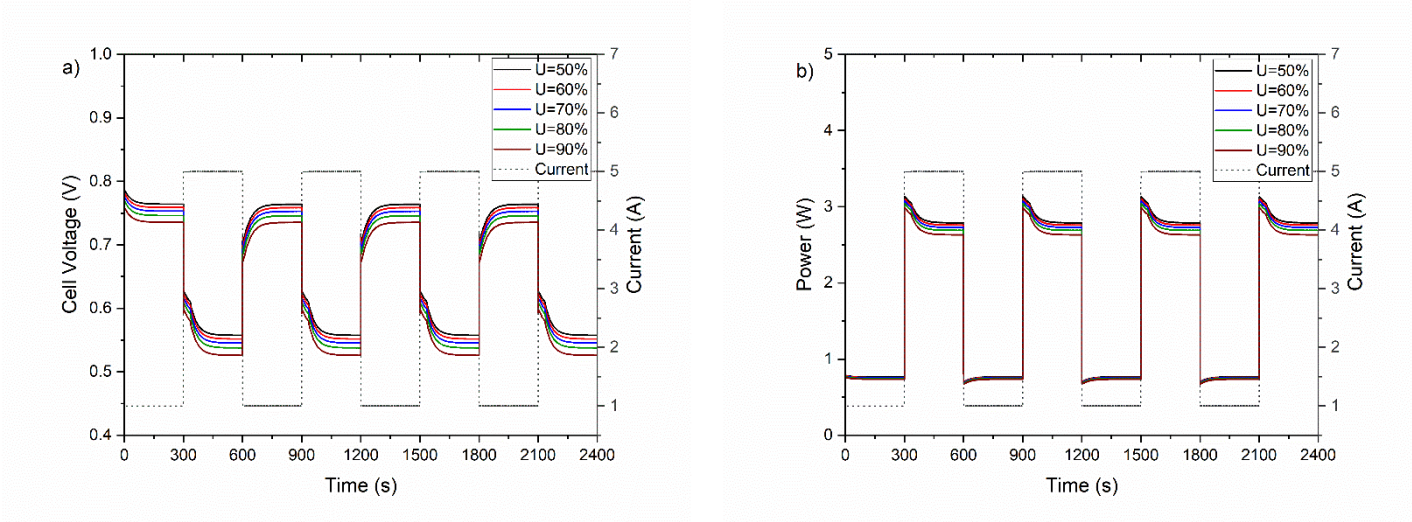

Figure 3.9 Transient profiles for: (a) voltage and (b) output power of the air breathing PEFC under a variety values of hydrogen utilisation for the ambient conditions of 20 °C and 40% relative humidity.

3.6 Conclusions

A dynamic model has been developed for an air-breathing PEFC to analyse its transient response to load changes and explore the sensitivity of this response to the ambient conditions, GDL parameters and hydrogen utilisation. A previously developed steady-state model for the fuel cell was directly linked to the dynamic model to provide the latter with the

data of the fuel cell temperature changing with the current density. The following are the key findings of the study:

- Relatively high ambient temperature and low ambient relative humidity result in significant overshoots when changing from low load (1 A) to high load (5 A) and this is due to the substantial increase in the ohmic losses, caused by the membrane dry-out, under the above ambient conditions. 20 °C was found to be the optimum ambient temperature at which the fuel cell demonstrates less overshoot and better steady state performance as a good balance between the activation and the ohmic losses is achieved at this ambient temperature. On the other hand, the transient and the steady state performances of the fuel cell were found to be improve with increasing relative humidity due to the same reasons mentioned for the optimum temperature of 20 °C.

- The cathode GDL thickness requires to be optimised to ensure reasonable transient and steady state cell performances; it was found to be 500 µm in this study. Too thin GDL (e.g. 100 µm) increases the supply rate of oxygen to the catalyst layer but at the same time increases the rejection rate of water required for the humidification of the membrane phase, thus resulting in high ohmic losses, significant overshoot and poor performance when changing to a high load. On the other hand, too thick GDL (e.g. 700 µm) ensures a good retention of water required for the membrane humidification but impacts on the transport rate of oxygen to the catalyst layer.

- The thermal conductivity of the cathode GDL requires to be reasonably high (e.g. ~ 30 $\mathrm{W/(m.K)}$). Extremely low thermal conductivity (e.g. 1 $\mathrm{W/(m.K)}$) hinders the rate of heat dissipation, thus leading to an unacceptable decrease in the ionic conductivity

of the membrane phase and a subsequent increase in the ohmic losses that ultimately results in a high overshoot and poor performance. On the other hand, no performance gain was observed beyond a GDL thermal conductivity of 30 $\mathrm{W/(m.K)}$.

- Hydrogen utilisation has no effect on the dynamic response of the fuel cell to the load changes. However, as it decreases, the fuel cell performance becomes slightly better as the amount of hydrogen supplied to the anodic compartment increases, increasing the partial pressure of hydrogen and subsequently the theoretical open circuit voltage (i.e. Nernst voltage) of the fuel cell. However, hydrogen utilisation is typically aimed to be maximised in order to save the fuel cost.

Acknowledgements

Fatma Calili thanks the Ministry of National Education at the Republic of Turkey for funding her PhD studentship at the University of Sheffield.

Nomenclature

Roman symbols

a	Water activity
A_{act}	Active area of the fuel cell, $\mathrm{m^2}$
$D_{H_2O}^{eff}$	Effective diffusivity of water into air, $\mathrm{m^2/s}$
$D_{H_2O,air}$	Binary diffusivity of water into air, $\mathrm{m^2/s}$
$D_{O_2}^{eff}$	Effective diffusivity of oxygen into air, $\mathrm{m^2/s}$
$D_{O_{2,}air}$	Binary diffusivity of oxygen into air $\mathrm{m^2/s}$
E	Nernst Voltage, V
E_a	Activation energy, $\mathrm{J/mol}$
E_0	Standard fuel cell voltage, V
F	Faraday's constant, $\mathrm{C/mol}$
j	Current density, $\mathrm{A/m^2}$

j_0	Reference exchange current density, $\mathrm{A/m^2}$
I	Electric current, A
k_{GDL}	GDL Thermal conductivity, $\mathrm{W/(m.K)}$
K_{H_2}	Hydrogen valve constant, $\mathrm{mol/(atm.s)}$
L_{GDL}	GDL thickness, m
L_{mem}	Membrane thickness, m
n_{H_2}	Number of hydrogen moles
P	Ambient pressure, atm
P_{H_2}	Partial pressure of hydrogen, atm
P_{H_2O}	Partial pressure of water vapour, atm
P_{sat}	Water vapour saturation pressure, atm
P_{O_2}	Partial pressure of oxygen, atm
q_{H_2}	Hydrogen molar flow, $\mathrm{mol/s}$
R	Universal Gas Constant, $\mathrm{atm/(mol.K)}$
RH	Relative humidity, $\%$
R_{elec}	Lumped electrical cell resistance, Ω
R_{mem}	Membrane resistance, Ω
T	Absolute temperature, K
U	Utilization factor
V_{an}	Anode volume, $\mathrm{m^3}$
V_{cell}	Cell voltage, V
x	Mole fraction

Greek symbols

α	Charge transfer coefficient
ε	Porosity
η_{act}	Activation over voltage, V
η_{ohmic}	Ohmic over voltage, V
σ_{mem}	Ionic conductivity, $\mathrm{S/m}$
τ	Tortuosity
τ_{H_2}	Hydrogen time constant, s

Appendix A: Subsystems in Figure 3.1

The block diagram of a dynamic model for an air-breathing PEFC built in MATLAB/Simulink is shown in Figure 3.1. This model comprises into three fundamental subsystems: Nernst voltage, activation losses, and ohmic losses. Notably, the block diagram for the Nernst voltage subsystem is explicitly presented in Figure 3.2. This appendix provides the block diagrams of activation losses in Figure A. 1 and ohmic losses in Figure A. 2.

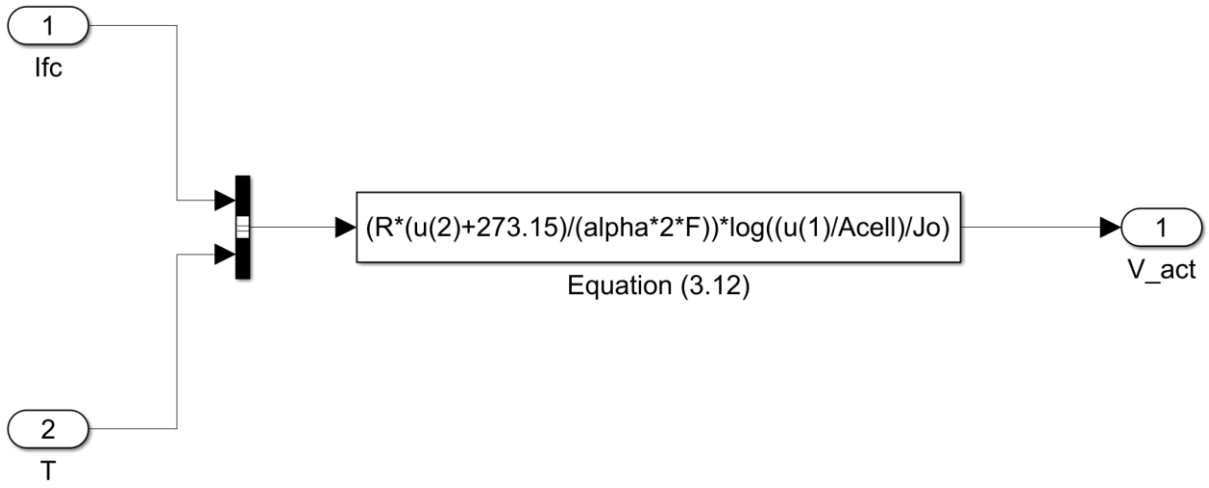

Figure A. 1 The block diagram of activation losses.

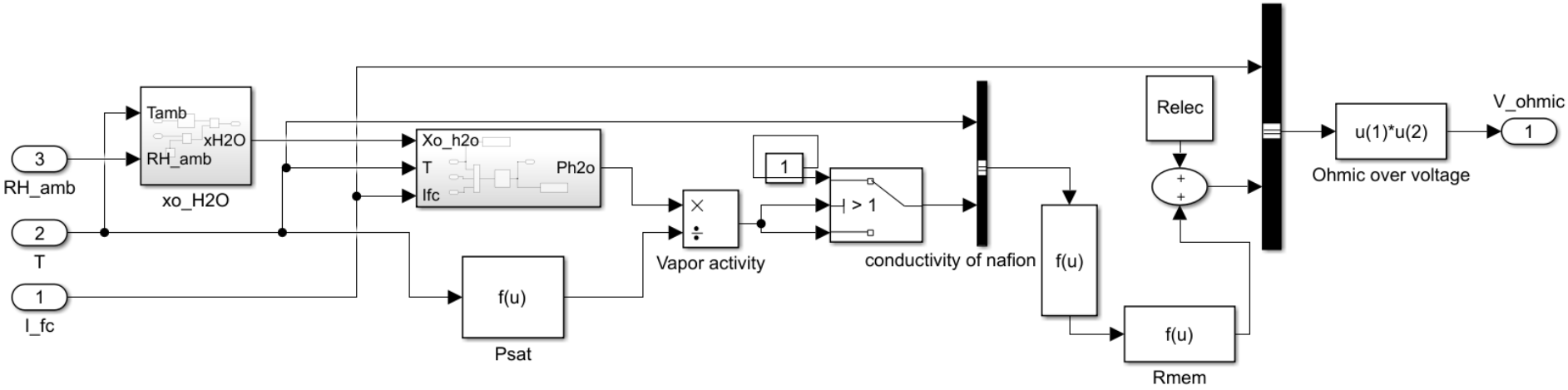

Figure A. 2 The block diagram of ohmic losses.

Appendix B: Derivation of Eq. (3.7)

Partial pressure of hydrogen flow in Laplace domain (Eq. (3.7)) can be derived by following steps:

$$q_{H_2}^{out} = K_{H_2}.P_{H_2} \tag{B.1}$$

Substituting Eq. (A.1) into Eq. (3.6):

$$\frac{d}{dt}P_{H_2} = \frac{RT}{V_{an}}(q_{H_2}^{in} - K_{H_2}.P_{H_2} - \frac{I}{2F}) \tag{B.2}$$

In Laplace domain:

$$\mathcal{L}\big(P_{H_2}(t)\big) = P_{H_2}(s) \tag{B.3}$$

$$\mathcal{L}\left(\frac{d}{dt}P_{H_2}(t)\right) = sP_{H_2}(s) \tag{B.4}$$

Substituting Eq. (B.3) and Eq. (B.4) into Eq. (B.3):

$$sP_{H_2}(s) = \frac{RT}{V_{an}}(q_{H_2}^{in} - K_{H_2}.P_{H_2}(s) - \frac{I}{2F}) \tag{B.5}$$

$P_{H_2}(s)$ can be determined as follows:

$$P_{H_2}(s) = \frac{{}^{1}/_{K_{H_2}}}{1 + \frac{V_{an}}{K_{H_2}RT}s}(q_{H_2}^{in} - \frac{I}{2F}) \tag{B.6}$$

where $\frac{V_{an}}{K_{H_2}RT}$ is hydrogen time constant, τ_{H_2} (Eq. (3.8)) and final form of the partial pressure of hydrogen flow in Laplace domain is given by:

$$P_{H_2}(s) = \frac{{}^{1}/_{K_{H_2}}}{1 + \tau_{H_2}s}(q_{H_2}^{in} - \frac{I}{2F}) \tag{B.7}$$

Appendix C: Fuel cell temperature as a function of current density

The fuel cell temperature is obtained using the following general form polynomial fitted using the data generated by a code developed by Ismail et al. [72]:

$$T = a_1.j^7 + a_2.j^6 + a_3.j^5 + a_4.j^4 + a_5.j^3 + a_6.j^2 + a_7.j + a_8 \quad (18)$$

where T is the cathode GDL surface temperature and j is the current density. a_1, a_2 … a_8 are coefficients given in Table C. 1.

Table C. 1 Values of coefficient in Eq. (C.1) at different ambient temperatures and an ambient relative humidity of 40%.

Coefficients	10 ℃	20 ℃	30 ℃
a_1	2.51×10^{-24}	7.02×10^{-24}	1.93×10^{-23}
a_2	-6.37×10^{-20}	-1.52×10^{-19}	-3.46×10^{-19}
a_3	6.34×10^{-16}	1.30×10^{-15}	2.43×10^{-15}
a_4	-3.13×10^{-12}	-5.50×10^{-12}	-8.49×10^{-12}
a_5	8.07×10^{-9}	1.20×10^{-8}	1.54×10^{-8}
a_6	-1.04×10^{-5}	-1.31×10^{-5}	-1.39×10^{-5}
a_7	1.36×10^{-2}	1.39×10^{-2}	1.34×10^{-2}
a_8	282.94	292.92	302.93

Chapter 4: Air-breathing versus Conventional Polymer Electrolyte Fuel Cells: A Parametric Numerical Study

---

This chapter is published as:

Calili-Cankir F, Ismail MS, Ingham DB, Hughes KJ, Ma L, Pourkashanian M. Air-breathing versus conventional polymer electrolyte fuel cells: A parametric numerical study. Energy. 2022 Jul 1;250:123827.

https://doi.org/10.1016/j.energy.2022.123827

Authorship statement

The principle author of the paper is Calili-Cankir F. The contribution of Calili-Cankir F is conceptualization, methodology, software, formal analysis, investigation, validation, writing original draft, review and editing.

4.1 Abstract

Two mathematical models have been built for air-breathing and conventional polymer electrolyte fuel cells to explore the reasons affecting the cell performance. A parametric study has been conducted to (i) investigate how each type of fuel cells responds to changes in some key parameters and (ii) consequently obtain some insights on how to improve the

performance of the air-breathing fuel cell. The conventional fuel cell significantly outperforms the air-breathing fuel cell and this is due to substantially higher forced convection-related heat and mass transfer coefficients associated with the conventional fuel cell as compared with natural convection-related heat and mass transfer coefficients associated with air-breathing fuel cell. The two types of fuel cell respond differently to changes in porosity and thickness of gas diffusion layer: the conventional fuel cell performs better with increasing porosity of gas diffusion layer (from 0.4 to 0.8) and decreasing thickness of gas diffusion layer (from 700 to 100 μm) while the air-breathing fuel cell performs better with decreasing porosity and increasing thickness of gas diffusion layer. Further, the air-breathing fuel cell was found to be more sensitive to membrane thickness and less sensitive to electrical resistance compared to conventional fuel cell.

Keywords: Air-breathing PEFCs; Conventional PEFCs; Natural convection; Forced convection; Heat and mass transfer

4.2 Introduction

There is an increasingly urgent need to convert to renewable energy sources in order to avoid the detrimental consequences of climate change phenomena [174-176]. In this regard, polymer electrolyte fuel cells (PEFCs) are promising zero-emission power conversion technologies which form a central pillar in hydrogen economy and this is due to their high efficiency, low operating temperature and rapid start-up [28, 177]. In conventional polymer electrolyte fuel cells (PEFCs), the reactants (hydrogen and oxygen), and products (water vapour) are transported from/to the flow channels to/from the membrane electrode assembly (MEA) of the fuel cell by mainly forced convection using auxiliary components such as compressors and flow controllers. Further, the reactant gasses are normally required to

be humidified by an external humidifier before entering the fuel cell to ensure appropriate initial membrane hydration and subsequently reasonably good ionic conductivity [178-180]. These auxiliary components (e.g., the compressors and humidifiers) substantially increase the overall size and the weight and subsequently the cost and complexity of the fuel cell system. On the other hand, small electronic devices (e.g., smartphones and tablets) have become increasingly essential in our daily life and they consequently form a huge market [17]. The powering components of these devices should be ideally very small to ease carrying and handling. Therefore, the conventional PEFC system should be substantially simplified to reduce its size and weight if it is to compete with the commonly-used rechargeable batteries. To this end, air-breathing PEFC technology has been proposed.

In air-breathing PEFCs, the cathode side of the fuel cell is open to the ambient and this allows for the oxidant (air) and humidifying water to be directly extracted from the ambient by natural convection, thus eliminating the need to have an oxygen storage device, a mass flow controller, a humidifier, and a pumping device. However, natural convection-related heat and mass transfer coefficients are significantly smaller than those of forced convection, imposing increased heat and mass transfer resistance for air-breathing PEFCs and significantly limiting the cell performance when compared with conventional PEFCs. Mathematical modelling is one of the most efficient and cost-effective ways to better understand the physics within the fuel cells and/or look into ways (either design-wise or material-wise) to improve their performance. There have been numerous models in the literature for the conventional PEFCs; see for example [157, 181-186]. On the other hand, the number of air-breathing PEFC numerical models is scarce and this is clearly due to the limited number of applications in which this technology is used. In the following paragraphs, we

summarise the key findings of the mathematical models for the air-breathing fuel cells that were encountered while performing the literature review.

Zhang and Pitchumani [57] built a two-dimensional and non-isothermal model for an air-breathing PEFC with a dual-cell hydrogen cartridge to investigate the effects of cell geometry and operating conditions on the performance of the fuel cell. They found that the performance of the fuel cell is improved by reducing the side length of the fuel cell and this is due to better the exposure to ambient air, thus enhancing the utilisation of the active area. They also found that the fuel cell performs better with increasing the anode pressure and relative humidity. In another study performed by the same research group, Zhang et al. [56] developed a three-dimensional and non-isothermal mathematical model to investigate the effect of geometrical parameters of an air-breathing PEFC stack, consisting of two cells sharing a hydrogen chamber. They concluded that the vertical gap between the fuel cell and the substrate requires to be minimum in order to improve the supply of air to the cathode catalyst layers and, therefore, improve the cell performance.

O'Hayre et al. [59] developed a one-dimensional and non-isothermal model for an air-breathing PEFC and they found that the fuel cell behaviour is adversely and significantly influenced by the fact that the boundary layer of natural convection is the main barrier that restricts heat and mass transfer to the open cathode of the fuel cell. They also showed that the cell performance is strongly affected by even slight forced convection. Litster et al. [65] proposed a two-dimensional numerical model for an air-breathing PEFC with a nano-porous gas diffusion layer (GDL). They showed that air is mainly transported by Knudsen diffusion in the proposed GDL, which provides sufficient amount of oxygen to the active side of the cathode catalyst layer. Calili et al. [22] built a dynamic model for an air-breathing PEFC and

investigated the effects of ambient conditions and GDL parameters (i.e. the GDL thickness and thermal conductivity) on the dynamic response of the fuel cell during load changes. They found that there exist an optimum ambient temperature (20 °C) and GDL thickness (i.e. 500 μm) at which the fuel cell shows better steady-state performance and less overshoots in the voltage during the load changes. They also found that the thermal conductivity of the GDL needs to be reasonably high in order to improve the performance and load following ability of the fuel cell. Rajani and Kolar [66] developed a two-dimensional model for an air-breathing PEFC and investigated the effect of ambient conditions (20-80% relative humidity and 10-40 °C) on the performance of the fuel cell. They reported that the ambient temperature predominantly influences the performance of the fuel cell compared to the ambient relative humidity. Chen et al. [73] proposed a mathematical model in order to investigate the effect of hydrogen relative humidity on the performance of air-breathing PEFCs at different ambient temperatures (10, 20 and 30 °C). They found that the hydrogen relative humidity significantly influences the performance of the fuel cell; for example, the limiting current density could increase by more than 40% when the hydrogen relative humidity increases from 0% to 100% at an ambient temperature of 30 °C. Matamoros and Brüggemann [64] created a three-dimensional model for an air-breathing PEFC and investigated the effects of the ambient conditions on the concentration and ohmic losses. They found that the performance of the fuel cell improves with increasing ambient temperature due to the fact that the increase in the temperature gradient enhances natural convection. They also demonstrated that mass transport losses dominantly influence the performance of the fuel cell compared to ohmic losses at different ambient conditions.

Ying et al. [70] built a two-dimensional model for a channel-based air-breathing PEFC. They found that there exists an optimum opening ratio for the open cathode at which the fuel cell performance is maximized. In their subsequent works, they developed three-dimensional and non-isothermal models for air-breathing PEFCs to investigate: (i) the temperature distribution and cell performance [68], (ii) the effects of the channel configuration [69] and (iii) interactions between electrochemical reactions, heat and mass transfer in the fuel cell [71]. Hwang [62] created a three-dimensional model for an air-breathing PEFC with an array of circular holes at the cathode current collector. They suggested that the fuel cell with the staggered arrangement for holes shows slightly better performance than that with the in-line arrangement for the holes. They also found that the optimum opening ratio for both arrangements is about 30%, which provides a balance between the mass transport losses and the ohmic losses. A two-dimensional model for an air-breathing PEFC with rectangular vertical opening at the cathode current collector was developed by Schmitz et al. [61]. Their results showed that the cell performance enhances when the opening ratio of the current collector increases from 33 to 80%.

Kumar and Kolar [89] developed a three-dimensional and non-isothermal model for an air-breathing PEFC and investigated the effects of cathode collector type (channel- and window-based) on the fuel cell performance. They showed that the fuel cell performs better with window-based cathode current collector than with the channel based current collectors due to the fact that the rate of transport rate of the produced water and heat is higher in the fuel cell equipped with the former current collector type.

A three-dimensional mathematical model for a commercial air-breathing PEFC was developed by Henriques et al. [187]. The model was used to predict the performance of the

fuel cell when the transversal channels (barriers in the channels to increase contact resistance) in the original design of the fuel cell is eliminated. The redesigned fuel cell was fabricated and experimentally tested. They validated the model with the experimental data and concluded that the efficiency of the fuel cell improved by about 26% after redesigning.

Ismail et al. [55] built a two-dimensional thermal model for an air-breathing PEFC. They showed that the Joule heating has a significant impact on the modelled thermal parameters. They also demonstrated that although the effect of entropic heat is not as significant as the Joule heating, it cannot be ignored at low current densities. Later, they [72] developed a non-isothermal mathematical model under steady-state conditions to investigate the impacts of heat sources on the performance of air-breathing PEFCs. They found that the fuel cell performance is significantly over-predicted if the entropic heat and/or Joule heat are neglected.

Recently, Yan et al. [125] performed a numerical simulation for an air-breathing PEFC stack applying different cathode flow channel designs in order to enhance the performance of the fuel cell. The numerical results were validated by experimental data and showed that the optimum opening ratio is between 50 and 60% shows a better performance due to reduced and uniform stack temperature. Lee et al. [188] developed a three-dimensional, two-phase and multiscale model for an air-breathing PEFC to parametrically investigate the transport of water and heat. They found that the performance of the fuel cell improves with the use of a thinner membrane and higher ionomer fraction in the cathode catalyst layer due to reduced ionic resistance of the membrane phase. Al-Anazi et al. [75] performed a computational investigation using a three-dimensional, non-isothermal, steady-state model for an air-breathing PEFC stack to investigate the effect of ambient conditions in Riyadh City

(Saudi Arabia) on the performance of the fuel cell. They found that the fuel cell stack performs better with warm and humid ambient conditions (summer time) where the humidification of the membrane is adequately maintained. On the other hand, the performance of fuel cell stack during the winter time was found to be around 12% less than that in summer time. Lee et al. [189] built a three-dimensional air-breathing PEFC model incorporating an innovative cathode flow-field design. They found that the proposed cathode flow-field configuration increases the water-retaining capability of the fuel cell by around 10% compared to that of the conventional cathode flow-field configuration where the channels are parallel.

To the best of the authors' knowledge, there have been no modelling studies in the literature that simultaneously compared and analysed the outcomes of the air-breathing and the conventional PEFCs. To this end, two steady-state, non-isothermal and efficient mathematical models have been developed for both conventional and air-breathing PEFCs to conduct for the first time a parametric study to (i) explore the parameters that impact each type of fuel cells and subsequently (ii) obtain insights on how to improve the air-breathing fuel cell performance. To achieve this goal, the sensitivity analysis of both modelled fuel cells to some key parameters (i.e. the porosity and the thickness of the GDL, the membrane thickness and the overall electrical resistance) has been performed. These parameters have been selected because they could be practically changed in order to improve the performance of the fuel cells. Namely, the porosity and the thickness of the GDL could be easily adapted by employing different types of GDLs or refining the existing GDLs. This note also applies to the thickness of the membrane electrolyte which is the only parameter that could be changed assuming using the conventionally-used Nafion® membranes. The overall

electrical resistance is mainly due to contact resistance between the various components of the fuel cells and could be controlled through varying the assembling compression. The parametric study has not included in the impact of the operating conditions (the temperature and relative humidity) as these parameters are dictated by those of the ambient adjacent to the open cathode of the air-breathing PEFCs; this is not the case for the conventional PEFC where the operating conditions could be controlled. Therefore, commonly-encountered ambient conditions (20 °C and 40% relative humidity) where fixed and used for both air-breathing and conventional PEFCs. It should be noted we have investigated the impact of the ambient conditions on the performance of air-breathing PEFCs in a previous work [22]. It is noteworthy that the model has been originally developed for the air-breathing PEFC [72]. However, some improvements and adaptations to the model have been made. Namely, the membrane electrolyte and the anode compartment have been included into the model and, consequently, the relevant physics (the heat transport in the anode GDL and the electrolyte, the transport of gases in the anode and the transport of dissolved water through the membrane) have been accounted for. Further, for the purpose of this comparative study, the physics of the model have been adapted to represent the corresponding conventional PEFC.

4.3 Model formulation

Most of the equations listed in this section are applicable for both types of fuel cells: conventional and air-breathing PEFCs. The modelled air-breathing PEFC was originally reported by Fabian et al. [60]. The cell geometry and MEA properties of the modelled conventional PEFC have been set to be the same as those of the air-breathing PEFC described by Fabian et al. [60]. The following assumptions and considerations have been employed for the models:

- The fuel cells operate under steady state conditions.
- Water exists only in vapour form.
- The reactant gases are treated as ideal gases.
- The anode of the air-breathing PEFC is in dead-end mode.
- The main mode of transport in GDLs is diffusion and therefore the contribution of the convective flow in GDLs is negligible.
- The cathode catalyst layer is infinitely thin so that it is treated as an interface between the membrane and the GDLs.
- The water activity is in equilibrium with water vapour activity in the catalyst layers.
- The concentration losses are neglected as the water activity has been always less than unity and the amount of reactants available for the reactions have been always sufficient for all the investigated cases.
- The only heat source occurs at the cathode catalyst layer and all the other heat sources are neglected due to their small amounts.

Figure 4.1 shows the schematics of the modelled cells displaying the key components and the heat and mass fluxes for each fuel cell type.

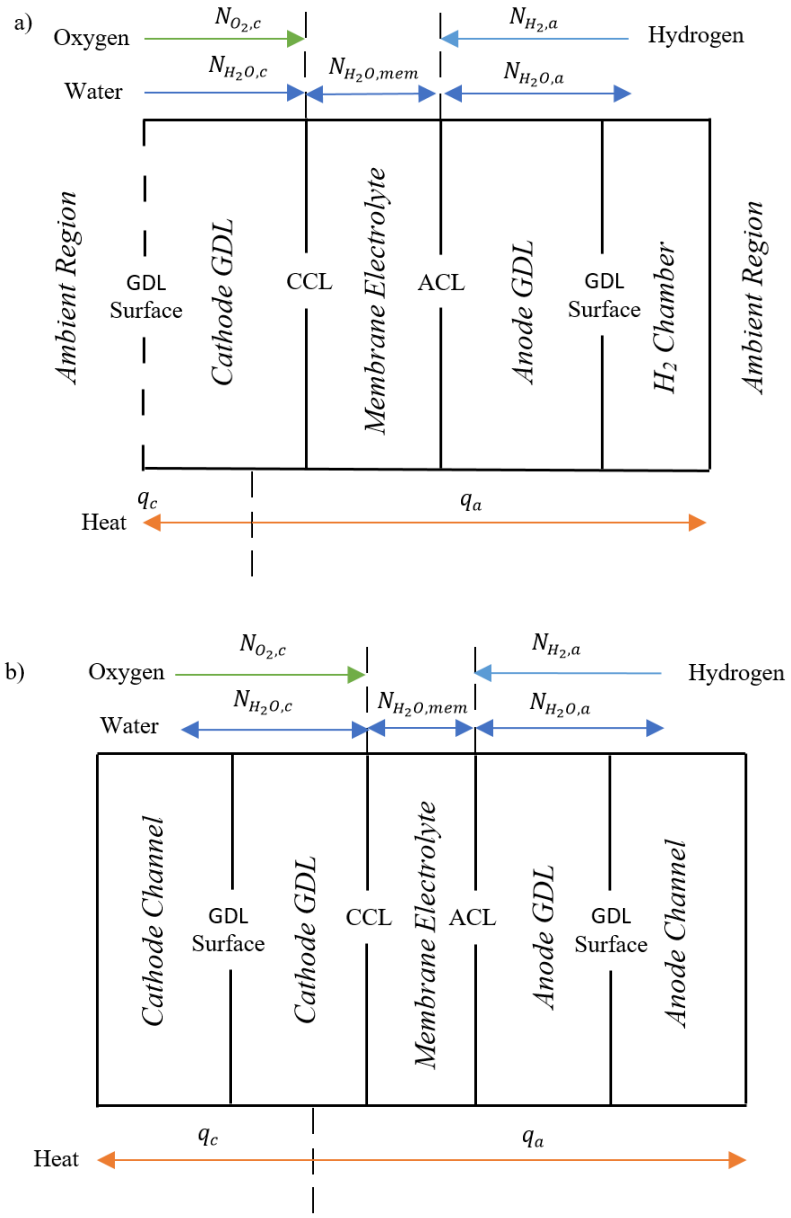

Figure 4.1 Schematic representations of the modelled: (a) air-breathing and (b) conventional PEFCs. Note that the symbol 'N' stands for molar flux, 'q' for heat flux, 'CCL' for cathode catalyst layer and 'ACL' for anode catalyst layer, the subscript 'a' for anode and the subscript 'c' for cathode.

Note that Fabian et al. [60] reported that some water accumulates at the cathode of the air-breathing PEFC, particularly at the intermediate current densities for low temperatures and high humidity conditions. However, accumulation of liquid water starts to diminish as the current density increases since the running air-breathing fuel cell was of high-performance. This is due to the exponential increase in the cell temperature at high current densities. The sharp decline in the cell potential at high current densities is, therefore, primarily due to

membrane dehydration, not water flooding. Therefore (considering that water flooding may only occur in the intermediate current densities of the modelled fuel cell and this does not change the overall trends of the outcomes of the models), water is, for simplification, assumed to exist in water vapour form only [22]. This assumption/simplification was also considered by O'Hayre et al. [59] and Ismail et al. [72].

4.3.1 Cell voltage

The cell voltage, V_{cell}, is calculated as follows:

$$V_{cell} = E - \eta_{act} - \eta_{ohmic} \tag{4.1}$$

where E is the reversible (or Nernst) voltage, η_{act} is the activation losses and η_{ohmic} is the ohmic losses. The reversible voltage is obtained using the Nernst equation [8]:

$$E = \frac{-\Delta H + T\Delta S}{2F} + \frac{RT}{2F}\ln\left(\frac{P_{H_2}.P_{O_2}^{1/2}}{P_{H_2O}}\right) \tag{4.2}$$

where P_{H_2}, $P_{O_2}$and P_{H_2O} are the partial pressures of hydrogen, oxygen and water under equilibrium conditions, respectively. T is the absolute temperature, R is the universal gas constant and F is the Faraday's constant. ΔH and ΔS are the enthalpy and entropy changes for the overall reaction, respectively. The activation losses are obtained using the following expression [8, 59]:

$$\eta_{act} = \frac{RT}{2\alpha F}\ln\left(\frac{C_{O_2}^{\infty/ch} j}{C_{O_2}^{ccl} j_0}\right) \tag{4.3}$$

where $C_{O_2}^{\infty/\mathrm{ch}}$ and $C_{O_2}^{ccl}$ are the molar concentrations of oxygen at the ambient/flow channel and the cathode catalyst layer, respectively. α is the charge transfer coefficient, j is the

current density and j_0 is the reference exchange current density, corrected for temperature by the following expression:

$$j_0 = j^0_{298\,K} \exp\left[\frac{E_a}{R}\left(\frac{1}{298} - \frac{1}{T}\right)\right] \tag{4.4}$$

where E_a is the activation energy. The ohmic losses can be expressed as follows [22, 59, 72]:

$$\eta_{ohmic} = jA_{act}(R_{elec} + R_{mem}) \tag{4.5}$$

where A_{act} represents the active area of the fuel cell, R_{elec} and R_{mem} are respectively the lumped electrical resistance of the cell and the membrane resistance. R_{mem} is given by:

$$R_{mem} = \frac{\delta_{mem}}{A_{act}\sigma_{mem}} \tag{4.6}$$

where δ_{mem} is the thickness of the Nafion® membrane. The ionic conductivity of the membrane, σ_{mem} can be calculated using the following empirical correlation for the air-breathing PEFC [79]:

$$\sigma_{mem} = (3.46a^3 + 0.0161a^2 + 1.45a - 0.175) \exp\left[1268\left(\frac{1}{303} - \frac{1}{T}\right)\right] \tag{4.7}$$

and using the well-known Springer's model for the conventional PEFCs [1, 77]:

$$\sigma_{mem} = [0.514\lambda - 0.326] \exp\left[1268\left(\frac{1}{303} - \frac{1}{T}\right)\right] \tag{4.8}$$

where λ represents the water content of the membrane and is given by [190]:

$$\lambda = \begin{cases} 0.043 + 17.81a - 39.85a^2 + 36a^3, & 0 < a \leq 1 \\ 14 + 1.4(a-1), & 1 < a \leq 3 \end{cases} \tag{4.9}$$

The water activity, a is defined as follows [8]:

$$a = \frac{P_{H_2O}}{P_{sat}} \tag{4.10}$$

where P_{H_2O} and P_{sat} represent the partial pressure and the saturation pressure of water vapour at the catalyst layers, respectively. P_{sat}, in atm, is given by [77, 191]:

$$\begin{aligned} log_{10}P_{sat} = {} & -2.1794 + 0.02953(T - 273.15) - 9.1837 \\ & \times 10^{-5}(T - 273.15)^2 + 1.4454 \\ & \times 10^{-7}(T - 273.15)^3 \end{aligned} \tag{4.11}$$

It should be noted that the water activity has been limited to one when calculating the ionic conductivity of the membrane in the modelled air-breathing PEFC; water activity beyond unity results in unrealistic values for the ionic conductivity of the membrane [59, 72].

4.3.2 Heat transfer

Heat is mainly produced at the cathode catalyst layer as a result of the exothermic oxygen reduction reaction, thus creating a temperature difference between the cathode catalyst layer and the two outermost sides of the fuel cells. The generated heat is first conducted through the solid-phase of the fuel cell components (i.e. the GDLs, the membrane and the current collectors) and is then transported at the interfaces with the ambient through convection. As schematically illustrated in Figure 4.1, the temperature gradients are created between the cathode catalyst layer interface (where most of the heat sources exist) and the ambient regions at both sides of the fuel cell. The heat generated in the fuel cell is mathematically given as [72]:

$$q = q_c + q_a = j\left(\eta_{act} + \eta_{ohm} + \frac{T\Delta S}{2F}\right) \tag{4.12}$$

The left-hand side heat flux, q_c (see Figure 4.1), may be expressed as follows:

$$q_c = \begin{cases} k_{GDL}\dfrac{T_{ccl} - T_{gdl,c}}{\delta_{gdl,c}} = h\left(T_{gdl,c} - T_{\infty}\right) \text{ for air-breathing PEFC} \\ k_{GDL}\dfrac{T_{ccl} - T_{gdl,c}}{\delta_{gdl,c}} = h\left(T_{gdl,c} - T_{cell}\right) \text{ for conventional PEFC} \end{cases} \quad (4.13)$$

and the right-hand side heat flux, q_a (see Figure 4.1), may be given by:

$$q_a = \begin{cases} \dfrac{T_{ccl} - T_{gdl,a}}{\left(\dfrac{\delta_{mem}}{k_{mem}} + \dfrac{\delta_{gdl,a}}{k_{gdl}}\right)} = h\left(T_{gdl,a} - T_{\infty}\right) \text{ for air-breathing PEFC} \\ \dfrac{T_{ccl} - T_{gdl,a}}{\left(\dfrac{\delta_{mem}}{k_{mem}} + \dfrac{\delta_{gdl,a}}{k_{gdl}}\right)} = h\left(T_{gdl,a} - T_{cell}\right) \text{ for conventional PEFC} \end{cases} \quad (4.14)$$

where T_{∞}, T_{cell}, T_{ccl}, $T_{gdl,c}$ and $T_{gdl,a}$ respectively represent the ambient temperature, the cell temperature (which is equivalent to the temperature of the gases flowing in the channel) and the temperatures at the cathode catalyst layer, at the cathode GDL surface and at the anode GDL surface. The cathode GDL, the anode GDL and the membrane thickness are designated as $\delta_{gdl,c}$, $\delta_{gdl,a}$ and δ_{mem}, respectively. k_{gdl} and k_{mem} are the thermal conductivities of the GDL and the membrane, respectively.

h is the heat transfer coefficients the fuel cell has with the ambient or the flow channel. h for either side of the air-breathing PEFCs is the sum of the radiative heat transfer coefficient h_{rad} and the convective heat transfer coefficient h_{conv} [192]:

$$h_{rad} = 2e\sigma_{Bolt}(T_{gdl}^2 + T_{\infty}^2)(T_{gdl} + T_{\infty}) \quad (4.15)$$

$$h_{conv} = \frac{Nu.\, k_{air}}{L_{ch}} \quad (4.16)$$

where e and σ_{Bolt} are the emissivity and the Stephan-Boltzmann constant, respectively. k_{air} is the thermal conductivity of air and L_{ch} is the characteristic length for heat transfer which is, for the air-breathing fuel cell, equal to 7 cm. Nu is the Nusselt number which is obtained

for a horizontally-oriented iso-flux heated plate (representing the air-breathing PEFC modelled in this work) using the following expressions [192, 193]:

$$Nu_c = 0.16Ra_c^{1/3} \tag{4.17}$$

$$Ra = \frac{g\beta q L_{ch}^4}{\nu_{air}\alpha_{air}k_{air}} \tag{4.18}$$

where Ra is the Rayleigh number. ν_{air} and α_{air} are the kinematic viscosity and the thermal diffusivity of air, respectively. All the thermo-physical properties of air used in the equations have been estimated using the tabulated data in [192] at the film temperature. The film temperature at the interface between the ambient and the cathode GDL, T_f, is defined as the arithmetic mean of the temperature of the cathode GDL surface, T_{gdl}, and the ambient temperature, T_∞. The thermal expansion coefficient at the interface, β is estimated as follows [72]:

$$\beta = {}^{1}/_{T_f} \tag{4.19}$$

On the other hand, h for the conventional fuel cell is represented by only the convective heat transfer coefficient and this is (as evidenced from not shown simulations) due to negligible dissipation of heat through radiation [192]:

$$h_{conv} = \frac{Nu.k_i}{L_{ch}} \tag{4.20}$$

where k_i is the thermal conductivity of the species i (air in the cathode flow channel and hydrogen in the anode flow channel). The characteristic length L_{ch} is the hydraulic diameter of the channel which is in this case the side length of the square cross-section (i.e., $1\ \mathrm{mm}$).

The Nusselt number for an iso-flux fully developed laminar flow in a rectangular channel is given by [192]:

$$Nu = 3.61 \qquad (4.21)$$

4.3.3 Mass transfer

Oxygen and water are transported by natural convection between the ambient and the cathode GDL in the air-breathing PEFC. On the other hand, oxygen, hydrogen and water vapour are transported by forced convection between the flow channel and the cathode/anode GDL of the conventional PEFC. The anode of the air-breathing PEFC is dead-ended and therefore, the concentration of dry hydrogen at the surface of the anode GDL is assumed to be that of the hydrogen chamber (see Figure 4.1). All the gases in both types of the fuel cells are mainly transported by diffusion within the GDLs. The driving force for the transport of the gases between the ambient/channel and the catalyst layer is the consumption/generation of these gases at the catalyst layers. All the above description could be mathematically described as follows:

$$N_i = \frac{j}{nF} = D_{ij}^{eff} \frac{C_i^{gdl} - C_i^{cl}}{\delta_{gdl}} = h_{m,i}\left(C_i^{gdl} - C_i^{\infty/ch}\right) \qquad (4.22)$$

The second term in the above equation is the Faraday's second law of electrolysis. N_i is the molar flux of the species i (oxygen, hydrogen or water vapour), j is the current density of the fuel cell, n is the number of electrons transferred per one mole of oxygen (4), water (2) or hydrogen (2).It is important to note that the models have indirectly accounted for the influence of nitrogen on the mass transfer by incorporating the initial concentration of oxygen in the ambient air and the binary diffusion coefficient of oxygen into nitrogen. Also,

it is worth mentioning that the impact of carbon dioxide has been considered to be insignificant due to the extremely low concentration of oxygen in the ambient air (i.e., 421 ppm) and the assumption of fuelling with pure hydrogen.

C_i^{gdl}, C_i^{cl} and $C_i^{\infty/ch}$ are respectively the molar concentration of the species i at the GDL surface, at the catalyst layer and in the ambient/flow channel and C_i^{cl} is the molar concentration of the species i in the catalyst layer. The effective diffusion coefficient on the cathode side, D_{ij}^{eff} is effective diffusion coefficient of the species i into j (oxygen and water vapour into air in the cathode GDL or hydrogen into water vapour in the anode GDL) and is estimated using the following expression [7]:

$$D_{ij}^{eff} = f(\varepsilon).D_{ij}\left(\frac{T_{gdl}}{T_{ref}}\right)^{1.5}\left(\frac{P_{ref}}{P}\right) \qquad (4.23)$$

where D_{ij} is the binary diffusion coefficient of the species i into j at the reference temperature (T_{ref}) and pressure (P_{ref}). Both the operational pressure (P) and the reference pressure are equal to the ambient pressure, i.e. 1 atm, and therefore the last term in Eq. (23) is unity. Note that T_{gdl} in Eq. (23) is taken to be the arithmetic mean of the surface temperature of the GDL and the temperature at the catalyst layer. The diffusibility, $f(\varepsilon)$, is a function of the porosity of the GDL and is calculated using the following empirical correlation [194]:

$$f(\varepsilon) = 1 - 2.72\varepsilon\cosh(2.53\varepsilon - 1.61)\left(\frac{3(1-\varepsilon)}{3-\varepsilon}\right) \qquad (4.24)$$

The mass transfer coefficient of the species i ($h_{m,i}$) is estimated as follows:

$$h_{m,i} = \frac{Sh_i.D_{ij}}{L_{ch,m}} \qquad (4.25)$$

where $L_{ch,m}$ is the characteristic length related to the mass transfer (which is equal to the side length of the square channel for the conventional fuel cell ($1\ \mathrm{mm}$) and equal to the side length of active area for the air-breathing fuel cell ($3\ \mathrm{cm}$)). Sh is Sherwood number and is, making use of the analogy between heat transfer and mass transfer, given as [192, 193]:

$$Sh_i = \begin{cases} 3.61 & \text{for conventional PEFC} \\ 0.16Ra_{m,i}^{1/3} & \text{for air-breathing PEFC} \end{cases} \tag{4.26}$$

$Ra_{m,i}$ is the Rayleigh number associated with the mass transfer for the species i and can be calculated using the following expression [193]:

$$Ra_{m,i} = \frac{g\gamma(x_i^{\infty} - x_i)L_{ch,m}^3}{\nu_i D_{ij}} \tag{4.27}$$

where g is the acceleration due to gravity, x_i^{∞} is the mole fraction of the species i in the ambient region, x_i is the mole fraction of the species i at the surface of the GDL and ν_i is the kinematic viscosity of the species i. Due to the fact that the nitrogen concentration within the cell and the ambient region remains almost constant, a binary mixture of ideal gases of oxygen and water vapour can be assumed; therefore, the volumetric expansion coefficient of species i due to the concentration gradients, γ, is estimated as follows [193]:

$$\gamma = \frac{M_{O_2} - M_{H_2O}}{M_{mix}} \tag{4.28}$$

where M_{O_2} and M_{H_2O} are the molecular weights of oxygen and water, respectively. The molecular weight of the binary mixture, M_{mix}, has been taken to be the arithmetic mean of the molecular weights of the binary mixture in the ambient region, M_{mix}^{∞}, and at the GDL surface, M_{mix}^{gdl} [72]:

$$M_{mix} = \frac{M_{mix}^{\infty} + M_{mix}^{\mathrm{gdl}}}{2} \tag{4.29}$$

where M_{mix}^{∞} is given by:

$$M_{mix}^{\infty} = \frac{C_{O_2}^{\infty}}{C_{O_2}^{\infty} + C_{H_2O}^{\infty}} M_{O_2} + \frac{C_{H_2O}^{\infty}}{C_{O_2}^{\infty} + C_{H_2O}^{\infty}} M_{H_2O} \quad (4.30)$$

$C_{O_2}^{\infty}$ is the molar concentration of oxygen in the ambient region:

$$C_{O_2}^{\infty} = 0.21(C_{tot}^{\infty} - C_{H_2O}^{\infty}) \quad (4.31)$$

The molar concentration of water in the ambient air, $C_{H_2O}^{\infty}$ is given by:

$$C_{H_2O}^{\infty} = \frac{P_{sat}^{\infty}.RH}{RT_{\infty}} \quad (4.32)$$

where RH represents the water relative humidity of the ambient. The water vapour saturation pressure P_{sat}^{∞} is obtained using Eq. (4.11).

The molar concentration of ambient air C_{tot}^{∞} is obtained using the ideal gas law:

$$C_{tot}^{\infty} = \frac{P}{RT_{\infty}} \quad (4.33)$$

In a similar way, M_{mix}^{gdl} is calculated using Eq. (4.30) by replacing the molar concentrations of oxygen and water in the ambient with those at the surface of the cathode GDL.

It should be noted that the membrane electrolyte is impermeable to oxygen, hydrogen and nitrogen but allows for water (in dissolved form) to transport within it by electro-osmotic drag (driven by the proton transport and is from the anode side to cathode side of the membrane) and back diffusion which is normally from the cathode side to anode side. To this end, the molar flux of water N_{H_2O} at either the cathode or the anode catalyst layer (calculated using Eq. (4.22)) is equal to the net water flux resulting as a result of the competing transport phenomena of electro-osmotic drag and back diffusion [195]:

$$N_{H_2O} = \begin{cases} n_d \frac{j}{F} - D_w \frac{C_{H_2O}^{ccl} - C_{H_2O}^{acl}}{\delta_{mem}} & \text{at the cathode catalyst layer} \\ D_w \frac{C_{H_2O}^{ccl} - C_{H_2O}^{acl}}{\delta_{mem}} - n_d \frac{j}{F} & \text{at the anode catalyst layer} \end{cases} \quad (4.34)$$

where $C_{H_2O}^{ccl}$ and $C_{H_2O}^{acl}$ are the molar concentrations of water at the cathode and the anode catalyst layers respectively. D_w is the dissolved water diffusivity in the membrane and n_d is the electro-osmotic drag coefficient. These two parameters are given as follows [195]:

$$D_w = \begin{cases} 3.1 \times 10^{-7} \lambda (\exp(0.28\lambda) - 1) \exp\left(-\frac{2346}{T}\right) & for\ 0 < \lambda < 3 \\ 4.17 \times 10^{-8} \lambda (161 \exp(-\lambda) + 1) \exp\left(-\frac{2346}{T}\right) & for\ \lambda \geq 3 \end{cases} \quad (4.35)$$

and

$$n_d = \begin{cases} 1 & for\ \ \lambda \leq 14 \\ 0.1875\lambda - 1.625 & for\ \lambda > 14 \end{cases} \quad (4.36)$$

The water content of the membrane, λ, is calculated using Eqs. (4.8-4.10). It should be noted that the water diffusivity and the electro-osmotic drag coefficient have been taken to be the arithmetic mean of their values at the temperatures of the anode and cathode catalyst layers.

4.3.4 Numerical Procedure

The computational domain of each fuel cell consists of a cathode GDL, cathode catalyst layer, membrane electrolyte, anode catalyst layer and anode GDL (Figure 4.1). The boundary layers next to the cathode of air-breathing PEFC are induced by natural convection and are for temperature and concentrations. The initial cell temperature of the conventional PEFC has been set to be the same with the ambient temperature. Table 4.1 shows the physical parameters used for the modelled of the air-breathing and conventional fuel cells; except for the characteristic lengths, the parameters for both models have been kept the same for

comparative purposes. All the physical parameters and constants of the fuel cells have been declared for each model and all the equations mentioned in Section 4.3.1, 4.3.2 and 4.3.3 have been appropriately listed in an m-file within MATLAB®. Eqs (4.1), (4.12-4.14), (4.22) and (4.34) have been then solved for current density, concentrations and temperatures at different cell potentials and interfaces using the nonlinear solver 'fsolve'.

Table 4.1 Physical parameters and constants used for the base cases of the models [59, 60, 72].

Parameters	**Value**
Universal gas constant, R	$8.314\ \mathrm{J/(mol.K)}$
Faraday's constant, F	$96485\ \mathrm{C/mol}$
Stephan-Boltzmann constant, σ_{Bolt}	$5.67\times10^{-8}\ \mathrm{W/(m^2.K^4)}$
Gravitational acceleration, g	$9.81\ \mathrm{m/s^2}$
Ambient/cell pressure, P	$1\ \mathrm{atm}$
Oxygen/nitrogen molar ratio	21/79
Ambient temperature, T_∞	20 °C
Initial cell temperature of conventional PEFC, T	20 °C
Binary diffusivity of O_2 in air, $D_{O_2,air}$	$2.20\times10^{-5}\ \mathrm{m^2/s}$
Binary diffusivity of H_2O in air, $D_{H_2O,air}$	$2.56\times10^{-5}\ \mathrm{m^2/s}$
Binary diffusivity of H_2 into water vapour, D_{H_2}	$2.59\times10^{-10}\ \mathrm{m^2/s}$ [57]
Cell active area, A_{act}	$9.00\times10^{-3}\ \mathrm{m^2}$
Membrane thickness, δ_{mem}	$5.20\times10^{-5}\ \mathrm{m}$
GDL thickness, δ_{gdl}	$3.00\times10^{-4}\ \mathrm{m}$
GDL porosity, ε	0.70
GDL tortuosity, τ	3
GDL thermal conductivity, k_{gdl}	$1\ \mathrm{W/(m.K)}$
Membrane thermal conductivity, k_{mem}	$0.17\ \mathrm{W/(m.K)}$
Emissivity, e	0.90
Reference exchange current density, $j^0_{298\ K}$	$3\ \mathrm{mA/cm^2}$
Lumped cell electrical resistance, R_{elec}	$12\ \mathrm{m\Omega}$
Charge transfer coefficient, α	0.41
Enthalpy change, ΔH	$-241.98\times10^3\ \mathrm{J/mol}$

Entropy change, ΔS	-44.43×10³ $\mathrm{J/mol}$
Activation energy, E_a	50.00×10³ $\mathrm{J/mol}$

4.4 Results and Discussion

Figure 4.2(a-b) shows that the polarisation curve and the surface temperature of the cathode GDL of the modelled air-breathing PEFC at ambient temperature and relative humidity of 20 °C and 40% are in very good agreement with the corresponding experimental data reported in [60]. Further, the model nicely captures the experimentally observed sharp decline in the cell performance (Figure 4.2a) and exponential increase in the cell temperature (Figure 4.2b) at high current densities. The graphs in Figure 4.2(a-b) also present the data generated by the modelled conventional PEFC at 20 °C cell temperature and 40% relative humidity of inlet gases. It is worth noting that the model for the conventional PEFC has not been validated by the experimental data. This is because the cell geometry and MEA properties has been set to be the same as those of air-breathing PEFC, in order to maintain consistent conditions for comparative purposes with the conventional PEFC. It is clear from Figure 4.2a that the conventional PEFC significantly outperforms the air-breathing PEFC as primarily evidenced by the decreased limiting current density demonstrated by the latter fuel cell. Some more data have been generated from both models and plotted in order to highlight the underlying reasons behind the above performance difference between the two types of fuel cells; see Figure 4.2(c-f).

Both the ohmic (Figure 4.2c) and to a lesser extent the activation (Figure 4.2d) losses participate towards the superiority of the conventional fuel cell over the air-breathing fuel cell in particular at high current densities (> 500 $\mathrm{mA/cm^2}$). The ohmic losses generally

correlate to the cell temperature which has been set in this study to be that of the cathode catalyst layer; this is a reasonable arrangement as the temperature difference between the cathode catalyst layer (where temperature is a maximum) and the outermost sides of the fuel cells is, for a given current density, less than 2 ℃. As the cell temperature increases, the water activity (calculated by Eq. (4.10)) decreases. To this end, the exponential increase in air-breathing fuel cell temperature after 500 $\mathrm{mA/cm^2}$ causes a corresponding exponential increase in membrane resistance and in turn the ohmic losses. This exponential increase in air-breathing fuel cell temperature is attributed to the inability of the heat transfer coefficient (which is substantially lower than the corresponding forced convection heat transfer coefficient for the conventional fuel cell) to dissipate heat from the air-breathing fuel cell. As shown in Figure 4.2e, the natural convection heat transfer coefficient increases with increasing current density: however, this increase is not sufficiently high to mitigate the exponential increase in cell temperature and, consequently, the ohmic losses.

Likewise, the exponential increase in the air-breathing fuel cell temperature causes a higher increased activation losses compared to the conventional fuel cell; this is evident from Eq. (4.3). This equation also shows that the activation losses are a function of oxygen concentration at the cathode catalyst layer: as the oxygen concentration increases, the activation losses decrease. In this regard, the conventional fuel cell has substantially higher amount of oxygen available for the reaction at the cathode catalyst layer than the air-breathing fuel cell (not shown) and this is due to significantly higher mass transfer coefficient demonstrated by the conventional fuel cell (Figure 4.2f). It is noteworthy that both forced and natural mass transfer coefficient slightly increase with increasing current density as both

are a function of diffusivity coefficient which scale with temperature as evidenced from Eq. (4.23) and Eq. (4.25).

In the following subsections, we conduct parametric studies to evaluate the effects of some key parameters (i.e., the GDL porosity, the GDL thickness, the membrane thickness and the electrical resistance) on the performance of both air-breathing and conventional fuel cells. This is performed in order to obtain insights on how the performance of air-breathing PEFC could be improved through analysing the differences in the outputs of the two types of the modelled fuel cells.

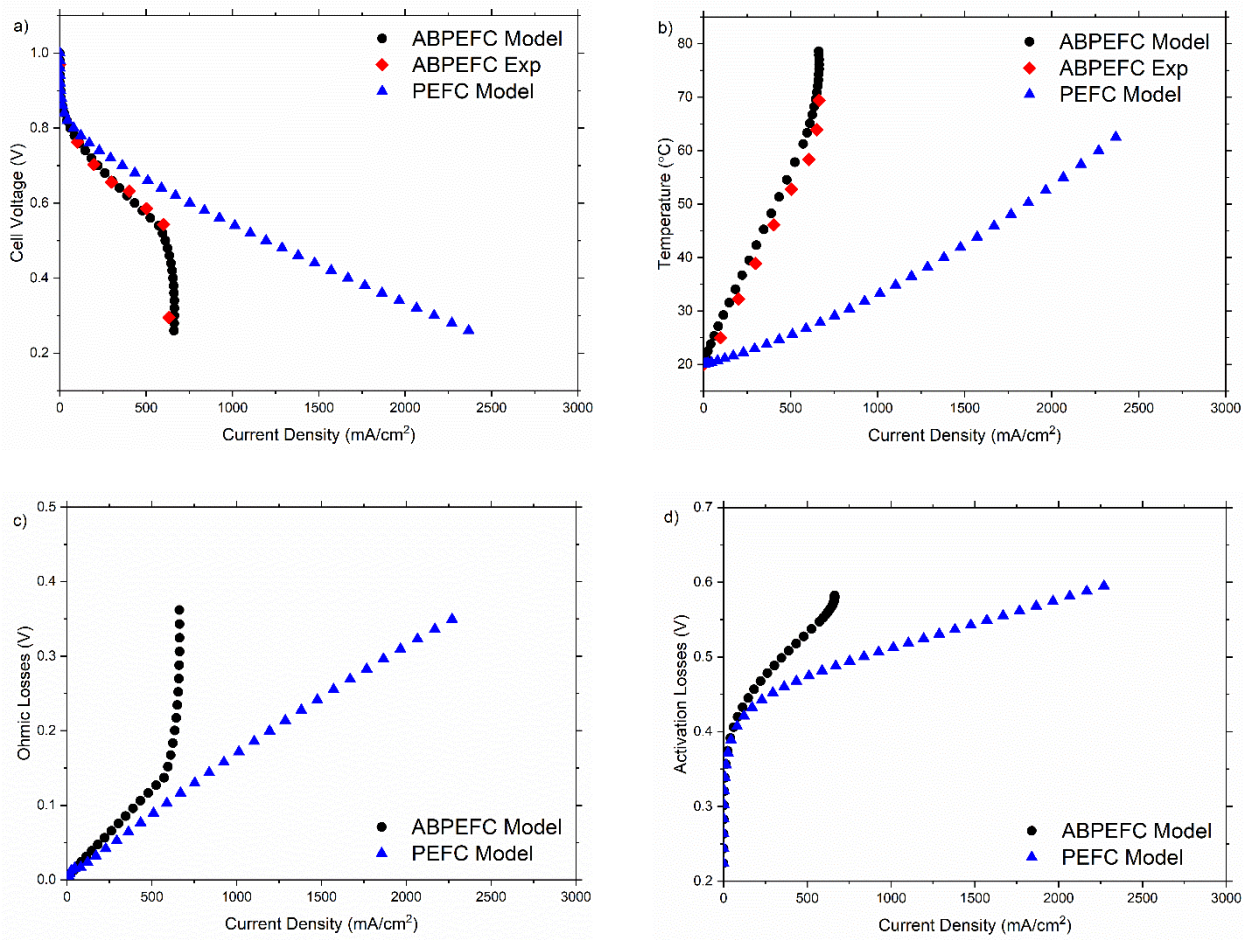

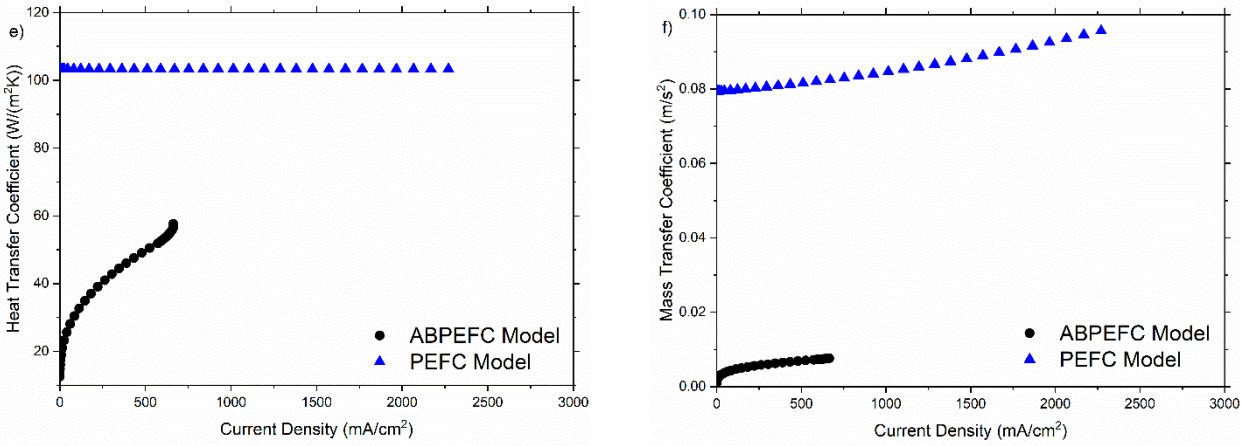

Figure 4.2 The outputs of the modelled air-breathing and conventional PEFCs at 20 °C and 40% relative humidity: (a) cell voltage, (b) cell temperature, (c) ohmic losses, (d) activation losses, (e) heat transfer coefficient and (f) mass transfer coefficient of oxygen as a function of current density.

4.4.1 Porosity of Gas Diffusion Layers

Figure 4.3 shows the impact of the cathode GDL porosity on the performance of the modelled fuel cells. Interestingly, the performance of the air breathing PEFC improves with decreasing cathode GDL porosity while the conventional one shows a slight performance increase with increasing cathode GDL porosity (Figure 4.3a). As expected, the increase in the cathode GDL porosity allows for more oxygen to be transported to the catalyst layers of the fuel cells (Figure 4.3e). Equally, more water is removed from the cathode catalyst layer as the cathode GDL porosity increases (Figure 4.3f). As heat transfer coefficient at the open cathode of the air-breathing PEFC is not sufficiently high to lower the exponential increase of the cell temperature (Figure 4.3b), the amount of water needed to hydrate the polymer electrolyte membrane become a rate limiting factor. As the water concentration at the cathode catalyst layer (and the membrane electrolyte) of the air-breathing fuel cell decreases, the membrane resistance and subsequently the ohmic losses (Figure 4.3c) increase, thus resulting in lower limiting current density (Figure 4.3a). On the other hand, the

heat transfer coefficients associated with the conventional fuel cell are sufficiently high to dissipate heat from the fuel cell and maintain well membrane hydration. As the porosity of the cathode GDL of the conventional fuel cell increases, more oxygen is transported to the cathode catalyst layer, thus leading to less activation losses (Figure 4.3d) and better fuel cell performance (Figure 4.3a).

The impact of anode GDL porosity on the performance of the modelled fuel cells are similar to but less than that of the cathode GDL porosity; see Figure 4.4. Namely, as the anode GDL porosity of the air-breathing fuel cell increases, the amount of water being removed from the anode catalyst layer (Figure 4.4f) and the ohmic losses (Figure 4.4c) increase. However, such an increase in the ohmic losses is less than that when the cathode GDL porosity increases considering the fact that water is generated at the cathode catalyst layer. On the other hand, the modelled conventional fuel cell is not heat transfer-limited and the increase in the anode GDL porosity leads to an increase in hydrogen available for the reaction at the anode catalyst layer (not shown) and a very slight non-noticeable improvement in the fuel cell performance (Figure 4.4a).

Overall, considering the outcomes of this study, it is recommended that GDLs with relatively low porosity (~ 0.4) should be used for air-breathing PEFCs, particularly for the cathode side of the fuel cell.

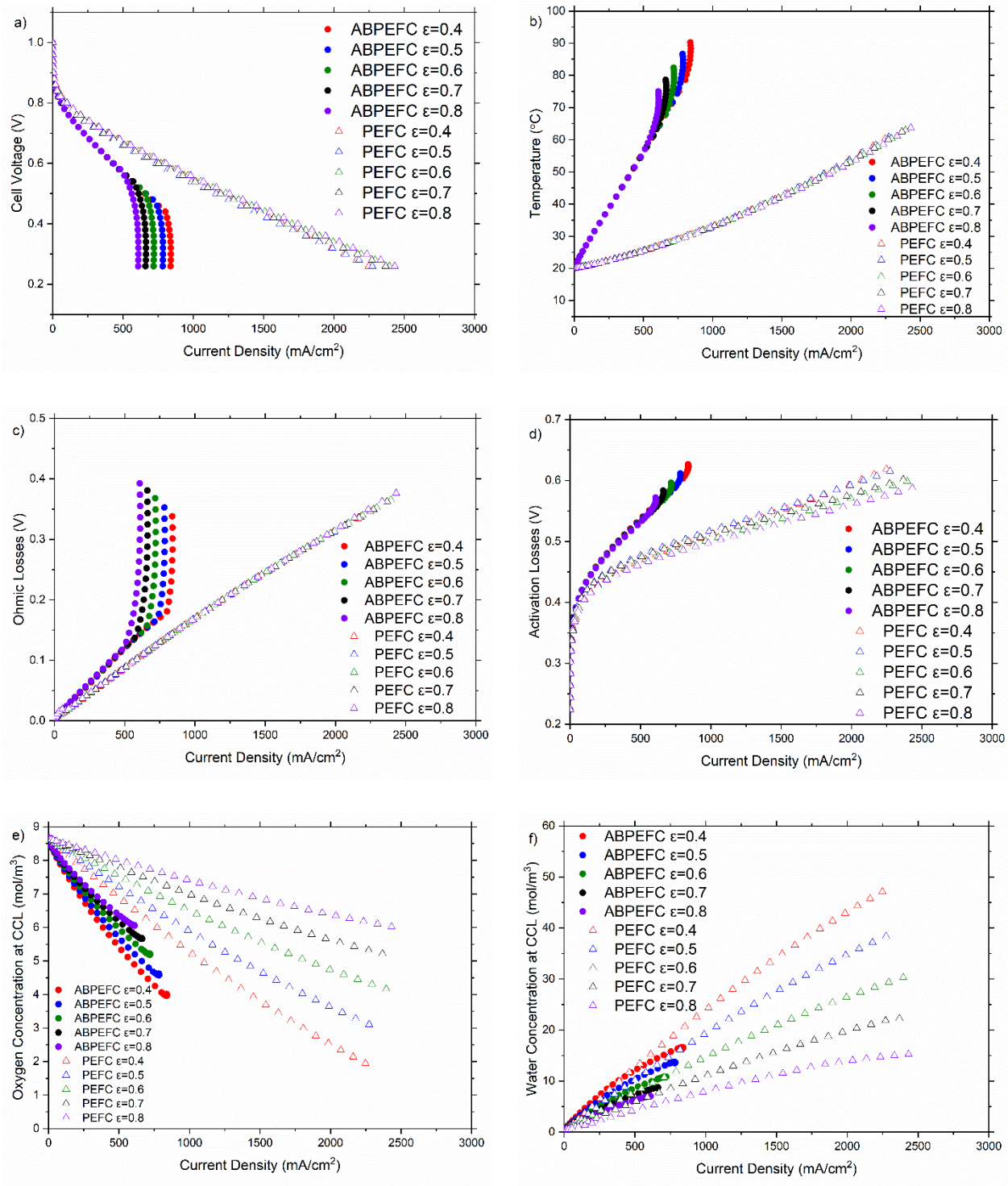

Figure 4.3 The outputs of the modelled air-breathing and conventional PEFCs at 20 °C and 40% relative humidity and variable cathode GDL porosity: (a) cell voltage, (b) cell temperature, (c) ohmic losses, (d) activation losses, (e) oxygen concentration at the cathode catalyst layer and (f) water concentration at the cathode catalyst layer as a function of current density.

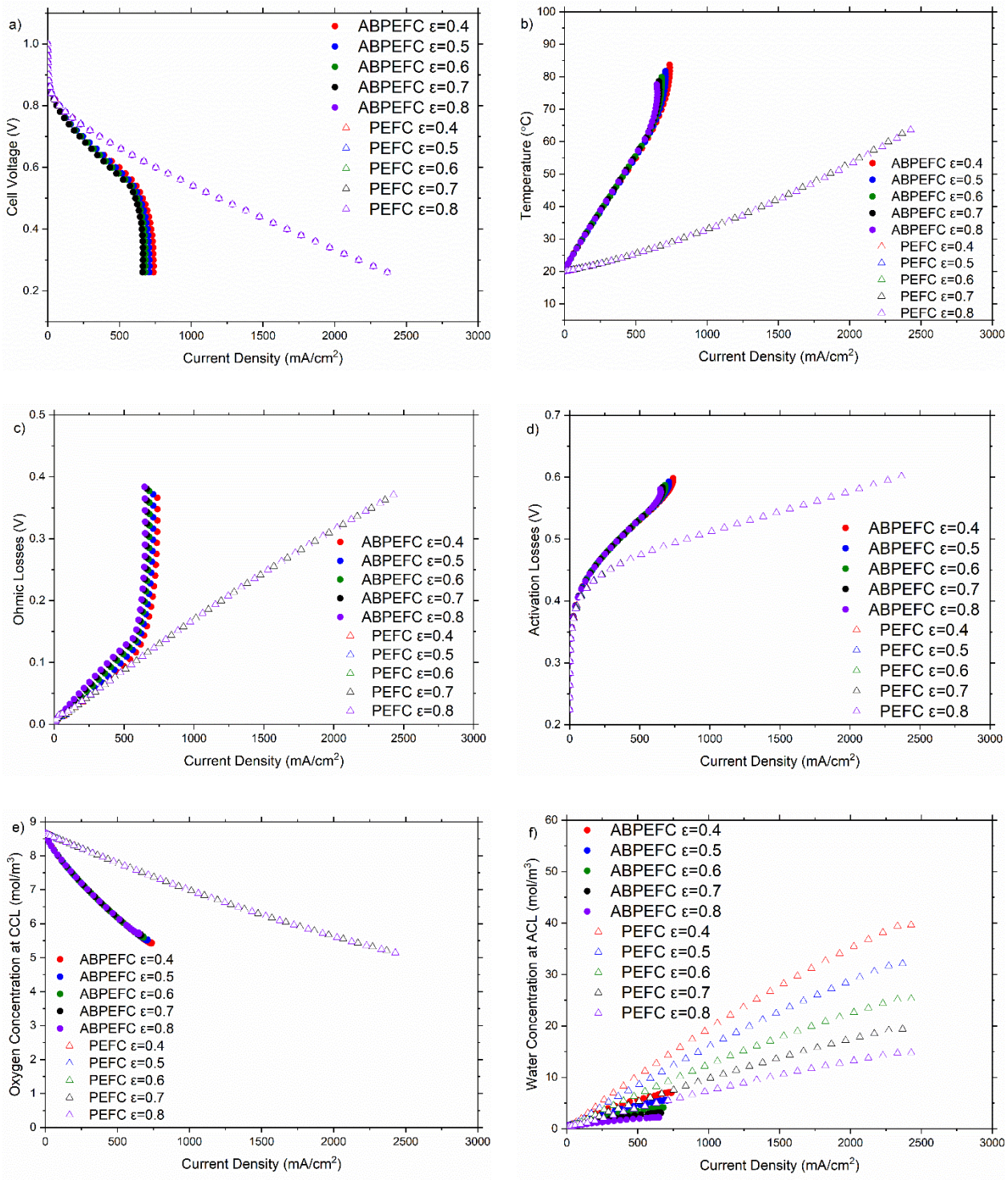

Figure 4.4 The outputs of the modelled air-breathing and conventional PEFCs at 20 °C and 40% relative humidity and variable anode GDL porosity: (a) cell voltage, (b) cell temperature, (c) ohmic losses, (d) activation losses, (e) oxygen concentration at the cathode catalyst layer and (f) water concentration at the anode catalyst layer as a function of current density.

4.4.2 Thickness of Gas Diffusion Layers

Figure 4.5 and Figure 4.6 show the impact of the thickness of the cathode GDL and the anode GDL respectively on the performance of the modelled fuel cells. It is clear that the impact of the GDL thickness is similar to that of the porosity. Namely, the performance of the air-breathing of the fuel cell improves as the cathode or anode GDL thickness increases (Figure 4.5a and Figure 4.6a). As the GDL thickness increases, less water is removed from the catalyst layers and the membrane (Figure 4.5 f and Figure 4.6f), thus reducing the membrane resistance and subsequently the ohmic losses (Figure 4.5c and Figure 4.6c). On the other hand, the conventional fuel cell is not heat transfer limited due to high transfer coefficients that allow for reasonable cell temperatures compared to those of air-breathing fuel cells Figure 4.5b and Figure 4.6b). To this end, thin GDLs are of benefits to the conventional fuel cell as it permits more oxygen to be supplied to the catalyst layers (Figure 4.5e) and/or more heat to be dissipated from the fuel cell leading to less cell temperatures (Figure 4.5b and Figure 4.6b), less activation losses (Figure 4.5d and Figure 4.6d) and slightly better performance (Figure 4.5a and Figure 4.6a). It should be noted that, as with the impact of the GDL porosity, the impact of the cathode GDL thickness on the performance of either the air-breathing or the conventional fuel cell is more profound than that of the anode GDL thickness and this is due to two factors: (i) more water is available at the cathode catalyst layer where it is produced and (ii) activation losses are mainly associated with the cathode catalyst layer. One more observation is that the cell temperature of the conventional fuel cell is more sensitive to the thickness of the anode GDL than the cathode GDL. This could be attributed to the longer thermal pathway that heat generated at the cathode catalyst layer need to travel through to the surface of the anode GDL compared to the surface of the cathode GDL; see Figure 4.1. Therefore, any reduction in the anode GDL thickness will have

greater (and better) impact on the surface temperature compared to that of the cathode GDL thickness. Overall, GDLs with relatively high thickness (> 500 µm) are favoured to be used for air-breathing PEFCs, particularly for the cathode side of the fuel cell.

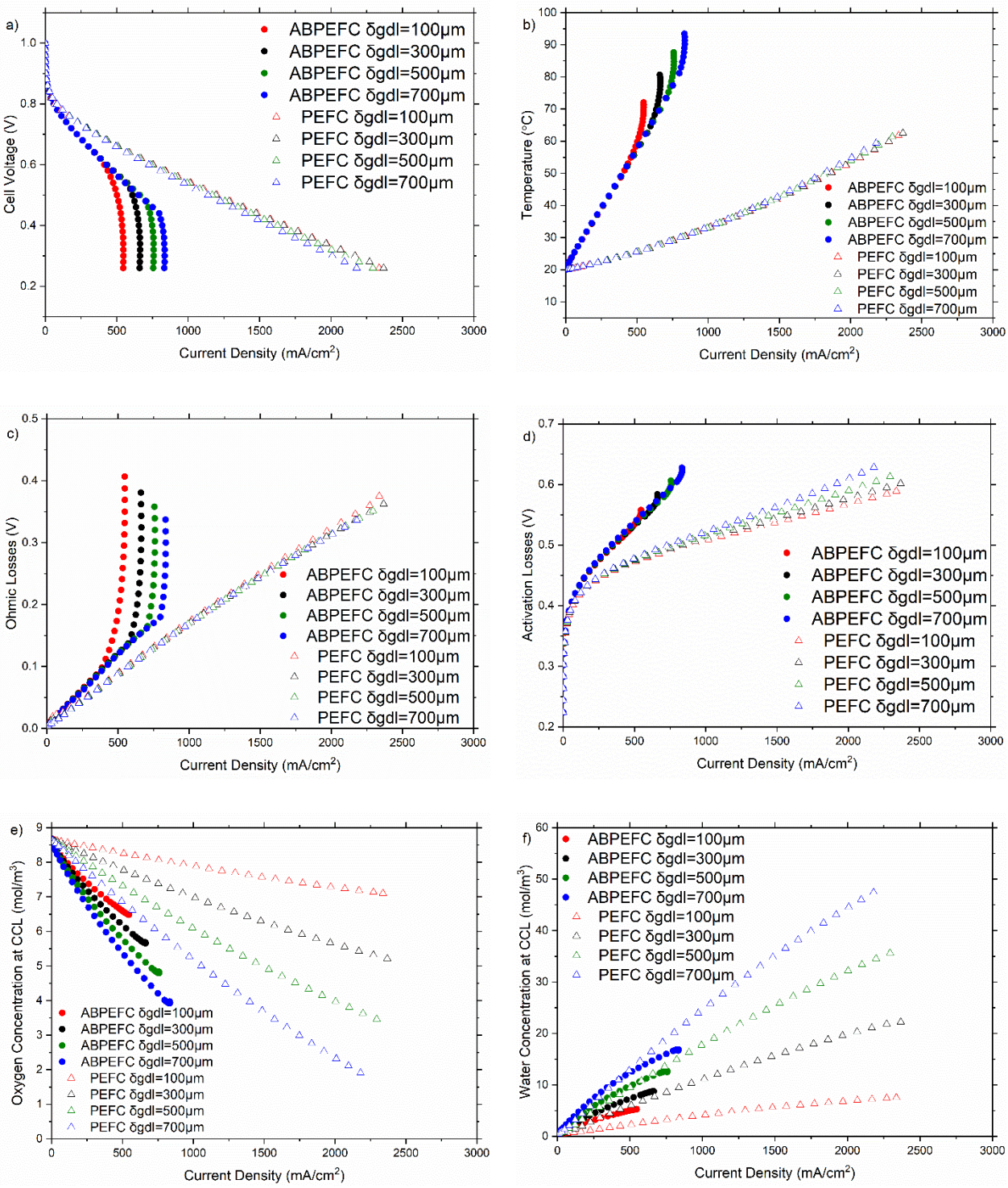

Figure 4.5 The outputs of the modelled air-breathing and conventional PEFCs at 20 °C and 40% relative humidity and variable cathode GDL thickness: (a) cell voltage, (b) cell temperature, (c) ohmic losses, (d)

activation losses, (e) oxygen concentration at the cathode catalyst layer and (f) water concentration at the cathode catalyst layer as a function of current density.

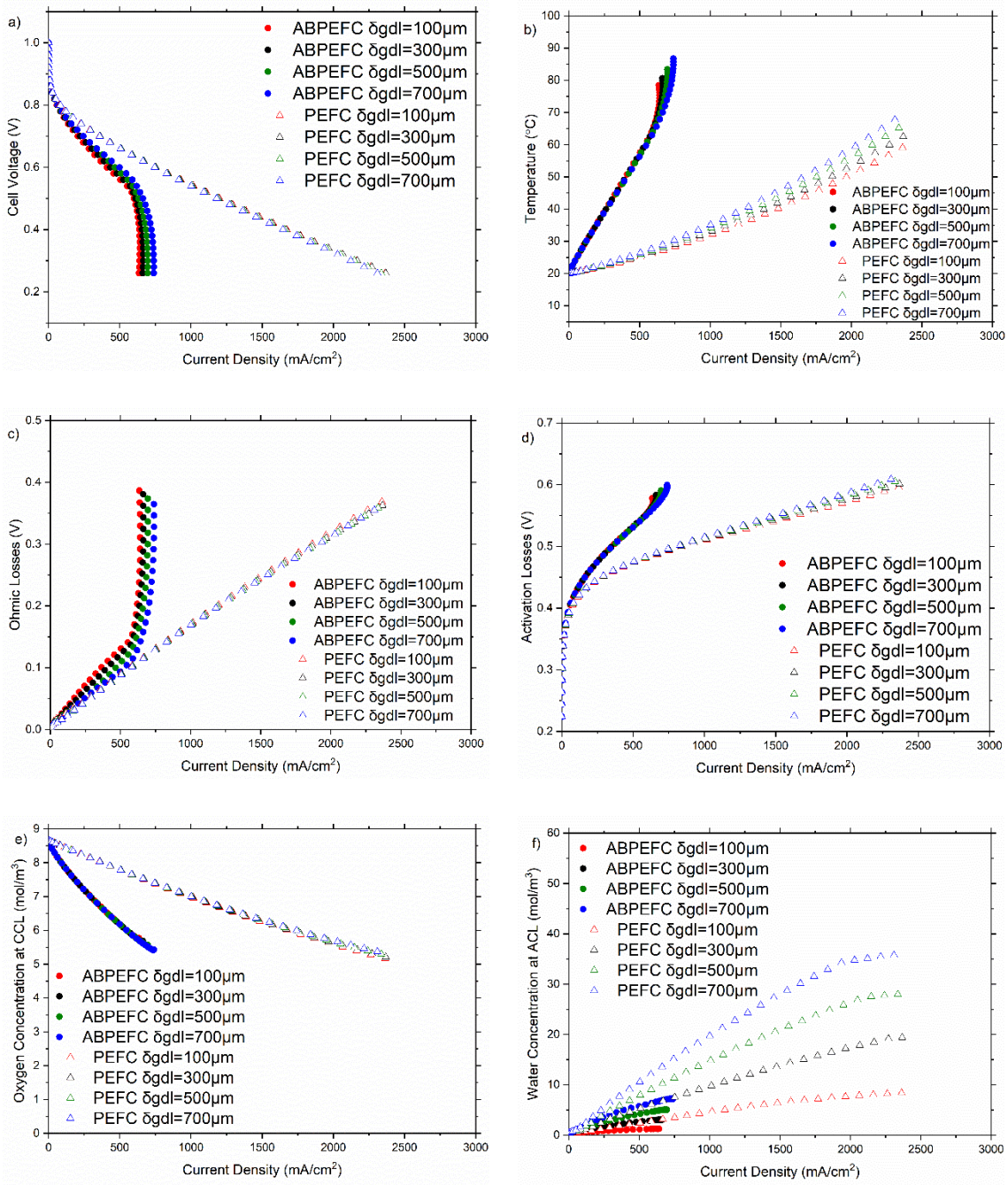

Figure 4.6 The outputs of the modelled air-breathing and conventional PEFCs at 20 °C and 40% relative humidity and variable anode GDL thickness: (a) cell voltage, (b) cell temperature, (c) ohmic losses, (d) activation losses, (e) oxygen concentration at the cathode catalyst layer and (f) water concentration at the anode catalyst layer as a function of current density.

4.4.3 Membrane Thickness

Figure 4.7 shows the impact of the membrane thickness on the performance of the modelled fuel cells. For this parametric study, membrane thicknesses have been changed in equally-spaced intervals from 20 to 140 μm. Overall, the fuel cell performance degrades with increasing membrane thickness for either the air-breathing or the conventional fuel cell. Evidently, as the membrane thickness increases, the ionic resistance of the membrane and subsequently the ohmic losses increases (Figure 4.7c). Also, the overall thermal resistance of the fuel cell increases with increasing membrane thickness, thus causing (along with increasing ohmic losses) an increase in cell temperature (Figure 4.7b) and consequently activation losses (Figure 4.7d). It is noteworthy that the fuel cell performance becomes less limited by the membrane thickness as the latter increases. For example, the limiting current density of the air-breathing fuel cell decreases by about 22% when changing the membrane thickness from 20 to 50 μm and by about 9% when changing the membrane thickness from 110 to 140 μm.

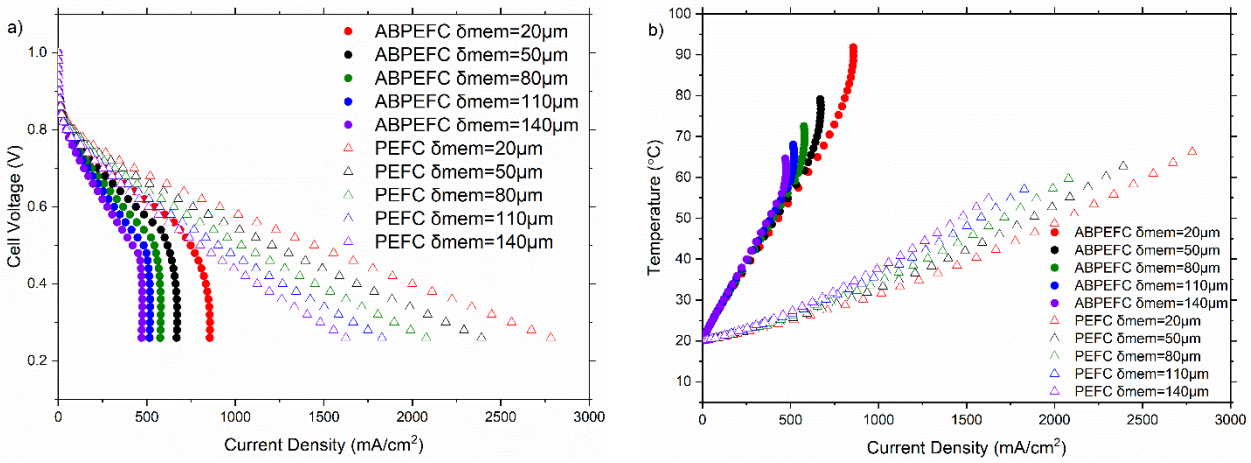

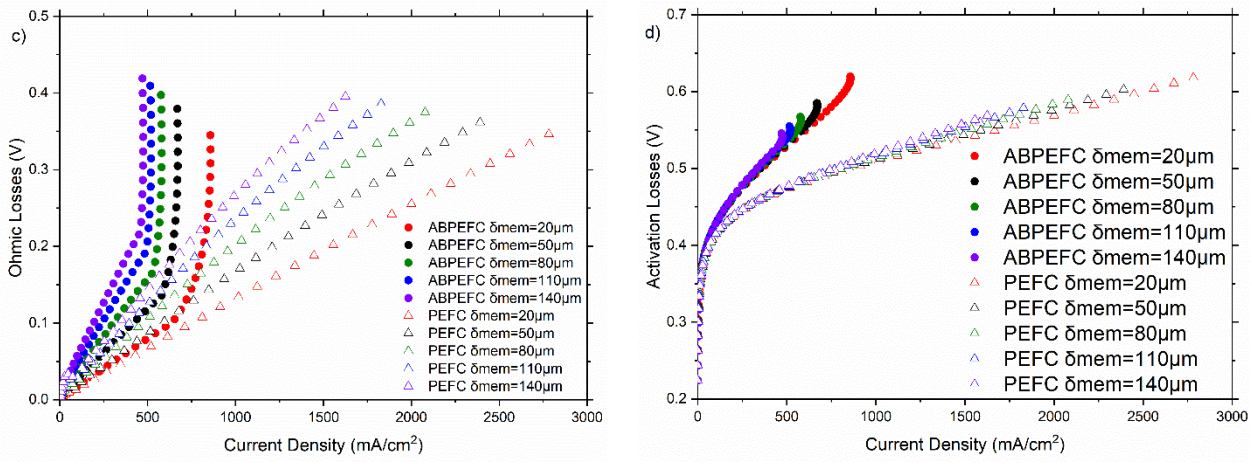

Figure 4.7 The outputs of the modelled air-breathing and conventional PEFCs at 20°C and 40% relative humidity and variable membrane thickness: (a) cell voltage, (b) cell temperature, (c) ohmic losses and (d) activation losses.

4.4.4 Electrical Resistance

Figure 4.8 shows the impact of the total electrical resistance on the performance of the modelled fuel cells. For the given range of the electrical resistance (6-18 $m\Omega$), the performance of the air-breathing fuel cell in the intermediate current density region slightly degrades with increasing electrical resistance and ohmic losses (Figure 4.8c); however, this effect diminishes as the current density increases as evidenced by the almost invariant limiting current densities of all the cases (Figure 4.8a). The fuel cell resistance is, as could be seen from Eq. (4.5), broken down into electrical resistance and membrane (ionic) resistance. As the current density of the air-breathing fuel cell increases, more heat is generated due to increasing ohmic (Figure 4.8c) and activation losses (Figure 4.8d). The relatively poor heat dissipation from the air-breathing fuel cell results in an exponential increase of the cell temperature at high current densities which substantially lower the water activity and increase the membrane resistance (Figure 4.8e) and eventually mask the impact of the electrical resistance. As can be seen from Figure 4.8e, the values of the membrane resistance

are almost the same at very high current densities justifying the almost invariant current densities of all the investigated cases for the air-breathing fuel cell. On the other hand, the conventional fuel cell (compared to the air-breathing one) enjoys better heat dissipation which even allow the membrane conductivity to increase with linearly increasing cell temperature (see Eq. (4.8)). This in turn allows for the impact of the electrical resistance to be fully realised along the entire range of the current density of the conventional fuel cell: the fuel cell performance gradually degrades with increasing electrical resistance.

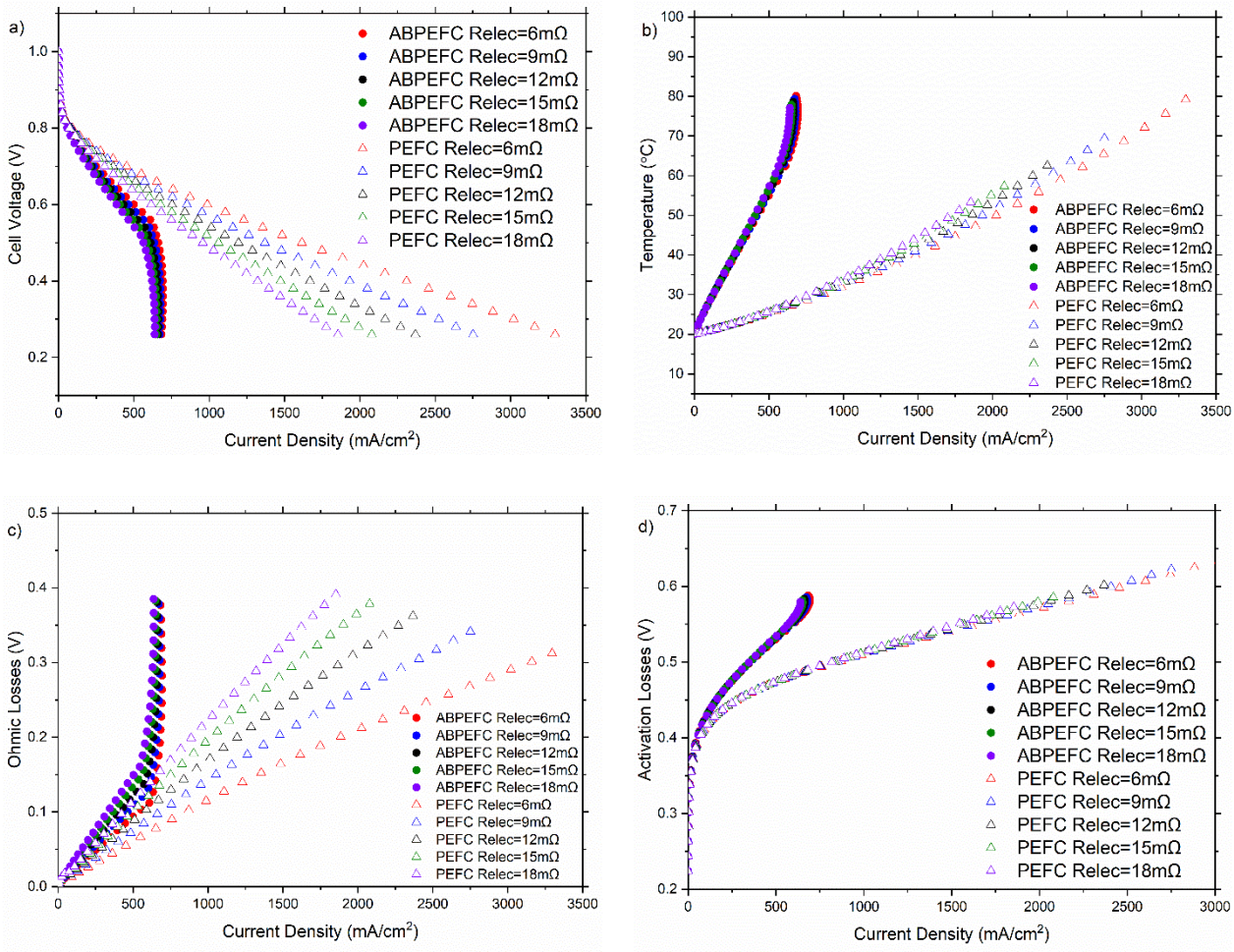

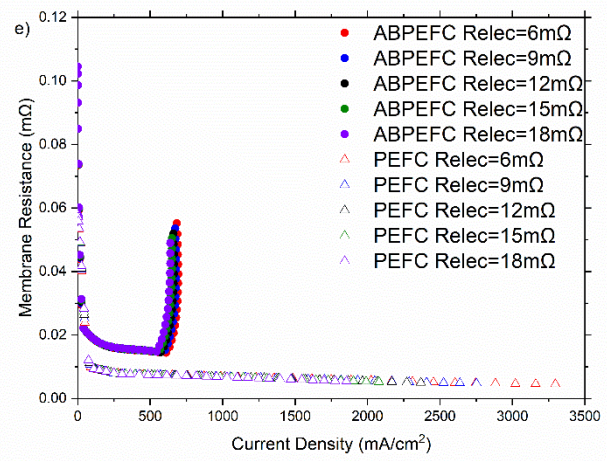

Figure 4.8 The outputs of the modelled air-breathing and conventional PEFCs at 20 °C and 40% relative humidity and variable electrical resistance: (a) cell voltage, (b) cell temperature, (c) ohmic losses, (d) activation losses and (e) membrane resistance.

4.5 Conclusions

Two steady-state, non-isothermal mathematical models have been developed for air-breathing and conventional PEFCs in order to undertake a parametric study that elucidates the key factors that influence the performance of each type of fuel cells and subsequently obtain better insights on how to improve the performance of the air-breathing fuel cell. Namely, some key parameters (i.e., the porosity and the thickness of the GDL, the membrane thickness and the overall electrical resistance) have been selected to comparatively assess the performance for each type of fuel cells and identify the underlying reasons behind the clear difference in performance. The key findings of this study are as follows:

- The conventional PEFC significantly outperforms the air-breathing PEFC and this is due to substantially higher heat and mass transfer coefficients demonstrated by the former type of fuel cells. Poor heat dissipation, due to reliance on natural heat convection, in case of the air-breathing PEFC leads to, compared to the conventional PEFC, an exponential increase in cell temperature at high current densities which

ultimately lower the membrane hydration and increase the ohmic losses. Likewise, poor supply of oxygen to the cathode catalyst layer of the air-breathing PEFC results in increased activation losses.

- The porosity and the thickness of the GDL impact the performance of the air-breathing and conventional PEFCs differently. As the GDL porosity increases from 0.4 to 0.8 or the GDL thickness decreases from 700 to 100 μm in case of the air-breathing PEFC, the rate of water transport away from the catalyst layer (and the membrane) increases, lowering the hydration level of the membrane and consequently increasing the ohmic losses and degrading cell performance especially at high current densities where cell temperature increases exponentially. On the other hand, the conventional PEFC is not, owing to relatively high heat transfer coefficient, heat transfer limited and therefore the increase in the GDL porosity or the decrease in the GDL thickness lead to better performance due to increased supply of oxygen/hydrogen to the catalyst layers without compromising the membrane hydration level.

- Both the air-breathing and conventional PEFCs perform better with the thinnest membrane (i.e. 20 μm) and this is evidently due to decreased membrane resistance and subsequently ohmic losses. However, the performance of the air-breathing PEFC is more sensitive to membrane thickness than the conventional PEFC and this is due to the fact that the former type of fuel cells is more heat transfer limited, meaning that thicker membranes result in higher thermal resistance and ultimately more pronounced impact on cell performance.

- In contrast, the performance of the conventional PEFC was found to be more sensitive to the overall electrical resistance than the air-breathing PEFC. The ohmic

losses in the air-breathing PEFC are, owing to insufficient heat dissipation at high current densities, dominantly influenced by the membrane resistance which largely mask the impact of the electrical resistance.

- As a recommendation out of this study, GDLs with relatively low porosity (~ 0.4) and high thickness (> 500 μm) should be ideally designed and/or used for air-breathing PEFCs, particularly for the cathode side of the fuel cell.

Acknowledgements

Fatma Calili thanks the Ministry of National Education at the Republic of Turkey for funding her PhD studentship at the University of Sheffield.

Nomenclature

Roman symbols

a	Water activity
A_{act}	Active area of the fuel cell, m^2
C	Molar Concentration, mol/m^3
D	Diffusion coefficient, m^2/s
e	Emissivity
E	Nernst Voltage, V
E_a	Activation energy, $\mathrm{J/mol}$
F	Faraday's constant, $\mathrm{C/mol}$
g	Gravitational acceleration, $\mathrm{m/s}^2$
h	Heat transfer coefficient, $\mathrm{W/(m^2.K)}$
h_m	Mass transfer coefficient, $\mathrm{m/s}$
ΔH	Enthalpy change for the reaction, $\mathrm{J/mol}$
j	Current density, $\mathrm{A/m}^2$
j_0	Reference exchange current density, $\mathrm{A/m}^2$

k	Thermal conductivity, $\mathrm{W/(m.K)}$
L_{ch}	Characteristic length, m
M	Molecular weight, , $\mathrm{kg/m^3}$
n	Number of electrons
n_d	Electro-osmotic drag coefficient
N	Molar flux, $\mathrm{mol/(m^2.s)}$
P	Ambient pressure, atm
P_{H_2}	Partial pressure of hydrogen, atm
P_{H_2O}	Partial pressure of water vapour, atm
P_{sat}	Water vapour saturation pressure, atm
P_{O_2}	Partial pressure of oxygen, atm
q	Heat flux, $\mathrm{W/m^2}$
R	Universal Gas Constant, $\mathrm{atm/(mol.K)}$
R_{elec}	Lumped electrical cell resistance, Ω
R_{mem}	Membrane resistance, Ω
Ra	Rayleigh number
RH	Relative humidity, %
ΔS	Entropy change for the reaction, $\mathrm{J/(mol.K)}$
Sh	Sherwood number
T	Absolute temperature, K
V_{cell}	Cell voltage, V
x	Mole fraction

Greek symbols

α	Charge transfer coefficient
β	Thermal expansion coefficient, $\mathrm{K^{-1}}$
γ	Volumetric expansion coefficient, $\mathrm{K^{-1}}$
δ	Thickness, m
ε	Porosity
η_{act}	Activation losses, V
η_{ohmic}	Ohmic losses, V
λ	Water content
σ_{Bolt}	Stephan-Boltzmann constant, $\mathrm{W/(m^2.K^4)}$
σ_{mem}	Ionic conductivity, $\mathrm{S/m}$

Abbreviations

ABPEFC	Air-breathing Polymer Electrolyte Fuel Cell
ACL	Anode Catalyst Layer
CCL	Cathode Catalyst Layer
GDL	Gas Diffusion Layer
MEA	Membrane Electrode Assembly
PEFC	Polymer Electrolyte Fuel Cell

Chapter 5: Dynamic Models for Air-breathing and Conventional Polymer Electrolyte Fuel Cells: A Comparative Study

---

This chapter is published as:

Calili-Cankir F, Ismail MS, Berber MR, Alrowaili ZA, Ingham DB, Hughes KJ, Ma L, Pourkashanian M. Dynamic models for air-breathing and conventional polymer electrolyte fuel cells: A comparative study. Renewable Energy. 2022 Aug 1;195:1001-14.

https://doi.org/10.1016/j.renene.2022.06.092

Authorship statement

The principle author of the paper is Calili-Cankir F. The contribution of Calili-Cankir F is conceptualization, methodology, software, formal analysis, investigation, validation, writing original draft, review and editing.

5.1 Abstract

Two dynamic models have been built for air-breathing and conventional polymer electrolyte fuel cells (PEFCs) in order to comparatively investigate the impacts of some key parameters on the transient response to load alterations and the steady-state performance for each fuel cell type. It was found that with load alterations, the dynamic response of the air-breathing

PEFC is significantly slower than that of the conventional PEFC and this is due to significantly slower heat transfer coefficients associated with natural convection taking place at the surface of the exposed-to-the ambient cathode GDL. Namely, lower heat transfer coefficient results in poor heat dissipation that eventually leads to: significantly higher and less-responsive-to-load changes cell temperature (compared to those of the conventional PEFC) and subsequently higher ohmic and activation losses. Further, the dynamic and the steady-state performance of the air-breathing PEFC was found to increase with decreasing GDL porosity, decreasing membrane thickness and, to a lesser extent, decreasing overall electrical resistance. These effects are significantly less profound on the performance of the conventional PEFC. All the above findings have been described and discussed in the paper.

Keywords: Air-breathing PEFCs; Conventional PEFCs; Dynamic model; Transient response; Load alterations

5.2 Introduction

Polymer electrolyte fuel cells (PEFCs) are promising clean power conversion technologies for a multitude of portable, automotive and stationary applications as they feature high efficiency and rapid start-up [28-30, 196, 197]. Conventional PEFCs typically require some auxiliary components (e.g. fans, compressors and humidifiers) to supply and humidify the reactant gases. These auxiliary components bring additional weight and volume and increase the cost of entire fuel cell system. Focusing on power sources for small portable devices, the number of the auxiliary components should be minimised to allow for significant size reduction of the fuel cell system and subsequently compete with the conventionally used non-environmentally friendly batteries [17, 148, 149]. In air-breathing PEFCs, the cathode is open to the ambient, and this means that the cathode gas diffusion layer is in direct contact

with the ambient, and that oxygen (required for the oxygen reduction half reaction at the cathode electrode) and water vapour (required for the initial humidification of the membrane electrolyte) are directly extracted from the ambient air through natural convection [70, 82, 87]. To this end, storage, pumping and humidifying devices are no longer required for the cathode sides of the fuel cell, thus significantly simplifying the fuel cell system. However, the performance of the air-breathing PEFC is significantly inferior to that of the conventional PEFC. Evidently, this is due to the substantially lower heat and mass transfer coefficients associated with natural convection at the open cathode of the air-breathing PEFC (compared to those of the cathode flow channels of the conventional PEFC or an open cathode with an integrated fan). This often leads to inadequate heat and mass exchange between the cathode catalyst layer and the ambient [111].

In the past two decades, there has been research work that has compared the effects of the natural and forced convection on the performance of the PEFCs. Santa Rosa et al. [122] developed an eight-cell air-breathing PEFC stack in order to investigate the difference between forced air-convection and natural air convection. They reported that the fuel cell performance with forced air convection is, for a typical voltage (i.e. 4 V), more than two times higher than the one with natural convection. Fernandez-Moreno et al. [39] built a portable system using an air-breathing PEFC for power generation and tested it with and without using a cathodic fan. They showed that the use of fan mitigated water flooding at the cathode of the fuel cell and the maximum current density of the PEFC with the fan is 0.37 $\mathrm{A/cm^2}$ while it is 0.24 $\mathrm{A/cm^2}$ if the operation of the fuel only relies on natural convection. Ferreira-Aparicio and Chaparro [102] studied different cathode designs to optimise the cathode architecture to reduce mass transport resistance of an air-breathing PEFC.

Enlighten by performance tests that were performed under natural and forced convection conditions, they showed the importance of the cathode design on the performance of the air-breathing PEFCs. Namely, as the opening of the open cathode collector increases, the cell performance in general improves. Jung et al.[110] added hydrophilic silica nano-particles to the anode catalyst layer to improve water management in air-breathing and air-blowing PEFCs. They showed that the proposed method improved the performance of both air-breathing and air-blowing PEFCs by around 27% and 44%, respectively. Ous and Arcoumanis [117] examined the effect of air stoichiometry on the formation of the water droplets under natural and forced convections in a PEFC with open cathodes. They observed that there was no droplet formation for the first 5 min at the lowest reported current density (i.e. 80 $\mathrm{mA/cm^2}$) and then small and few droplets formed under natural convection. However, the current density almost doubled and that the number and size of droplets significantly increased when a fan was operated to provide increased air flow rates. Calili-Cankir et al. [23] developed two mathematical steady-state models for air-breathing and conventional PEFCs to conduct a parametric investigation on how natural convection affects the performance of the air-breathing PEFC. They showed that the conventional PEFC outperforms the air-breathing PEFC and this is due to the substantially higher heat and mass transfer coefficients associated with the former fuel cell type. They also found that the air-breathing PEFC is, compared to the conventional PEFC, more sensitive to the membrane thickness and less sensitive to the electrical conductivity.

However, there have been no studies that have thoroughly investigated the effect of natural convection on the transient response of the air-breathing PEFC. Air-breathing PEFCs should be reasonably responsive to the rapid and/or high load variations in order to meet the power

requirements of the small electronic devices. In a previous work [22], we investigated the transient response of the air-breathing PEFC at different ambient conditions (temperature and relative humidity), GDL parameters (thickness and thermal conductivity) and hydrogen utilisation. In this study, two dynamic models for air-breathing and conventional PEFCs have been developed within the platform of MATLAB/Simulink to investigate, for the first time, the effect of natural convection on the transient response of the air-breathing PEFC by simultaneously comparing with the outcomes of both dynamic models. Furthermore, the effects of the GDL porosity, the membrane thickness and the electrical resistance on the transient response of both types of fuel cells have been comparatively assessed in this study to provide better insights on how some key design parameters should be varied to improve the dynamic response of the air-breathing PEFC.

5.3 Dynamic Modelling of Fuel Cells

5.3.1 Model Assumptions

Two dynamic models for single air-breathing and conventional PEFCs are developed within the platform of MATLAB/Simulink. The modelled air-breathing PEFC was originally described and reported by Fabian and his co-workers [60] and the geometry and the physical parameters of the conventional PEFC have been considered to be the same as those of the air breathing PEFC; see Table 5.1. Figure 5.1 demonstrates the schematic representations of key components of the fuel cells modelled in this study. It should be noted that we have not listed the dimensions of the hydrogen chamber (for the air-breathing PEFC) and the flow channels (for the conventional PEFC) in Table 5.1 as they were not used in the calculations; the concentrations and temperature at the surfaces of the GDLs were assumed to be the same as those of the chamber and the flow channels.

Table 5.1 Physical parameters and constants used in the dynamic models [22].

Parameters	**Value**
Universal gas constant, R	8.315 J/(mol. K)
Faraday's constant, F	96500 C/mol
Standard reversible fuel cell voltage, E_0	1.23 V
Ambient/cell pressure, P	1 atm
Ambient temperature, T_∞	20 °C
Initial cell temperature of conventional PEFC, T	20 °C
Binary diffusivity of O_2 in air, $D_{O_{2,}air}$	2.1×10^{-5} m^2/s
Binary diffusivity of H_2O in air, $D_{H_2O,air}$	2.6×10^{-5} m^2/s
Length of active cell side (square), L_a	0.03 m
Cell active area, A_{act}	0.0009 m^2
Membrane thickness, δ_{mem}	5.2×10^{-5} m
GDL thickness, δ_{gdl}	3.0×10^{-4} m
GDL porosity, ε	0.4
GDL tortuosity,τ	3.0
GDL thermal conductivity, k_{gdl}	10 W/(m. K)
Exchange current density, j_0	2.5×10^{-5}A/cm^2
Lumped cell electrical resistance, R_{elec}	12 mΩ
Charge transfer coefficient, α	0.28
Utilization factor, U	0.7
Hydrogen time constant, τ_{H_2}	0.3096 s
Oxygen time constant, τ_{O_2}	0.7784 s
Water vapour time constant, τ_{H_2O}	0.9288 s
Hydrogen valve constant, K_{H_2}	3.627×10^{-5} mol/(s. atm)
Oxygen valve constant, K_{O_2}	1.443×10^{-5} mol/(s. atm)
Water vapour valve constant, K_{H_2O}	1.209×10^{-5} mol/(s. atm)

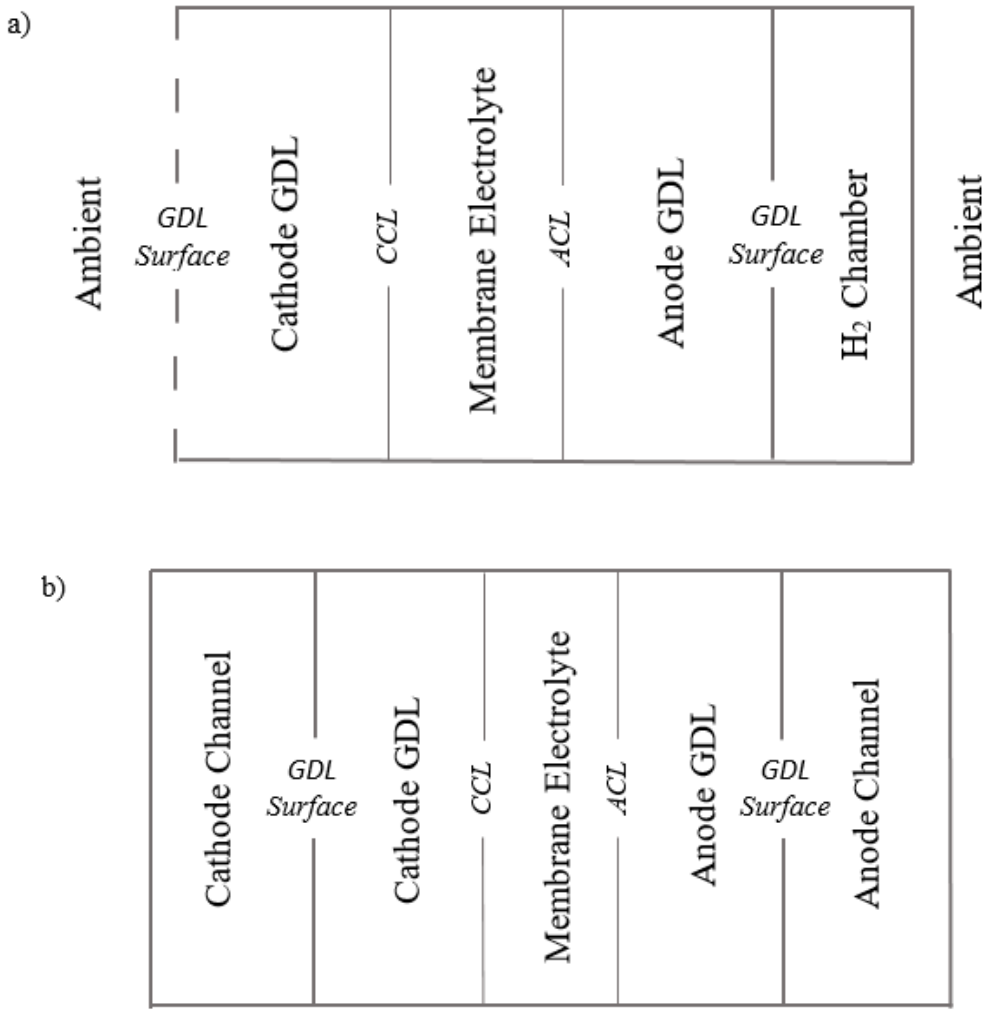

Figure 5.1 Schematic diagrams of the modelled: (a) air-breathing and (b) conventional PEFCs (adapted from [23]). Note that the abbreviations 'CCL' and 'ACL' stand for cathode catalyst and anode catalyst layers respectively. The dimensions of the key components are listed in Table 5.1.

The following assumptions and considerations have been taken into account for the developed dynamic models:

- Water exists only in vapour form.
- The reactant gases are ideal.
- The anode is dead-ended in the air-breathing PEFC.
- The catalyst layers are treated as interfaces between the membrane and the GDLs as they are infinitely thin.

- The water activity within the membrane is in equilibrium with water vapour activity in the catalyst layers.

- The properties of all the fuel cell components are assumed to be uniform.

As shown in Figure 5.2, the dynamic models, expressed in the Laplace domain, consist of three main blocks: Nernst voltage, activation losses and ohmic losses. The outputs of the models are the cell voltage and power. It has been previously reported that the sharp decline in the cell voltage of the modelled air-breathing PEFC at high current densities was found to be primarily due to the membrane dehydration [22, 59, 60, 72]; hence, we assume that, for simplification and comparative purposes, the concentration losses, typically induced by water flooding and/or insufficient supply of the reactant gasses to the catalyst layers at high current densities, are negligible for the dynamic models. The 'Cell Temperature' block in Figure 5.2 is a link to steady-state models for the fuel cells that were built in a previous work [23] in order to feed the dynamic models with the temperature of the cathode catalyst layer. The steady-state models were called as a function in the dynamic models that runs these steady-state models for a given set of parameters and operating conditions and curve-fits the temperature-current density data in order to use the corresponding curve-fitting equation as an input for the dynamic models. This temperature was treated as the cell temperature; this is a reasonable approximation as: (i) the temperature of the cathode catalyst layer is the highest compared to other parts of the fuel cell and (ii) the temperature variation across the fuel cell is normally less than 2 °C [23]. It is noteworthy that the details of the steady-state models were not mentioned in the present study in order to maintain flow of the paper and to avoid distracting readers from its main focus, which is the transient response of

the fuel cells; the interested readers are referred to [23] for further details regarding the steady-state models.

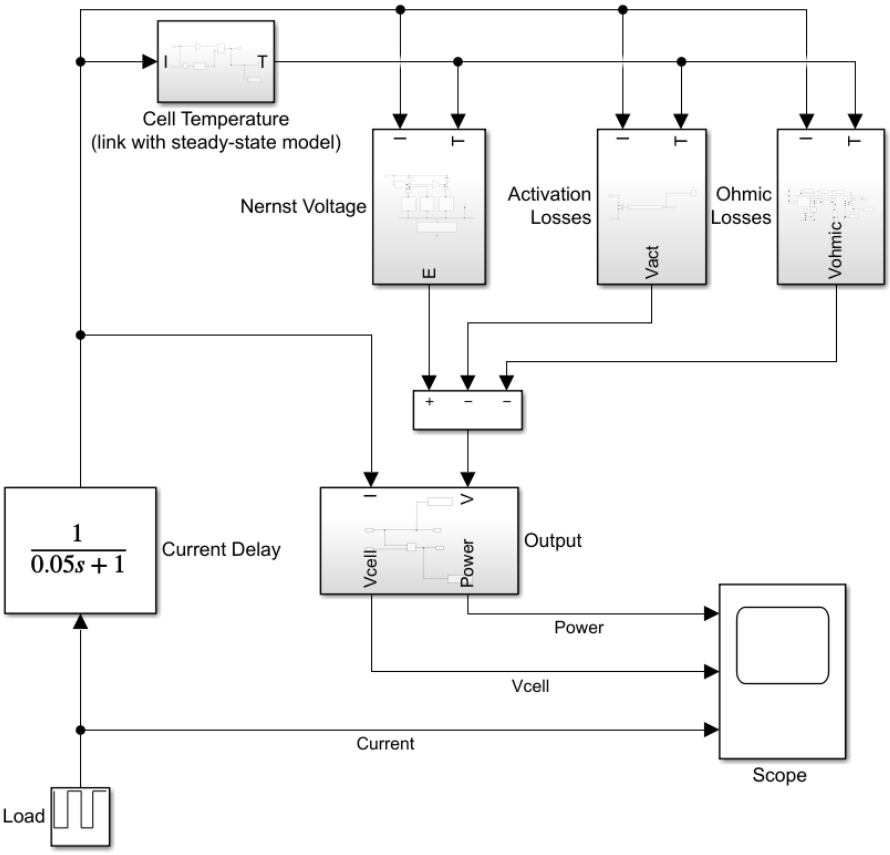

Figure 5.2 The block diagram of the dynamic model for the fuel cells.

5.3.2 Model Formulation

The cell potential for both types of fuel cells, V_{cell}, is calculated as follows [3]:

$$V_{cell} = E - \eta_{act} - \eta_{ohmic} \tag{5.1}$$

where E is the Nernst (the reversible) voltage and η_{act} and η_{ohmic} are the activation and ohmic losses, respectively. As shown below, the equations used for each dynamic model were compiled in a subsection to avoid confusion starting with those specific to air-breathing

PEFCs. Where equations are common for both fuel cell types, the necessary notes and references are given in the conventional PEFC subsections.

Air-breathing PEFC

The Nernst voltage is obtained by [8]:

$$E = E_0 + \frac{RT}{2F}\ln\left(P_{H_2}.P_{O_2}^{1/2}\right) \qquad (5.2)$$

where E_0 is the standard reversible fuel cell voltage, T is the absolute temperature, R is the universal gas constant and F is the Faraday's constant. P_{H_2} and P_{O_2} are the partial pressures of hydrogen and oxygen, respectively. Figure 5.3 illustrates the block diagram of the Nernst voltage for the air-breathing PEFC.

The partial pressure of oxygen in the open cathode compartment is calculated by [22, 74]:

$$P_{O_2} = x_{O_2}P = x_{O_2}^0 - \delta_{GDL}\frac{jRT}{4FD_{O_2}^{eff}} \qquad (5.3)$$

where $x_{O_2}^0$ is the mole fraction of the oxygen in the ambient air (i.e. 0.21), δ_{GDL} is the GDL thickness, j is the current density and P is the ambient pressure. The effective diffusivity of oxygen into air, $D_{O_2}^{eff}$, is calculated using the following expression:

$$D_{O_2}^{eff} = \frac{\varepsilon}{\tau}D_{O_2,air} \qquad (5.4)$$

where ε and τ are the porosity and tortuosity of the porous diffusion medium, respectively and $D_{O_{2,}air}$ is the binary diffusivity of oxygen into air.

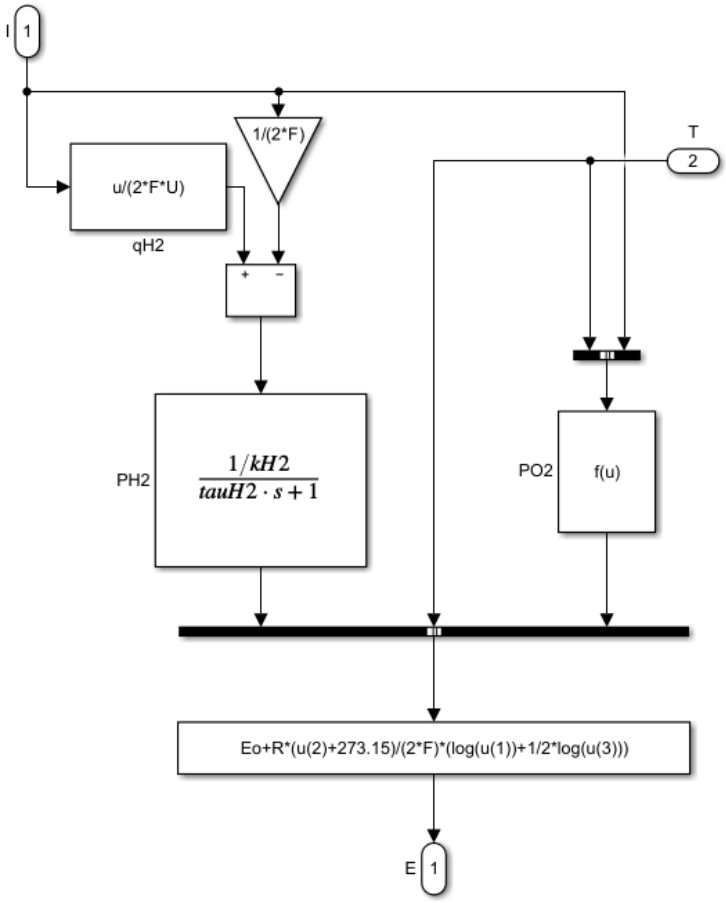

Figure 5.3 The block diagram of the Nernst voltage for the air-breathing PEFC.

The relationship of the hydrogen molar flow through a valve with its partial pressure inside the flow channel can be expressed as follows [160]:

$$\frac{q_{H_2}}{P_{H_2}} = \frac{k_{an}}{\sqrt{M_{H_2}}} = K_{H_2} \tag{5.5}$$

where k_{an} and K_{H_2} are the anode valve constant and the molar valve constant for hydrogen, respectively. M_{H_2} is the molar mass of hydrogen. The derivative of the partial pressure of hydrogen is determined using the ideal gas law and written in the Laplace transform domain as follows [160]:

$$P_{H_2} V_{an} = n_{H_2} RT \tag{5.6}$$

where V_{an} and n_{H_2} are the volume of the anode compartment and the number of hydrogen moles in the anode channel, respectively. The time derivation of Eq. (5.6) can be obtained by:

$$\frac{d}{dt}P_{H_2} = \frac{RT}{V_{an}}q_{H_2} \tag{5.7}$$

where q_{H_2} is the molar flow rate of hydrogen and given by:

$$q_{H_2} = q_{H_2}^{in} - K_{H_2}P_{H_2} - q_{H_2}^{r} \tag{5.8}$$

where $q_{H_2}^{in}$ and $q_{H_2}^{r}$ are the inlet flow rate of hydrogen and the flow rate of reacting hydrogen, respectively.

The molar flow rate of reacting hydrogen can be obtained as a function of the fuel cell current I using Faraday's second law of electrolysis:

$$q_{H_2}^{r} = \frac{I}{2F} \tag{5.9}$$

After substituting Eq. (5.8) and Eq. (5.9) into Eq. (5.7), the derivation of partial pressure of oxygen can be rewritten as follows:

$$\frac{d}{dt}P_{H_2} = \frac{RT}{V_{an}}(q_{H_2}^{in} - K_{H_2}P_{H_2} - \frac{I}{2F}) \tag{5.10}$$

And its expression in the Laplace domain [22, 74]:

$$P_{H_2} = \frac{1/K_{H_2}}{1 + \tau_{H_2}s}(q_{H_2}^{in} - \frac{I}{2F}) \tag{5.11}$$

The hydrogen time constant, τ_{H_2}, is given by:

$$\tau_{H_2} = \frac{V_{an}}{K_{H_2}RT} \tag{5.12}$$

The activation losses are expressed as follows [22]:

$$\eta_{act} = \frac{RT}{2\alpha F} \ln\left(\frac{j}{j_0}\right) \tag{5.13}$$

where α and j_0 are the charge transfer coefficient and the exchange current density, respectively. Note that the exchange current density is a function of temperature as evident from Eq. (3.13) in Chapter 3. The exchange current density shown in Table 5.1 was obtained after correcting the reference exchange current density at 30 ℃ (i.e. $5\times10^{-5}\mathrm{A/cm^2}$) for the temperature which is initially 20 ℃ in our case. However, for simplification, the sensitivity of the exchange current density to temperatures beyond 20 ℃ was assumed to be negligible. Relaxing this assumption was found to result in an almost negligible impact on the performance of the modelled fuel cells at the selected currents (an increase up to 0.03 for the air-breathing PEFC and up to 0.01 V for the conventional PEFC).

The ohmic losses can be obtained using the equation [72]:

$$\eta_{ohmic} = jA_{act}(R_{elec} + R_{mem}) \tag{5.14}$$

where A_{act} is the active area of the fuel cell and R_{elec} is the lumped electrical resistance of the cell. The membrane resistance, R_{mem}, is defined as follows:

$$R_{mem} = \frac{\delta_{mem}}{A_{act}\sigma_{mem}} \tag{5.15}$$

where δ_{mem} is the thickness of the polymer electrolyte membrane. The ionic conductivity of the membrane, σ_{mem}, can be calculated using following empirical expression that is more appropriate for air-breathing PEFC than the well-known Springer's model [79]:

$$\sigma_{mem} = (3.46a^3 + 0.0161a^2 + 1.45a - 0.175)\exp\left[1268\left(\frac{1}{303} - \frac{1}{T}\right)\right] \quad (5.16)$$

where a is the water activity and given by [8]:

$$a = \frac{P_{H_2O}}{P_{sat}} \quad (5.17)$$

where P_{H_2O} and P_{sat} are the partial pressure and saturation pressure of water vapour at the cell temperature, respectively. The partial pressure of water is obtained as follows [22, 74]:

$$P_{H_2O} = x_{H_2O}P = x^0_{H_2O} + \delta_{GDL}\frac{jRT}{2FD^{eff}_{H_2O}} \quad (5.18)$$

where $x^0_{H_2O}$ is the mole fraction of the water vapour in the ambient air as a function of ambient relative humidity (RH) and $D^{eff}_{H_2O}$ is the effective diffusivity of water into air. These quantities are obtained as follows:

$$x^0_{H_2O} = \frac{RH \times P_{sat}}{100} \quad (5.19)$$

and

$$D^{eff}_{H_2O} = \frac{\varepsilon}{\tau}D_{H_2O,air} \quad (5.20)$$

The saturation pressure of water vapour is calculated by [77]:

$$log_{10}P_{sat} = -2.1794 + 0.02953(T - 273.15) - 9.1837 \times 10^{-5}(T - 273.15)^2 + 1.4454 \times 10^{-7}(T - 273.15)^3 \quad (5.21)$$

Conventional PEFC

As with the air-breathing PEFC, the relationship between the hydrogen molar flow through a valve and its partial pressure inside the flow channel is given by Eq. (5.5). The detailed derivation of the partial pressure of hydrogen in the Laplace transform domain is shown in Eqs (5.6)-(5.11).

Similarly, it may be considered that the molar flows of oxygen (q_{O_2}) and water vapour (q_{H_2O}) through the valve are proportional to their partial pressures inside the flow channel of the fuel cell. The valve molar constants of oxygen (K_{O_2}) and water (K_{H_2O}) can be obtained as follows:

$$\frac{q_{O_2}}{P_{O_2}} = \frac{k_{ca}}{\sqrt{M_{O_2}}} = K_{O_2} \tag{5.22}$$

and

$$\frac{q_{H_2O}}{P_{H_2O}} = \frac{k_{an}}{\sqrt{M_{H_2O}}} = K_{H_2O} \tag{5.23}$$

where k_{ca} and k_{an} are respectively valve constants of the cathode and anode compartments. M_{O_2} and M_{H_2O} are molar masses of oxygen and water vapour, respectively. P_{O_2} and P_{H_2O} are the partial pressures of oxygen and water, respectively.

For oxygen and water, the derivatives of their partial pressures can be obtained using the ideal gas law and rewritten in the Laplace transform domain as follows [161]:

$$P_{O_2} = \frac{1/K_{O_2}}{1 + \tau_{O_2} s}\left(q_{O_2}^{in} - \frac{I}{4F}\right) \tag{5.24}$$

and

$$P_{H_2O} = \frac{1/K_{H_2O}}{1 + \tau_{H_2O} s} \left(\frac{I}{2F}\right) \tag{5.25}$$

where τ_{O_2} and τ_{H_2O} are respectively oxygen and water time constants and they can be expressed as follows:

$$\tau_{O_2} = \frac{V_{ca}}{K_{O_2} RT} \tag{5.26}$$

and

$$\tau_{H_2O} = \frac{V_{an}}{K_{H_2O} RT} \tag{5.27}$$

The Nernst Voltage for a conventional PEFC can be written as [3]:

$$E = E_0 + \frac{RT}{2F} \ln\left(\frac{P_{H_2} . P_{O_2}^{1/2}}{P_{H_2O}}\right) \tag{5.28}$$

Using Eqs. (5.11), (5.24), (5.25) and (5.28), the Nernst voltage of the conventional fuel cell can be depicted as shown in Figure 5.4.

The activation and ohmic losses are calculated using Eq. (5.13) and Eq. (5.14), respectively. The ionic conductivity of the membrane, σ_{mem}, is estimated using the well-known Springer's model [77]:

$$\sigma_{mem} = [0.514\lambda - 0.326] \exp\left[1268\left(\frac{1}{303} - \frac{1}{T}\right)\right] \tag{5.29}$$

where λ represents the water content of the membrane and is calculated using the following expression:

$$\lambda = \begin{cases} 0.043 + 17.81a - 39.85a^2 + 36a^3, & 0 < a \leq 1 \\ 14 + 1.4(a - 1), & 1 < a \leq 3 \end{cases} \tag{5.30}$$

where a is the water activity which is given in Eq. (5.17). P_{H_2O} that is required to calculate water activity is estimated using Eq. (5.25).

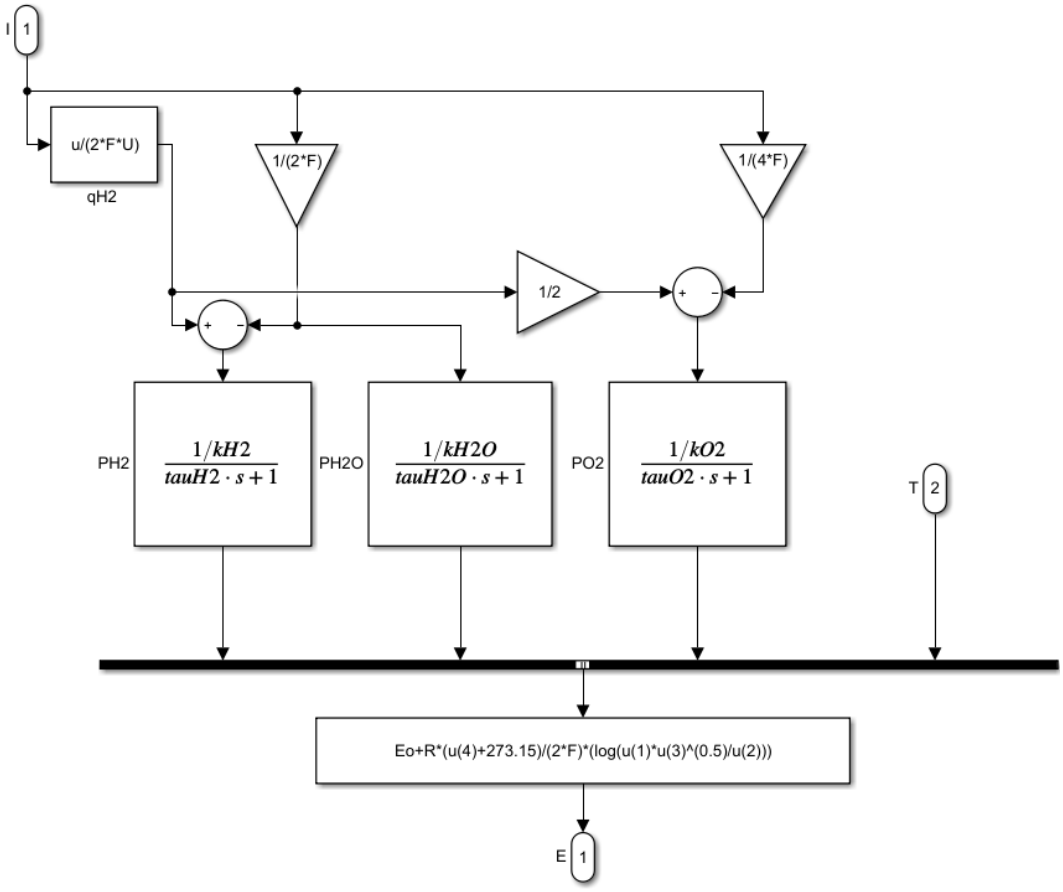

Figure 5.4 The block diagram of the Nernst voltage for the conventional PEFC.

5.4 Results and Discussion

Figure 5.5 demonstrates the polarisation curves and the surface temperature of the cathode GDL generated by the dynamic models of the fuel cells at 20 °C and 40% relative humidity. The steady-state output of the dynamic model of the air-breathing PEFC is validated against the experimental data reported by Fabian et al. [60]. The sharp decline in the performance and the sharp increase in the GDL surface temperature at high current densities are captured by the dynamic model of the air-breathing PEFC. Figure 5.5 also shows that the dynamic modelling data of both type of fuel cells under steady-state conditions are in very good

agreement with the corresponding steady-state modelling data previously reported in [23]. Note that the solution was found to be insensitive to time steps below 0.05 s and as such the latter time step was selected for the simulations.

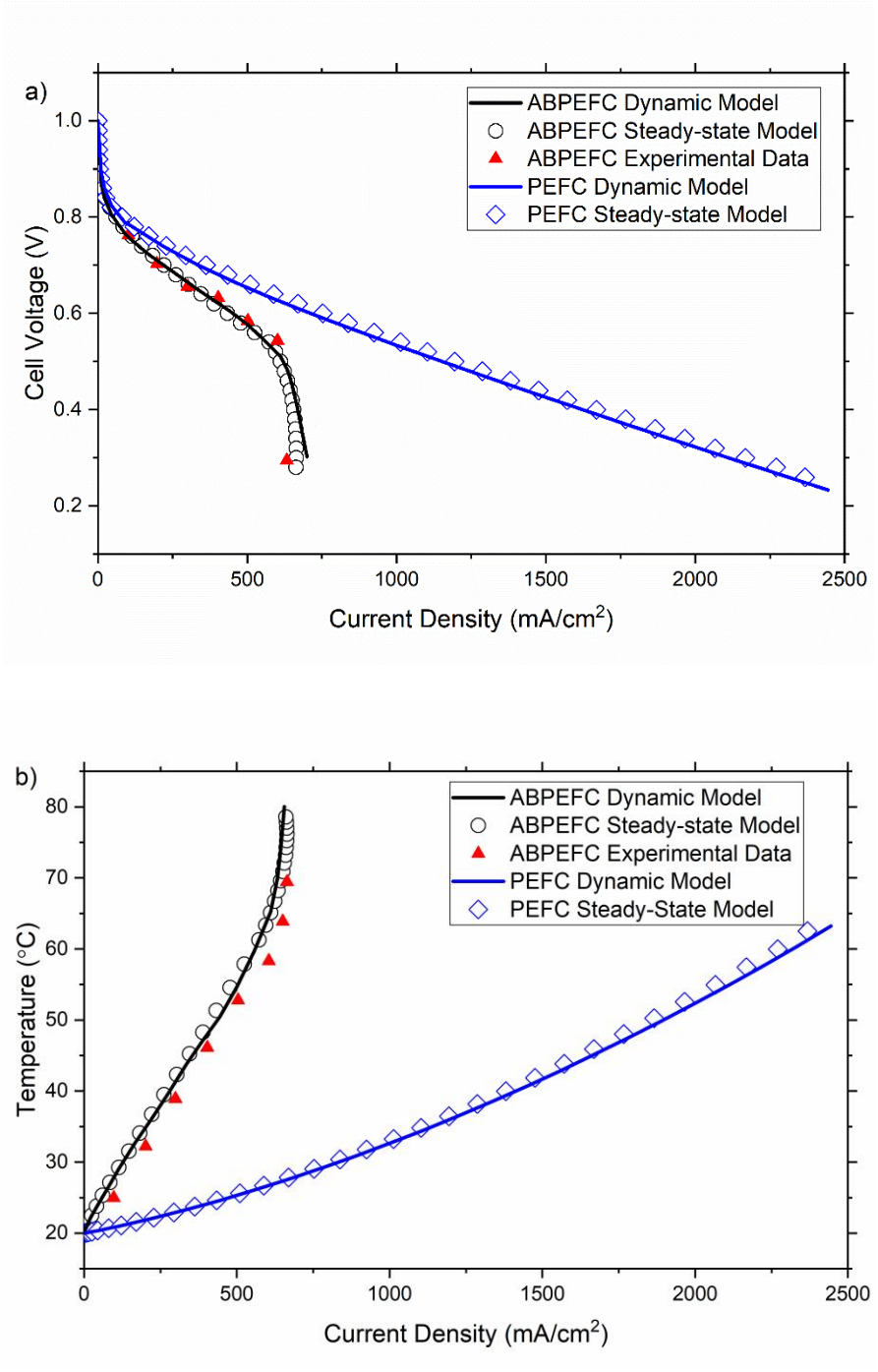

Figure 5.5 Dynamic model outputs of the fuel cells against the steady-state modelling data [23] and the experimental data [60] at 20 °C and 40% relative humidity: (a) cell voltage and (b) cell temperature.

In the following subsections, we conduct a study to first investigate the impact of type of convection at the cathode side (natural convection for the air-breathing PEFC versus forced convection for the conventional PEFC) on the fuel cell performance. This is followed by a parametric study that investigates the effects of the GDL porosity, the membrane ionic resistance and the electrical resistance on the transient response for each type of the fuel cells. This parametric study is primarily performed in order to: (i) evaluate the impact of natural convection on the transient response of the air-breathing PEFC to sudden and large load changes and (ii) have better insights on how to improve this transient response through refining the investigated parameters (i.e. the GDL porosity, the ionic resistance of the membrane and the overall electronic resistance of the fuel cell).

5.4.1 Transient Operation

Two load current values (i.e. 1 and 5 A) were chosen to simulate a large current step change considering the air-breathing PEFC. The "Repeating Sequence Stairs" built-in function in Simulink was used in order to program rapid load alterations between low and high current steps after each 300 s for 2100 s; 300 s was experimentally found to be sufficient for the potential of the air-breathing PEFC to stabilise [60]. According to Kim et al. [171] the evolution of the cell temperature with time under rapid load alteration is given by:

$$T(t) = T_2 + (T_1 - T_2) \times \exp\left(-\frac{h}{mC_p}t\right) \qquad (5.31)$$

where T_1 and T_2 are the steady cell temperature before and after applying the current step change, respectively. h is the heat transfer coefficient and mC_p is the heat capacitance of the fuel cell.

It should be noted that the cell temperature as a function of current density data were generated for each variable investigated in this study (i.e. convection type, the GDL porosity, the membrane thickness and the overall electrical conductivity) using previously-developed steady-state models reported in [23, 72]. These data were fitted to high order polynomials and directly linked to the corresponding dynamic models so that the steady-state temperatures T_1 and T_2 are supplied and used in Eq. (5.31); an example of some high-order polynomial curve fitting equations were presented in a previous work [22]. In the earlier work [22], $\frac{h}{mC_p}$ value was estimated as $0.0295\ s^{-1}$ for the air-breathing PEFC. Further, the mean heat transfer coefficients were found to be 41.95 and 103.29 $\mathrm{W/(m^2.K)}$ for the air-breathing and conventional PEFCs respectively [23]. To this end, $\frac{h}{mC_p}$ for the conventional PEFC could be estimated as 0.0726 s^{-1}.

Figure 5.6 shows that the load current of the fuel cells as it suddenly changes between low (1 A) and high (5 A) currents at 20 °C and 40% relative humidity. The cell temperature for both types of fuel cell follow the sudden load changes and sharply increases/decreases before stabilisation. From the graph, it is clear that the time needed to stabilise cell temperature for the air-breathing PEFC is longer than that of the conventional PEFC.

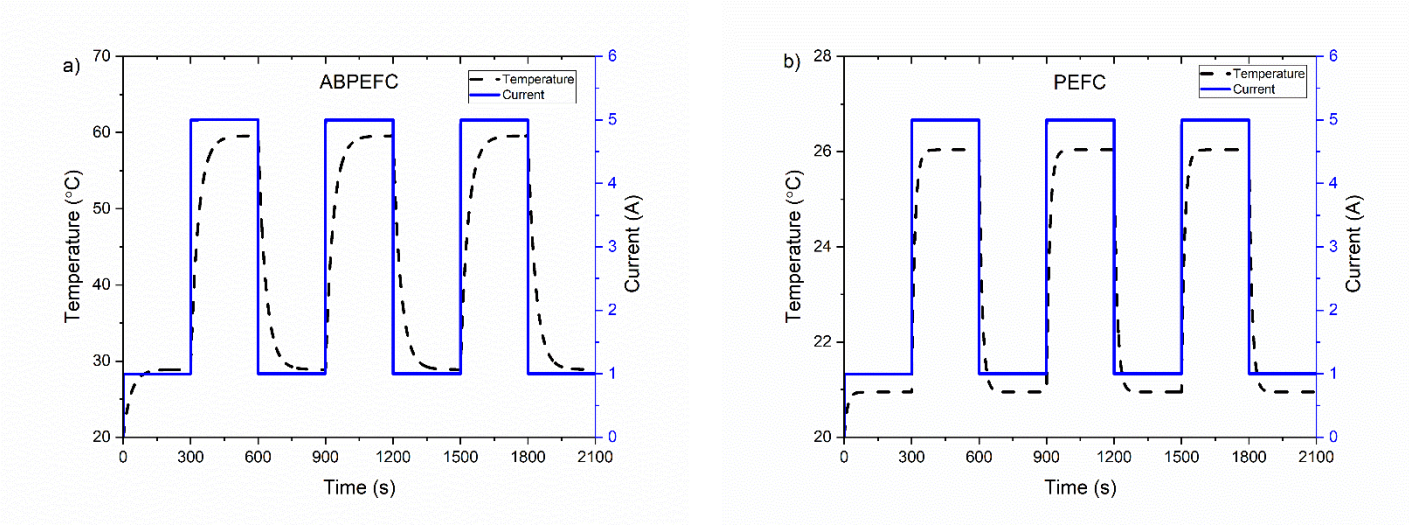

Figure 5.6 The cell temperature as it changes with alternating 4-A step changes in the load current under 20 ℃ and 40% relative humidity for: (a) air-breathing PEFC and (b) conventional PEFC.

5.4.2 Type of Convection Effect

Figure 5.7 shows the impact of convection type (i.e. natural versus forced convection) on the transient response of the fuel cell at typical values of 20 ℃ and 40% relative humidity. It is clear from the figure that the dynamic response of the conventional PEFC is more stable than the air-breathing PEFC as it (i.e. the air-breathing PEFC) demonstrates substantially less overshoots and faster response times. When the load is step-changed from 1 A to 5 A, the power of air-breathing PEFC sharply increases from 0.75 W to 3.05 W and then stabilises at 2.75 W after around 100 s while the power of the conventional PEFC sharply increases from 0.78 W to 3.25 W and then stabilises at 3.2 W after around 25 s (Figure 5.7a). Thus, the time that requires for the air-breathing PEFC to stabilise is about 4 times higher than that of the conventional PEFC when changing from low load (1 A) to high load (5 A). On the other hand, when the load is reversely step-changed from high to low currents, the power of the air-breathing PEFC suddenly decreases from 2.75 W to 0.69 W and then stabilises at 0.75 W while the power of the conventional PEFC sharply decreases from 3.2 W to 0.76 W and stabilises at 0.78 W. The observation that the output power demonstrates significantly higher overshoots

than the conventional PEFC is attributed to the profiles of the activation (Figure 5.7b) and the ohmic (Figure 5.7c) losses. It is seen clearly from these two figures that the activation and the ohmic losses of the air-breathing PEFC are significantly less responsive to load alterations. These dynamic profiles for the activation and ohmic losses (which are both stronger function of temperature as shown in Section 5.3.2) are linked to the dynamic profiles of the fuel cell temperature (Figure 5.6) where the cell temperature of the air-breathing PEFC is significantly higher and less responsive to load changes than the conventional PEFC. This is evidently due to significantly lower heat transfer coefficient at the surface of the open cathode of the air-breathing PEFC compared to that of the cathode flow channel of the conventional PEFC.

It is noteworthy that, when step-changed to 5 A, the ohmic losses associated with the air-breathing PEFC firstly decrease and then increase (Figure 5.7c); this is attributed to the two-field effect of the temperature described in our previous work [22]. Namely, when load is suddenly increased to 5 A, the resulting sudden increase in the cell temperature causes an initial increase in the ionic conductivity of the membrane (Eq. (5.16)) and as such the ohmic losses decreases. As time passes, such a positive impact of the cell temperature on the ionic conductivity is, however, countered by the exponential increase in the saturation pressure of water vapour (Eq. (5.21)) that eventually decreases the ionic conductivity of the membrane (and increases the ohmic losses) before reaching steady-state values.

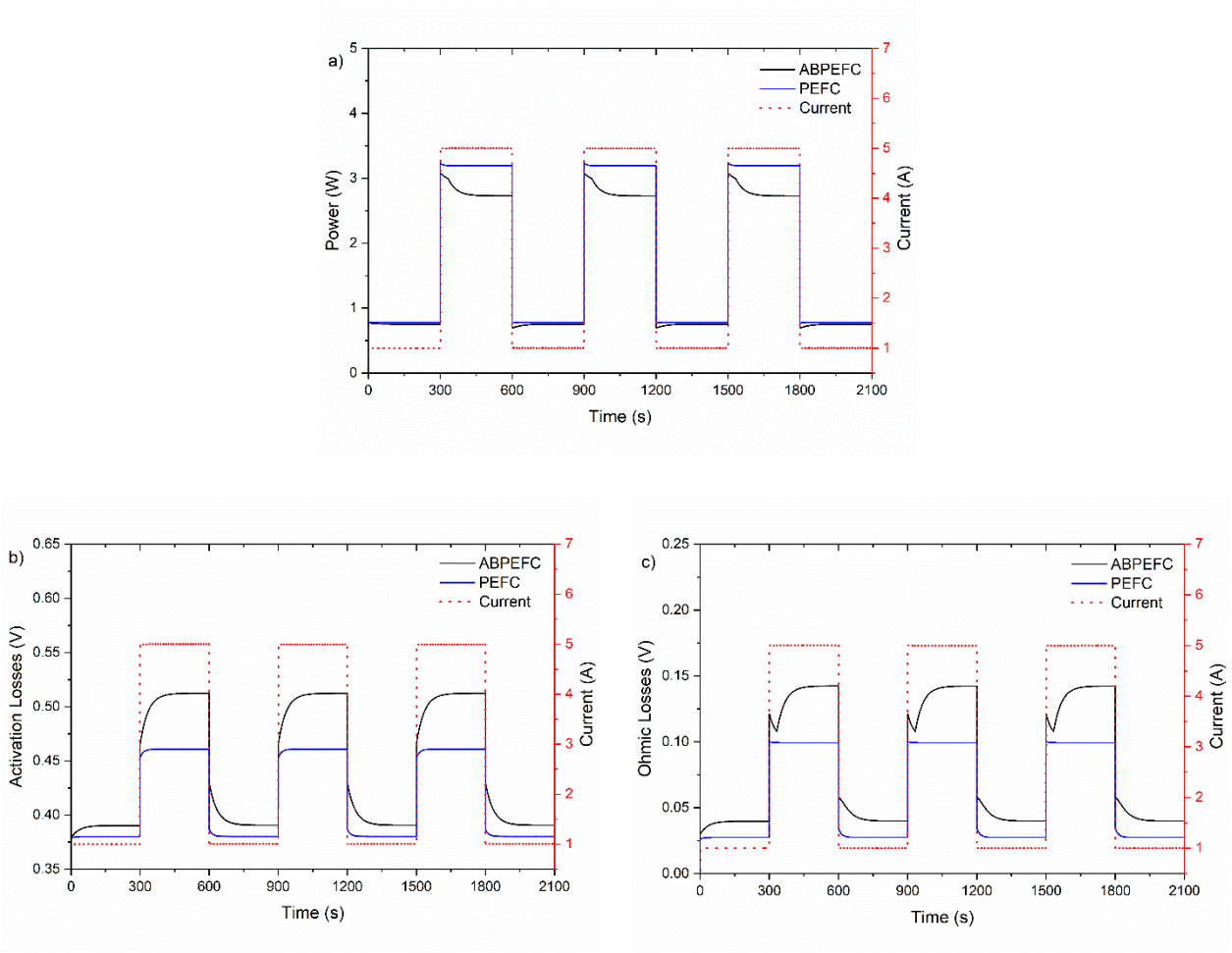

Figure 5.7 Transient profiles of the modelled fuel cells for: (a) output power, (b) activation losses and (c) ohmic losses at 20 °C and 40% relative humidity.

5.4.3 GDL Porosity Effect

Figure 5.8 shows the impact of the GDL porosity on the dynamic and the steady-state performances of the air-breathing PEFC. Note that the porosity of both cathode and anode GDLs have been simultaneously changed with the same values. It should be also noted that, for simplification, the microporous layers (MPLs) were not explicitly considered in the models; they were implicitly accounted for by relatively low GDL porosity values: 0.6 and 0.4. Adding MPLs to the model implies adding a new set of mass and heat transfer equations for the steady-state models; this may provide a marginal gain in terms of prediction accuracy but would unnecessarily complicate the modelling framework. Figure 5.8b shows that the overshoots in the output power decrease with decreasing GDL porosity at high currents. In

addition, the figure shows the performance of the air-breathing PEFC improves with decreasing porosity; this is more evident with 5 A that with 1 A as the values of and the variation in the ohmic losses are higher in the former case (Figure 5.8d). This improvement in the cell performance with decreasing GDL porosity is attributed to the decreased transfer rate of water from the catalyst layer (particularly from the cathode catalyst layer where water is produced) to the surface of the GDL (and then to the ambient) with decreasing GDL porosity. This allows for more water to be available for the humidification of the membrane phase; this is evident from the Figure 5.8c which shows that the water activity at the cathode catalyst layer increases and demonstrates less overshooting with decreasing porosity. As the water activity of the membrane phase increases, the ionic conductivity increases and the ohmic losses of the cell decreases (Figure 5.8d). It should be noted that poor heat dissipation at the cathode of the air-breathing PEFC due to low heat transfer coefficients results in relatively high temperatures (Figure 5.8a) which substantially increase the saturation pressures of water vapour and render the water required for membrane humidification a performance limiting factor.

Figure 5.9 shows the impact of the GDL porosity on the dynamic and the steady-state performances of the conventional PEFC. Figure 5.9b indicates that the output power of the conventional PEFC is considerably less affected by the GDL porosity compared to the air-breathing PEFC at current load changes between 1 A and 5 A (particularly in the intermediate current density region for the conventional PEFC); the conventional fuel cell shows very slight improvement with decreasing GDL porosity. This is primarily due to the high heat transfer coefficients that lead to relatively low temperatures for the conventional PEFC at low (~ 21°C) and high (~ 26°C) currents; see Figure 5.9a. This situation, compared to that of

the air-breathing PEFC, ensures lower saturation pressures of water vapour, higher water activity values (Figure 5.9c), less ohmic losses (Figure 5.9d) and ultimately that the fuel cell becomes less sensitive to GDL porosity and amount of water required for the humidification of the membrane phase. It is worth mentioning that the cell temperature profiles in Figure 5.8 and Figure 5.9 more or less overlap each other as the sensitivity of the cell temperature to the GDL porosity is almost negligible at 1 and 5 A. However, as shown in Figure 4.3b in our previous work presented in Chapter 4 [23], the GDL porosity impacts the limiting current density which in turns impacts on the temperature of the fuel cells; this is particularly more evident for the air-breathing fuel cell. Namely, the lower is the porosity, the higher is the limiting current density and subsequently the higher is the cell temperature. Conversely, in the high current density region, the performance of the conventional PEFC improves with higher GDL porosity. This increase facilitates the transportation of more oxygen to the cathode catalyst layer, resulting in reduced activation losses (Figure 4.3d) and enhanced fuel cell performance (Figure 4.3a).

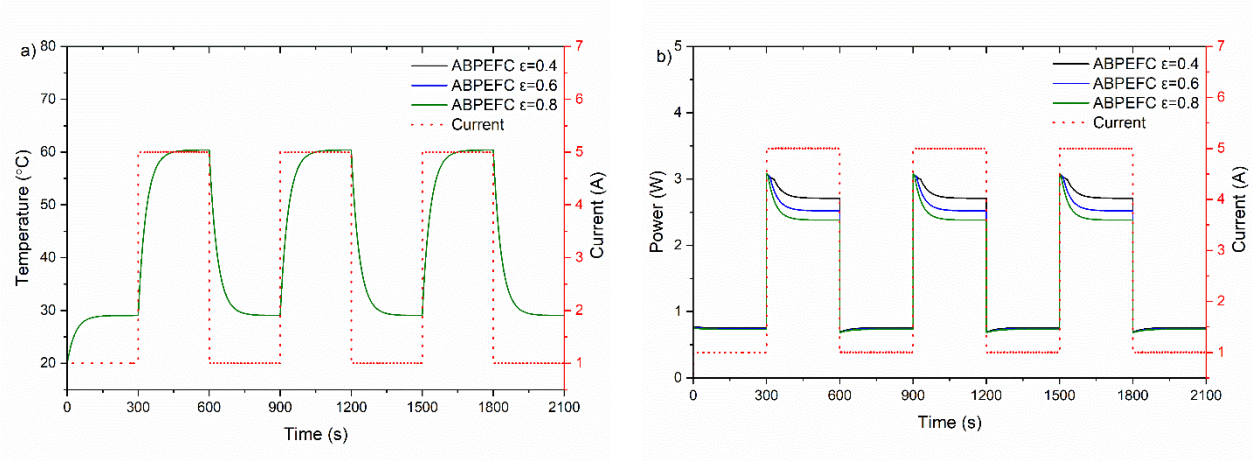

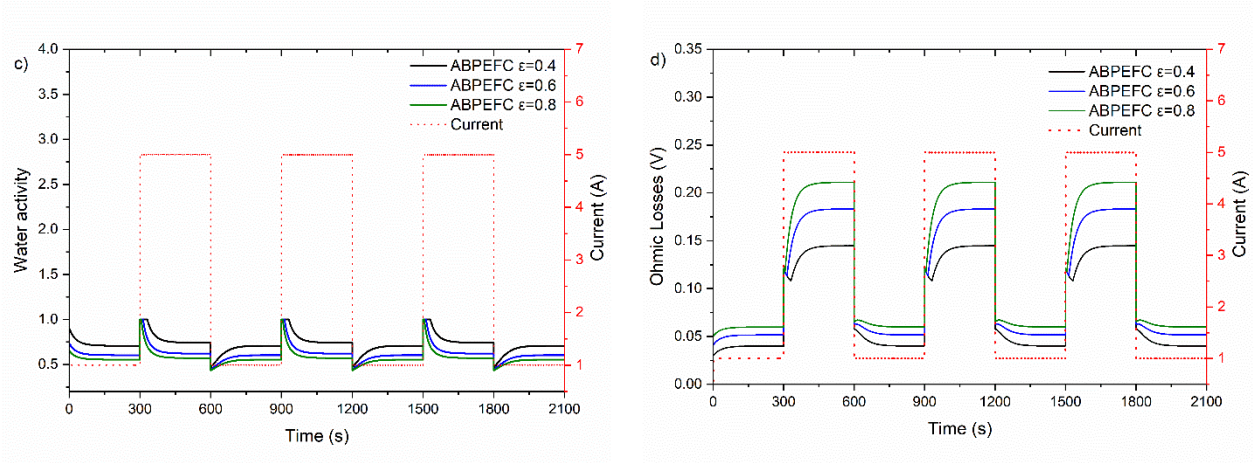

Figure 5.8 Transient profiles of the modelled air-breathing PEFC for: (a) cell temperature, (b) output power, (c) water activity and (d) ohmic losses under different values for the GDL porosity at 20 °C and 40% relative humidity.

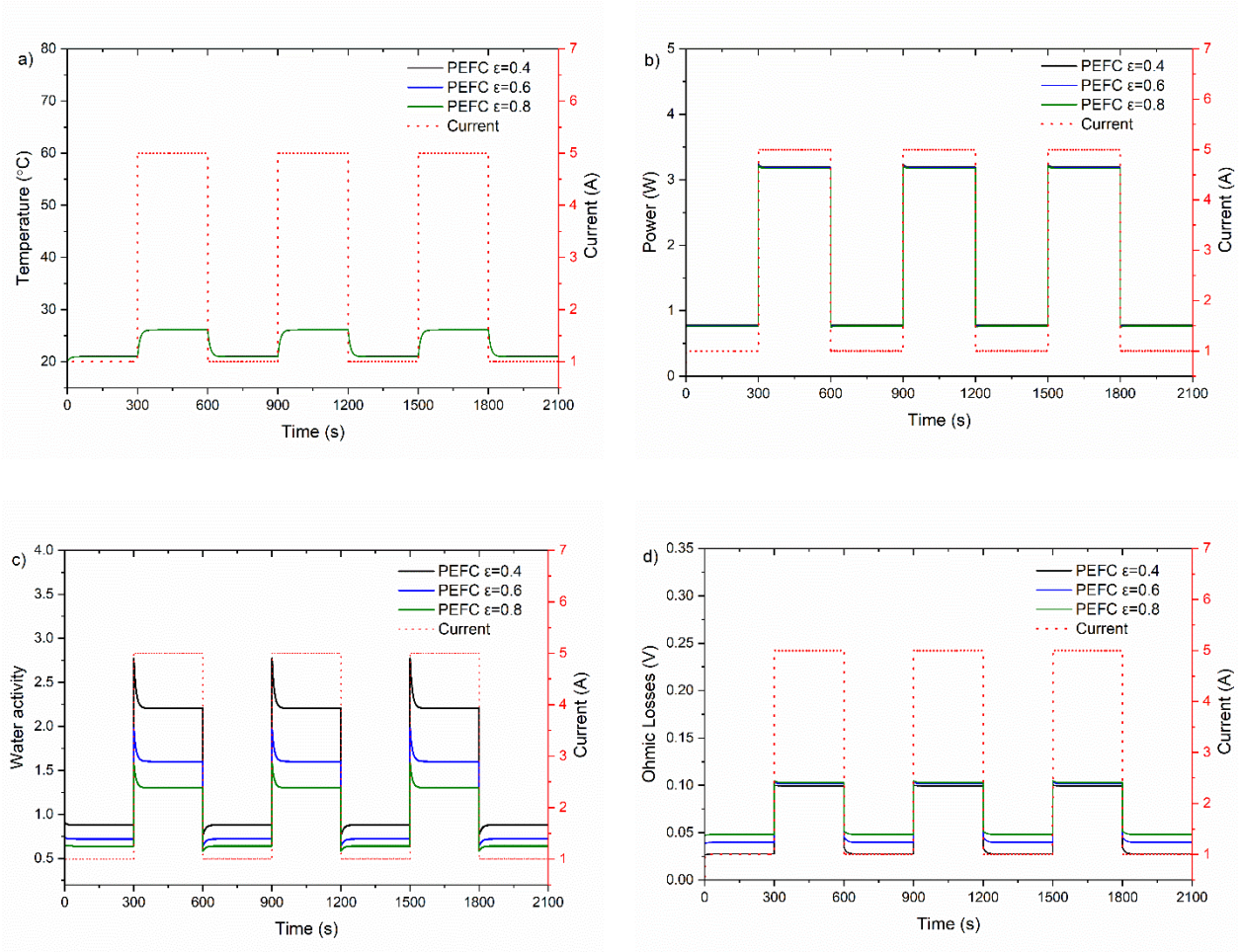

Figure 5.9 Transient profiles of the modelled conventional PEFC for: (a) cell temperature, (b) output power, (c) water activity and (d) ohmic losses under different values for the GDL porosity at 20 °C and 40% relative humidity.

5.4.4 Membrane Thickness Effect

Figure 5.10 and Figure 5.11 show the impact of the membrane thickness on the dynamic and the steady-state performance of the air-breathing and conventional PEFCs, respectively. Overall, the figure expectedly demonstrates that the performance of the both types of the fuel cell improves with decreasing membrane thickness; however, the dynamic and the steady-state performances of the air-breathing PEFC is significantly more sensitive to the membrane thickness that the conventional PEFC; Figure 5.10b and Figure 5.11b. This is primary due to the poorer heat dissipation demonstrated by the air-breathing PEFC compared to the conventional PEFC; this is manifested through the significantly higher temperatures of the air-breathing PEFC; compare Figure 5.10a and Figure 5.11a. As the membrane thickness increases, the ionic resistance of the membrane electrolyte increases (Eq. (5.15)) and subsequently the ohmic losses increases (Figure 5.10d and Figure 5.11d). This leads to an increased Joule heating (which is heat source and a product of the current density and the ohmic losses) and increased cell temperature (Figure 5.10a and Figure 5.11a). As the cell temperature increases, the activation losses in turn, as can be inferred from Eq. (5.13), increases; this could be clearly seen in Figure 5.10c and to a much lesser extent in Figure 5.11c.

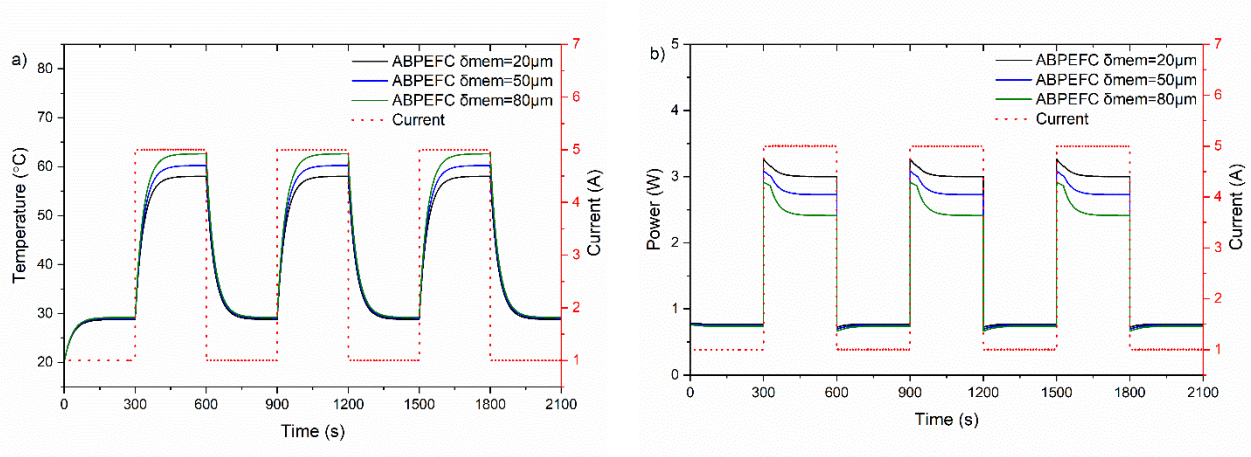

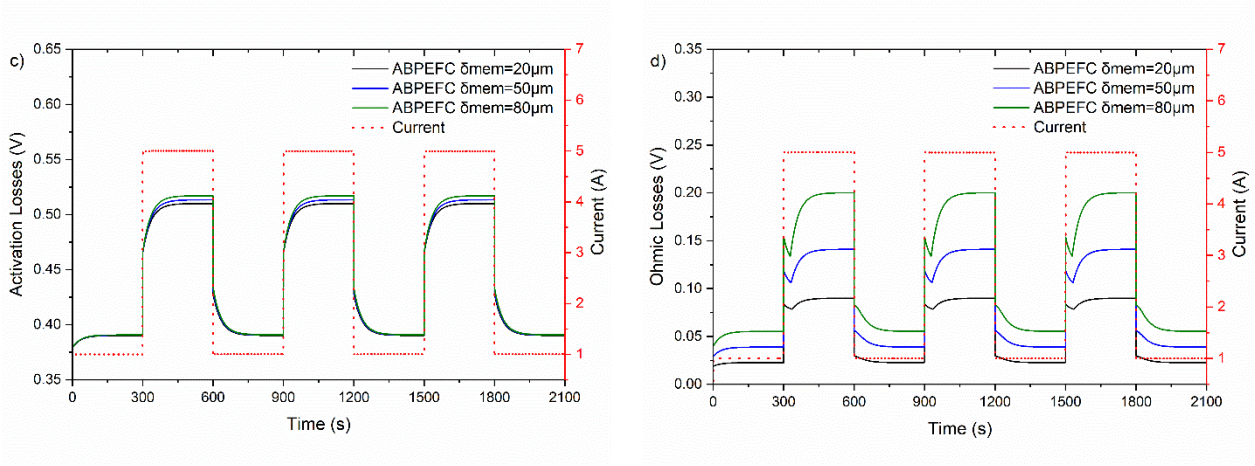

Figure 5.10 Transient profiles of the modelled air-breathing PEFC for: (a) cell temperature, (b) output power, (c) activation losses and (d) ohmic losses under different values for the membrane thickness at 20 °C and 40% relative humidity.

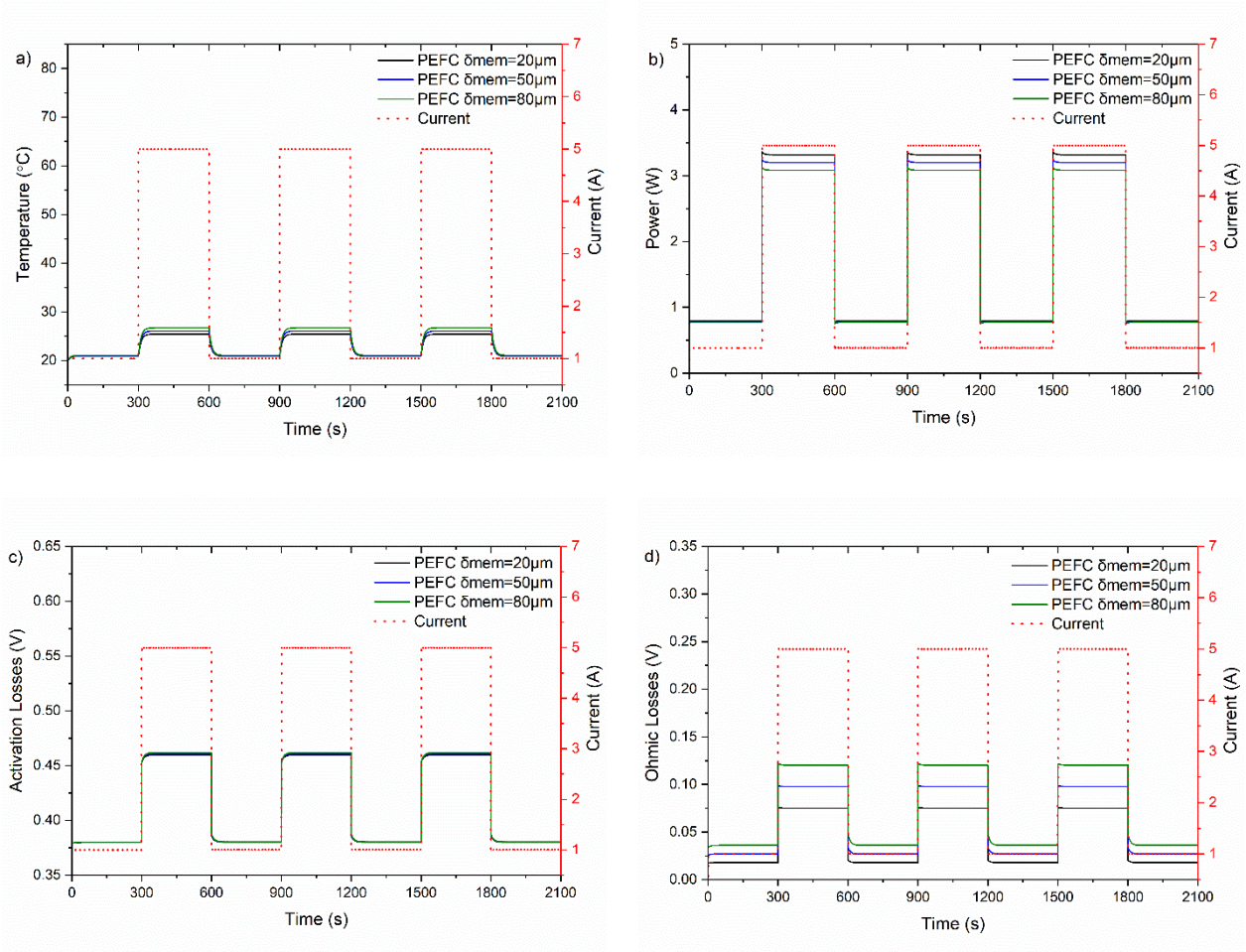

Figure 5.11 Transient profiles of the modelled conventional PEFC for: (a) cell temperature, (b) output power, (c) activation losses and (d) ohmic losses under different values for the membrane thickness at 20 °C and 40% relative humidity.

5.4.5 Electrical Resistance Effect

Figure 5.12 and Figure 5.13 respectively show the impact of the lumped electrical resistance of all the electrically conducting components (i.e. the GDLs, the catalyst layers and the flow-field plates) on the dynamic and the steady-state performances of the modelled air-breathing and conventional PEFCs. As expected, the performance of both types of the fuel cell improves with decreasing the electrical resistance (Figure 5.12b and Figure 5.13b).

As with the impact of the membrane thickness, the increased electrical resistance leads to an increase in (i) the ohmic losses (Figure 5.12d and Figure 5.13d), (ii) the source term associated with the Joule heating, (iii) the cell temperature (Figure 5.12a and Figure 5.13a) and (iv) activation losses (Figure 5.12c and Figure 5.13c). For the given realistically selected ranges for the membrane thickness and the electrical resistance, the impact of the electrical resistance on either the dynamic or the steady-state performance of the fuel cell is less than that of the membrane thickness. Clearly, this is due to less ohmic losses obtained for the given values of the electrical resistance; compare for example Figure 5.10d and Figure 5.12d. For the same reason the impact of the electrical resistance appears to be quantitatively similar on the steady-state performance of the air-breathing and the conventional PEFCs.

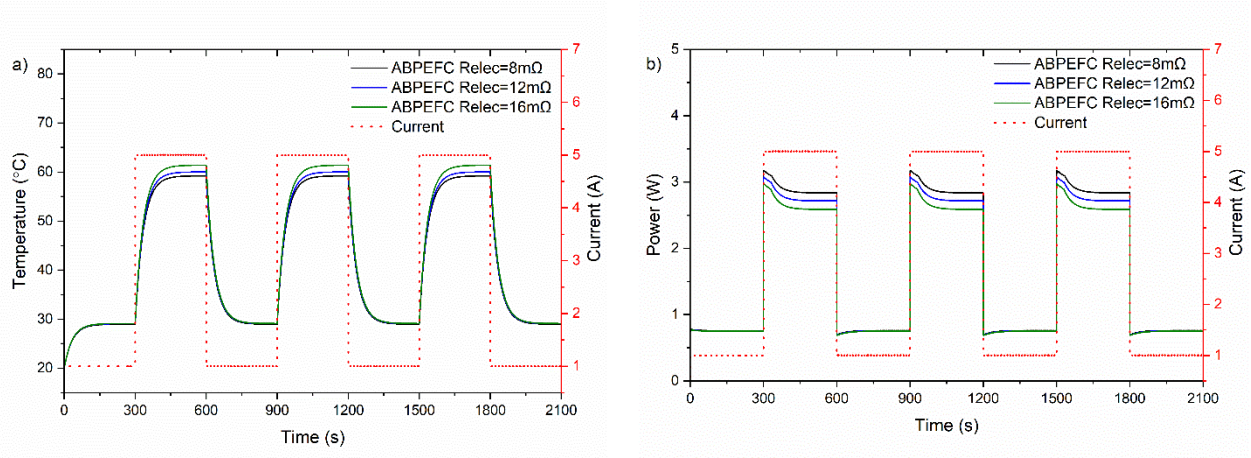

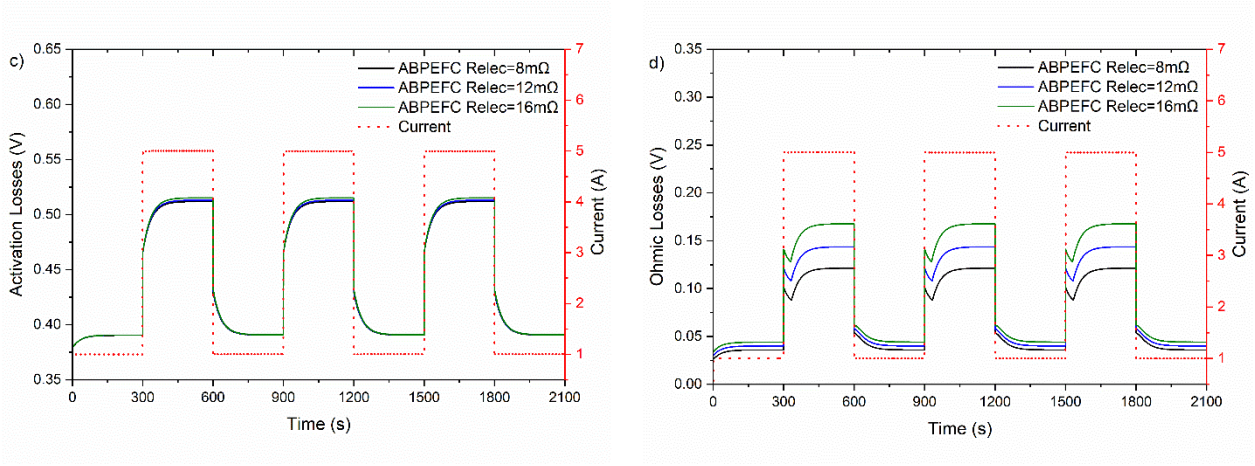

Figure 5.12 Transient profiles of the modelled air-breathing PEFC for: (a) cell temperature, (b) output power, (c) activation losses and (d) ohmic losses under different values for the electric resistance at 20 °C and 40% relative humidity.

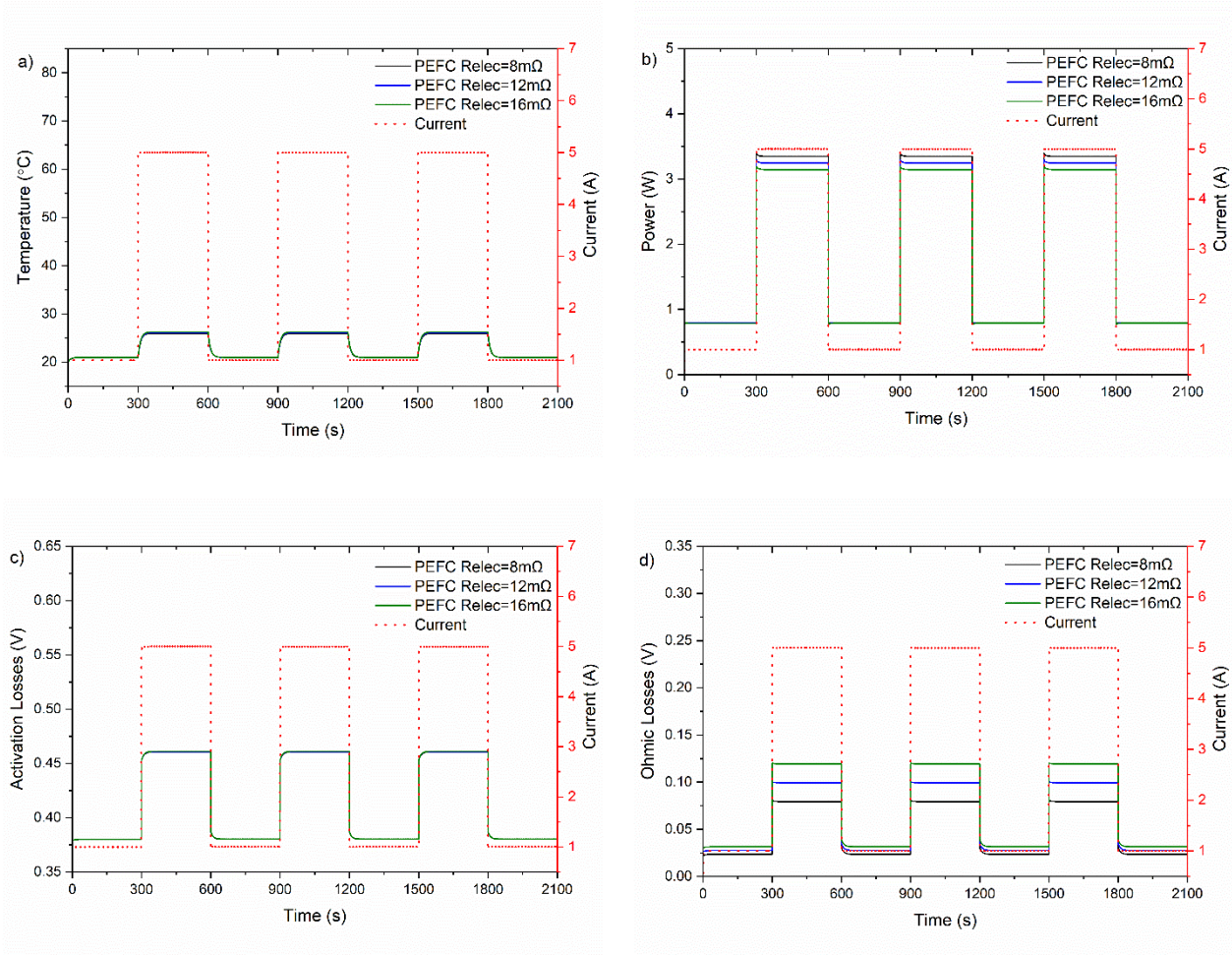

Figure 5.13 Transient profiles of the modelled conventional PEFC for: (a) cell temperature, (b) output power, (c) activation losses and (d) ohmic losses under different values for the electric resistance at 20 °C and 40% relative humidity.

5.5 Conclusions

Two dynamic models have been developed for air-breathing and conventional PEFCs in order to investigate the sensitivity of the transient response and the performance of each type of the fuel cell to some key design parameters. This has been performed to obtain much better insights on how to improve the transient response of the air-breathing PEFC through comparing and contrasting the outcomes of its dynamic model with those of the dynamic model of the higher-in-performance and more responsive conventional PEFC. The following are the key findings of the study:

- The air-breathing PEFC is much less responsive to load changes than the conventional PEFC and this is primarily due to poor heat dissipation from the open cathode of the former type of the fuel cell caused by substantially lower natural convection-related heat transfer coefficients. This leads to significantly higher and less-responsive-to-load-changes cell temperature compared to the conventional PEFC and subsequently higher ohmic and activation losses.

- It is recommended that the porosity of the GDLs are designed to be relatively low to enhance the dynamic and the steady-state performances of the air-breathing PEFC. Higher GDL porosity values increases the removal rate of water required for the humidification of the membrane electrolyte, thus causing higher ohmic losses, significant overshoots with load alterations and poorer performance compared to lower GDL porosity values.

- The dynamic and the steady-state performance of the air-breathing PEFC improves with decreasing membrane thickness and, to a lesser extent, decreasing the overall electrical resistance. This is because the increase in the membrane thickness or

electrical resistance leads to higher ohmic and activation losses. This impact is less profound on the performance of the conventional PEFC and this is clearly due to better heat dissipation demonstrated by this type of fuel cell.

Acknowledgements

The authors highly appreciate the Deputyship for Research & Innovation, Ministry of Education in Saudi Arabia for funding this work through the project number "375213500". The authors extend their sincere appreciation to the central laboratory at Jouf University for supporting this study. Fatma Calili-Cankir thanks the Ministry of National Education at the Republic of Turkey for funding her PhD studentship at the University of Sheffield.

Nomenclature

Roman symbols

a	Water activity
A_{act}	Active area of the fuel cell, m^2
$D_{H_2O}^{eff}$	Effective diffusivity of water into air, m^2/s
$D_{H_2O,air}$	Binary diffusivity of water into air, m^2/s
$D_{O_2}^{eff}$	Effective diffusivity of oxygen into air, m^2/s
$D_{O_{2,}air}$	Binary diffusivity of oxygen into air, m^2/s
E	Nernst Voltage, V
E_0	Standard fuel cell voltage, V
F	Faraday's constant, $\mathrm{C/mol}$
j	Current density, $\mathrm{A/m}^2$
j_0	Exchange current density,$\mathrm{A/m}^2$
I	Electric current, A
k_{an}	Anode valve constant, $\sqrt{\mathrm{mol.\,g}}/(\mathrm{atm.\,s})$
k_{ca}	Cathode valve constant, $\sqrt{\mathrm{mol.\,g}}/(\mathrm{atm.\,s})$
K_{H_2}	Hydrogen valve constant, $\mathrm{mol}/(\mathrm{atm.\,s})$
K_{H_2O}	Water valve constant, $\mathrm{mol}/(\mathrm{atm.\,s})$

K_{O_2}	Oxygen valve constant, $\mathrm{mol/(atm.\,s)}$
M	Molar mass, $\mathrm{g/mol}$
n	Number of moles
P	Ambient pressure, atm
P_{H_2}	Partial pressure of hydrogen, atm
P_{H_2O}	Partial pressure of water vapour, atm
P_{sat}	Water vapour saturation pressure, atm
P_{O_2}	Partial pressure of oxygen, atm
q_{H_2}	Hydrogen molar flow, $\mathrm{mol/s}$
R	Universal Gas Constant, $\mathrm{atm/(mol.\,K)}$
RH	Relative humidity, %
R_{elec}	Lumped electrical cell resistance, Ω
R_{mem}	Membrane resistance, Ω
T	Absolute temperature, K
U	Utilization factor
V_{an}	Anode volume, $\mathrm{m^3}$
V_{ca}	Cathode volume, $\mathrm{m^3}$
V_{cell}	Cell voltage, V
x	Mole fraction

Greek symbols

α	Charge transfer coefficient
δ	Thickness, m
ε	Porosity
η_{act}	Activation over voltage, V
η_{ohmic}	Ohmic over voltage, V
λ	Water content
σ_{mem}	Ionic conductivity, $\mathrm{S/m}$
τ	Tortuosity
τ_{H_2}	Hydrogen time constant, s
τ_{H_2O}	Water time constant, s
τ_{O_2}	Oxygen time constant, s

Chapter 6: Conclusions and Future Work

6.1 Conclusions

Air-breathing PEFCs are promising energy converters to power small electronic devices due to their appealing features; they are system-wise simpler than conventional PEFCs, and they feature longer times between recharges compared to batteries. However, compared to conventional PEFCs, the performance and operation stability of this type of fuel cell are relatively low due to the low heat and mass transfer coefficients associated with natural convection. The main focus of this thesis was to numerically investigate and optimise the dynamic and steady-state performances of the air-breathing PEFC. For this purpose, two dynamic models and two steady-state models were developed for air-breathing and conventional PEFCs. These models were then validated using experimental data reported in the literature.

A comprehensive review of air-breathing PEFCs was initially carried out to primarily explore the recent developments in this technology. This review revealed that the design parameters, such as the opening ratio of the cathode current collector and the GDL thickness, should be optimised to ensure efficient water management and sufficient oxygen supply. Also, the review identified that the ambient conditions, which are beyond the control of the user, have a substantial impact on the performance of the air-breathing PEFC due to the passive supply of atmospheric oxygen to the open cathode of the fuel cell. The studies in the literature showed that better performance is realised when the air-breathing fuel cell is

oriented vertically or horizontally facing upwards compared to horizontally facing downward cell orientation as the former two cell orientations improve the heat and mass transports between the cathode compartment and the ambient air. The review listed the conservation equations and showed how to adapt them to account for natural convection. Also, it showed that there have been very few investigations on hydrogen storage and delivery, air-breathing PEFC stacks and air-breathing PEFC systems; one of the main aims of these investigations is to minimize the fuel cell system and maximize the cell performance so that the air-breathing technology becomes commercially attractive for portable applications. The review concluded that more research on the air-breathing PEFCs is required to overcome technical and economic issues (e.g. reliability of operation under extreme ambient conditions; safe operation in terms of hydrogen storage; size and weight reduction; and cost reduction) to make a sizeable market penetration.

Chapter 3 presents a parametric analysis of the dynamic response of the air-breathing PEFC to the rapid and large load alterations. The main objective of this study was to investigate the sensitivity of the transient response of the air-breathing fuel cell to the ambient conditions, GDL parameters and fuel utilisation. It was found that low ambient relative humidity and high ambient temperature lead to a significant increase in the ohmic losses due to the membrane dry-out, thus negatively affecting the transient response of the fuel cell when changing from low current to high current steps. The transient and steady-state performances of the air-breathing PEFC were found to improve with increasing ambient relative humidity as well-hydrated membrane mitigates the ohmic losses. It was found that there exists an optimum ambient temperature (i.e. 20 °C) and a GDL thickness (i.e. 500 μm) where the fuel cell performs better and shows less overshoots and this is due to a good

balance between activation and ohmic losses. It was found that the thermal conductivity of the cathode GDL should be reasonably high to achieve sufficient heat dissipation, prevent an extreme increase in the cell temperature and eventually decrease in the ohmic losses, thus improving the transient and steady-state performances of the fuel cell. Further, hydrogen utilisation was found to have no impact on the transient response of the air-breathing PEFC to the load alterations. However, the steady-state performance of the fuel cell was found to be slightly better with an increasing amount of hydrogen supplied to the anode and this is due to the increase in the partial pressure of hydrogen which leads to an increase in the Nernst Voltage of the fuel cell.

Chapter 4 presents a comparative parametric study using two steady-state, non-isothermal mathematical models for air-breathing and conventional PEFCs. The porosity and the thickness of the GDL, the membrane thickness and the electrical resistance were studied to comparatively investigate the performance of each fuel cell type and understand the main reasons behind the performance difference between them. The conventional PEFC was found to substantially outperform the air-breathing PEFC since the former fuel cell type has significantly higher heat and mass transfer coefficients. The cell temperature of the air-breathing PEFC was found to exponentially increase at high current densities due to poor heat dissipation; this results in membrane dry-out and ultimately increases the ohmic losses. Similarly, it was found that the passive supply of oxygen by natural convection causes an increase in the activation losses. This study showed that the changes in the porosity and the thickness of the GDL influence the performance of the air-breathing and conventional PEFCs differently; namely, the performance of the former type of fuel cell improves with decreasing porosity and increasing thickness of GDL whereas the latter type of the fuel cell shows better

performance with increasing porosity of GDL and decreasing thickness of GDL. Moreover, the air-breathing PEFC, compared to the conventional PEFC, was found to be more sensitive to membrane thickness and less sensitive to overall electrical resistance and this is attributed to the lower heat transfer coefficient associated with natural convection; this results in higher thermal resistance, poor heat dissipation and higher ionic resistance.

Chapter 5 presents a comparative parametric study using two dynamic models for air-breathing and conventional PEFCs. This study aimed to: (i) investigate the sensitivity of the dynamic response and the performance of these two fuel cell types to the type of convection, the porosity of the GDL, the membrane thickness and the overall electrical resistance, and (ii) ultimately have better insights on how to make the air-breathing PEFC more responsive to the rapid and large load alterations. The transient response of the air-breathing PEFC was found to be much slower to the load changes than that of the conventional PEFC and this is because of the insufficient heat dissipation induced by the reliance of the air-breathing PEFC on the natural convection, thus leading to higher ohmic and activation losses. The study suggested that the porosity of the GDL should be designed to be relatively small to improve the performance and transient response of the air-breathing PEFC as the removal rate of the water (required for membrane hydration) increases with increasing GDL porosity, leading to higher ohmic losses and significant overshoots when load changes. The steady-state performance and the transient response of the air-breathing PEFC under load alterations were found to enhance with decreasing membrane thickness and decreasing the overall electrical resistance. Overall, the effect of these parameters on performance was found to be less pronounced in the conventional PEFC due to its superior heat dissipation capability over air-breathing PEFCs.

Consequently, these studies attempt to better understand the key factors that may affect the performance of the air-breathing PEFCs, both in terms of their steady-state performance and their dynamic response to sudden and substantial load changes, and how to improve their overall performance. The outcomes of these studies show that, due to the reliance on natural convection, both the steady-state performance of the modelled air-breathing PEFC and its transient response are highly sensitive to ambient conditions. Furthermore, the findings indicate that some design parameters that could be optimised have significant impacts on the dynamic and steady-state performances of the air-breathing PEFC.

6.2 Future Work

In this thesis, numerical studies on how to enhance the dynamic and steady-state performances of a single air-breathing PEFC were presented. However, future investigations are necessary to fully understand the dynamic behaviour of the air-breathing PEFC under different conditions and to refine existing mathematical models.

As a future work, it would be of interest to develop higher-dimensional steady-state (1-D, 2-D or 3-D) models for the air-breathing and conventional PEFCs to fully capture the dimensional effects on the fuel cell performance (the steady-state models in the present work are zero-dimensional). This would provide a more comprehensive and comparative investigation and assist in obtaining deeper insights on how to design an efficient air-breathing PEFC.

Further, it would be of a great interest to link the higher-dimensional models to the corresponding dynamic models through feeding these dynamic models with some parameters obtained from the steady-state models, e.g. the surface temperature of the cathode GDL. In doing so, the impact of more parameters on the dynamic and steady-state

performances of the air-breathing PEFC could be investigated. For example, it would be interesting to create innovative designs for the open cathode by developing 3-D mathematical models and investigate the effect of these designs on the steady-state and dynamic performance of the air-breathing PEFC.

Another future work is to complement the computational work described in this work with relevant experiments. One of the interesting topics is to experimentally investigate the effect of cathode GDL surface treatment with hydrophobic and/or hydrophilic agents on the performance of the air-breathing PEFC. The experimentally-obtained temperature data are then used to generate curve-fitting equations that could be fed into the corresponding dynamic models in order to investigate the impact of the surface treatment of the GDL on the transient response of the fuel cell. These studies may provide new insights into how to design efficient air-breathing PEFCs with not only higher steady-state performance but also faster transient response to the load alterations.

Furthermore, future research is required to investigate the dynamic performance of an entire portable system powered by an air-breathing PEFC. Namely, it would be interesting to integrate the proposed dynamic model for an air-breathing PEFC into a larger-in-scale dynamic model for a system powering a small portable device and investigate the impacts of the ambient conditions, the operating conditions and the key design parameters on the dynamic response of the fuel cell system to the temporal load changes.

References

[1] Xing, L., Shi, W., Su, H., Xu, Q., Das, P.K., Mao, B. and Scott, K., 2019. Membrane electrode assemblies for PEM fuel cells: A review of functional graded design and optimization. *Energy*, *177*, pp.445-464. https://doi.org/10.1016/j.energy.2019.04.084

[2] Huang, B., Qi, Y. and Murshed, A.M., 2013. *Dynamic modeling and predictive control in solid oxide fuel cells: first principle and data-based approaches*. John Wiley & Sons.

[3] Barbir F. PEM Fuel Cells: Theory and Practice. Sustain World Ser. 2005:1-433.

[4] USA Department of Energy,2023. *DOE Technical Targets for Fuel Cell Systems and Stacks for Transportation Applications.* Available from: https://www.energy.gov/eere/fuelcells/doe-technical-targets-fuel-cell-systems-and-stacks-transportation-applications.

[5] USA Department of Energy,2023. Technical Targets for Fuel Cell Systems for Portable Power and Auxiliary Power Applications. Available from: https://bit.ly/45ONoRj.

[6] Ferriday, T.B. and Middleton, P.H., 2021. Alkaline fuel cell technology-A review. *International journal of hydrogen energy*, 46(35), pp.18489-18510. https://doi.org/10.1016/j.ijhydene.2021.02.203

[7] Mench MM, Wiley I. Fuel cell engines. Hoboken, N.J: John Wiley & Sons; 2008.

[8] O'Hayre RP, O'Hayre RP, VleBooks. Fuel cell fundamentals. 3rd ed. Hoboken, New Jersey: Wiley; 2016.

[9] Fuel cell energy,2023. Available from: https://www.fuelcellenergy.com/.

[10] Golkhatmi, S.Z., Asghar, M.I. and Lund, P.D., 2022. A review on solid oxide fuel cell durability: Latest progress, mechanisms, and study tools. *Renewable and Sustainable Energy Reviews*, *161*, p.112339. https://doi.org/10.1016/j.rser.2022.112339

[11] Da Rosa, A.V. and Ordóñez, J.C., 2021. *Fundamentals of renewable energy processes*. Academic Press.

[12] Dicks, A.L. and Rand, D.A., 2018. *Fuel cell systems explained*. John Wiley & Sons.

[13] Litster, S. and McLean, G.J., 2004. PEM fuel cell electrodes. *Journal of power sources*, *130*(1-2), pp.61-76. https://doi.org/10.1016/j.jpowsour.2003.12.055

[14] Zaidi, J. and Matsuura, T. eds., 2008. *Polymer membranes for fuel cells*. Springer Science & Business Media.

[15] Kundu, P.P. and Dutta, K., 2016. Hydrogen fuel cells for portable applications. In *Compendium of hydrogen energy* (pp. 111-131). Woodhead Publishing.

[16] Kamarudin, S.K., Achmad, F. and Daud, W.R.W., 2009. Overview on the application of direct methanol fuel cell (DMFC) for portable electronic devices. *International Journal of hydrogen energy*, *34*(16), pp.6902-6916. https://doi.org/10.1016/j.ijhydene.2009.06.013

[17] Wilberforce, T., Alaswad, A., Palumbo, A., Dassisti, M. and Olabi, A.G., 2016. Advances in stationary and portable fuel cell applications. International journal of hydrogen energy, 41(37), pp.16509-16522. https://doi.org/10.1016/j.ijhydene.2016.02.057

[18] Han, J. and Liu, H., 2007. Real time measurements of methanol crossover in a DMFC. Journal of Power Sources, 164(1), pp.166-173. https://doi.org/10.1016/j.jpowsour.2006.09.105

[19] Goor, M., Menkin, S. and Peled, E., 2019. High power direct methanol fuel cell for mobility and portable applications. International Journal of Hydrogen Energy, 44(5), pp.3138-3143. https://doi.org/10.1016/j.ijhydene.2018.12.019

[20] Metzger, N. and Li, X., 2022. Technical and economic analysis of fuel cells for forklift applications. ACS omega, 7(22), pp.18267-18275. CC-BY-NC-ND 4.0.

[21] Calili-Cankir, F., Ismail, M.S., Ingham, D.B., Hughes, K.J., Ma, L. and Pourkashanian, M., 2023. *Air-breathing polymer electrolyte fuel cells: A review.* Renewable Energy. https://doi.org/10.1016/j.renene.2023.05.134

[22] Calili, F., Ismail, M.S., Ingham, D.B., Hughes, K.J., Ma, L. and Pourkashanian, M., 2021. *A dynamic model of air-breathing polymer electrolyte fuel cell (PEFC): A parametric study.* International Journal of Hydrogen Energy, 46(33), pp.17343-17357. https://doi.org/10.1016/j.ijhydene.2021.02.133

[23] Calili-Cankir, F., Ismail, M.S., Ingham, D.B., Hughes, K.J., Ma, L. and Pourkashanian, M., 2022. Air-breathing versus conventional polymer electrolyte fuel cells: A parametric numerical study. *Energy*, *250*, p.123827. https://doi.org/10.1016/j.energy.2022.123827

[24] Calili-Cankir, F., Ismail, M.S., Berber, M.R., Alrowaili, Z.A., Ingham, D.B., Hughes, K.J., Ma, L. and Pourkashanian, M., 2022. Dynamic models for air-breathing and conventional polymer electrolyte fuel cells: A comparative study. *Renewable Energy*, *195*, pp.1001-1014. https://doi.org/10.1016/j.renene.2022.06.092

[25] Staffell, I., Scamman, D., Abad, A.V., Balcombe, P., Dodds, P.E., Ekins, P., Shah, N. and Ward, K.R., 2019. The role of hydrogen and fuel cells in the global energy system. *Energy & Environmental Science*, *12*(2), pp.463-491. 10.1039/C8EE01157E

[26] Falama, R.Z., Saidi, A.S., Soulouknga, M.H. and Salah, C.B., 2023. A techno-economic comparative study of renewable energy systems based different storage devices. *Energy*, *266*, p.126411. https://doi.org/10.1016/j.energy.2022.126411

[27] Hong, S., Kim, E. and Jeong, S., 2023. Evaluating the sustainability of the hydrogen economy using multi-criteria decision-making analysis in Korea. *Renewable Energy*, *204*, pp.485-492. https://doi.org/10.1016/j.renene.2023.01.037

[28] Daud, W.R.W., Rosli, R.E., Majlan, E.H., Hamid, S.A.A., Mohamed, R. and Husaini, T., 2017. PEM fuel cell system control: A review. *Renewable Energy*, *113*, pp.620-638. https://doi.org/10.1016/j.renene.2017.06.027

[29] Qin, Y., Guo, Q., Chen, R., Zhuang, Y. and Wang, Y., 2021. Numerical investigation of water droplet impact on PEM fuel cell flow channel surface. *Renewable Energy*, *168*, pp.750-763. https://doi.org/10.1016/j.renene.2020.12.075

[30] Solati, A., Nasiri, B., Mohammadi-Ahmar, A., Mohammadi, K. and Safari, A.H., 2019. Numerical investigation of the effect of different layers configurations on the performance of radial PEM fuel cells. *Renewable energy*, *143*, pp.1877-1889. https://doi.org/10.1016/j.renene.2019.06.003

[31] Ismail, M.S., Ingham, D.B. and Pourkashanian, M., 2018. Modeling of portable fuel cells. In *Portable Hydrogen Energy Systems* (pp. 51-66). Academic Press. https://doi.org/10.1016/B978-0-12-813128-2.00004-8

[32] Sun, J., Li, J., Zhou, T., Yang, K., Wei, S., Tang, N., Dang, N., Li, H., Qiu, X. and Chen, L., 2016. Toxicity, a serious concern of thermal runaway from commercial Li-ion battery. *Nano Energy*, *27*, pp.313-319. https://doi.org/10.1016/j.nanoen.2016.06.031

[33] Ferreira-Aparicio P, Conde, J.J. and Chaparro, A.M. . Fundamentals and components of portable hydrogen fuel-cell systems. Portable Hydrogen Energy System: Academic Press; 2018. https://doi.org/10.1016/B978-0-12-813128-2.00002-4

[34] Moreno, N.G., Molina, M.C., Gervasio, D. and Robles, J.F.P., 2015. Approaches to polymer electrolyte membrane fuel cells (PEMFCs) and their cost. *Renewable and Sustainable Energy Reviews*, *52*, pp.897-906. https://doi.org/10.1016/j.rser.2015.07.157

[35] Belmonte, N., Luetto, C., Staulo, S., Rizzi, P. and Baricco, M., Case studies of energy storage with fuel cells and batteries for stationary and mobile applications. *Challenges* 2017; 8: 9. https://doi.org/10.3390/challe8010009

[36] Kundu, A., Jang, J.H., Gil, J.H., Jung, C.R., Lee, H.R., Kim, S.H., Ku, B. and Oh, Y.S., 2007. Micro-fuel cells—Current development and applications. *Journal of Power Sources*, *170*(1), pp.67-78. https://doi.org/10.1016/j.jpowsour.2007.03.066

[37] Davis, F. and Higson, S.P., 2007. Biofuel cells—recent advances and applications. *Biosensors and bioelectronics*, 22(7), pp.1224-1235. https://doi.org/10.1016/j.bios.2006.04.029

[38] Bullen, R.A., Arnot, T.C., Lakeman, J.B. and Walsh, F.C., 2006. Biofuel cells and their development. *Biosensors and Bioelectronics*, *21*(11), pp.2015-2045. https://doi.org/10.1016/j.bios.2006.01.030

[39] Fernández-Moreno, J., Guelbenzu, G., Martín, A.J., Folgado, M.A., Ferreira-Aparicio, P. and Chaparro, A.M., 2013. A portable system powered with hydrogen and one single air-breathing PEM fuel cell. *Applied energy*, *109*, pp.60-66. https://doi.org/10.1016/j.apenergy.2013.03.076

[40] Song, W.J., Chen, H., Guo, H., Ye, F. and Li, J.R., 2022. Research progress of proton exchange membrane fuel cells utilizing in high altitude environments. *International Journal of Hydrogen Energy*, *47*(59), pp.24945-24962. https://doi.org/10.1016/j.ijhydene.2022.05.238

[41] Wang, Y., Diaz, D.F.R., Chen, K.S., Wang, Z. and Adroher, X.C., 2020. Materials, technological status, and fundamentals of PEM fuel cells–a review. *Materials today*, *32*, pp.178-203. https://doi.org/10.1016/j.mattod.2019.06.005

[42] Wu, H.W., 2016. A review of recent development: Transport and performance modeling of PEM fuel cells. *Applied energy*, *165*, pp.81-106.

https://doi.org/10.1016/j.apenergy.2015.12.075

[43] Cheng, X., Shi, Z., Glass, N., Zhang, L., Zhang, J., Song, D., Liu, Z.S., Wang, H. and Shen, J., 2007. A review of PEM hydrogen fuel cell contamination: Impacts, mechanisms, and mitigation. *Journal of Power Sources*, *165*(2), pp.739-756.

https://doi.org/10.1016/j.jpowsour.2006.12.012

[44] Wu, J., Yuan, X.Z., Martin, J.J., Wang, H., Zhang, J., Shen, J., Wu, S. and Merida, W., 2008. A review of PEM fuel cell durability: Degradation mechanisms and mitigation strategies. *Journal of Power Sources*, *184*(1), pp.104-119.

https://doi.org/10.1016/j.jpowsour.2008.06.006

[45] Mehta, V. and Cooper, J.S., 2003. Review and analysis of PEM fuel cell design and manufacturing. *Journal of power sources*, *114*(1), pp.32-53. https://doi.org/10.1016/S0378-7753(02)00542-6

[46] Kurnia, J.C., Chaedir, B.A., Sasmito, A.P. and Shamim, T., 2021. Progress on open cathode proton exchange membrane fuel cell: Performance, designs, challenges and future directions. *Applied Energy*, *283*, p.116359. https://doi.org/10.1016/j.apenergy.2020.116359

[47] Lee, K.I., Lee, S.W., Park, M.S. and Chu, C.N., 2010. The development of air-breathing proton exchange membrane fuel cell (PEMFC) with a cylindrical configuration. *International Journal of Hydrogen Energy*, *35*(21), pp.11844-11854.

https://doi.org/10.1016/j.ijhydene.2010.08.105

[48] Lee, K.I., Chung, D.K., Park, M.S. and Chu, C.N., 2013. The development of a cylindrical proton exchange membrane fuel cell with an integrated metal-hydride container. *International Journal of Precision Engineering and Manufacturing*, *14*, pp.1065-1070. https://doi.org/10.1007/s12541-013-0143-6

[49] Tüber, K., Zobel, M., Schmidt, H. and Hebling, C., 2003. A polymer electrolyte membrane fuel cell system for powering portable computers. *Journal of Power Sources*, *122*(1), pp.1-8. https://doi.org/10.1016/S0378-7753(03)00428-2

[50] Han, H.S., Cho, C., Kim, S.Y. and Hyun, J.M., 2013. Performance evaluation of a polymer electrolyte membrane fuel cell system for powering portable freezer. Applied energy, 105, pp.125-137. https://doi.org/10.1016/j.apenergy.2012.12.056

[51] Kim, S.H., Miesse, C.M., Lee, H.B., Chang, I.W., Hwang, Y.S., Jang, J.H. and Cha, S.W., 2014. Ultra compact direct hydrogen fuel cell prototype using a metal hydride hydrogen storage tank for a mobile phone. *Applied energy*, *134*, pp.382-391. https://doi.org/10.1016/j.apenergy.2014.08.019

[52] Orogbemi, O.M., Ingham, D.B., Ismail, M.S., Hughes, K.J., Ma, L. and Pourkashanian, M., 2016. The effects of the composition of microporous layers on the permeability of gas diffusion layers used in polymer electrolyte fuel cells. *International Journal of Hydrogen Energy*, *41*(46), pp.21345-21351. https://doi.org/10.1016/j.ijhydene.2016.09.160

[53] Zhang, X., Yang, J., Ma, X., Zhuge, W. and Shuai, S., 2022. Modelling and analysis on effects of penetration of microporous layer into gas diffusion layer in PEM fuel cells: Focusing on mass transport. *Energy*, *254*, p.124103. https://doi.org/10.1016/j.energy.2022.124103

[54] Büchi, F.N. and Srinivasan, S., 1997. Operating proton exchange membrane fuel cells without external humidification of the reactant gases: Fundamental aspects. *Journal of the Electrochemical Society*, *144*(8), p.2767. DOI 10.1149/1.1837893

[55] Ismail, M.S., Ingham, D.B., Hughes, K.J., Ma, L. and Pourkashanian, M., 2013. Thermal modelling of the cathode in air-breathing PEM fuel cells. *Applied energy*, *111*, pp.529-537. https://doi.org/10.1016/j.apenergy.2013.05.007

[56] Zhang, Y., Mawardi, A. and Pitchumani, R., 2007. Numerical studies on an air-breathing proton exchange membrane (PEM) fuel cell stack. *Journal of Power Sources*, *173*(1), pp.264-276. https://doi.org/10.1016/j.jpowsour.2007.05.008

[57] Zhang, Y. and Pitchumani, R., 2007. Numerical studies on an air-breathing proton exchange membrane (PEM) fuel cell. *International Journal of Heat and Mass Transfer*, *50*(23-24), pp.4698-4712. https://doi.org/10.1016/j.ijheatmasstransfer.2007.03.044

[58] Hamel, S. and Fréchette, L.G., 2011. Critical importance of humidification of the anode in miniature air-breathing polymer electrolyte membrane fuel cells. *Journal of Power Sources*, *196*(15), pp.6242-6248. https://doi.org/10.1016/j.jpowsour.2011.04.020

[59] O'Hayre, R., Fabian, T., Litster, S., Prinz, F.B. and Santiago, J.G., 2007. Engineering model of a passive planar air breathing fuel cell cathode. *Journal of Power Sources*, *167*(1), pp.118-129. https://doi.org/10.1016/j.jpowsour.2007.01.073

[60] Fabian, T., Posner, J.D., O'Hayre, R., Cha, S.W., Eaton, J.K., Prinz, F.B. and Santiago, J.G., 2006. The role of ambient conditions on the performance of a planar, air-breathing hydrogen PEM fuel cell. *Journal of power Sources*, *161*(1), pp.168-182. https://doi.org/10.1016/j.jpowsour.2006.03.054

[61] Schmitz, A., Ziegler, C., Schumacher, J.O., Tranitz, M., Fontes, E. and Hebling, C., 2004. Modelling Approach for Planar Self-Breathing PEMFC and Comparison with Experimental Results. *Fuel Cells*, *4*(4), pp.358-364. https://doi.org/10.1002/fuce.200400034

[62] Hwang, J.J., 2006. Species-electrochemical modeling of an air-breathing cathode of a planar fuel cell. *Journal of the Electrochemical Society*, *153*(8), p.A1584. DOI 10.1149/1.2209567

[63] Tabe, Y., Park, S.K., Kikuta, K., Chikahisa, T. and Hishinuma, Y., 2006. Effect of cathode separator structure on performance characteristics of free-breathing PEMFCs. *Journal of power sources*, *162*(1), pp.58-65. https://doi.org/10.1016/j.jpowsour.2006.06.093

[64] Matamoros, L. and Brüggemann, D., 2007. Concentration and ohmic losses in free-breathing PEMFC. *Journal of power sources*, *173*(1), pp.367-374. https://doi.org/10.1016/j.jpowsour.2007.02.091

[65] Litster, S., Pharoah, J.G., McLean, G. and Djilali, N., 2006. Computational analysis of heat and mass transfer in a micro-structured PEMFC cathode. *Journal of Power Sources*, *156*(2), pp.334-344. https://doi.org/10.1016/j.jpowsour.2005.05.064

[66] Rajani, B.P.M. and Kolar, A.K., 2007. A model for a vertical planar air breathing PEM fuel cell. *Journal of power sources*, *164*(1), pp.210-221. https://doi.org/10.1016/j.jpowsour.2006.10.055

[67] Hottinen, T., Himanen, O. and Lund, P., 2004. Effect of cathode structure on planar free-breathing PEMFC. *Journal of Power Sources*, *138*(1-2), pp.205-210. https://doi.org/10.1016/j.jpowsour.2004.06.044

[68] Ying, W., Sohn, Y.J., Lee, W.Y., Ke, J. and Kim, C.S., 2005. Three-dimensional modeling and experimental investigation for an air-breathing polymer electrolyte membrane fuel cell (PEMFC). *Journal of Power Sources*, *145*(2), pp.563-571. https://doi.org/10.1016/j.jpowsour.2005.01.083

[69] Ying, W., Yang, T.H., Lee, W.Y., Ke, J. and Kim, C.S., 2005. Three-dimensional analysis for effect of channel configuration on the performance of a small air-breathing proton exchange membrane fuel cell (PEMFC). *Journal of Power Sources*, *145*(2), pp.572-581. https://doi.org/10.1016/j.jpowsour.2005.02.066

[70] Ying, W., Ke, J., Lee, W.Y., Yang, T.H. and Kim, C.S., 2005. Effects of cathode channel configurations on the performance of an air-breathing PEMFC. *International Journal of Hydrogen Energy*, *30*(12), pp.1351-1361. https://doi.org/10.1016/j.ijhydene.2005.04.009

[71] Wang, Y. and Ouyang, M., 2007. Three-dimensional heat and mass transfer analysis in an air-breathing proton exchange membrane fuel cell. *Journal of Power Sources*, *164*(2), pp.721-729. https://doi.org/10.1016/j.jpowsour.2006.11.056

[72] Ismail, M.S., Ingham, D.B., Hughes, K.J., Ma, L. and Pourkashanian, M., 2014. An efficient mathematical model for air-breathing PEM fuel cells. Applied energy, 135, pp.490-503. https://doi.org/10.1016/j.apenergy.2014.08.113

[73] Chen, Z., Ingham, D., Ismail, M., Ma, L., Hughes, K.J. and Pourkashanian, M., 2020. Effects of hydrogen relative humidity on the performance of an air-breathing PEM fuel cell: a numerical study. International Journal of Numerical Methods for Heat & Fluid Flow, 30(4), pp.2077-2097. https://doi.org/10.1108/HFF-11-2018-0674

[74] Yalcinoz, T. and Alam, M.S., 2008. Dynamic modeling and simulation of air-breathing proton exchange membrane fuel cell. *Journal of power sources*, *182*(1), pp.168-174. https://doi.org/10.1016/j.jpowsour.2008.03.076

[75] Al-Anazi, A., Wilberforce, T., Khatib, F.N., Vichare, P. and Olabi, A.G., 2021. Performance evaluation of an air breathing polymer electrolyte membrane (PEM) fuel cell in harsh environments–A case study under Saudi Arabia's ambient condition. *International Journal of Hydrogen Energy*, *46*(45), pp.23463-23479. https://doi.org/10.1016/j.ijhydene.2020.10.258

[76] Ismail, M.S., Hughes, K.J., Ingham, D.B., Ma, L. and Pourkashanian, M., 2012. Effects of anisotropic permeability and electrical conductivity of gas diffusion layers on the performance of proton exchange membrane fuel cells. *Applied energy*, *95*, pp.50-63. https://doi.org/10.1016/j.apenergy.2012.02.003

[77] Springer, T.E., Zawodzinski, T.A. and Gottesfeld, S., 1991. Polymer electrolyte fuel cell model. *Journal of the electrochemical society*, *138*(8), p.2334. DOI 10.1149/1.2085971

[78] Litster, S. and Djilali, N., 2007. Mathematical modelling of ambient air-breathing fuel cells for portable devices. *Electrochimica Acta*, *52*(11), pp.3849-3862. https://doi.org/10.1016/j.electacta.2006.11.002

[79] Sone, Y., Ekdunge, P. and Simonsson, D., 1996. Proton conductivity of Nafion 117 as measured by a four-electrode AC impedance method. Journal of the Electrochemical Society, 143(4), p.1254. DOI 10.1149/1.1836625

[80] Schmitz, A., Tranitz, M., Wagner, S., Hahn, R. and Hebling, C., 2003. Planar self-breathing fuel cells. *Journal of Power Sources*, *118*(1-2), pp.162-171. https://doi.org/10.1016/S0378-7753(03)00080-6

[81] Schmitz, A., Tranitz, M., Eccarius, S., Weil, A. and Hebling, C., 2006. Influence of cathode opening size and wetting properties of diffusion layers on the performance of air-breathing PEMFCs. *Journal of Power Sources*, *154*(2), pp.437-447. https://doi.org/10.1016/j.jpowsour.2005.10.070

[82] Jeong, S.U., Cho, E.A., Kim, H.J., Lim, T.H., Oh, I.H. and Kim, S.H., 2006. Effects of cathode open area and relative humidity on the performance of air-breathing polymer electrolyte membrane fuel cells. *Journal of power sources*, *158*(1), pp.348-353. https://doi.org/10.1016/j.jpowsour.2005.09.044

[83] Bussayajarn, N., Ming, H., Hoong, K.K., Stephen, W.Y.M. and Hwa, C.S., 2009. Planar air breathing PEMFC with self-humidifying MEA and open cathode geometry design for portable applications. *International Journal of Hydrogen Energy*, 34(18), pp.7761-7767. https://doi.org/10.1016/j.ijhydene.2009.07.077

[84] Kim, S.H., Cha, H.Y., Miesse, C.M., Jang, J.H., Oh, Y.S. and Cha, S.W., 2009. Air-breathing miniature planar stack using the flexible printed circuit board as a current collector. *international journal of hydrogen energy*, *34*(1), pp.459-466. https://doi.org/10.1016/j.ijhydene.2008.09.088

[85] Hottinen, T., Mikkola, M. and Lund, P., 2004. Evaluation of planar free-breathing polymer electrolyte membrane fuel cell design. *Journal of Power Sources*, *129*(1), pp.68-72. https://doi.org/10.1016/j.jpowsour.2003.11.012

[86] Babcock, B., Tupper, A.J., Clark, D., Fabian, T. and O'Hayre, R., 2010. Optimization of passive air breathing fuel cell cathodes. https://doi.org/10.1115/1.3177381

[87] Kumar, P.M. and Kolar, A.K., 2010. Effect of cathode channel dimensions on the performance of an air-breathing PEM fuel cell. *International journal of thermal sciences*, 49(5), pp.844-857. https://doi.org/10.1016/j.ijthermalsci.2009.12.002

[88] Kumar, P.M. and Parthasarathy, V., 2013. A passive method of water management for an air-breathing proton exchange membrane fuel cell. *Energy*, 51, pp.457-461. https://doi.org/10.1016/j.energy.2012.12.015

[89] Kumar, P.M. and Kolar, A.K., 2010. Effect of cathode design on the performance of an air-breathing PEM fuel cell. *International journal of hydrogen energy*, 35(2), pp.671-681. https://doi.org/10.1016/j.ijhydene.2009.10.086

[90] Chun, D., Kim, D., Williamson, Z.R., Lee, T. and Squibb, C.W., 2013. Investigation of fin based oxygen supply modules on the performance of air-breathing polymer electrolyte membrane fuel cells. *Applied thermal engineering*, 50(1), pp.293-301. https://doi.org/10.1016/j.applthermaleng.2012.06.039

[91] Willamson, Z.R., Chun, D., Kwon, K., Lee, T., Squibb, C.W. and Kim, D., 2013. Evaluation of fin structure effects on a heated air-breathing polymer electrolyte membrane (PEM) fuel cell. Applied thermal engineering, 56(1-2), pp.54-61. https://doi.org/10.1016/j.applthermaleng.2013.02.036

[92] Karst, N., Faucheux, V., Martinent, A., Bouillon, P., Laurent, J.Y., Druart, F. and Simonato, J.P., 2010. Innovative water management in micro air-breathing polymer electrolyte membrane fuel cells. *Journal of Power Sources*, *195*(4), pp.1156-1162. https://doi.org/10.1016/j.jpowsour.2009.08.068

[93] Suseendiran, S.R., Pearn-Rowe, S. and Rengaswamy, R., 2020. Development of cylindrical PEM fuel cells with semi-cylindrical cathode current collectors. *International Journal of Hydrogen Energy*, *45*(17), pp.10549-10558. https://doi.org/10.1016/j.ijhydene.2019.09.113

[94] Giddey, S., Badwal, S.P.S., Ciacchi, F.T., Fini, D., Sexton, B.A., Glenn, F. and Leech, P.W., 2010. Investigations on fabrication and lifetime performance of self–air breathing direct hydrogen micro fuel cells. *International journal of hydrogen energy*, *35*(6), pp.2506-2516. https://doi.org/10.1016/j.ijhydene.2009.12.158

[95] Hsieh, S.S., Kuo, J.K., Hwang, C.F. and Tsai, H.H., 2004. A novel design and microfabrication for a micro PEMFC. *Microsystem Technologies*, *10*, pp.121-126. https://doi.org/10.1007/s00542-003-0321-z

[96] Yu, J., Cheng, P., Ma, Z. and Yi, B., 2003. Fabrication of a miniature twin-fuel-cell on silicon wafer. *Electrochimica Acta*, *48*(11), pp.1537-1541. https://doi.org/10.1016/S0013-4686(03)00034-3

[97] Yu, J., Cheng, P., Ma, Z. and Yi, B., 2003. Fabrication of miniature silicon wafer fuel cells with improved performance. *Journal of Power Sources*, *124*(1), pp.40-46. https://doi.org/10.1016/S0378-7753(03)00618-9

[98] Lee, S.J., Chang-Chien, A., Cha, S.W., O'hayre, R., Park, Y.I., Saito, Y. and Prinz, F.B., 2002. Design and fabrication of a micro fuel cell array with "flip-flop" interconnection. *Journal of Power Sources*, *112*(2), pp.410-418. https://doi.org/10.1016/S0378-7753(02)00393-2

[99] Jaouen, F., Haasl, S., van der Wijngaart, W., Lundblad, A., Lindbergh, G. and Stemme, G., 2005. Adhesive copper films for an air-breathing polymer electrolyte fuel cell. *Journal of power sources*, *144*(1), pp.113-121. https://doi.org/10.1016/j.jpowsour.2004.12.048

[100] Schmitz, A., Wagner, S., Hahn, R., Uzun, H. and Hebling, C., 2004. Stability of planar PEMFC in printed circuit board technology. *Journal of Power Sources*, *127*(1-2), pp.197-205. https://doi.org/10.1016/j.jpowsour.2003.09.023

[101] O'Hayre, R., Braithwaite, D., Hermann, W., Lee, S.J., Fabian, T., Cha, S.W., Saito, Y. and Prinz, F.B., 2003. Development of portable fuel cell arrays with printed-circuit technology. *Journal of Power Sources*, *124*(2), pp.459-472. https://doi.org/10.1016/S0378-7753(03)00802-4

[102] Ferreira-Aparicio, P. and Chaparro, A.M., 2014. Influence of the gas diffusion cathode structure on the performance of an air-breathing proton exchange membrane fuel cell. *International journal of hydrogen energy*, *39*(8), pp.3997-4004. https://doi.org/10.1016/j.ijhydene.2013.06.082

[103] Jeong, S.U., Cho, E.A., Kim, H.J., Lim, T.H., Oh, I.H. and Kim, S.H., 2006. A study on cathode structure and water transport in air-breathing PEM fuel cells. *Journal of Power Sources*, *159*(2), pp.1089-1094. https://doi.org/10.1016/j.jpowsour.2005.12.046

[104] Liao, S., Dang, D., Tian, X., Hou, S., Liu, F., Peng, H. and Fu, Z., 2015. Enhanced water management in the cathode of an air-breathing PEMFC using a dual catalyst layer and optimizing the gas diffusion and microporous layers. *International Journal of Hydrogen Energy*, *40*(10), pp.3961-3967. https://doi.org/10.1016/j.ijhydene.2015.01.091

[105] Baroutaji, A., Carton, J.G., Stokes, J. and Olabi, A.G., 2017. Application of open pore cellular foam for air breathing PEM fuel cell. *international journal of hydrogen energy*, *42*(40), pp.25630-25638. https://doi.org/10.1016/j.ijhydene.2017.05.114

[106] Tsai, B.T., Tseng, C.J., Liu, Z.S., Wang, C.H., Lee, C.I., Yang, C.C. and Lo, S.K., 2012. Effects of flow field design on the performance of a PEM fuel cell with metal foam as the flow distributor. *International Journal of Hydrogen Energy*, *37*(17), pp.13060-13066. https://doi.org/10.1016/j.ijhydene.2012.05.008

[107] Tseng, C.J., Tsai, B.T., Liu, Z.S., Cheng, T.C., Chang, W.C. and Lo, S.K., 2012. A PEM fuel cell with metal foam as flow distributor. *Energy Conversion and Management*, *62*, pp.14-21. https://doi.org/10.1016/j.enconman.2012.03.018

[108] Kumar, A. and Reddy, R.G., 2004. Materials and design development for bipolar/end plates in fuel cells. *Journal of Power Sources*, *129*(1), pp.62-67. https://doi.org/10.1016/j.jpowsour.2003.11.011

[109] Dang, D., Zeng, R., Chen, X., Su, X., Yang, X., Su, H., Wu, C. and Zhang, L., 2021. Natural wood derived robust carbon sheets with perpendicular channels as gas diffusion layers in air-breathing proton exchange membrane fuel cells (PEMFCs). *Catalysis Communications*, *159*, p.106351. https://doi.org/10.1016/j.catcom.2021.106351

[110] Jung, U.H., Jeong, S.U., Park, K.T., Lee, H.M., Chun, K., Choi, D.W. and Kim, S.H., 2007. Improvement of water management in air-breathing and air-blowing PEMFC at low

temperature using hydrophilic silica nano-particles. *International Journal of Hydrogen Energy*, *32*(17), pp.4459-4465. https://doi.org/10.1016/j.ijhydene.2007.05.008

[111] Li, P.W., Zhang, T., Wang, Q.M., Schaefer, L. and Chyu, M.K., 2003. The performance of PEM fuel cells fed with oxygen through the free-convection mode. *Journal of Power Sources*, *114*(1), pp.63-69. https://doi.org/10.1016/S0378-7753(02)00535-9

[112] Obeisun, O.A., Meyer, Q., Engebretsen, E., Finegan, D.P., Robinson, J.B., Hinds, G., Shearing, P.R. and Brett, D.J., 2015. Study of water accumulation dynamics in the channels of an open-cathode fuel cell through electro-thermal characterisation and droplet visualisation. *International Journal of Hydrogen Energy*, *40*(46), pp.16786-16796. https://doi.org/10.1016/j.ijhydene.2015.07.066

[113] Vijay Babu, A.R., Manoj Kumar, P. and Srinivasa Rao, G., 2016. Effect of design and operating parameters on the performance of planar and ducted cathode structures of an air-breathing PEM fuel cell. *Arabian Journal for Science and Engineering*, *41*(9), pp.3415-3423. https://doi.org/10.1007/s13369-015-1890-8

[114] Hottinen, T., Noponen, M., Mennola, T., Himanen, O., Mikkola, M. and Lund, P., 2003. Effect of ambient conditions on performance and current distribution of a polymer electrolyte membrane fuel cell. *Journal of Applied Electrochemistry*, *33*, pp.265-271. https://doi.org/10.1023/A:1024184824662

[115] Chu, D., Jiang, R. and Walker, C., 2000. Analysis of PEM fuel cell stacks using an empirical current–voltage equation. *Journal of Applied Electrochemistry*, *30*, pp.365-370. https://doi.org/10.1023/A:1003905109007

[116] Chu, D. and Jiang, R., 1999. Performance of polymer electrolyte membrane fuel cell (PEMFC) stacks: Part I. Evaluation and simulation of an air-breathing PEMFC stack. *Journal of Power Sources*, *83*(1-2), pp.128-133. https://doi.org/10.1016/S0378-7753(99)00285-2

[117] Ous, T. and Arcoumanis, C., 2009. The formation of water droplets in an air-breathing PEMFC. *International journal of hydrogen energy*, *34*(8), pp.3476-3487. https://doi.org/10.1016/j.ijhydene.2009.02.037

[118] Ma, H.K. and Huang, S.H., 2009. Innovative design of an air-breathing proton exchange membrane fuel cell with a piezoelectric device. *Journal of Electrochemical Energy Conversion and Storage,* 6(3): 034501. https://doi.org/10.1115/1.3005581

[119] Fabian, T., O'Hayre, R., Litster, S., Prinz, F.B. and Santiago, J.G., 2010. Passive water management at the cathode of a planar air-breathing proton exchange membrane fuel cell. *Journal of Power Sources*, *195*(10), pp.3201-3206. https://doi.org/10.1016/j.jpowsour.2009.12.030

[120] Fabian, T., O'Hayre, R., Litster, S., Prinz, F.B. and Santiago, J.G., 2010. Active water management at the cathode of a planar air-breathing polymer electrolyte membrane fuel cell using an electroosmotic pump. *Journal of Power Sources*, *195*(11), pp.3640-3644. https://doi.org/10.1016/j.jpowsour.2009.12.025

[121] Coz, E., Théry, J., Boillat, P., Faucheux, V., Alincant, D., Capron, P. and Gébel, G., 2016. Water management in a planar air-breathing fuel cell array using operando neutron imaging. *Journal of Power Sources*, *331*, pp.535-543. https://doi.org/10.1016/j.jpowsour.2016.09.041

[122] Santa Rosa, D.T., Pinto, D.G., Silva, V.S., Silva, R.A. and Rangel, C.M., 2007. High performance PEMFC stack with open-cathode at ambient pressure and temperature conditions. *International Journal of Hydrogen Energy*, *32*(17), pp.4350-4357. https://doi.org/10.1016/j.ijhydene.2007.05.042

[123] Yang, T. and Shi, P., 2008. A preliminary study of a six-cell stack with dead-end anode and open-slits cathode. *International journal of hydrogen energy*, *33*(11), pp.2795-2801. https://doi.org/10.1016/j.ijhydene.2008.03.025

[124] Isanaka, S.P., Sparks, T.E., Liou, F.F. and Newkirk, J.W., 2016. Design strategy for reducing manufacturing and assembly complexity of air-breathing Proton Exchange Membrane Fuel Cells (PEMFC). *Journal of Manufacturing Systems*, *38*, pp.165-171. https://doi.org/10.1016/j.jmsy.2015.10.004

[125] Yan, W.M., Zeng, M.S., Yang, T.F., Chen, C.Y., Amani, M. and Amani, P., 2020. Performance improvement of air-breathing proton exchange membrane fuel cell stacks by thermal management. *International Journal of Hydrogen Energy*, *45*(42), pp.22324-22339. https://doi.org/10.1016/j.ijhydene.2019.08.146

[126] Barthélémy, H., Weber, M. and Barbier, F., 2017. Hydrogen storage: Recent improvements and industrial perspectives. *International Journal of Hydrogen Energy*, *42*(11), pp.7254-7262. https://doi.org/10.1016/j.ijhydene.2016.03.178

[127] Gkanas, E.I., 2018. Metal hydrides: Modeling of metal hydrides to be operated in a fuel cell. In *Portable Hydrogen Energy Systems* (pp. 67-90). Academic Press. https://doi.org/10.1016/B978-0-12-813128-2.00005-X

[128] Rusman, N.A.A. and Dahari, M., 2016. A review on the current progress of metal hydrides material for solid-state hydrogen storage applications. *International Journal of Hydrogen Energy*, *41*(28), pp.12108-12126. https://doi.org/10.1016/j.ijhydene.2016.05.244

[129] Schlapbach, L. and Züttel, A., 2001. Hydrogen-storage materials for mobile applications. *nature*, *414*(6861), pp.353-358. https://doi.org/10.1038/35104634

[130] Bhattacharyya, R. and Mohan, S., 2015. Solid state storage of hydrogen and its isotopes: an engineering overview. *Renewable and Sustainable Energy Reviews*, *41*, pp.872-883. https://doi.org/10.1016/j.rser.2014.09.004

[131] Tarasov, B.P., Fursikov, P.V., Volodin, A.A., Bocharnikov, M.S., Shimkus, Y.Y., Kashin, A.M., Yartys, V.A., Chidziva, S., Pasupathi, S. and Lototskyy, M.V., 2021. Metal hydride hydrogen storage and compression systems for energy storage technologies. *International Journal of Hydrogen Energy*, *46*(25), pp.13647-13657. https://doi.org/10.1016/j.ijhydene.2020.07.085

[132] Hoffman, K.C., Reilly, J.J., Salzano, F.J., Waide, C.H., Wiswall, R.H. and Winsche, W.E., 1976. Metal hydride storage for mobile and stationary applications. *International Journal of Hydrogen Energy*, *1*(2), pp.133-151. https://doi.org/10.1016/0360-3199(76)90067-7

[133] Gkanas, E.I., Grant, D.M., Khzouz, M., Stuart, A.D., Manickam, K. and Walker, G.S., 2016. Efficient hydrogen storage in up-scale metal hydride tanks as possible metal hydride compression agents equipped with aluminium extended surfaces. *international journal of hydrogen energy*, *41*(25), pp.10795-10810. https://doi.org/10.1016/j.ijhydene.2016.04.035

[134] Ferreira-Aparicio, P., Conde, J.J. and Chaparro, A.M., 2018. Hydrogen storage options for portable fuel-cell systems. In *Portable Hydrogen Energy Systems* (pp. 41-50). Academic Press. https://doi.org/10.1016/B978-0-12-813128-2.00003-6

[135] Lototskyy, M.V., Tolj, I., Pickering, L., Sita, C., Barbir, F. and Yartys, V., 2017. The use of metal hydrides in fuel cell applications. *Progress in Natural Science: Materials International*, *27*(1), pp.3-20. https://doi.org/10.1016/j.pnsc.2017.01.008

[136] Horizon, 2022. Available from: https://www.horizoneducational.com/hydrostik-pro/p1222.

[137] HBank, 2022. Available from: http://www.hbank.com.tw

[138] Horizon, 2022. Available from: https://www.horizonfuelcell.com.

[139] Hwang, J.J., 2013. Effect of hydrogen delivery schemes on fuel cell efficiency. *Journal of Power Sources*, *239*, pp.54-63. https://doi.org/10.1016/j.jpowsour.2013.03.090

[140] Kurnia, J.C., Sasmito, A.P. and Shamim, T., 2019. Advances in proton exchange membrane fuel cell with dead-end anode operation: A review. *Applied Energy*, *252*, p.113416. https://doi.org/10.1016/j.apenergy.2019.113416

[141] Rodatz, P., Tsukada, A., Mladek, M. and Guzzella, L., 2002. Efficiency improvements by pulsed hydrogen supply in PEM fuel cell systems. *IFAC Proceedings Volumes*, *35*(1), pp.259-264. https://doi.org/10.3182/20020721-6-ES-1901.01511

[142] Jiang, D., Zeng, R., Wang, S., Jiang, L. and Varcoe, J.R., 2014. Paradox phenomena of proton exchange membrane fuel cells operating under dead-end anode mode. *Journal of Power Sources*, *265*, pp.45-49. https://doi.org/10.1016/j.jpowsour.2014.04.086

[143] Nikiforow, K., Karimäki, H., Keränen, T.M. and Ihonen, J., 2013. Optimization study of purge cycle in proton exchange membrane fuel cell system. *Journal of power sources*, *238*, pp.336-344. https://doi.org/10.1016/j.jpowsour.2012.11.153

[144] Siegel, J.B., Bohac, S.V., Stefanopoulou, A.G. and Yesilyurt, S., 2010. Nitrogen front evolution in purged polymer electrolyte membrane fuel cell with dead-ended anode. *Journal of the Electrochemical Society*, *157*(7), p.B1081. DOI 10.1149/1.3425743

[145] Matsuura, T., Chen, J., Siegel, J.B. and Stefanopoulou, A.G., 2013. Degradation phenomena in PEM fuel cell with dead-ended anode. *International Journal of Hydrogen Energy*, *38*(26), pp.11346-11356. https://doi.org/10.1016/j.ijhydene.2013.06.096

[146] Himanen, O., Hottinen, T. and Tuurala, S., 2007. Operation of a planar free-breathing PEMFC in a dead-end mode. *Electrochemistry communications*, *9*(5), pp.891-894. https://doi.org/10.1016/j.elecom.2006.12.002

[147] Chiche, A., Lindbergh, G., Stenius, I. and Lagergren, C., 2021. Design of experiment to predict the time between hydrogen purges for an air-breathing PEM fuel cell in dead-end mode in a closed environment. *International Journal of Hydrogen Energy*, *46*(26), pp.13806-13817. https://doi.org/10.1016/j.ijhydene.2021.01.035

[148] Chaparro, A.M. and Ferreira-Aparicio, P., 2018. Why portable electricity with hydrogen fuel cells?. In *Portable Hydrogen Energy Systems* (pp. 1-13). Academic Press. https://doi.org/10.1016/B978-0-12-813128-2.00001-2

[149] Al-Baghdadi, M.A.S., 2009. Performance comparison between airflow-channel and ambient air-breathing PEM fuel cells using three-dimensional computational fluid dynamics models. *Renewable Energy*, *34*(7), pp.1812-1824. https://doi.org/10.1016/j.renene.2008.12.002

[150] Ferreira-Aparicio, P., 2018. Technology indicators of portable power based on hydrogen-fed fuel cells. In *Portable Hydrogen Energy Systems* (pp. 175-192). Academic Press. https://doi.org/10.1016/B978-0-12-813128-2.00010-3

[151] Alink, R., Haußmann, J., Markötter, H., Schwager, M., Manke, I. and Gerteisen, D., 2013. The influence of porous transport layer modifications on the water management in polymer electrolyte membrane fuel cells. *Journal of Power Sources*, *233*, pp.358-368. https://doi.org/10.1016/j.jpowsour.2013.01.085

[152] Lee, F.C., Ismail, M.S., Ingham, D.B., Hughes, K.J., Ma, L., Lyth, S.M. and Pourkashanian, M., 2022. Alternative architectures and materials for PEMFC gas diffusion layers: A review and outlook. *Renewable and Sustainable Energy Reviews*, *166*, p.112640. https://doi.org/10.1016/j.rser.2022.112640

[153] Forner-Cuenca, A., Biesdorf, J., Gubler, L., Kristiansen, P.M., Schmidt, T.J. and Boillat, P., 2015. Engineered water highways in fuel cells: radiation grafting of gas diffusion layers. *Advanced materials*, *27*(41), pp.6317-6322. https://doi.org/10.1002/adma.201503557

[154] Cho, J., Lee, S., Shim, B.S., Jung, S.Y., Kim, D. and Park, S., 2021. Unveiling water drainage through microporous layer with laser-ablated open furrows in proton exchange membrane fuel cells. *Journal of Power Sources*, *491*, p.229563. https://doi.org/10.1016/j.jpowsour.2021.229563

[155] Fu, Y., Hou, M., Xu, H., Hou, Z., Ming, P., Shao, Z. and Yi, B., 2008. Ag–polytetrafluoroethylene composite coating on stainless steel as bipolar plate of proton exchange membrane fuel cell. *Journal of Power Sources*, *182*(2), pp.580-584. https://doi.org/10.1016/j.jpowsour.2008.04.051

[156] Baroutaji, A., Carton, J.G., Oladoye, A.M., Stokes, J., Twomey, B. and Olabi, A.G., 2017. Ex-situ evaluation of PTFE coated metals in a proton exchange membrane fuel cell environment. *Surface and Coatings Technology*, *323*, pp.10-17. https://doi.org/10.1016/j.surfcoat.2016.11.105

[157] Carton, J.G., Lawlor, V., Olabi, A.G., Hochenauer, C. and Zauner, G., 2012. Water droplet accumulation and motion in PEM (Proton Exchange Membrane) fuel cell mini-channels. *Energy*, *39*(1), pp.63-73. https://doi.org/10.1016/j.energy.2011.10.023

[158] Ferreira-Aparicio, P. and Chaparro, A.M., 2014. Influence of the cathode architecture in the frequency response of self-breathing proton exchange membrane fuel cells. *Journal of Power Sources*, *272*, pp.79-89. https://doi.org/10.1016/j.jpowsour.2014.08.046

[159] Javed, A., Shahid, M.A., Sharif, M. and Yasmin, M., 2017. Energy consumption in mobile phones. *International Journal of Computer Network and Information Security*, *10*(12), p.18.

[160] Padulles, J., Ault, G.W. and McDonald, J.R., 2000. An integrated SOFC plant dynamic model for power systems simulation. *Journal of Power sources*, *86*(1-2), pp.495-500. https://doi.org/10.1016/S0378-7753(99)00430-9

[161] El-Sharkh, M.Y., Rahman, A., Alam, M.S., Byrne, P.C., Sakla, A.A. and Thomas, T., 2004. A dynamic model for a stand-alone PEM fuel cell power plant for residential applications. *Journal of Power Sources*, *138*(1-2), pp.199-204. https://doi.org/10.1016/j.jpowsour.2004.06.037

[162] Uzunoglu, M. and Alam, M.S., 2006. Dynamic modeling, design, and simulation of a combined PEM fuel cell and ultracapacitor system for stand-alone residential applications. *IEEE transactions on energy conversion*, *21*(3), pp.767-775. 10.1109/TEC.2006.875468

[163] Uzunoglu, M., Onar, O.C. and Alam, M.S., 2007. Dynamic behavior of PEM FCPPs under various load conditions and voltage stability analysis for stand-alone residential applications. *Journal of Power Sources*, *168*(1), pp.240-250. https://doi.org/10.1016/j.jpowsour.2007.02.045

[164] Yalcinoz, T., 2018, June. A dynamic model and analysis of PEM fuel cells for an electric bicycle. In *2018 IEEE International Conference on Environment and Electrical Engineering and 2018 IEEE Industrial and Commercial Power Systems Europe (EEEIC/I&CPS Europe)* (pp. 1-5). IEEE. 10.1109/EEEIC.2018.8493821

[165] Benchouia, N.E., Derghal, A., Mahmah, B., Madi, B., Khochemane, L. and Aoul, E.H., 2015. An adaptive fuzzy logic controller (AFLC) for PEMFC fuel cell. *International Journal of Hydrogen Energy*, *40*(39), pp.13806-13819. https://doi.org/10.1016/j.ijhydene.2015.05.189

[166] Hemi, H., Ghouili, J. and Cheriti, A., 2014. A real time fuzzy logic power management strategy for a fuel cell vehicle. *Energy conversion and Management*, *80*, pp.63-70. https://doi.org/10.1016/j.enconman.2013.12.040

[167] Sakhare, A., Davari, A. and Feliachi, A., 2004. Fuzzy logic control of fuel cell for stand-alone and grid connection. *Journal of Power Sources*, *135*(1-2), pp.165-176. https://doi.org/10.1016/j.jpowsour.2004.04.013

[168] Ou, K., Yuan, W.W., Choi, M., Yang, S. and Kim, Y.B., 2017. Performance increase for an open-cathode PEM fuel cell with humidity and temperature control. *International Journal of Hydrogen Energy*, *42*(50), pp.29852-29862. https://doi.org/10.1016/j.ijhydene.2017.10.087

[169] Morner, S.O. and Klein, S.A., 2001. Experimental evaluation of the dynamic behavior of an air-breathing fuel cell stack. *J. Sol. Energy Eng.*, *123*(3), pp.225-231. https://doi.org/10.1115/1.1385202

[170] Alnejaili, T., Drid, S., Mehdi, D., Chrifi-Alaoui, L., Belarbi, R. and Hamdouni, A., 2015. Dynamic control and advanced load management of a stand-alone hybrid renewable power system for remote housing. *Energy Conversion and Management*, *105*, pp.377-392. https://doi.org/10.1016/j.enconman.2015.07.080

[171] Kim, H.I., Cho, C.Y., Nam, J.H., Shin, D. and Chung, T.Y., 2010. A simple dynamic model for polymer electrolyte membrane fuel cell (PEMFC) power modules: Parameter estimation and model prediction. *International journal of hydrogen energy*, *35*(8), pp.3656-3663. https://doi.org/10.1016/j.ijhydene.2010.02.002

[172] Alhazmi, N., Ingham, D.B., Ismail, M.S., Hughes, K., Ma, L. and Pourkashanian, M., 2014. The through-plane thermal conductivity and the contact resistance of the components of the membrane electrode assembly and gas diffusion layer in proton exchange membrane fuel cells. *Journal of Power Sources*, *270*, pp.59-67.

https://doi.org/10.1016/j.jpowsour.2014.07.082

[173] Alhazmi, N., Ismail, M.S., Ingham, D.B., Hughes, K.J., Ma, L. and Pourkashanian, M., 2013. The in-plane thermal conductivity and the contact resistance of the components of the membrane electrode assembly in proton exchange membrane fuel cells. *Journal of power sources*, *241*, pp.136-145. https://doi.org/10.1016/j.jpowsour.2013.04.100

[174] Karatayev, M., Lisiakiewicz, R., Gródek-Szostak, Z., Kotulewicz-Wisińska, K. and Nizamova, M., 2021. The promotion of renewable energy technologies in the former Soviet bloc: Why, how, and with what prospects?. *Energy Reports*, *7*, pp.6983-6994. https://doi.org/10.1016/j.egyr.2021.10.068

[175] Hekimoğlu, G., Sarı, A., Kar, T., Keleş, S., Kaygusuz, K., Yıldırım, N., Tyagi, V.V., Sharma, R.K. and Saleh, T.A., 2021. Carbonized waste hazelnut wood-based shape-stable composite phase change materials for thermal management implementations. *International Journal of Energy Research*, *45*(7), pp.10271-10284.

https://doi.org/10.1002/er.6514

[176] Sarı, A., Saleh, T.A., Hekimoğlu, G., Tyagi, V.V. and Sharma, R.K., 2021. Microencapsulated heptadecane with calcium carbonate as thermal conductivity-enhanced phase change material for thermal energy storage. *Journal of Molecular Liquids*, *328*, p.115508. https://doi.org/10.1016/j.molliq.2021.115508

[177] Moazeni, F. and Khazaei, J., 2020. Electrochemical optimization and small-signal analysis of grid-connected polymer electrolyte membrane (PEM) fuel cells for renewable energy integration. *Renewable Energy*, *155*, pp.848-861.

https://doi.org/10.1016/j.renene.2020.03.165

[178] Rosli, M.I., Borman, D.J., Ingham, D.B., Ismail, M.S., Ma, L. and Pourkashanian, M., 2010. Transparent PEM fuel cells for direct visualization experiments. https://doi.org/10.1115/1.4001353

[179] Wilberforce, T., Ijaodola, O., Khatib, F.N., Ogungbemi, E.O., El Hassan, Z., Thompson, J. and Olabi, A.G., 2019. Effect of humidification of reactive gases on the performance of a proton exchange membrane fuel cell. *Science of the Total Environment*, *688*, pp.1016-1035. https://doi.org/10.1016/j.scitotenv.2019.06.397

[180] Cha, D., Yang, W. and Kim, Y., 2019. Performance improvement of self-humidifying PEM fuel cells using water injection at various start-up conditions. *Energy*, *183*, pp.514-524. https://doi.org/10.1016/j.energy.2019.06.154

[181] Tohidi, M., Mansouri, S.H. and Amiri, H., 2010. Effect of primary parameters on the performance of PEM fuel cell. *International Journal of Hydrogen Energy*, *35*(17), pp.9338-9348. https://doi.org/10.1016/j.ijhydene.2010.03.112

[182] Carcadea, E., Varlam, M., Ismail, M., Ingham, D.B., Marinoiu, A., Raceanu, M., Jianu, C., Patularu, L. and Ion-Ebrasu, D., 2020. PEM fuel cell performance improvement through numerical optimization of the parameters of the porous layers. *International Journal of Hydrogen Energy*, *45*(14), pp.7968-7980. https://doi.org/10.1016/j.ijhydene.2019.08.219

[183] Turkmen, A.C. and Celik, C., 2018. The effect of different gas diffusion layer porosity on proton exchange membrane fuel cells. *Fuel*, *222*, pp.465-474. https://doi.org/10.1016/j.fuel.2018.02.058

[184] Kahveci, E.E. and Taymaz, I., 2018. Assessment of single-serpentine PEM fuel cell model developed by computational fluid dynamics. *Fuel*, *217*, pp.51-58. https://doi.org/10.1016/j.fuel.2017.12.073

[185] Carton, J.G. and Olabi, A.G., 2017. Three-dimensional proton exchange membrane fuel cell model: comparison of double channel and open pore cellular foam flow plates. *Energy*, *136*, pp.185-195. https://doi.org/10.1016/j.energy.2016.02.010

[186] Dong, P., Xie, G. and Ni, M., 2021. Improved energy performance of a PEM fuel cell by introducing discontinuous S-shaped and crescent ribs into flowing channels. *Energy*, *222*, p.119920. https://doi.org/10.1016/j.energy.2021.119920

[187] Henriques, T., César, B. and Branco, P.C., 2010. Increasing the efficiency of a portable PEM fuel cell by altering the cathode channel geometry: A numerical and experimental study. *Applied Energy*, *87*(4), pp.1400-1409. https://doi.org/10.1016/j.apenergy.2009.09.001

[188] Lee, N., Lee, J., Lee, S.W., Jang, S.S. and Ju, H., 2020. Parametric study of passive air-cooled polymer electrolyte membrane fuel cell stacks. *International Journal of Heat and Mass Transfer*, *156*, p.119886. https://doi.org/10.1016/j.ijheatmasstransfer.2020.119886

[189] Lee, J., Gundu, M.H., Lee, N., Lim, K., Lee, S.W., Jang, S.S., Kim, J.Y. and Ju, H., 2020. Innovative cathode flow-field design for passive air-cooled polymer electrolyte membrane (PEM) fuel cell stacks. *International Journal of Hydrogen Energy*, *45*(20), pp.11704-11713. https://doi.org/10.1016/j.ijhydene.2019.07.128

[190] Atyabi, S.A., Afshari, E., Wongwises, S., Yan, W.M., Hadjadj, A. and Shadloo, M.S., 2019. Effects of assembly pressure on PEM fuel cell performance by taking into accounts electrical and thermal contact resistances. *Energy*, *179*, pp.490-501. https://doi.org/10.1016/j.energy.2019.05.031

[191] Miao, D., Chen, W., Zhao, W. and Demsas, T., 2020. Parameter estimation of PEM fuel cells employing the hybrid grey wolf optimization method. *Energy*, *193*, p.116616. https://doi.org/10.1016/j.energy.2019.116616

[192] Bergman, T.L., 2011. *Fundamentals of heat and mass transfer*. John Wiley & Sons.

[193] Ghiaasiaan, S.M., 2018. *Convective heat and mass transfer*. CRC Press.

[194] Unsworth, G., Dong, L. and Li, X., 2013. Improved experimental method for measuring gas diffusivity through thin porous media. *AIChE Journal*, *59*(4), pp.1409-1419. https://doi.org/10.1002/aic.13911

[195] Jiao, K. and Li, X., 2011. Water transport in polymer electrolyte membrane fuel cells. *Progress in energy and combustion Science*, *37*(3), pp.221-291. https://doi.org/10.1016/j.pecs.2010.06.002

[196] Dhimish, M., Vieira, R.G. and Badran, G., 2021. Investigating the stability and degradation of hydrogen PEM fuel cell. *International Journal of Hydrogen Energy*, *46*(74), pp.37017-37028. https://doi.org/10.1016/j.ijhydene.2021.08.183

[197] Rahimi-Esbo, M., Ranjbar, A.A. and Rahgoshay, S.M., 2020. Analysis of water management in PEM fuel cell stack at dead-end mode using direct visualization. *Renewable Energy*, *162*, pp.212-221. https://doi.org/10.1016/j.renene.2020.06.078